UC Irvine
UC Irvine Electronic Theses and Dissertations

Title

Using mechanical stimulation to improve tissue-engineered articular cartilage for implantation in the knee joint

Permalink

Author

Salinas, Evelia

Publication Date

2020

Copyright Information

Peer reviewed|Thesis/dissertation

UNIVERSITY OF CALIFORNIA,

IRVINE

Using mechanical stimulation to improve tissue-engineered articular cartilage for implantation in the knee joint

DISSERTATION

Submitted in partial satisfaction of the requirements for the degree of

DOCTOR OF PHILOSOPHY

in Biomedical Engineering

By

Evelia Yareli Salinas

Dissertation committee

Dr. Kyriacos A. Athanasiou, Chair

Dr. Anna Grosberg

Dr. Jerry C. Hu

2020

DEDICATION

To

My parents, Maria Isabel and Jose Marcos Salinas, who were my first teachers, role models, and forever cheerleaders

Mis abuelos Pruneda y mis abuelos Salinas, llevo su amor conmigo a donde quiera que vaya

And my sister, Isabella Salinas, who has been, and will forever be, my best friend

TABLE OF CONTENTS

ACKNOWLEDGEMENTS

As a child, people ask what you want to be when you grow up, and my response was usually, "If I could go to school forever, I would." At that time, I didn't think that was an option. When I learned about graduate school, I saw it as an opportunity to gain scientific knowledge, grow professionally, and, as a bonus, extend my time as a student. When I started graduate school, I didn't realize that it would, indeed, make me a student forever. The pursuit of a doctoral degree teaches you something extremely valuable, how to learn about anything you want. This asset comes second only to the invaluable relationships I have made along the way.

First, and foremost, I would like to thank Dr. Kyriacos Athanasiou for his incredible mentorship, undeniable kindness, honest advice, and unwavering dedication to excellence. I would also like to thank Dr. Jerry C. Hu, for his mentorship and boundless creativity for solving problems. I am extremely fortunate to be taught by Dr. Athanasiou and Jerry, and I am forever grateful for the patience and support they have shared with me on this journey.

Dr. Athanasiou and Jerry have cultivated a laboratory with some of the highest quality people I have ever met, let alone worked with. Jarrett, thank you so much for your partnership and friendship, the *in vivo* study would have been close to insurmountable without your companionship. Erik, I feel fortunate to rub shoulders with you and bounce ideas off of you both in and outside the laboratory. Ryan, Gaston, Rachel, Gaby, Ben, Wendy, and Heenam you make the quest for data and understanding a pleasure, and I am honored work with you and share in your space. Of course, I would also like to thank past members of the lab, especially Dr. Aryaei and Dr. Paschos, for always being an email away and leaving behind impeccable lab notes. Finally, I would like to thank Jessica Herrera, the absolute best undergraduate mentee. You have been a wonderful student and partner, and I am so proud of you.

VITA

Evelia Y. Salinas

2015   B.S. Biophysics, St. Mary's University, San Antonio, Texas

2018   M.S Biomedical Engineering, University of California, Irvine

2016-2017   Teaching Assistant University of California, Davis

2018   Teaching Assistant University of California, Irvine

FIELD OF STUDY

Biomedical Engineering

PUBLICATIONS

1.   Salinas EY, Hu JC, Athanasiou KA, A guide for using mechanical stimulation to enhance tissue-engineered articular cartilage, *Tissue Engineering Part C* (2018)

2.   Salinas EY, Aryaei A, Paschos N, Berson E, Kwon H, Hu JC, Athanasiou KA, Shear stress induced by fluid-flow produces improvements in tissue-engineered cartilage, *Biofabrication (2020)*

3.   Link JM*, Salinas EY*, Hu JC, Athanasiou KA, The tribology of cartilage: mechanisms, experimental techniques, and relevance to translational tissue engineering, *Clinical Biomechanics (2019)*

4.   Salinas EY, Williams AE, King CE, Effect of controlling group heterogeneity on student performance in a graphical programming course, *IEEE Frontiers in Education* (2019)

ABSTRACT OF THE DISSERTATION

Using mechanical stimulation to improve tissue-engineered articular cartilage for implantation in the knee joint

By

Evelia Yareli Salinas

Doctor of Philosophy in Biomedical Engineering

University of California, Irvine 2020

Dr. Kyriacos Athanasiou, Chair

Hyaline articular cartilage, the smooth, white, tissue that is found at the ends of long bones, does not regenerate. Although it is a mechanically robust tissue that repeatedly supports up to six-times body weight, its innate lack of vasculature limits access to nutrients and progenitor cells that are necessary for tissue repair. Currently, clinicians attempt to limit further degeneration when focal defects are manifested on the articular cartilage surface. Unfortunately, for the 250,000 Americans that receive clinical treatment each year, the available options do not produce biomimetic repair tissue necessary to substantiate a long-term treatment option. Tissue-engineered articular cartilage can be designed and manipulated *in vitro* to fill this significant clinical need. In particular, mechanical stimulation during neocartilage culture can be used to enhance mechanical properties and drive extracellular matrix content toward biomimetic levels. However, before an effective tissue-engineering strategy for treating focal articular cartilage defects can be translated to the clinic, the FDA requires that both local and systemic safety be rigorously demonstrated in a large animal model. Thus, toward translating tissue engineering technologies to clinical applications, the global objectives of this research are: 1) to

enhance the mechanical and extracellular matrix properties of neocartilage using mechanical stimulation and bioactive factors, and 2) to evaluate the local and systemic safety of neocartilage implanted in an orthotopic location in a large animal model.

To address these objectives, this research: 1) enhanced the mechanical and extracellular matrix properties of neocartilage using shear stress stimulation, 2) further improved neocartilage properties by exploring combinations of mechanical stimulation strategies with bioactive factors, and 3) evaluated the safety of mechanically stimulated neocartilage implanted in the femoral condyles of Yucatan minipigs.

Shear stress stimulation was shown to improve compressive moduli and extracellular matrix content in neocartilage created from bovine articular chondrocytes, minipig costochondrocytes, and human articular chondrocytes. In particular, it was shown that fluid-induced shear stress applied within a range of 0.05-0.21Pa improved the compressive moduli by 72% - 450% in all types of self-assembled neocartilage. Additionally, the modes of action for fluid-induced shear stress were investigated and it was determined that shear stress upregulated genes encoding a mechanically gated ion channel on the primary cilia of chondrocytes, which have previously been shown to be key sensors of mechanical stimulation. These results indicated that fluid-induced shear stress is an effective strategy for the improvement of mechanical properties in neocartilage constructs.

Shear stress was combined with other forms of mechanical stimulation (i.e. compression stress or tension stress). The tensile properties of neocartilage constructs that were stimulated with a combination of tension and shear stress were significantly improved over shear stress only constructs. Compressive properties were also significantly improved over non-stimulated controls, but not over neocartilage stimulated with only shear stress. However, when bioactive factors were included, the neocartilage constructs that received only shear stress and bioactive

factors were the most mechanically robust in both compressive and tensile properties. This research indicates that neocartilage should be stimulated with bioactive factors and shear stress before implantation.

Finally, to assess the local and systemic safety of mechanically stimulated implants, an *in vivo* study was performed in the femoral condyles of Yucatan minipigs. It was found that the implants did not elicit local or systemic inflammatory responses in minipigs. In particular, there were no adverse effects in the gross morphology of the native tissue surrounding the implants. Furthermore, histological staining did not show evidence of fibrosis or infiltrating immune cells. Finally, the systemic evaluation of the minipigs via complete blood count and blood phenotyping chemistry panels did not show differences between animals that received implants and animals that did not receive implants. These large animal *in vivo* studies conclude that there are no adverse local or systemic safety effects of neocartilage implants that are treated with mechanical stimulation and bioactive factors.

Overall, this research is significant because it has elucidated strategies to improve the properties of neocartilage toward native articular cartilage, as well as demonstrated the safety of neocartilage implants in a clinically relevant location in a large animal model. This work is foundational for future preclinical studies because it has presented evidence of both the local and systemic safety of self-assembled, mechanically stimulated, neocartilage implants. With further research, the efficacy of tissue-engineered neocartilage implants can be investigated and have the potential to transform clinical treatment options for patients suffering from articular cartilage degeneration.

INTRODUCTION

Hyaline articular cartilage is a smooth, white tissue found at the ends of bones in diarthrodial joints. Hyaline articular cartilage distributes the forces generated in diarthrodial joints during locomotion, allowing subchondral bone to withstand rigorous biomechanical environments with loads approaching six times body weight. The mechanical robustness of articular cartilage is attributed to specialized proteins and macromolecules. In particular, the collagens and proteoglycans that interact with charged synovial fluid give articular cartilage the frictionless and viscoelastic properties necessary to endure compressive, tensile, and shear stresses. Although, the presence of articular cartilage gives rise to extremely durable and resilient synovial joints, slight imbalances in biological processes, overuse, and trauma can lead to cumulative and progressive changes over decades of use.

Because articular cartilage is avascular, it does not have abundant access to nutrients and circulating progenitor cells, which limits its ability to produce a sufficient healing response when damaged. Articular cartilage's inability to heal causes even minor tissue degradation and failure to cascade into larger defects and eventually osteoarthritis. However, before osteoarthritis is manifested in patients, clinicians attempt to repair focal defects with microfracture, chondroplasty, mosaicplasty, or chondrocyte implantation. These surgeries occur about 250,000 times a year in the U.S alone. Unfortunately, these current clinical treatment options are inadequate because of their inability to produce hyaline articular cartilage, failure to integrate with native tissue, and even fill the entire defect. The void of substantial long-term treatment options for articular cartilage defects can be filled with tissue-engineered articular cartilage, which can be designed and manipulated to possess native-like biochemical and biomechanical properties, fill shape-specific defects, and integrate with surrounding native tissue.

1

The self-assembling process is a tissue-engineering strategy used to produce neocartilage constructs. The self-assembling process does not require the use of scaffolds, and instead relies on intrinsic minimization of free energy by chondrocytes. The process consists of four distinct phases: during the first phase chondrocytes are seeded into a non-adherent substrate; during the second phase chondrocytes ensue minimization of free energy via cell-to-cell adhesion; in the third phase chondrocytes start to produce extracellular matrix; in the fourth phase the neocartilage begins to mature and ceases extracellular matrix production. The self-assembling process has several advantages over traditional tissue engineering systems in that it does not rely on the use of scaffolds, which have been shown to leach degradation byproducts and contribute to an immune response following implantation. The self-assembling process uses biochemical and biomechanical stimuli during the tissue culture process to create robust neocartilage constructs for implantation. Overall, the use and manipulation of self-assembled neocartilage implants provides a potentially safe and promising option for articular cartilage tissue repair strategies.

The tissue engineering of articular cartilage typically requires the use of bioactive agents, such as enzymes and growth factors, to strengthen tissue and achieve biomimetic properties. In particular, it has been found that the use of bioactive agents (TGF-β1, C-ABC, and LOXL2) and biomechanical stimulation during the self-assembling of neocartilage yields stiffer and stronger constructs with enhanced extracellular matrix contents. In terms of biomechanical stimulation, compression, hydrostatic pressure, and tension stimulation have all been used to improve self-assembled neocartilage mechanical properties. Shear stress, and fluid-induced shear stress in particular, has not been investigated for use on self-assembled neocartilage constructs. Furthermore, the combination of mechanical stimulation strategies also has yet to be investigated. Biomechanical stimulation strategies have several advantages over bioactive factors. For example, TGF-β1 has pleiotropic effects leading to unknown, potentially harmful,

ramifications when implanted. The investigation of shear stress stimulation, both independently and in combination with other mechanical stimuli, has the potential to produce neocartilage that is on par with those that have been stimulated with bioactive factors.

Toward advancing neocartilage-engineering technologies safely to the clinic, the global objectives of this research are: 1) to determine the optimal combination of mechanical stimulation strategies for the production of mechanically robust neocartilage implants and 2) to assess the safety of orthotopic implantation of mechanically stimulated neocartilage constructs in a large animal model. To achieve the overarching goals of this work, three specific aims were performed:

Specific Aim 1: To enhance properties of neocartilage created with a variety of chondrocyte types under fluid-induced shear stress stimulation. The main objective of this aim is to drive the translatability of the fluid-induced shear stress culture regimen by applying it to neocartilage derived first from bovine articular chondrocytes, then minipig costochondrocytes, and finally from human articular chondrocytes. Costal cartilage is a favorable cell source for allogeneic neocartilage implants because it eliminates donor-site morbidity and cell scarcity. *The hypothesis of specific aim 1 is that fluid-induced shear stress will yield an increase in the mechanical properties of neocartilage created from a variety of cell sources.*

Specific Aim 2: To improve neocartilage properties by stimulating constructs with a combination of mechanical stimulation and bioactive factors. The objective of this aim is to determine which combination of mechanical stimulation strategies and bioactive factors are optimal for creating neocartilage with robust mechanical properties and biomimetic extracellular matrix content. Combinations of mechanical stimulation strategies (i.e. compression + shear stress, tension + shear stress) will be investigated in neocartilage created with minipig costochondrocytes to determine which would be optimal for pairing with bioactive factors. *The*

3

hypothesis of this aim is that a combination of mechanical stimulation strategies combined with bioactive factors will produce neocartilage with improved properties compared to statically cultured control groups or either form of stimulus alone.

Specific Aim 3: To evaluate the translatability and safety of neocartilage cultured under combined mechanical stimuli and bioactive factors with orthotopic implantation in a large animal model. The objective of this aim is to assess the safety and translatability of allogeneic, mechanically stimulated neocartilage via implantation in the articular cartilage of a minipig. The mechanical stimulation regimen yielding the most biomimetic neocartilage from aim 2 will be used to created implants studied *in vivo. It is hypothesized that allogeneic neocartilage cultured under mechanical stimulation will not produce a local or systemic immune response when implanted in an orthotopic location in a large animal model.*

All 7 chapters in the main body of this thesis, in addition to the three chapters in the appendix, are either already published works or represent full-sized publications of original research. The outcomes and future direction of this body of work are discussed in the Conclusions section. A brief description of each section is provided below.

Chapter 1 provides a background of mechanical stimulation strategies used in the field of articular cartilage tissue engineering. Specifically, mechanical stimulation strategies are described in terms of their implementation, modes of action, and resultant neocartilage properties.

Toward achieving specific aim 1, Chapter 2 and Chapter 3, investigate the application of fluid-induced shear stress on neocartilage implants. Chapter 2 focuses on the development of fluid-induced shear stress as a strategy to improve neocartilage tissue properties. This chapter begins with the design and development of a fluid-induced shear stress bioreactor, the investigation of the modes of action responsible for the improvement of neocartilage properties,

and the translation to human chondrocyte derived neocartilage. Chapter 3 further optimizes the fluid-induced shear stress regimen by determining when in the tissue culture period shear stress is most effective at improving neocartilage construct properties.

To satisfy specific aim 2, Chapter 4, Chapter 5, and Chapter 6 explore utilizing a combination of mechanical stimulation strategies to improve neocartilage properties. In Chapter 4, the combination of passive compressive stress and fluid-induced shear stress are investigated in both bovine neocartilage and minipig neocartilage. In Chapter 5, the combination of constant tensile stress and shear stress is explored in minipig neocartilage. For both Chapter 4 and Chapter 5, the combinations of mechanical stimuli are compared against nonstimulated controls and neocartilage treated with only one form of mechanical stimulus. In Chapter 6, the inclusion of bioactive factors was investigated with the combination of fluid-induced shear stress and constant tensile stress.

Finally, specific aim 3 was achieved by utilizing the knowledge gained from prior chapters to engineer mechanically robust neocartilage to be used for *in vivo* implantation in Chapter 7. Neocartilage implants were placed in defects created in the femoral condyles of Yucatan minipigs. This large animal *in vivo* study was divided into two surgical sets. The first surgical set was performed with three minipigs to determine an optimal fixation method and assess the local immune response to neocartilage implants. The second surgical set was performed with five minipigs, three of which received implants and two of which did not receive implants. The second surgical set was focused on assessing the systemic immune response to neocartilage implants.

It should be noted that additional work, completed in collaboration with colleagues and/or other departments, is included in the appendix. Appendix A presents a review of the tribology of cartilage, which includes mechanisms, experimental techniques, and relevance to translational

tissue engineering. Appendix B provides a characterization of adult and neonatal articular cartilage from the equine stifle joint. Finally, Appendix C was completed and published as part of a grant from the Division of Teaching Excellence and Innovation at the University of California, Irvine. The effect of controlling group heterogeneity on student performance in a graphical programing course was investigated in a large undergraduate level biomedical engineering classroom.

Overall, this work describes several advances in the field of neocartilage tissue engineering, as well as research aiming to improve the training of future engineers that will enter the field.

CHAPTER 1- A GUIDE FOR USING MECHANICAL STIMULATION TO IMPROVE TISSUE ENGINEERED CARTILAGE

ABSTRACT

The use of tissue-engineered articular cartilage (AC) constructs has the potential to become a powerful treatment option for cartilage lesions resulting from trauma or early stages of pathology. Although fundamental tissue-engineering strategies based on the use of scaffolds, cells, and signals have been developed, techniques that lead to biomimetic AC constructs that can be translated to *in vivo* use have yet to be fully confirmed. Mechanical stimulation during tissue culture can be an effective strategy to enhance the mechanical, structural, and cellular properties of tissue-engineered constructs toward mimicking those of native AC. *In vivo*, mechanical loading at maximal and supramaximal physiological levels has been shown to be detrimental to AC through the development of degenerative changes. In contrast, multiple studies have revealed that during culture, mechanical stimulation within narrow ranges of magnitude and duration can produce anisotropic, mechanically robust AC constructs with high cellular viability. Significant progress has been made in evaluating a variety of mechanical stimulation techniques on tissue-engineered AC, either alone or in combination with other stimuli. The objective is to list the qualitative and quantitative effects that can be attained when mechanical stimulation is used to engineer AC. Our goal is to provide a practical guide to their use and optimization of loading parameters. For each loading condition, we will also present and discuss benefits and limitations of bioreactor configurations that have been used. The intent is for this review to serve as a reference for including mechanical stimulation strategies as part of AC construct culture regimens.

INTRODUCTION

Degradation of articular cartilage (AC) is caused by trauma or over-use (1,2), which initiate a cascade of pathological events, leading to osteoarthritis (OA). According to the Center for Disease Control, OA affects over 30 million Americans per year. Even before OA is fully manifested, AC injuries can negatively impact the mobility of young patients.(3) Currently, there are no substantial, long-term treatment options to repair and halt the progression of AC injuries. Focal defects (~5mm dia.) are generally treated by microfracture and autologous chondrocyte implantation.(4) These strategies lead to the development of mechanically inferior fibrocartilage in the treated lesions, which places detrimental stresses on surrounding AC.(5) Tissue-engineering strategies show the potential to overcome the drawbacks of current treatment options by designing and developing biomimetic AC tissues for transplantation.

Native, healthy AC consists of a durable, low-friction, mechanically robust tissue, sparsely populated by chondrocytes. Physiologically, AC experiences and endures a myriad of mechanical forces including compression, shear, hydrostatic pressure (HP), and tension. To achieve translatable, biomimetic AC tissue, the design criteria of engineered AC follow those of native AC in both form and function: high compressive and tensile stiffness, a well-organized matrix rich in collagen type II and sulfated glycosaminoglycans (sGAG), viable cells of a healthy phenotype, low coefficient of friction, and *in vivo* durability.

To treat AC injuries, tissue-engineering has focused on developing constructs derived from chondrocytes, scaffolds, and signals. Signaling tools used to satisfy the aforementioned design criteria include bioactive and mechanical stimuli. In general, research in the field remains highly centralized on investigating bioactive factors alone because they can be easily applied in culture medium. Transforming growth factor-β1 (TGF-β1), insulin-like growth factor-1 (IGF-1), and bone morphogenetic protein-2 (BMP-2) are all effective in improving extracellular matrix (ECM) content and mechanical properties.(4) Mechanical stimulation also increases ECM content and mechanical properties, but, notably, fiber organization in response to mechanical

stimulation has also been observed.(5–7) This review focuses on the use of mechanical stimuli to address the design criteria that soluble factors have been able to influence and also those that the soluble factors have not shown efficacy toward.

Because articulating joints lack access to blood vessels, chondrocytes dwelling in AC rely on mechanical movement for nutrient delivery, signaling, and cellular waste disposal.(5) Mechanical stimulation research on tissue-engineered AC (TEAC) has largely been focused on direct compression (DC) and HP, but, more recently, shear and tension have also shown potential for increasing ECM content, preserving cellular viability, and promoting matrix organization. The mechanical stimulation parameters most commonly reported are magnitude and duration.(8) The optimal mechanical loading parameters will depend on the matrix or scaffold used for cell culture because of stress shielding on the chondrocytes. Alternatively, studies that use high-density chondrocyte culture and no initial matrix, will likely employ lower magnitudes of load. For this reason, it is important to report parameters in units that normalize to the matrix, such as percent strain. Frequency, waveform, and time of application are also important parameters (Figure 1), although less frequently investigated. To-date, a description of how specific design criteria can be achieved by manipulating mechanical stimulation parameters is lacking.

The first portion of this review defines specific design criteria, which include mechanical properties and matrix production, content, organization, and integration, as well as criteria specified by the FDA, such as durability.(9) The second portion introduces different types of mechanical stimulation and their mode of application with bioreactors. Subsections in each type of mechanical stimulation offer integrated discussion on how various design criteria are enhanced by the specified mode of stimulation. Of particular interest are descriptions of how certain design criteria can be addressed more effectively using mechanical stimuli because little or no data exist on how such properties can be manipulated using bioactive factors alone. The

limitations of mechanical stimuli are also discussed within the context of how they may be paired with bioactive factors.

FIGURE 1
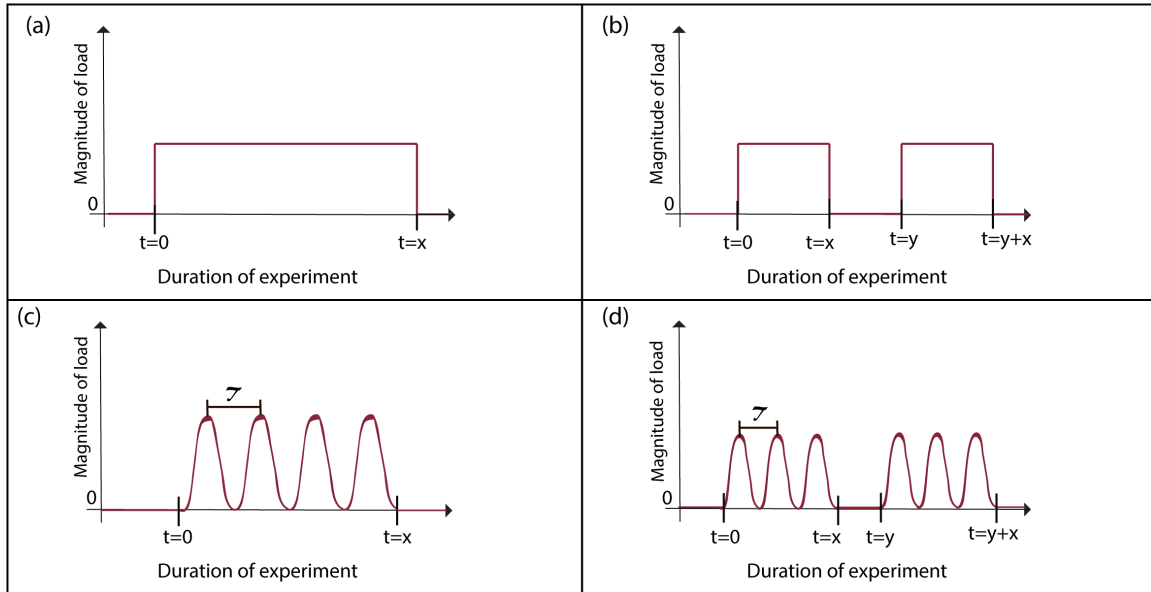
Figure 1 – Waveforms representing common loading patterns used in mechanical stimulation studies. **a)** continuous passive loading, **b)** intermittent passive loading, **c)** continuous dynamic loading, and **d)** intermittent dynamic loading. The x-axis represents the duration of the experiment, where t=0 represents the commencement of mechanical stimulation. *t = x* represents the duration of applied stimulation, and τ represents the wave period (frequency = $1/\tau$). In b) and d), t = y - x is the amount of time the tissue is in static culture between mechanical stimulation treatments. The y-axis represents the magnitude of load, which is commonly measured in units of stress, strain, or mass.

DESCRIPTION AND ASSESSMENT OF TISSUE ENGINEERED ARTICULAR CARTILAGE DESIGN CRITERIA

Compressive moduli

Sustaining compressive loads is a critical function of AC. Major weight-bearing joints, such as the hip and knee, experience compressive stress between 0.5-7.7MPa, which typically leads to about 13% strain.(1,10) Native AC in healthy people endures thousands of compressive loading

cycles per day without suffering injury, and failure to maintain loading on a regular basis leads to cartilage degradation and loss of AC function.(11) Thus, TEAC must similarly be capable of withstanding routine compressive cycles without failure.

Compressive moduli in TEAC are frequently represented by aggregate (H_A) and dynamic (E_D) moduli. The H_A is a measure of the equilibrium resistance of a solid-fluid mixture once fluid has stopped flowing.(12) The E_D is the ratio of stress to strain under cyclic loading conditions.(13) Native human AC tissue has an H_A of 0.08-2MPa.(14–16) The E_D of native AC has been shown to increase with increasing strain nonlinearly.(13,17) Though other compressive properties exist, investigators generally only measure and report one or two compressive moduli. Regardless of which modulus value is measured, the objective of this design criterion is for TEAC to match the compressive properties of native AC.

Tensile properties

Native AC sustains a constant state of static pre-tension caused by negatively charged proteoglycans retaining fluid throughout the ECM.(18) Consequently, the collagen in the cartilage matrix imposes tension that allows the tissue to swell without rupturing.(10,11) As a result of the Poisson effect, AC is also exposed to tension during compression as well as shear.(19) Tensile properties of AC are quantified using the Young's modulus (E_Y) and the ultimate tensile strength (UTS). The E_Y is defined as the slope of the linear portion of the stress-strain curve under conditions of uniaxial loading.(20) The UTS is defined as the maximum stress sustained by the material under strain and is considered the stress at failure. To match the tensile properties of native AC, TEAC must have a E_Y of 5-25MPa and UTS of 2-8MPa.(15,21,22) Because native AC experiences macroscopic tension indirectly as an effect of compressive and shear loads, tensile properties have not historically been investigated as much as compressive properties, but this characteristic is gaining recognition of its importance.

Collagen content

Two-thirds of the dry mass of AC is collagen. The most abundant collagen type in AC is collagen II, but collagen types III, VI, IX, X, XI, XII, and XIV also contribute to a mature AC matrix.(23) Collagen types II, IX, and XI form a reinforcing heteropolymer in the ECM, while collagen type X contributes to regulating ossification of cartilage.(24) Collagen X is also found in excess in ECM of OA patients, making it a marker for the disease.(25) The goal of this design criterion is to engineer AC constructs with high collagen II content and without collagens that are indicative of fibrocartilage or bone (e.g., collagen I and X).(26)

Collagen content is recorded in almost all TEAC studies. Generally, a hydroxyproline assay is used when quantifying collagen content in TEAC constructs.(27) This assay is not specific to any collagen type and measures total collagen content. Immunohistochemical staining and ELISA assays may be performed to assess collagen type II content in an AC constructs.(28) Collagen fibril diameter and crosslinks, such as pyridinoline (29), are also important aspects of the collagen fibril network found in AC ECM, though they are not often reported in mechanical stimulation studies. Investigating specific collagen type, crosslinks, and fibril/fiber dimensions could be helpful for determining what aspects of the collagen network are affected by mechanical loading and if these contribute to mechanical properties.

Glycosaminoglycan content

The highly anionic GAGs found in AC contribute to resisting compressive loads by binding to water molecules.(30) GAG takes up about 25% of the dry weight of native AC, of which most are chondroitin and keratan sulfate chains and hyaluronan.(31) GAGs have functional roles in tissue remodeling, up-take of proteins, intracellular signaling, and cell migration.(15,32) Aggrecan is the major type of proteoglycan found in AC and is made of a protein core attached to many 4- or 6- sulfated chondroitin chains.(31,33) In particular, sGAGs are responsible for

withstanding high mechanical loads, and their synthesis is regulated by exposure to compressive forces.(34) However, excessive loading, such as strenuous exercise, depletes sGAGs, resulting in reduced HP and compromised compressive properties.(34) Some studies only report GAG content instead of sGAG content, but it is crucial to obtain these data because sGAG depletion gives insight to excessive loads in mechanical stimulation studies.

The 1,9-dimethylmethylene blue (DMMB) dye assay is widely used to quantify total sGAG, but it cannot differentiate amongst sGAGs nor detect non-sulfated hyaluronan.(32,35) However, fluorophore-assisted carbohydrate electrophoresis is gaining recognition as a strategy that does differentiate amongst GAG types.(36)

Cellular performance

In static cultures, chondrocytes in the inner region of AC constructs have limited access to signals and nutrients causing them to lose function and their chondrocytic phenotype.(37) Cell viability and proliferation are measured using metabolic assays, and cellular content may be measured indirectly by quantifying DNA content. TEAC is biomimetic and employable for translation only if it houses viable chondrocytes with high proliferative potential and AC-specific ECM production.(38)

Investigating mechanical stimulation on AC constructs shows that there is significant increase in chondrocyte viability when AC constructs are cultured under a dynamic regimen.(5,11) For example, when DC is induced dynamically it has resulted in five-fold increase of viable cells when compared to passive DC cultures.(6) Higher chondrocyte viability in dynamic cultures is attributed to higher nutrient and sulfate accessibility compared to passively stimulated or static cultures.(11)

Fiber organization

Though ECM content has been attributed as the main contributor to AC mechanical properties (39,40), fiber organization has increasingly gained recognition for playing a major role in AC mechanical functionality.(41,42) When tested under confined or unconfined compression, as well as tension, zonal architecture and anisotropy have been found to play salient roles in the mechanical properties of native AC.(41,43,44) A robust TEAC with zonal architecture has not yet been achieved. The challenge in replicating the zonal architecture of AC comes from the uniqueness of each zone. For example, reconstruction of the superficial zone would require replication of lubricin and superficial zone protein content.(45,46) Efforts have been made to study and culture individual zonal subpopulations of chondrocytes under mechanical stimulation.(47) For instance, superficial zone chondrocytes have been found to have an increased response to tensile stimulation, whereas deep zone chondrocytes have been found to respond better to HP.(48,49) Crosslink content, such as pyridinoline, has also been shown to play a large role in the structure-function relationship of AC.(50,51) ECM content, structure, and crosslinking are salient aspects of AC constructs and should be fully characterized.

Investigators may also aim to reconstruct zonal architecture to enhance the functionality and biomimicry of TEAC. Both zonal structure and surface anisotropy are important aspects of fiber organization in AC, but only surface anisotropy has been successfully achieved in TEAC with the use of mechanical stimulation. Surface-anisotropy in native AC can be tested using split lines.(44,52) Although, split lines have never been observed in TEAC, anisotropy may also be assessed using scanning electron microscopy.(53)

Tribology

Native AC demonstrates exceptionally low friction even under large and repetitive mechanical loads.(54) Although the intrinsic nature of AC is not conducive to regeneration, a low coefficient of friction keeps the tissue functional for decades.(54) Its low friction and efficient lubrication can

be attributed to several mechanisms: lubricin, hyaluronic acid, surface-active phospholipids (55), and interstitial pressurization.(56) In AC, the minimum fluid film thickness between articulating surfaces, in conjunction with the surface roughness, loading speed, and magnitude determine the lubrication mode.(15,57) In hydrodynamic lubrication, usually a low mechanical load is transmitted at a high speed via a thin layer of fluid lubricant between two articulating surfaces; under this mode, the friction coefficient of native AC may reach 0.001.(15,57) In boundary lubrication, a high mechanical load is transmitted directly on the surface of AC at a low speed.(15,58) In native AC, the measured friction coefficient at boundary lubrication may be between 0.01-0.12.(15,59) Tribology properties are usually measured with shear-tests and tribometers by sliding a probe with a smooth spherical tip across the tissue surface.(59) Tribology properties are sparsely investigated in TEAC mechanical stimulation studies, but they are salient in maintaining healthy and functional ECM.

Integration and durability

Toward clinical translation, integration and durability are salient properties in TEAC and are crucial design criteria for functionality and success in translation to the clinic. Unfortunately, only a few mechanical stimulation studies on TEAC have assessed construct durability and integration *in vivo* or *in vitro*. Instead, studies have typically been focused on immobilization to show the effects of how durability decreases in the absence of mechanical stimuli.(60–63) In preclinical studies with animal models, the FDA recommends "a minimum of one year in length to provide an adequate period for completion of healing, allowing assessment of durability of the therapeutic response, and of the integrity of the product. For clinical studies, the FDA recommends "a minimum of two-year follow up clinical information" for phase 2 and "a minimum of five years follow up" in phase 3.(9) These guidelines demonstrate the necessity for further investigation on the durability properties of TEAC cultured under mechanical stimulation. Routine mechanical stimulation is important for AC maintenance, but how mechanical

stimulation during culture affects implant durability and integration remains an area that lacks sufficient data.(9)

TYPES OF MECHANICAL STIMULATION AND THEIR EFFECTS ON TISSUE-ENGINEERED ARTICULAR CARTILAGE DESIGN CRITERIA

<u>Direct compression</u>

DC is the most abundantly investigated mechanical stimulation strategy in TEAC. DC is applied by directly loading the surface of an AC construct (Figure 2a). Studies show that both passive and dynamic DC at less than 10% strain is beneficial for mechanical and biochemical properties.(6,64–66) Similarly, studies using stress as a measurement of load show that properties benefit only up to a peak stress.(67,68) For example, it was found that in a self-assembling culture system, TEAC properties were improved only between 3.3kPa and 5kPa of stress.(68) Stress, and correspondingly deformation, is a critical parameter of DC stimulation for obtaining beneficial responses in TEAC.

DC bioreactors: Bioreactors used to apply passive DC are simple in design; Weights coated with agarose, are placed on top of AC constructs.(67,68) These weights produce low compressive stresses, with corresponding strains under 10%. The weights rest on top of constructs during culture and are removed during media change. The duration of loading and the magnitude of stress are determined based on cell-type and scaffold material properties.

Bioreactors used for dynamic DC stimulation use pistons or springs to load and unload the platen cyclically on the constructs. Dynamic DC alleviates the diffusion limitations of waste and nutrients that are experienced in passive DC and static culture. This mass transport is produced by pressure gradients within the matrix in addition to the physical mixing of the surrounding media.(11,69) Commercial bioreactors allow for exchanging media through a

reservoir and may also allow the investigator to assess mechanical properties throughout culture.(70) Alternatively, dynamic DC bioreactors have been developed in-house, and have achieved frequency ranges between 0.01-10Hz and displacements of 0.1-15mm.(71,72) The decision to use either a commercial or in-house dynamic DC bioreactor is made by considering study needs.

TABLE 1: DIRECT COMPRESSION

Reference	Cell + Scaffold Type	Loading Parameters	Waveform	Bioactive Factors (Y/N)	Enhanced Design Criteria
Nebelung et al. (11)	Human chondrocytes + col I hydrogel	10% strain 0.3Hz 28 days	Dynamic Continuous	N	5.9-fold increase in col II
Kisiday et al. (10)	Juvenile bovine chondrocytes + peptide hydrogel	2.5% strain 1Hz 39 days	Dynamic Continuous	N	18% increase in H_A 53% increase in sGAG 20% increase in cell viability
El-Ayoubi et al. (6)	Canine chondrocytes +	10% strain 1 Hz	Dynamic Continuou	N	"cell number was significantly higher in stimulated groups"

	PLLA scaffold	14 days	s		
Mauck et al. (7)	Juvenile bovine chondrocytes + agarose	10% strain 1Hz 5 days	Dynamic Intermittent	Y	• 90% increase in H_A • 105% increase in col II • 35% increase in GAG
Mauck et al. (17)	Juvenile bovine chondrocytes + agarose hydrogel	10% strain 1Hz 28 days	Dynamic Intermittent	N	• 6-fold increase in H_A • 60% increase in sGAG
Elder et al. (13)	Juvenile bovine chondrocytes + scaffold-free	0.5kPa 4 days	Passive Continuous	N	• 40% increase in E_Y • 52% increase in total col
Huwe et al. (14)	Bovine costal chondrocytes + scaffold-free	5kPa 4 days	Passive Continuous	Y	• 39% increase in E_r • 1.62-fold increase in E_Y • 61% increase in total col
MacBarb et al. (63)	Juvenile ovine chondrocytes and meniscus cells +	10g 4 days	Passive Continuous	N	• 96% increase in E_r • 1.5-fold increase in E_i • 2.5-fold increase in

	scaffold-free				E_y
					● 2.7-fold increase in UTS
					● 27% increase in total col
					● 67% increase in GAG

Table of research articles on direct compression stimulation on AC constructs. The quantitative results reported in the column labeled "enhanced design criteria" were either taken directly from the referenced article, or calculated from their reported data. Quotations directly from the referenced article were used when quantitative data were not available. Abbreviations: Aggregate (H_A), Instantaneous (E_i), Relaxation (E_r), Young's (E_y) moduli; Ultimate Tensile Strength (UTS); Collagen (col); Glycosaminoglycans (GAG).

DC improvements of TEAC compressive moduli: Dynamic DC loading has typically been applied at 1Hz (14,64,72) because it is similar to the pace of human gait, although it remains to be seen if other frequencies can also be efficacious in engineering cartilage. In particular, at 1Hz of 20% strain for 21 days and 28 days yielded three-fold and six-fold increases in aggregate modulus, respectively.(72) These studies demonstrate that adding dynamic DC stimulation to culture regimes improves compressive moduli in TEAC.

Passive DC has also improved compressive moduli in self-assembled AC constructs. The instantaneous and relaxation moduli of passively compressed, self-assembled cartilage constructs under 5kPa of stress were increased significantly to about 700kPa and 275kPa

respectfully.(67) Stress magnitude studies of compressive loading on self-assembling costal chondrocytes showed that compressive properties improve only up to a peak load of 5kPa.(68) Passive loads at higher stresses were found to yield insignificant and even detrimental results in H_A and E_r, demonstrating the importance of identifying a range of beneficial loading parameters.(68)

DC increases of TEAC collagen and GAG content: A compressive stress of 0.5kPa significantly increased collagen content in self-assembling AC to 1.5-fold of free-swelling controls.(67) A separate study found that collagen content was enhanced by 61% when AC derived from costal chondrocytes was cultured with a combination of passive DC at 5kPa and bioactive stimuli.(68) This study showed that collagen content trended lower in constructs stimulated at higher loads, suggesting that an excess of compressive loads may indeed lead to degeneration of salient ECM proteins (Figure 3). Fibrocartilage derived from meniscus and articular chondrocyte cocultures also yielded a 27% increase in collagen content when stimulated passively with a 0.1N DC load.(73) Although collagen II content specifically needs to be investigated more thoroughly, these studies show that DC is a potent regimen for increasing total collagen content.

Dynamic DC has also been shown to increase GAG content by 60% in chondrocyte-seeded agarose gels.(14,72) When combined with bioactive factor IGF-1, dynamic DC stimulation on these AC constructs yielded GAG content at 50% that of native AC.(72) Additionally, chondrocytes in monolayer stimulated with 20% compressive strain at 2Hz exhibited an estimated 45% upregulation of GAG production.(37) These studies along with others shown in Table 1, confirm the benefits that DC stimulation has on GAG content in AC constructs.(8,11)

FIGURE 2
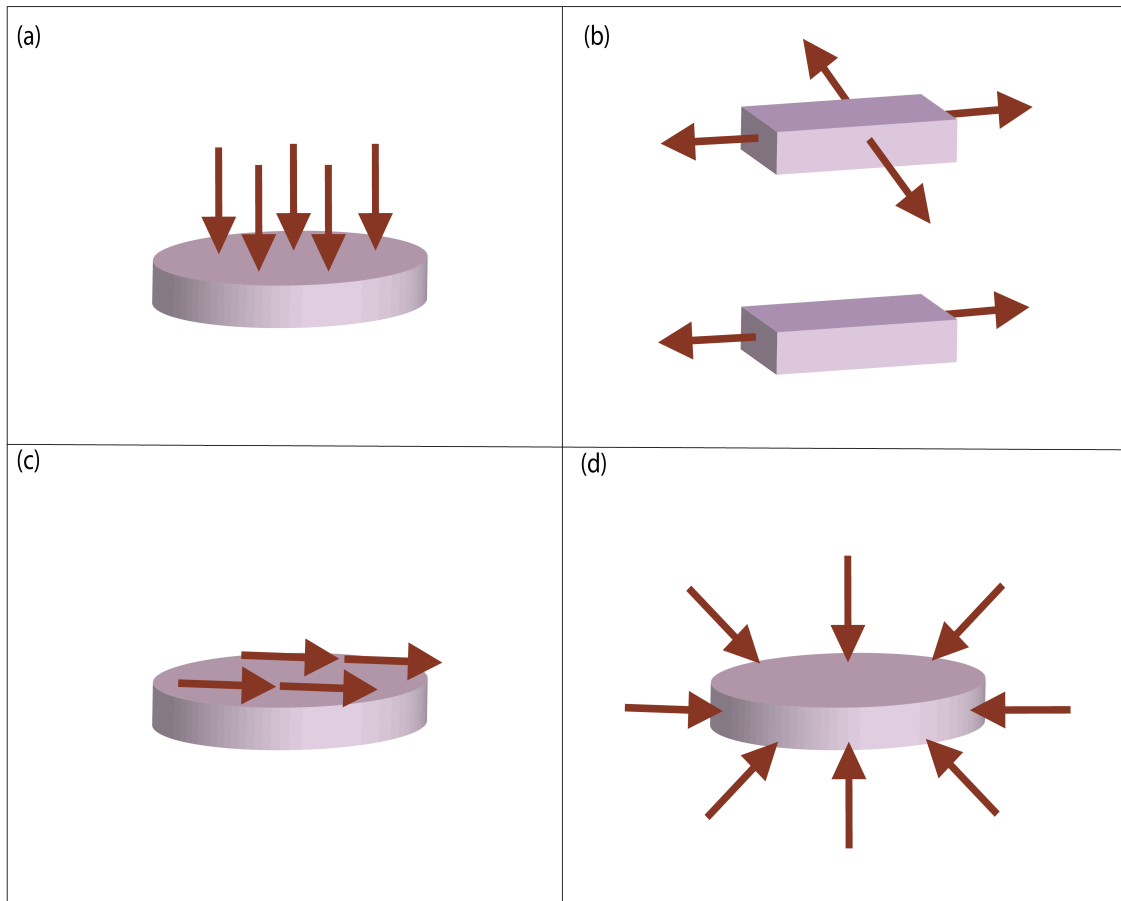
Figure 2 – Arrows indicate the direction of mechanical loads acting on tissue-engineered articular cartilage during mechanical stimulation. **a)** direct compression, **b)** biaxial tension (top), uniaxial tension (bottom), **c)** shear, and **d)** hydrostatic pressure

Shear

AC experiences shear stresses during normal physiological movement and loading.(11) Shear stress is thought to be detrimental to native AC because it causes wear, tear, and degradation over time. However, *in vitro*, at low frequencies (<1Hz) and magnitudes of stress (<0.5Pa), shear stimulation is suggested to yield enhanced AC construct properties.(74–76) Shear stress is applied along the horizontal plane of the tissue (Figure 2c), causing ECM and chondrocytes to slide upon each other in an antiparallel manner. Shear stress is applied by flowing fluid across TEAC, or as direct shear by sliding a solid sphere or platen along the surface of the AC

construct. A common loading pattern of shear stress used in both fluid and direct shear bioreactors is oscillatory shear stress because of its similarities to physiological joint movement.(77–79) Although up-regulation in ECM proteins, such as collagen II, has been found with shear stimulation, it is still unclear whether it is caused by shear forces exerted on the constructs or by increased nutrient perfusion.(80,81) There have been no studies to uncouple the response to shear stimulation and perfusion. Further study is needed to determine the cause of positive responses in TEAC cultured under shear stress, but multiple studies have shown that it is an effective tactic for the enhancement of mechanical properties (Table 2) and 40-140% increases in collagen II content.(74–76,81)

Shear bioreactors: Fluid-induced shear stimulation requires fluid flow across the surface of TEAC. Many of the bioreactors used for fluid-induced shear stimulation are known as perfusion bioreactors because, in many configurations, medium moves through the pores of the tissue as well. Mechanically stirred bioreactors include spinner-flasks, which produce a high-shear and turbulent environment.(11) Positive outcomes include improved ECM retention, but the high-shear environment results in increased levels of apoptosis and cell lysis.(11,82) In contrast, low-shear bioreactors employ rotating-walls or parallel plates. The mechanical force applied in low-shear bioreactors is usually below 0.5Pa and conducive to increased ECM content and chondrogenic phenotypes without being harmful to cells.(11)

To ensure sustained contact for shear application, direct-shear bioreactors typically compress constructs while applying shear stress to mimic the compressive rolling action of articulating joints.(83) Thus, TEAC in direct-shear bioreactors often experience 2-10% compressive strain and 0.1-1Pa shear stress.(66,77,78,83,84) However, direct-shear has shown conflicting results, ranging from no significant differences in ECM content, to a 35% increase in GAG content and 40% increase in collagen II content.(66,85,86)

TABLE 2: SHEAR

Reference	Cell + Scaffold Type	Loading Parameters	Waveform	Bioactive Factors (Y/N)	Enhanced Design Criteria
Freyria et al. (26)	Juvenile bovine chondrocytes + col I sponge	30RPM 30 days	Fluid Oscillatory	N	• 2-fold increase in cell proliferation
Pei et al. (99)	Caprine bone marrow MSCs + β-TCP scaffold	300RPM 14 days	Fluid Continuous	N	• "significant increase in col 2"
Gemmiti et al. (20)	Juvenile bovine chondrocytes + scaffold-free	0.1Pa 7 days	Fluid Continuous	N	• 79% increase in E_Y • 86% increase in UTS • 100% increase in col II
Gemmiti et al. (19)	Juvenile bovine chondrocytes + scaffold-free	0.15Pa 3 days	Fluid Continuous	N	• 2.5-fold increase in E_Y • 42% increase in

					UTS ● 1.4-fold increase in col II
Waldman et al. (31)	Juvenile bovine chondrocytes + porous calcium phosphate	2% strain 1Hz 7days	Direct Oscillatory	N	● 40% increase in col II ● 35% increase in GAG
Grad et al. (46)	Juvenile bovine chondrocytes + polyurethane scaffold	15% strain 1Hz 21 days	Direct Oscillatory	N	● 37% decrease in friction coefficient ● "More pronounced staining for col 2"

Table of research articles studying shear stress stimulation on AC constructs. The quantitative increases reported in the column labeled "enhanced design criteria" refer to comparisons between non-stimulated controls with no bioactive factors and stimulated controls. The results were either taken directly from the referenced article, or calculated from their reported data. Quotations directly from the referenced article were used when quantitative data was not available. Abbreviations: Aggregate (H_A), Instantaneous (E_i), Relaxation (E_r), Young's (E_y) moduli; Ultimate tensile Strength (UTS) ; Collagen (col); Glycosaminoglycans (GAG)

Shear stress improvements of TEAC tensile properties: Fluid-induced shear stress has yielded increases in tensile properties of scaffold-free TEAC. A parallel plate bioreactor was used to induce a shear stress of 0.15Pa on TEAC. The E_Y of the stimulated tissue increased to 2.28MPa compared to the 1.55MPa of statically cultured controls.[74] A second study employing the same methods tested shear stimulation at 0.1Pa and showed E_Y and UTS improve to 5MPa and 1.3MPa respectively.[75] These studies show that shear is an effective tactic for increasing tensile properties and that the benefits may be optimized within a narrow range of stress.

Shear stress increases of TEAC collagen content: Enhancement in collagen deposition may be attained with shear stimulation.[74,75,86] Using a solid sphere, at 2% strain, shear elicited a 40% increase in collagen II content compared to non-stimulated controls. Conversely, groups stimulated at 6% and 12% shear strain exhibited deleterious effects on collagen II content.[86] Studies investigating the effects of fluid-induced shear also found that 0.1Pa yielded the highest percentage of collagen II (7.5%) compared to nonstimulated controls (3.7%).[75] These studies show that collagen II content increases significantly in AC constructs when cultured under low magnitudes of shear.

Direct shear improvements of TEAC tribology: The application of direct shear on chondrocyte-seeded polyurethane scaffolds yielded a significant decrease in the boundary lubrication friction coefficient from 0.681 to 0.427.[76] Certain bioactive factors, such as interleukin-1β (IL-1β), TGF-β1, and oncostatin M (OSM) have also been found to alter the frictional properties of AC constructs, but they have not been tested in combination with mechanical stimulation.[87] It was also found that TEAC that underwent shear forces in two directions had an even lower friction coefficient (0.251) than those loaded in only one direction.[76] This was shown to validate that gliding motions on the articulating surface of TEAC during culture significantly decreases friction coefficients.[88]

Shear stress-aided integration: Although there have been few studies on the effect of mechanical stimulation on integration, there is some evidence that suggests the use of fluid shear bioreactors, such as spinner-flasks, promotes integration of TEAC with native AC.(89,90) It has been shown that shear-stimulated TEAC was better integrated with surrounding tissues in an *in vivo* model than TEAC that was cultured statically. It was also found that collagen matrix organization was better in the shear-stimulated groups.(90) A separate study used a spinner flask to enhance integration in an *in vitro* model. This study created defects in native AC explants, press-fitted them with TEAC, and cultured the pair in a spinner-flask set to 90RPM, showing better integration with the surrounding native AC tissue.(89) Although the mechanisms behind the results of these studies are unclear, the potential for using mechanical stimulation, such as continuous passive motion (CPM), early on in post-operative physical therapies to promote integration has been elucidated.(89) To investigate further, mechanical stimulation studies that include *in vivo* phases may consider the use of CPM to enhance integration and functionality of the implant.

FIGURE 3
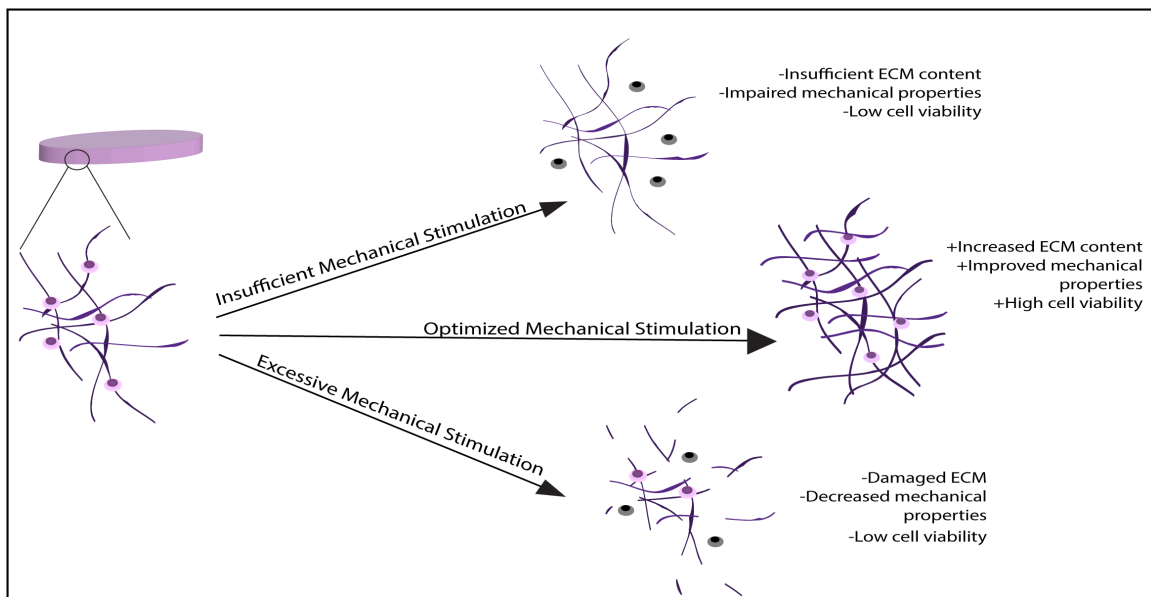
Figure 3 – The importance of optimizing mechanical stimulation parameters: Insufficient mechanical stimulation results in low levels of signaling and nutrient diffusion causing low cell viability, ECM content, and mechanical properties. Excessive mechanical stimulation impairs mechanotransduction pathways by physically damaging ECM and sending chondrocytes to apoptosis, which leads to low mechanical properties. Optimized mechanical sitmulation yields high cell viability, robust ECM, and improved mechanical properties by delivering nutrients and signaling cells to produce robust ECM components. Abbreviations: (ECM) extracellular matrix.

Hydrostatic pressure

Under HP, tissues and cells experience uniform and normal compression on all surfaces (Figure 2d). HP has been a popular form of mechanical stimulation in the field for over 15 years because it is experienced by native AC in every aspect of joint movement.(18) Native AC encounters HP when negatively charged proteoglycans trap fluid within the cartilage matrix during joint loading.(18) Physiologically, AC typically experiences 3-10MPa of HP.(91,92) Because HP does not shear or deform the essentially incompressible tissues, damage to the ECM is minimized during *in vitro* stimulation.(11)

HP bioreactors: HP bioreactors have a fluid-filled chamber and a piston that applies pressure to the chamber and subsequently the tissue.(93–96) Research has focused on stimulating TEAC with HP at magnitudes ranging from 3-18MPa, and in general should not exceed 30MPa because it alters chondrocyte proteoglycan synthesis.(91,93,97) Both passive and dynamic (up to 1Hz) HP have been investigated, yielding improved mechanical properties, ECM protein expression, and ECM content.(91,92,98,99) As an example, dynamic HP stimulation (0.5MPa at 0.5Hz) is used commercially to enhance sGAG production in constructs.(100,101) These applications suggest that HP can be a necessary accessory toward increasing matrix synthesis in TEAC.

TABLE 3: HYDROSTATIC PRESSURE

Reference	Cell + Scaffold Type	Loading Parameters	Waveform	Bioactive Factors (Y/N)	Enhanced Design Criteria
Kraft et al. (77)	Porcine chondrocytes + scaffold-free	5MPa 0.1Hz 21 days	Dynamic Intermittent	N	• 12% increase in total col • 64% increase in GAG
Correia et al. (16)	Human adipose SCs + gellan gum hydrogels	5MPa 0.5Hz 28 days	Dynamic Intermittent	N	• 57% increase in GAG
Elder et al. (53)	Juvenile bovine chondrocytes + scaffold-free	10MPa 4 days	Passive Intermittent	Y	• 1.6-fold increase in H_A • 2.3-fold increase in E_Y • 1.7-fold increase in total col • 84% increase in GAG
Gunja et al. (41)	Mature leporine meniscus cells	10MPa	Passive Intermitten	Y	• 100% increase in E_i

	+ PLLA scaffold	28 days	t		• 100% increase in E_r • 2.75-fold increase in total col
Chen et al. (38)	Porcine chondrocytes + PGA scaffold	5MPa 56 days	Passive Intermittent	N	• 5 fold increase in E_Y
Gunja et al. (37)	Mature leporine meniscus cells + PLLA scaffold	10MPa 28 days	Passive Intermittent	N	• 60% increase in Ei • 100% increase in E_r • 2-fold increase in total col • 2-fold increase in GAG
Heyland et al. (36)	Porcine chondrocytes + alginate beads	0.3MPa 7 days	Passive Intermittent	N	• "65% increase in col2/col1 ratio"
Elder et al.[34]	Juvenile bovine chondrocytes + scaffold-free	10MPa 4 days	Passive Continuous	N	• 1.6-fold increase in H_A • 63% increase in E_Y

Table of research articles on hydrostatic pressure stimulation on AC constructs. The quantitative increases reported in the column labeled "enhanced design criteria" refer to comparisons between non-stimulated controls with no bioactive factors and stimulated controls. The results were either taken directly from the referenced article, or calculated from their reported data. Quotations directly from the referenced article were used when quantitative data were not available. Abbreviations: Aggregate (H_A), Instantaneous (E_i), Relaxation (E_r), Young's (E_y) moduli; Ultimate Tensile Strength (UTS); Collagen (col); Glycosaminoglycans (GAG).

HP enhancements of TEAC compressive moduli: A few studies have found that passive HP culturing regimes result in an enhancement of compressive moduli in self-assembling cartilage tissues. For example, H_A peaked at 238kPa in self-assembling cartilage constructs stimulated at stresses under 10MPa for 1hr a day for 14 days. HP stimulation for longer than 14 days was deleterious to compressive moduli.(102) The combination of TGF-β1 and passive HP of 10MPa increased the H_A by nearly two-fold when compared to either stimulus alone.(103) Although the effects of HP stimulation on TEAC mechanical properties have not been heavily investigated, these studies suggest that short-term HP is a potent stimulus for enhancing compressive moduli.

HP increases of TEAC (s)GAG content: A 1.3-fold increase in sGAG was found in AC constructs derived from deep zone chondrocytes when exposed to HP compared to static controls.(49) Self-aggregating suspension cultures stimulated with passive HP yielded a significant increase of 64% more GAG per chondrocyte.(104) When stimulated between 7-10MPa, GAG content was significantly increased in tissues derived from juvenile chondrocytes.(49,98,103) These studies, along with others shown in Table 3, show that HP stimulation enhances GAG content in TEAC.

Tension

Tensile forces are applied on engineered tissues by directly pulling the tissue outward along the edges (Figure 2b) resulting in axial strain. Tension may be delivered to TEAC in a uniaxial or biaxial manner (Figure 2b). Very few studies have explored the effects of tensile stimulation on TEAC. However, the potential for developing robust AC constructs by using passive uniaxial tension to stimulate mechanosensitive TRPV 4 ion channels has been elucidated and has yielded TEAC at 90% native AC tensile properties and collagen content.(105)

Tension bioreactors: In the most common uniaxial tension bioreactor, the tissue is draped over hooks, or clamped, along the opposing edges and pulled away.(106) Biaxial tension bioreactors stimulate mechanically by employing equidistant rakes attached along all edges of the tissue that move apart and remain equidistant during loading to attain uniform deformation across the tissue.(107,108) Both uniaxial and biaxial tension are applied passively or dynamically usually within 2-15% strain, but the most promising outcomes thus far have followed passive uniaxial tension in combination with bioactive factors such as TGF- β 1.(105)

TABLE 4: TENSION

Reference	Cell + Scaffold Type	Loading Parameters	Waveform	Bioactive Factors (Y/N)	Enhanced Design Criteria
Vanderploeg et al. (64)	Juvenile bovine chondrocytes + fibrin gel	10% strain 1Hz 2 days	Uniaxial Dynamic Continuous	N	● "further increased DNA content ….and cell viability"

Vanderploeg et al. (75)	Juvenile bovine chondrocytes + fibrin hydrogel	5% strain 1Hz 3 days	Uniaxial Dynamic Intermittent	N	• 12.3% increase in total col • 12.9% increase in sGAG
Connelly et al. (65)	Juvenile bovine BMSCs + Fibrin gel	10% strain 1Hz 14 days	Uniaxial Dynamic Intermittent	N	• 27% increase in total col • 12.5% increase in sGAG
Lee et al. (42)	Human chondrocytes + scaffold-free	4-15% strain 5 days	Uniaxial Passive Continuous	Y	• 3-fold increase in H_A • 4-fold increase in E_Y • 4.3-fold increase in UTS
Fan et al. (55)	Juvenile bovine chondrocytes + scaffold-free	16%strain 28 days	Biaxial Passive Intermittent	N	• 1.2-fold increase in total col

Table of research articles on tensile stimulation on AC constructs. The quantitative increases reported in the column labeled "enhanced design criteria" refer to comparisons between non-stimulated controls with no bioactive factors and stimulated controls. The results were either taken directly from the referenced article, or calculated from their reported data. Quotations directly from the referenced article were used when quantitative data were not available. Abbreviations: Aggregate (H_A), Instantaneous (E_i), Relaxation (E_r), Young's (E_y) moduli; Ultimate Tensile Strength (UTS); Collagen (col); Glycosaminoglycans (GAG).

Passive uniaxial tension enhancements of TEAC tensile properties: One recent study produced tensile stiffness reaching 94% and 60% of native AC E_Y and UTS with application of continuous passive tension stimulation. The constructs were strained to 12-15% on the first day of stimulation and an additional 4-5% per day for 5 days.(105) In this study, a bioactive regimen of TGF-β1, C-ABC, and LOXL2 was combined with passive tensile stimulation on self-assembling AC constructs derived from human chondrocytes.(105) When compared to non-stimulated controls, the addition of passive tensile stimulation and bioactive stimuli elicited a six-fold increase in both E_Y and UTS. Uniaxial tension is seldom investigated for enhancing mechanical properties in TEAC, but the results presented here suggest it is a potent regimen for improving tensile properties.

Tension increases of TEAC GAG content: Uniaxial tensile loading has been found to enhance GAG content in self-assembling AC constructs by an estimated 33%.(105) The effect of tension stimulation has also been investigated on AC constructs derived from chondrocytes of the deep zone, middle zone, and superficial zone of bovine AC. In particular, superficial zone chondrocytes are significantly more responsive to tensile loading, leading to a 20.6% increase in sGAG production.(48) Although studies in tensile stimulation are limited, current research shows encouraging results toward increased GAG production.

Uniaxial tension-aided organization of TEAC ECM: Uniaxial tension develops surface anisotropy that is similar to that of native AC.(105) Fiber organization in TEAC is not improved upon the addition of bioactive factors alone. However, when used together, uniaxial tension and C-ABC lead to a dramatic change in anisotropy.(105) Fiber organization is achieved because the catabolic enzyme chondroitinase-ABC cleaves and removes excess GAGs while uniaxial tension provides physical reorganization of the ECM.(105)

PERSPECTIVES

The role of mechanical stimulation has been experimentally confirmed *in vitro* as a way to enhance design criteria in TEAC. It has been shown that TEAC properties benefit from a narrow range of loading magnitudes and durations in DC and HP stimulation because both excessive and insufficient loading can lead to deleterious consequences. For example, compressive moduli increase with the application of either DC or HP, and they both show that excessive stress (>10MPa) and strain (>20%) can be detrimental (Figure 3). Although dynamic DC is beneficial for long durations, studies in HP have shown short-term passive stimulation to work best for improving compressive moduli. This suggests that different types of mechanical stimulation may be applied in tandem to further improve multiple design criteria. The different mechanotransduction mechanisms through which DC and HP affect the engineered tissue should be elucidated to clarify this difference in optimal loading regimens.

TEAC research in tension and shear stimulation is not as extensive as in DC and HP. This may be due to the association of shear and tensile loads to cartilage damage *in vivo*. However, shear stimulation has produced up to a 257% increase in E_Y, and tension stimulation has produced AC with nearly biomimetic E_Y and UTS. Furthermore, both shear stress and tension have led to enhancements in TEAC properties, such as fiber organization and integration, which have been elusive under static cultures or DC and HP. Beneficial loading

parameters for tension and shear stimulation should be further investigated and expanded upon by assessing all design criteria.

There is also a stark unevenness in the amount of research and literature amongst TEAC design criteria. For example, attaining biomimetic tensile properties in TEAC has proven to be a challenging feat, yet the effects of mechanical stimulation on tensile properties have been scarcely investigated. On the other hand, an extensive number of studies show that TEAC cultured with DC, tension, and HP stimulation yield increases in GAG composition. Research on GAG composition in TEAC is quite extensive: for example, a comparison of HP and tension stimulation studies suggests that GAG production is partially regulated by tensile stimulation in superficial zone chondrocytes and by HP in deep zone chondrocytes. To engineer AC to translatability, salient design criteria (e.g compressive and tensile properties, ECM content, cellular viability, ECM organization, tribology, integration, durability) in must be investigated fully in mechanical stimulation studies.

To identify ranges of beneficial loading for each type of mechanical stimulation technique, investigators must adequately report loading parameters and TEAC characteristics. Adequately reporting loading parameters includes specifying the mechanical loads in units that normalize to the characteristics of the TEAC scaffold or matrix. For example, when reporting deformation, units of strain should be used instead of length. Although frequency, magnitude, and duration of load are commonly described, specific waveforms are currently not reported. Furthermore, not all mechanical stimulation studies report construct characteristics fully. In particular, mechanical and tribology properties should be reported, collagen fibril dimensions, organization, and specific type should be included with total content, and *in vivo* durability must be assessed whenever possible. Thus, this information must be included in all studies where mechanical stimulation is investigated to avoid reaching incomplete conclusions.

Mechanical stimulation has proven itself a powerful addition to AC engineering procedures. Static cultures are inadequate in AC engineering because the lack of inherent vascularization and mechanical loading leads to limited nutrient and waste transport. The studies shown here confirm that, when compared to static AC tissue cultures, mechanical stimulation is a valuable promoter of ECM synthesis and concomitant mechanical property enhancement. Furthermore, the addition of mechanical stimulation has also yielded characteristics, such as matrix organization, that were not previously attainable with bioactive factors alone. Combinations of bioactive factors and mechanical stimulation have led to the most mechanically robust and biomimetic AC constructs to date. From the physical pressure gradients that lead to mass nutrient transport in dynamic DC and shear, to the tension-driven activation of TRPV 4 ion channels, mechanical stimulation strategies drive the increase of important ECM components and enhance mechanical properties. Toward expanding translatability, the vast potential of mechanical stimulation needs to be explored to aid integration of TEAC within the diarthrodial joint. The routine inclusion of mechanical stimulation in culture regimes may lead to additive and synergistic enhancements in design criteria necessary for the successful tissue-engineering of AC.

REFERENCES

1.   Afoke N., Byers P., Hutton W. Contact pressures in the human hip joint. J Bone Jt. Surg Br. **69**, 536, 1984;

2.   Eisenhart R., Adam C., Steinlechner M., Eckstein F. Quantitative determination of joint incongruity and pressure distribution during simulated gait and cartilage thickness in the human hip joint. J. Orthop. Res. **17**, 532, 1999;

3.   Kalichman L., Li L., Kim D., Guermazi A., Donnell C., Hoffmann U., et al. Facet joint osteoarthritis and low back pain in the community-based population. Spine (Phila. Pa. 1976). **33**, 2560, 2011;

4.   Makris E., Gomoll A., Malizos K., Hu J., Athanasiou K. Repair and tissue engineering techniques for articular cartilage. Nat. Rev. Rheumatol. Nature Publishing Group; **11**, 21, 2014;

5.   Li K., Zhang C., Qiu L., Gao L., Zhang X. Advances in application of mechanical stimuli in bioreactors for cartilage tissue engineering. Tissue Eng. Part B. **23**, 399, 2017;

6.   El-Ayoubi R., DeGrandpre C., DiRaddo R., Yousefi A. Design and dynamic culture of 3D-scaffolds for cartilage tissue engineering. J. Biomater. Appl. **25**, 429, 2011;

7.   Mauck R., Nicoll S., Seyhan S., Ateshian G., Hung C. Synergistic action of growth factors and dynamic loading for articular cartilage tissue engineering. Tissue Eng. **9**, 597, 2003;

8.   Natenstedt J., Kok A., Dankelman J., Tuijthof G. What quantitative mechanical loading stimulates in vitro cultivation best? J. Exp. Orhtopaedics. Journal of Experimental Orthopaedics; **2**, 1, 2015;

9.   FDA. Guidance for industry: preparation of IDEs and INDs for products intended to repair or replace knee cartilage. 2011.

10.   Grad S., Eglin D., Alini M., Stoddart M. Physical stimulation of chondrogenic cells In vitro: a review. Clin. Orthop. Relat. Res. **469**, 2764, 2011;

11.   Darling E., Athanasiou K. Articular cartilage bioreactors and bioprocesses. Tissue Eng. **9**, 9, 2003;

12.   Williamson A., Chen A., Sah R. Compressive properties and function-composition relationships of developing bovine articular cartilage. J. Orthop. Res. **19**, 1113, 2001;

13.   Park S., Hung C., Ateshian G. Mechanical response of bovine articular cartilage under dynamic unconfined compression loading at physiological stress levels. Osteoarthr. Cartil. **12**, 65, 2004;

14.   Athanasiou K., Responte D., Brown W., Hu J. Harnessing biomechanics to develop cartilage regeneration strategies. J Biomech Eng. **137**, 1, 2015;

15.   Athanasiou K., Darling E., Hu J., Durain G., Reddi H. Articular Cartilage. 2017.

16.   Athanasiou K., Agarwal A., Dzida F. Comparative study of the intrinsic mechanical properties of the human acetabular and femoral head cartilage. J Orthop Res. **12**, 340, 1994;

17.   Desrochers J., Amrein M., Matyas J. Viscoelasticity of the articular cartilage surface in early osteoarthritis. Osteoarthr. Cartil. Elsevier Ltd; **20**, 413, 2012;

18.   Narmoneva D., Wang J., Setton L. Nonuniform swelling-induced residual strains in articular cartilage. J. Biomech. **32**, 401, 1999;

19.   Fan J., Waldman S. The effect of intermittent static biaxial tensile strains on tissue engineered cartilage. Ann. Biomed. Eng. **38**, 1672, 2010;

20.   Wortman J., Evans R. Young's modulus, shear modulus, and poisson's ratio in silicon and germanium. J. Appl. Phys. **36**, 153, 1965;

21.   Mansour J. Biomechanics of Cartilage. Biomech. Princ. p. 66–79.

22.   Williamson A., Chen A., Masuda K., Sah R. Tensile mechanical properties of bovine articular cartilage: Variations with growth and relationships to collagen network components. J. Orhtopaedic Res. **21**, 872, 2003;

23.   Eyre D. Collagen of articular cartilage. Arthritis Res. **4**, 30, 2001;

24.   Nieminen J. Effect of functional loading on remodelling in canine, and normal and collagen type II transgenic murine bone. 2009.

25.   Gelse K., Po E., Aigner T. Collagens — structure, function, and biosynthesis. Adv. Drug Deliv. Rev. **55**, 1531, 2003;

26.   Viguet-carrin S., Garnero P., Delmas P. The role of collagen in bone strength. Osteoporos. Int. **17**, 319, 2006;

27.   Cissell D., Link J., Hu J., Athanasiou K. A modified hydroxyproline assay based on hydrochloric acid in ehrlich's solution accurately measures tissue. Tissue Eng Part C. **23**, 243, 2017;

28.   Roberts S., Menage J., Sandell L., Evans E., Richardson J. Immunohistochemical study of collagen types I and II and procollagen IIA in human cartilage repair tissue following autologous chondrocyte implantation. Knee. **5**, 398, 2009;

29.   Eyre D., Weis M., Wu J. Advances in collagen cross-link analysis. Methods. **45**, 65, 2008;

30.   Buckwalter J., Mankin H. Articular cartilage: tissue design and chondrocyte-matrix interactions. Instr. Course Lect. **47**, 477—486, 1998;

31.   Bayliss M., Osborne D., Woodhouse S., Davidson C. Sulfation of chondroitin sulfate in human articular cartilage: The effect of age, topographical position, and zone of cartilage on tissue composition. J Bio Chem. **274**, 15892, 1999;

32.	Kuiper N., Sharma A. A detailed quantitative outcome measure of glycosaminoglycans in human articular cartilage for cell therapy and tissue engineering strategies. Osteoarthr. Cartil. **23**, 2233, 2015;

33.	Hascall V., Sajdera S. Physical Properties and Polydispersity of Proteoglycan from Bovine Nasal Cartilage. J. Biol. Chem. **245**, 4920, 1970;

34.	Siebelt M., Groen H., Koelewijn S., Blois E., Sandker M., Waarsing J., et al. Increased physical activity severely induces osteoarthritic changes in knee joints with papain induced sulfate-glycosaminoglycan depleted cartilage. Arthritis Res. Ther. **16**, 1, 2014;

35.	Farndale R., Buttle D., Barrett A. Improved quantitation and discrimination of sulphated glycosaminoglycans by use of dimethylmethylene blue. Biochem Biophys Acta. **2**, 173, 1986;

36.	Calabro A., Midura R., Wang A., West L., Plaas A., Hascall V. Fluorophore-assisted carbohydrate electrophoresis (FACE) of glycosaminoglycans. Osteoarthr. Cartil. **9**, 16, 2001;

37.	Lin W., Chang Y., Wang H., Yang T., Chiu T., Huang S., et al. The study of the frequency effect of dynamic compressive loading on primary articular chondrocyte functions using a microcell culture system. Biomed. Res. Int. **2014**, 1, 2014;

38.	Van Susante L., Pieper J., Buma P., Van Kuppevelt T., Van Beuningen H., Van Der Kraan P., et al. Linkage of chondroitin-sulfate to type I collagen scaffolds stimulates the bioactivity of seeded chondrocytes in vitro. Biomaterials. **22**, 2359, 2001;

39.	Sophia Fox A., Bedi A., Rodeo S. The basic science of articular cartilage: structure, composition, and function. Sports Health. **1**, 461, 2009;

40. Silverberg J., Barrett A., Das M., Petersen P., Bonassar L., Cohen I. Structure-function relations and rigidity percolation in the shear properties of articular cartilage. Biophys. J. **7**, 2014;

41. Stolz M., Raiteri R. ., Daniels A., Vanlandingham M., Baschong W. Dynamic elastic modulus of porcine articular cartilage determined at two different levels of tissue organization by indentation-type atomic force microscopy. Biophys. J. Elsevier; **86**(5), 3269, 2004;

42. Fazaeli S., Ghazanfari S., Everts V., Smit T., Koolstra J. The contribution of collagen fibers to the mechanical compressive properties of the temporomandibular joint disc. Osteoarthr. Cartil. Elsevier Ltd; **24**, 1292, 2016;

43. Jurvelin J., Buschmann M., Hunziker E. Mechanical anisotropy of the human knee articular cartilage in compression. Proc. Inst. Mech. Eng. H. IMECHE; **217**, 215, 2003;

44. Julkunen P., Jurvelin J., Isaksson H. Contribution of tissue composition and structure to mechanical response of articular cartilage under different loading geometries and strain rates. Biomech Model Mechanobiol. **9**, 237, 2010;

45. Peng G., McNary S., Athanasiou K., Reddi H. Surface zone articular chondrocytes modulate the bulk and surface mechanical properties of the tissue-engineered cartilage. Tissue Eng Part A. **20**(23-24), 3332, 2045;

46. Jay G., Waller K. The biology of lubricin: near frictionless joint motion. Matrix Biol. **39**, 17, 2014;

47. Schuurman W., Klein J., Dhert W., Van Weeren P., Hutmacher D., Malda J. Cartilage regeneration using zonal chondrocyte subpopulations: a promising approach or an overcomplicated strategy? J Tissue Eng Regen Med. **9**(6), 669, 2015;

48. Vanderploeg E., Wilson C., Levenston M. Articular chondrocytes derived from distinct tissue zones differentially respond to in vitro oscillatory tensile loading. Osteoarthr. Cartil. **16**, 1228, 2012;

49. Mizuno S., Ogawa R. Using changes in hydrostatic and osmotic pressure to manipulate metabolic function in chondrocytes. Am. J. Physiol. Cell. Phyiosl. **300**, 1234, 2011;

50. Robins S., Duncan A. Cross-linking of collagen: location of pyridinoline in bovine articular cartilage at two sites of the molecule. Biochem. J. **1**, 175, 1983;

51. McNerny E., Gardinier J., Kohn D. Exercise increases pyridinoline cross-linking and counters the mechanical effects of concurrent lathyrogenic treatment. Bone. **81**, 327, 2015;

52. Below S., Arnoczky S., Dodds J., Kooima C., Walter N. The split-line pattern of the distal femur : a consideration in the orientation of autologous cartilage grafts. Arthroscopy. **18**, 613, 2002;

53. Gruber H., Wiggins W. Methods for transmission and scanning electron microscopy of bone and cartilage. In: An YH, Martin KL, editors. Handb. Histol. Methods Bone Cartil. Humana Press; p. 497–504, 2003.

54. Kienle S., Boettcher K., Wiegleb L., Urban J., Burgkart R., Lieleg O., et al. Comparison of friction and wear of articular cartilage on different length scales. J. Biomech. Biomech. Elsevier; **48**, 3052, 2015;

55. Chang D., Guilak F., Jay G., Zauscher S. Interaction of lubricin with type II collagen surfaces: adsorption, friction, and normal forces. J Biomech. Elsevier; **47**, 659, 2014;

56. Setton L., Zhu W., Mow V. The biphasic poroviscoelasic behavior of articular cartilage role of the surface zone in governing the compressive behavior. J. Biomech. **26**, 581, 1993;

57. Gleghorn JP, Bonassar L. Lubrication mode analysis of articular cartilage using Stribeck surfaces. J. Biomech. **41**, 1910, 2008;

58. Atarod M., Ludwig T., Frank C., Schmidt T., Shrive N. Cartilage boundary lubrication of ovine synovial fluid following anterior cruciate ligament transection: a longitudinal study. Osteoarthr. Cartil. **23**, 640, 2015;

59. Blum M., Ovaert T. Low friction hydrogel for articular cartilage repair: evaluation of mechanical and tribological properties in comparison with natural cartilage tissue. Mater. Sci. Eng. C. Elsevier B.V.; **33**(7), 4377, 2013;

60. Responte D., Lee J., Hu J., Athanasiou K. Biomechanics-driven chondrogenesis: from embryo to adult. FASEB. **26**, 3614, 2017;

61. Roddy K., Prendergast P., Murphy P. Mechanical influences on morphogenesis of the knee joint revealed through morphological, molecular and computational analysis of immobilised embryos. PLoS One. **6**, e17526, 2011;

62. Hall B., Herring S. Paralysis and growth of the musculoskeletal system in the embryonic chick. J. Morphol. **206**, 45, 1990;

63. Nowlan N., Sharpe J., Roddy K., Prendergast P., Murphy P. Mechanobiology of embryonic skeletal development: insights from animal models. Birth Defects Res. C. Embryo Today. **90**, 203, 2010;

64. Kisiday J., Jin M., Dimicco M., Kurz B., Grodzinsky A. Effects of dynamic compressive loading on chondrocyte biosynthesis in self-assembling peptide scaffolds. J. Biomech. Biomech. **37**, 595, 2004;

65. Nebelung S., Gavenis K., Lüring C., Zhou B., Mueller-rath R., Stoffel M., et al. Simultaneous anabolic and catabolic responses of human chondrocytes seeded in collagen hydrogels to long-term continuous dynamic compression. Ann. Anat. Elsevier GmbH.; **194**, 351, 2012;

66. Shahin K., Doran P. Tissue engineering of cartilage using a mechanobioreactor exerting simultaneous mechanical shear and compression to simulate the rolling action of articular joints. Biotechnol. Bioengeering. **109**, 1060, 2012;

67. Elder B., Athanasiou K. Effects of confinement on the mechanical properties of self-assembeled articular cartilage constructs in the direction orthogonal to the confinement surface. J. Orthop. Res. Res. **26**, 238, 2008;

68. Huwe L., Sullan G., Hu JC, Athanasiou K. Using costal chondrocytes to engineer articular cartilage with applications of passive axial compression and bioactive stimuli. Tissue Eng. Part A. **00**, 1, 2017;

69. Suh J. Dynamic unconfined compression of articular cartilage under a cyclic compressive load. Biorheology. **33**(4-5), 289304, 1996;

70. Tran S., Cooley A., Elder S. Effect of a mechanical stimulation bioreactor on tissue engineered , scaffold-free cartilage. Biotechnol. Bioengeering. **108**, 1421, 2011;

71. Correia C., Pereira A., Duarte A., Frias A., Pedro A., Oliveira T. Dynamic culturing of cartilage tissue: the significance of hydrostatic pressure. Tissue Eng Part A. **18**, 1979, 2012;

72.   Mauck R., Soltz M., Wang C., Wong D., Chao P., Ateshian G. Functional tissue engineering of articular cartilage through dynamic loading of chondrocyte-seeded agarose gels. J. Biomech. Eng. **122**, 252, 2000;

73.   MacBarb R., Paschos N., Abeug R., Makris E., Hu J., Athanasiou K. Passive strain-induced matrix synthesis and organization in shape-specific, cartilaginous neotissues. Tissue Eng. Part A. **20**, 3290, 2014;

74.   Gemmiti C., Guldberg R. Fluid flow increases type II collagen deposition and tissue-engineered cartilage. Tissue Eng. **12**, 7, 2006;

75.   Gemmiti C., Guldberg R. Shear stress magnitude and duration modulates matrix composition and tensile mechanical properties in engineered cartilaginous tissue. Biotechnol. Bioengeering. **104**, 809, 2010;

76.   Grad S., Loparic M., Peter R., Stolz M., Aebi U., Alini M. Sliding motion modulates stiffness and friction coefficient at the surface of tissue engineered cartilage. Osteoarthr. Cartil. Elsevier Ltd; **20**, 288, 2012;

77.   Stoddart M., Ettinger L., Jo H., Zu C. Enhanced matrix synthesis in de novo , scaffold free cartilage-like tissue subjected to compression and shear. Biotechnol. Bioengeering. **95**, 1043, 2006;

78.   Yusoff N., Azuan N., Osman A., Pingguan-murphy B. Design and validation of a bi-axial loading bioreactor for mechanical stimulation of engineered cartilage. Med. Eng. Phys. Institute of Physics and Engineering in Medicine; **33**, 782, 2011;

79.   Sun M., Lv D., Zhang C., Zhu L. Culturing functional cartilage tissue under a novel bionic mechanical condition. Med. Hypotheses. Elsevier Ltd; **75**, 657, 2010;

80. Zhu G., Mayer-wagner S., Schröder C., Woiczinski M., Blum H., Lavagi I., et al. Comparing effects of perfusion and hydrostatic pressure on gene profiles of human chondrocyte. J. Biotechnol. Elsevier B.V.; **210**, 59, 2015;

81. Freyria A., Cortial D., Ronziere M., Guerret S., Herbage D. Influence of medium composition , static and stirred conditions on the proliferation of and matrix protein expression of bovine articular chondrocytes cultured in a 3-D collagen scaffold. Biomaterials. **25**, 687, 2004;

82. Zhao J., Griffin M., Cai J., Li S., Bulter P., Kalaskar D. Bioreactors for tissue engineering: An update. Biochem Eng J. Elsevier B.V.; **109**, 268, 2016;

83. Gharravi A., Orazizadeh M., Ansari-asl K., Banoni S. Design and fabrication of anatomical bioreactor systems containing alginate scaffolds for cartilage tissue engineering. Avicenna J. Med Biotech. **4**, 65, 2012;

84. Di Federico E., Bader D., Shelton J. Design and validation of an in vitro loading system for the combined application of cyclic compression and shear to 3D chondrocytes-seeded agarose constructs. Med. Eng. Phys. Institute of Physics and Engineering in Medicine; **36**(4), 534, 2014;

85. Bian L., Fong J., Lima E., Stoker A., Ateshian G., Cook J. Dynamic mechanical loading enhances functional properties of tissue-engineered cartilage using mature canine chondrocytes. Tissue Eng Part A. **16**, 1781, 2010;

86. Waldman S., Spiteri C., Grynpas M., Pilliar R., Kandel R. Long-term intermittent shear deformation improves the quality of cartilaginous tissue formed in vitro. J. Orthop. Res. **21**, 590, 2003;

87. Gleghorn J., Jones A., Flannery C., Bonassar L. Alteration of articular cartilage frictional properties by transforming growth factor-beta, interleukin-1Beta, and oncostatin M. Arthritis Rheum. **60**, 440, 2009;

88. Wimmer M., Alini M., Grad S. The effect of sliding velocity on chondrocytes activity in 3D scaffolds. J. Biomech. **42**, 424, 2009;

89. Theodoropoulos J., DeCroos A., Petrera M., Park S., Kandel R. Mechanical stimulation enhances integration in an in vitro model of cartilage repair. Knee Surg. Sport. Traumatol. Arthosc. **24**(6), 2055, 2016;

90. Pei Y., Fan J., Zhang X., Zhang Z., Yu M. Repairing the osteochondral defect in goat with the tissue-engineered osteochondral graft preconstructed in a double-chamber stirring bioreactor. Biomed. Res. Int. **2014**, 1, 2014;

91. Elder B., Athanasiou K. Hydrostatic pressure in articular cartilage tissue engineering: from chondrocytes to tissue regeneration. Tissue Eng. Part B. **15**, 2009;

92. Smith L., Lin J., Trindade M., Shida J., Kajiyama G. Time-dependent effects of intermittent hydrostatic pressure on articular chondrocyte type II collagen and aggrecan mRNA expression. J. Rehabil. Res. Dev. **37**, 153, 2000;

93. Smith L., Rusk S., Ellison B., Wessels P., Tsuchiya K., Carter D. In vitro stimulation of articular chondrocyte mRNA and extracellular matrix synthesis by hydrostatic pressure. J. Orthop. Res. **14**, 53, 1996;

94. Heyland J., Wiegandt K., Goepfert C., Scumacher U., Portner R. Redifferentiation of chondrocytes and cartilage formation under intermittent hydrostatic pressure. Biotechnol. Lett. **28**, 1641, 2006;

95. Gunja N., Athanasiou K. Effects of hydrostatic pressure on leporine meniscus cell-seeded PLLA scaffolds. J. Biomed. Mater. Res. A. Wiley Subscription Services, Inc., A Wiley Company; **92A**, 896, 2010;

96. Chen J., Yuan Z., Liu Y., Zheng R., Dai Y., Tao R. Improvement of in vitro three-dimensional cartilage regeneration by a novel hydrostatic pressure bioreactor. Stem Cells Transl Med. **6**, 982, 2017;

97. Parkkinen J., Lammi M., Pelttari A., Helminen H., Tammi M., Virtanen I. Altered golgi apparatus in hydrostatically loaded articular cartilage chondrocytes. Ann. Rheum. Dis. **52**, 192, 1993;

98. Hu J., Athanasiou K. The effects of intermittent hydrostatic pressure on self-assembled articular cartilage constructs. Tissue Eng. **12**, 1337, 2006;

99. Gunja N., Uthamathil R., Athanasiou K. Effects of TGF-Beta1 and hydrostatic pressure on mensicus cell-seeded scaffolds. Biomaterials. **30**, 565, 2009;

100. Huang B., Hu J., Athanasiou K. Cell-based tissue engineering strategies used in the clinical repair of articular cartilage. Biomaterials. **98**(August 2016), 1, 2016;

101. Mizuno S., Kusanagi A., Tarrant L., Tokuno T., Smith R. System useful for repairing cartilage, comprises lyophilized acellular collagen matrix containing pores and bioactive agent disposed within the pores patent. 2013.

102. Elder B., Athanasiou K. Effects of temporal hydrostatic pressure on tissue-engineered bovine articular cartilage constructs. Tissue Eng. Part A Part A. **15**, 1151, 2009;

103. Elder B., Athanasiou K. Synergistic and additive effects of hydrostatic pressure and growth factors on tissue formation. PLoS One. (6), e2341, 2008;

104. Kraft J., Jeong C., Novotny J., Seacrist T., Chan G., Domzalski M., et al. Effects of
hydrostatic loading on a self-aggregating, suspension culture – derived cartilage tissue
analog. Cartilage. **2**, 254, 2011;

105. Lee J., Huwe L., Paschos N., Aryaei A., Gegg C., Hu J., et al. Tension stimulation drives
tissue formation in scaffold-free systems. Nat. Mater. **16**, 864, 2017;

106. Wu S., Wang Y., Streubel P., Duan B. Living nanofiber yarn-based woven biotextiles for
tendon tissue engineering using cell triculture and mechanical stimulation. Acta Biomater.
Acta Materialia Inc.; **62**, 102, 2017;

107. Bieler F., Ott C., Thompson M., Seidel R., Ahrens S, Epari D., et al. Biaxial cell
stimulation: a mechanical validation. J Biomech. **42**, 1692, 2009;

108. Wartella K., Wayne J. Bioreactor for biaxial mechanical stimulation to tissue engineered
constructs. J. Biomech. Eng. **131**, 1, 2017;

CHAPTER 2- SHEAR STRESS INDUCED BY FLUID FLOW PRODUCES IMPROVEMENTS IN TISSUE ENGINEERED CARTILAGE

ABSTRACT

Tissue engineering aims to create implantable biomaterials for the repair and regeneration of damaged tissues. *In vitro* tissue engineering is generally based on static culture, which limits access to nutrients and lacks mechanical signaling. Using shear stress is controversial because in some cases it can lead to cell death while in others it promotes tissue regeneration. To understand how shear stress works and how it may be used to improve neotissue function, a series of studies were performed. First, a tunable device was designed to determine optimal levels of shear stress for neotissue formation. Then, computational fluid dynamics modeling showed the device applies fluid-induced shear (FIS) stress spanning three orders of magnitude on tissue-engineered cartilage (neocartilage). A beneficial window of FIS stress was subsequently identified, resulting in up to 3.6-fold improvements in mechanical properties of neocartilage *in vitro*. *In vivo*, neocartilage matured as evidenced by the doubling of collagen content toward native values. Translation of FIS stress to human derived neocartilage was then demonstrated, yielding analogous improvements in mechanical properties, such as 168% increase in tensile modulus. To gain an understanding of the beneficial roles of FIS stress, a mechanistic study was performed revealing a mechanically gated complex on the primary cilia of chondrocytes that is activated by FIS stress. This series of studies places FIS stress into the arena as a meaningful mechanical stimulation strategy for creating robust and translatable neotissues, and demonstrates the ease of incorporating FIS stress in tissue culture.

INTRODUCTION

All tissues in the body require nutrient and waste transport, as well as signal transmission via both soluble and mechanical cues. For example, vasculature, the most abundant source of transport and transmission in the body, delivers both soluble factors and mechanical signals via fluid-induced shear stress. *In vitro* tissue engineering has not typically incorporated vasculature and, instead, relies on static culture, limiting the transfer of soluble factors and removing fluid-induced mechanical signals. Static cultures are widely used in part because high-levels of shear have been associated with elevated levels of apoptosis,[1] tissue degradation,[2] and secretion of proinflammatory factors.[3] Specifically in chondrocytes, shear stress has been linked to upregulation of proinflammatory factors and pro-apoptosis, and in cartilage tissue, shear stress has been linked to matrix degradation.[4, 5] However, for some cells, such as vascular endothelial cells and cardiomyocytes,[6] specific shear stress magnitudes have been identified as beneficial.[2] Motivated by the potential ease of using shear stress in tissue culture, we embarked on a comprehensive series of studies aimed to determine an optimal beneficial shear stress regimen, to investigate the translatability of this strategy, and to explore how shear stress mechanistically improves tissue engineering.

To study how fluid flow may be used to enhance neotissue properties, we selected self-assembled neocartilage as a model.[7, 8] Neocartilage is the ideal model system for this series of studies because native articular cartilage does not rely on vasculature for survival. At the same time, cartilage, which is subjected to shear forces due to interstitial fluid flow, requires mechanical stimuli to maintain homeostasis.[9] Cartilage injuries constitute some of the most vexing medical problems because of the tissue's innate inability to heal,[10] making it a prime candidate for tissue engineering.[11] To restore cartilage's biomechanical function, the use of tissue-engineered neocartilage as a model system holds clinical promise and translational potential for the 240 million people that suffer from articular cartilage degeneration worldwide.[2]

Establishing fluid-induced shear stress as a potent mechanical stimulation strategy in tissue engineering can contribute to the significant medical need for producing replacement cartilage.

Although native articular cartilage experiences shear stress, prior mechanical stimulation strategies have focused on applying hydrostatic pressure, compression, and recently, uniaxial tension, during tissue culture.[12] Optimal loading windows and, in some cases, cell-signaling pathways have been identified for these stimuli[13-15] but not for shear stress. Despite tantalizing hints of the ability of shear stress to improve tissue quality, such as collagen type II deposition,[16-18] a window of shear stress for optimal tissue formation has yet to be identified. How fluid-induced shear stress is transduced also remains largely unexplored for chondrocytes. Motivated by how shear stress loading maintains native articular cartilage, we sought to identify a window of fluid-induced shear stress magnitude that produces neocartilage robust enough to thrive in an *in vivo* environment. We also sought to elucidate the players in mechanotransducing shear stress toward enhanced neocartilage construct properties. Toward translation and demonstration that the stimulus functions across species, we also aimed to employ fluid-induced shear stress to produce human neocartilage.

In this series of studies, we designed and developed a device that applies shear stress to neocartilage by using an orbital shaker to create oscillatory fluid motion. The neocartilage is held in fixed positions as fluid flows over it, creating shear stress on the surface of the neocartilage constructs. We also identified an optimized fluid-induced shear (FIS) stress loading regimen on neocartilage and investigated a cell signaling pathway involved in producing improved extracellular matrix properties (Figure 1). We used computational fluid dynamics models to quantify the magnitudes of FIS stresses that were applied on neocartilage constructs with parameters including settings on the orbital shaker and location in the device. Contrary to the prevailing notion of avoiding shear stress in cartilage tissue culture,[1, 19, 20] we hypothesized that a window of shear stress could be identified that leads to the enhancement of

collagen content and mechanical properties of neocartilage. We then performed an *in vivo* rat study to examine whether FIS stress-induced improvements in neocartilage mechanical properties could be maintained for 8 weeks; another objective of the *in vivo* study was to test the hypothesis that implanted neocartilage extracellular matrix and cellular organization would remodel toward mature native tissue properties. Subsequently, we translated the optimal FIS stress loading conditions to engineer human neocartilage. We also examined how FIS stress initiates mechanotransduction to improve neocartilage properties. To elucidate how fluid-induced shear stress contributed to the observed results, we performed RNA sequencing and scanning electron microscopy imaging. The overall objective of this work was to establish fluid-induced shear stress as a meaningful mechanical stimulation strategy for creating robust and translatable neocartilage, as well as to demonstrate the ease and benefit of incorporating fluid-induced shear stress in tissue culture.

FIGURE 1
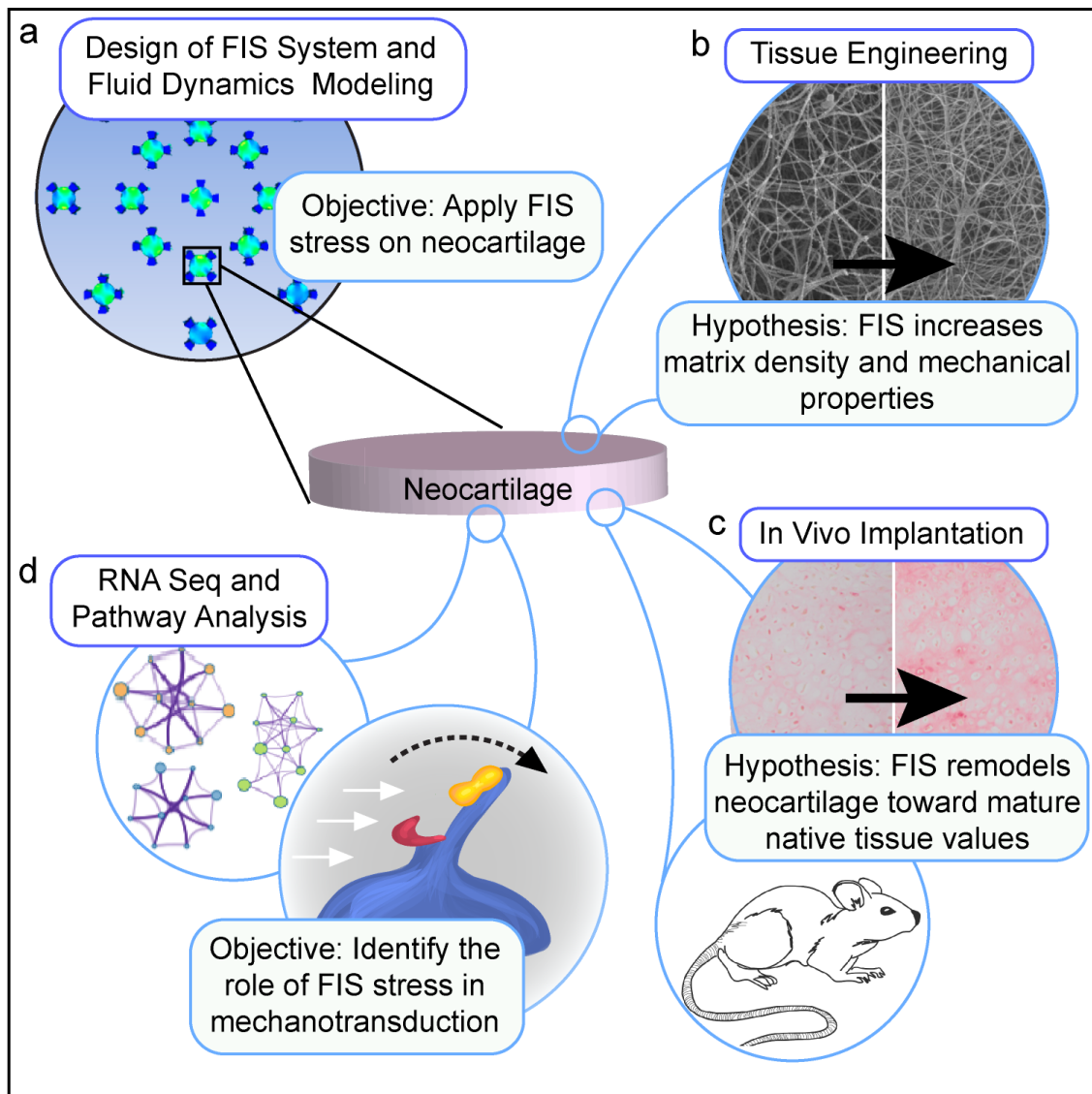
Figure 1- Overview of series of studies to elucidate the roles of fluid-induced shear (FIS) stress. a) Computational fluid dynamics models to determine shear stress magnitude imparted on neocartilage in the FIS stress device. **b)** Tissue engineering studies *in vitro* using bovine and human cells to test the hypothesis that FIS stress results in enhancements in neocartilage density and mechanical characteristics. **c)** *In vivo* studies in athymic mice to test the hypothesis that FIS stress-stimulated neocartilage remodels toward native values after implantation. **d)** RNA sequencing followed by pathway analysis to elucidate mechanotransduction pathways activated by FIS stress.

MATERIALS AND METHODS

Bovine chondrocyte harvest

Juvenile bovine (14-30 days) stifle joints were procured from Research 87. Articular cartilage was harvested from the distal femurs within 48 hours of slaughter. The harvested articular cartilage was digested in 0.2% collagenase type II (Worthington Biochemical Corp) solution for 18 hours to release the chondrocytes from the tissue matrix. Next, the chondrocytes were washed in a solution of Dulbecco's Modified Eagle's Medium (DMEM) and 1% penicillin-streptomycin-fungizone (PSF, Lonza BioWhittaker). For each study in this investigation, eight juvenile bovine stifle joints were used; chondrocytes from the eight animals were pooled and counted using a hemocytometer, and their viability was estimated using a trypan blue exclusion assay. Cells were stored at -80°C in freezing medium containing 90% fetal bovine serum and 10% dimethyl-sulfoxide serum until use.

Human chondrocyte harvest and expansion

Human knee articular chondrocytes were harvested from a Caucasian male donor, age 43, with no known musculoskeletal pathology (Musculoskeletal Transplant Foundation). The human chondrocytes were passaged and chondrotuned as previously described.[15] Briefly, the chondrocytes were expanded in a chondrogenic culture medium with bioactive factors TGF-β1 (1ng/ml), bFGF (10ng/ml), and PDGF-bb (10ng/ml) (all from Peprotech) to passage 3. Cells were then placed in a 3D aggregate culture for a duration of 7 days.[15] The resulting aggregates were digested using 0.2% collagenase to release the redifferentiated chondrocytes for construct seeding.[8]

The self-assembling process

Before seeding, 5mm diameter, non-adherent, sterilized, agarose (2% weight/volume phosphate-buffered saline (PBS)) wells were formed and pre-saturated with chondrogenic medium (DMEM with GlutaMAX (Gibco); nonessential amino acids (0.1mM) (Gibco); 1% insulin,

human transferrin, and selenous acid (ITS+; BD Biosciences); 1% PSF; dexamethasone (100nM) (Sigma-Aldrich); ascorbate-2-phosphate (50µg/mL) (Sigma-Aldrich); sodium pyruvate (100µg/mL) (Sigma-Aldrich) and L-proline (40µg/mL) (Sigma-Aldrich). In the non-adherent, agarose wells 4 million chondrocytes were seeded to form self-assembled, scaffold-free, neocartilage constructs; the constructs were fed 0.5ml of chondrogenic medium daily. Once the neocartilage constructs grew to the edge of the agarose wells (day 7), they were transferred to the FIS stress stimulation device. The neocartilage constructs have not been shown to grow significantly in diameter or thickness during culture under FIS. After FIS stress stimulation, constructs were transferred to a 48-well tissue culture treated plate and maintained in static culture with 1ml of chondrogenic medium exchanged per day for the remaining culture duration (total culture time = 28 days). For experimental groups treated with bioactive factors, TGF-β1 and LOXL2 were used. TGF-β1 (10ng/ml) was applied continuously. LOXL2 was applied on days 15-28 (0.15 µg/ml) (SignalChem) with copper sulfate (1.6 µg /ml) (Sigma-Aldrich) and hydroxylysine (0.146 µg /ml) (Sigma-Aldrich). For human-derived neotissues, C-ABC (Sigma-Aldrich) (2 U/ml) CHG was applied for 4 hours on day 7.

<u>FIS stress device fabrication</u>

The FIS stress device was made by first fabricating an acrylonitrile butadiene styrene (ABS) negative mold using the additive manufacturing process of the open source MakerBot. The ABS negative mold was sterilized in an autoclave before every use. To create the FIS stress device, 23ml of sterilized agarose in 2% weight/volume phosphate-buffered saline (PBS) was deposited into an 83mm diameter petri dish. The ABS negative mold was then placed on top of the agarose. Once the agarose gelled (15min), the ABS negative mold was removed and the resultant FIS stress device remained in the petri dish (Figure 2a, b, c, d). Agarose was used to create the device because of its cost effectiveness, and in order avoid rusting that results from using steel in a humid culture environment. Additionally, agarose is non-adherent to cells and

not a barrier to nutrient diffusion, as opposed to steel or acrylic. To induce FIS stress, the device

was first saturated with chondrogenic medium through three exchanges of 20ml of the medium,

then filled with 20ml of the medium and placed on an orbital shaker at 25, 50, or 100RPM.

Because the petri dish is only 100mm in diameter and a standard orbital shakers, 500 x 500mm,

can hold a single layer of about 20 petri dishes. The petri dishes may also be stacked, meaning

over 20 petri dishes can be mounted on the shaker at the same time.

FIGURE 2
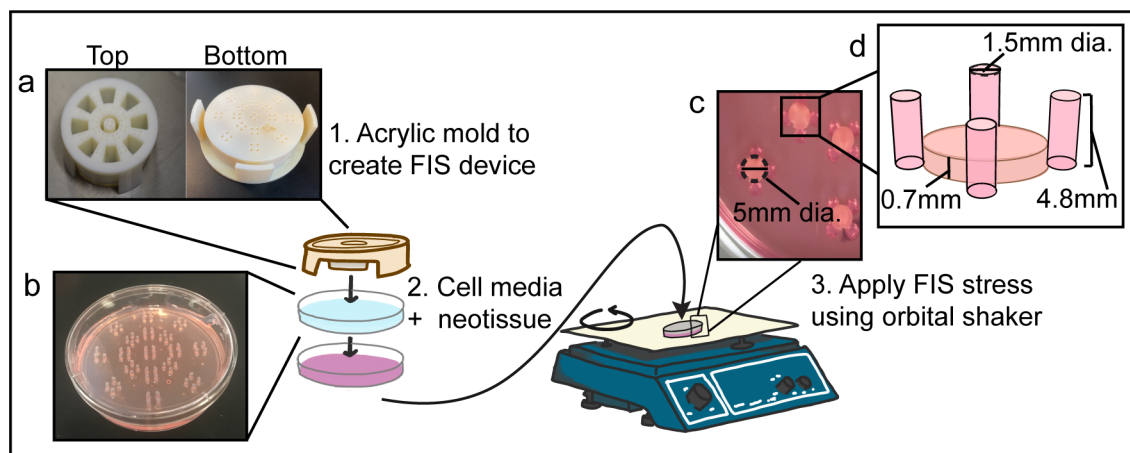
Figure 2- The fabrication and use of the FIS stress device a) A 3D-printed acrylic mold was used to form the FIS stress device. b) The FIS stress device was made of 2% agarose in a petri dish. A total of 16 constructs were held in place by four posts each. c) The constructs were placed in the FIS stress device for 6 or 12 days after 7 days of initial culture, and the device was filled with cell media. Placing the device on an orbital shaker initiated FIS stress stimulation. d) The neocartilage constructs sit in the device surrounded by 4 agarose posts that hold it in place.

Computation of shear stress in device

The unsteady, free-surface flow inside the device was modeled by solving three-dimensional

Navier-Stokes equations using the commercial CFD software ANSYS FLUENT 16.1. Three-

dimensional cylindrical renderings of the neocartilage constructs and the device were generated

using the preprocessor ANSYS ICEM CFD 16.1. Certain CFD modeling parameters, including

the dimensions of the neocartilage constructs, the dimensions of the device, and the orbital diameter, were held constant as follows: The diameter of the device was 83mm with 16 cylindrical constructs, each supported and held in place by four posts. Each neocartilage construct, modeled as a solid cylinder with a radius of 2.5mm and a thickness of 0.7mm, was supported by four posts that were 1.5mm thick and 4.8mm tall, in the positions shown in Figure 2d. The orbital diameter was set to fit the standard orbital shaker size of 19 mm. Theoretically, changes in the parameters that were held constant for the *in vitro* portion of this study; such as construct and device size and geometry may alter the shear stress generated in the device. However, previous studies have shown that to create a significant difference in the generated shear stress, the device would have to double in diameter. [52] Finally, the independent variables examined were orbital velocity at orbital shaker settings of 25, 50, or 100RPM and an inner or outer position on the device. An unstructured mesh of 1,001,750 tetrahedral shaped cells was applied to the volume. A higher mesh density was applied to the constructs, versus the bulk region, for proper resolution.

The volume of fluid (VOF) model was applied to track the liquid-air interface present in the system. In the model, both phases sharing the interface employed a combined set of momentum equations so that the volume fraction of each fluid in each cell can be tracked throughout the grid. The two phases were set with the default properties for air and water. The initial resting liquid height was set as 4mm. The mesh's orbital motion was specified by a user-defined function. The three orbital RPMs yielded three separate cases of FIS stress magnitude; frequency was not measured because the frequency and magnitude cannot be controlled independently using this device. A time step of 0.0001 was determined to be necessary for acceptable convergence. Techniques for modeling and determining convergence criteria, grid optimization, and time needed to reach steady state for the transient solution have been previously described.[21-23]

<u>FIS stress stimulation</u>

FIS stress stimulation was applied to neocartilage constructs starting at day 7. Five ranges of FIS stress magnitude were investigated by placing the device on the orbital shaker at 25, 50, or 100RPM. The FIS stress device induced a range of 0-0.01Pa at 25RPM, ranges of 0.07-0.15Pa and 0.05-0.21Pa at 50RPM, and ranges of 0.37-0.70Pa and 0.25-0.85Pa at 100RPM (Figure 3a, b, c). FIS stress stimulation durations of 6 days and 12 days were investigated.

FIGURE 3
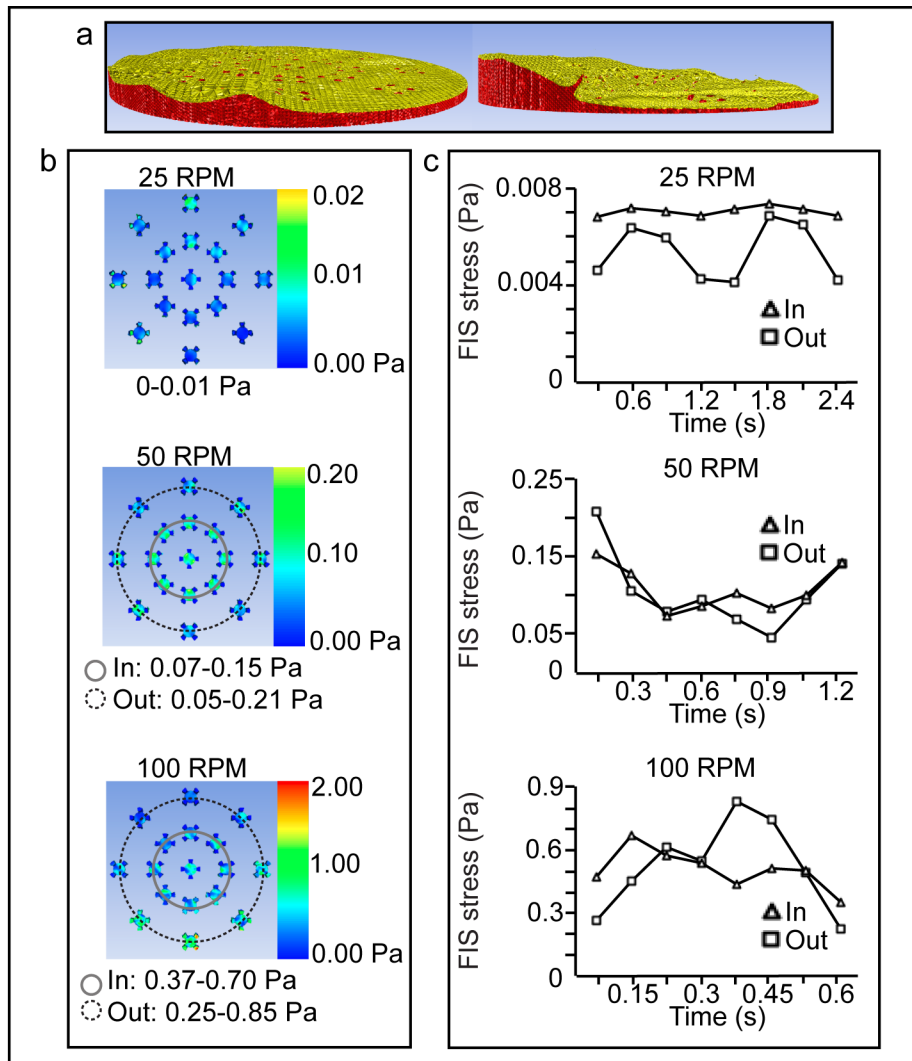
Figure 3- Computational fluid dynamics (CFD) was used to predict the magnitude of shear stress created in the FIS stress device. a) Snapshots of waveforms of the fluid flow created in the FIS stress device at 25RPM (left) and 100RPM (right) on the orbital shaker as predicted by CFD models. **b)** CFD modeling of the shear stress distribution in the FIS stress device during stimulation. At 50 and 100RPM, constructs placed in the inner circle of the FIS stress device experience a slightly different shear stress magnitude range than constructs placed in the outer circle. **c)** FIS stress experienced by a construct at varying time points of one orbital shaker cycle.

Mechanical testing

A 2.5mm diameter punch from the center of the neocartilage constructs was used for creep indentation testing using an automated indentation apparatus.[24, 25] Briefly, a 0.9 mm diameter, flat, porous, indenter tip was used to apply a 2g (0.02N) step mass onto the neocartilage construct to reach 10-15% strain. The indented neocartilage was allowed to creep to equilibrium as described previously.[26, 27] The aggregate modulus and shear modulus were estimated by analyzing the experimental data using a semianalytical, seminumerical, linear biphasic model in combination with finite element modeling.[26]

Tensile testing samples were taken in the shape of a dog bone, following ASTM standards, with a gauge length of 1mm. Paper was glued to the construct tabs outside the gauge and gripped by a mechanical tester (Test Resources, Inc.). The construct was pulled apart at 1% of the gauge length per second (0.01mm/s) until failure. Image-J was used to measure the cross-sectional area, and a stress-strain curve was generated to yield the tensile Young's modulus. The ultimate tensile strength (UTS) was obtained by measuring the maximum stress on the curve.

Biochemical analysis

Samples were weighed, lyophilized for 72hr, weighed again, and digested in 125µg/ml papain solution (Sigma), 2mM N-acetyl cysteine (Sigma), and 2mM EDTA (Sigma)) in phosphate buffer

(50mM, pH = 6.5) at 65°C for 18hr. Total DNA was quantified using PicoGreen dsDNA reagent (Invitrogen). Total GAG content was measured using a Blyscan assay kit from Biocolor, and total collagen content was quantified using a modified colorimetric chloramine-T hydroxyproline assay.[28] For the collagen assay, a Sircol collagen standard (Biocolor) was used to create a standard curve.

Genomic analysis

mRNA was isolated immediately after FIS stress stimulation ceased using an RNeasy Kit (Qiagen, Inc.). mRNA from samples that were not stimulated with FIS stress was also isolated at the same time as samples stimulated with FIS stress. RNA-Seq was performed by the UCI Genomics High-Throughput Facility (GHTF). The RNA Sequencing libraries used by the UCI GHTF were prepared with the mRNA-Seq sample preparation kit from Illumina and sequenced using the Illumina HiSeq 2000. In total, eight constructs were sequenced (four stimulated with the optimal FIS stress loading, and four non-stimulated controls). After applying quality control filters, paired-end libraries were used to perform differential expression analysis on a Linux platform using the Hypergeometric Optimization of Motif EnRichment (HOMER) modules tools suite.[29] The NIH's Database for Annotation, Visualization and Integrated Discovery (DAVID) was used to translate gene identification numbers to genes names, and Cytoscape was used to perform pathway analysis and cluster genes of similar function.

RT-PCR was performed on the genes of interest: IHH, PKD1, and PKD2, which encode for PC1 and PC2, respectively. RT-PCR was performed on both human and bovine derived neocartilage. Total RNA was reverse-transcribed using random primers (Integrated DNA technologies), with GAPDH primers used to control for cDNA concentration in separate RT-PCRs for all samples. Primers for bovine GAPDH, IHH, PKD1, and PKD2, and human B2M, IHH, PKD1, and PKD2 were designed using the Integrated DNA technologies PrimerQuest tool;

they are shown in Supplementary Table 5. The specificity of all primers was verified to be 100% with the NIH's National Library of Medicine online Nucleotide Blast tool. PerfeCTa SYBR Green SuperMix from Quanta Bio was added to each RT-PCR reaction (plated in triplicate) for a total reaction volume of 25ul. Ct values were normalized to GAPDH expression levels to obtain the relative expression of the gene of interest in comparison to GAPDH in both control and FIS-stimulated constructs.

In vivo study

The Institutional Animal Care and Use Committee (IACUC) of UC Davis approved the use of 12 6-8 week old athymic mice for this study. All neocartilage constructs were created using the self-assembling process for 4 weeks, as described above. After the initial 4 weeks of culture, 24 constructs were implanted *in vivo* for an additional 4 weeks, while six constructs were tested immediately after the initial 4 weeks of *in vitro* culture. In parallel, six constructs were left to culture *in vitro* for an additional 4 weeks to compare the effects of *in vitro* incubation vs *in vivo* implantation. A 1.5cm incision was formed on the dorsal side of the mice under general anesthesia. Two bilateral punches were created on either side of the mice, and a neocartilage construct was placed in each pouch with no mouse receiving two constructs from the same group (-FIS Stress/-TL, +FIS Stress/-TL, +FIS/+TCL). The investigators were not blinded to which constructs each mouse received. Following 4 weeks of implantation, mice were sacrificed, and the constructs were removed for mechanical and biochemical assessment as specified above.

Statistical analysis

Analysis of variance and Tukey's *post hoc* tests were used to compare biochemical and mechanical data for multiple group comparisons. Data are presented as mean + standard deviation. Six constructs were used per group to determine the optimal FIS stress stimulation

regimen (0.05-0.21Pa for 12 days). All six constructs were used for biochemical analysis and mechanical testing. Five constructs per group were used in the human neocartilage study to determine mechanical properties, and four constructs were used to determine biochemical properties. For RNA-Seq analysis and RT-PCR verification, four constructs per group were used. Four constructs per group were used in the *in vivo* animal study.

RESULTS

A fluid-induced shear (FIS) stress device generated shear stress ranging from 0-0.85Pa on self-assembled neocartilage.

A device capable of inducing FIS stress stimulation on 5 mm diameter, self-assembled neocartilage constructs was designed (Figure 2). Computational fluid dynamics (CFD) modeling was employed to relate fluid flow to ranges of FIS stress magnitudes (Figure 3a,, b, c). The CFD models predicted that the FIS stress device could induce a shear stress range of 0-0.01Pa at 25RPM, 0.07-0.15Pa and 0.05-0.21Pa at 50RPM, and 0.37-0.70Pa and 0.25-0.85Pa at 100RPM at different locations (Figure 3b). Figure 3c shows a detailed account of the shear stress experienced by the constructs through time. Each plot represents the time it takes for one full rotation of the orbital shaker. The constructs placed in the inner circle of the FIS stress device experienced slightly different shear stress magnitude ranges than constructs placed in the outer circle. By using an orbital shaker to apply FIS stress, magnitude and frequency of FIS stress loading cannot be studied independently; the frequency of FIS stress loading increases with increasing FIS stress magnitude. It was found that the FIS stress device is capable of imparting shear stress at multiple orders of magnitude on tissue-engineered constructs. Thus, we designed, developed, and implemented a device that successfully applies multiple ranges of FIS stress to neotissues.

An optimal range of FIS stress, 0.05-0.21Pa, improved the compressive modulus of neocartilage derived from bovine articular cartilage chondrocytes by 450%.

Of the five ranges of FIS stress magnitude that were considered in this study, 0.05-0.21Pa was found to result in significantly improved construct characteristics. In spite of previous studies indicating that shear stress might lead to degraded neocartilage[1, 19, 20, 30], the aggregate modulus of constructs stimulated by 0.05-0.21Pa of FIS stress (379±76kPa) improved to the level of native tissue.[31] Specifically, constructs that were stimulated with FIS stress for 6 days improved by 450% ($p < 0.05$) (Figure 3a, Supplementary Table 1) compared to the aggregate modulus of statically cultured controls (98±25kPa). This makes FIS stress a promising mechanical loading strategy to produce robust articular cartilage. Interestingly, other ranges of FIS stress decreased construct aggregate modulus values; samples stimulated with 0-0.01Pa or 0.25-0.85Pa yielded aggregate modulus values of 44±21kPa and 95±36kPa, respectively (Figure 4a, Supplementary Table 1). These findings suggest that although some ranges of shear stress can be harmful to neocartilage, self-assembled neocartilage compressive properties can be improved using a FIS stress magnitude between 0.05-0.21Pa (Figure 4a, Supplementary Table 1).

Optimization of the duration of an applied mechanical stimulus is necessary for mechanical stimulation studies. We also investigated the duration of FIS stress stimulation for 12 days at 50 and 100RPM. A FIS stress stimulation lasting 12 days at 50RPM was found to yield increased tensile properties, with a tensile Young's modulus of 1.87±0.59MPa ($p < 0.05$, over unstimulated controls) and ultimate tensile strength (UTS) of 0.60±0.15MPa ($p < 0.05$, over unstimulated controls) (Figure 4b, c, Supplementary Table 1). Thus, we discovered the optimal FIS stress stimulation regimen to be within the range of 0.05-0.21Pa implemented for 12 days.

In terms of biochemical properties, glycosaminoglycan, collagen, and DNA content were quantified and normalized to dry weight. Glycosaminoglycan content was not shown to increase or decrease in response to FIS stress stimulation for any of the ranges or durations of shear stress that were tested. (Supplementary table 1 A, B, C, D) Collagen content was also not affected by the implementation of FIS stress stimulation. (Supplementary table 1 A, B, C, D) This suggests that the improvements seen in mechanical properties are likely due to crosslinking of fibers. To determine if improvement in mechanical properties was due to an increase in cell quantities, cell growth was measured indirectly using a DNA quantification assay. The DNA/ %DW of neocartilage constructs was not affected by FIS stress stimulation.(Supplementary table 1 A, B, C, D)

FIGURE 4
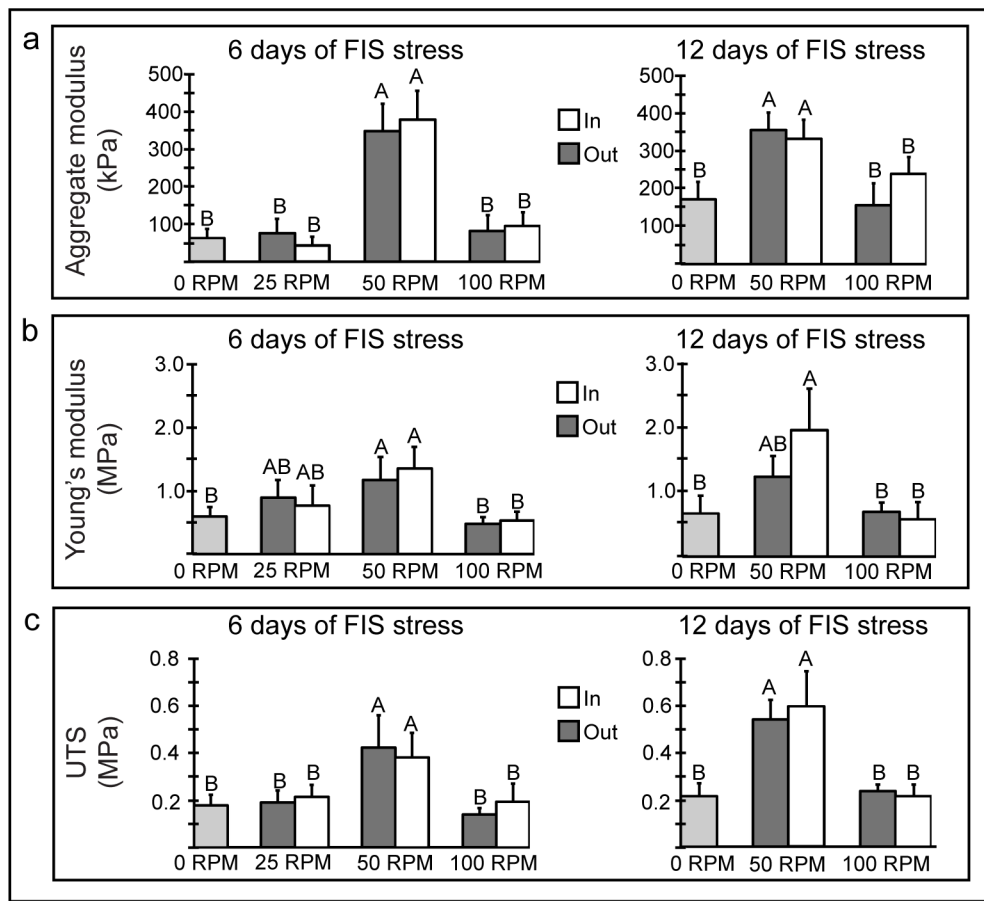
Figure 4- An optimized regimen of FIS stress was found to yield superior mechanical properties of neocartilage. The mechanical properties, **a)** aggregate modulus, **b)** Young's modulus, and **c.** ultimate tensile strength, of unstimulated neocartilage or stimulated with three different ranges of FIS stress. **a-c)** The position of constructs on the FIS stress device was also investigated (in vs. out), as well as duration of FIS stress stimulation (6 vs. 12 days). One-way analysis of variance ($p < 0.05$) was performed across all groups and letters placed on top of bar graphs indicate statistical significance amongst groups.

<u>FIS stress led to recapitulation of native tissue fiber density.</u>

To verify, visualize, and assess the improvements in extracellular matrix-level fiber organization stemming from FIS stress stimulation, we employed scanning electron microscopy to look at the surface of the neocartilage constructs. Fiber density on the constructs stimulated with the optimal FIS stress regimen was significantly higher than in statically cultured control constructs (Figure 5a, b). Specifically, the fiber density of FIS stress-stimulated constructs improved to 88±3% from 61±3% of unstimulated constructs ($p < 0.05$). FIS stress stimulation served to increase extracellular matrix properties and, ultimately, led to the enhancement of mechanical properties.

To ensure that the fiber density observed on the surface of the neocartilage constructs was uniform throughout the inside of the construct, histological staining of top-to-bottom cross-sections was performed. Safranin O staining was more pronounced in neocartilage constructs stimulated with FIS stress, suggesting an increase in proteoglycan content. Furthermore, the stain was uniform throughout FIS stress stimulated constructs, which suggests that the beneficial effects of FIS stress are not localized to the surface of the neocartilage (Figure 5c).

FIGURE 5
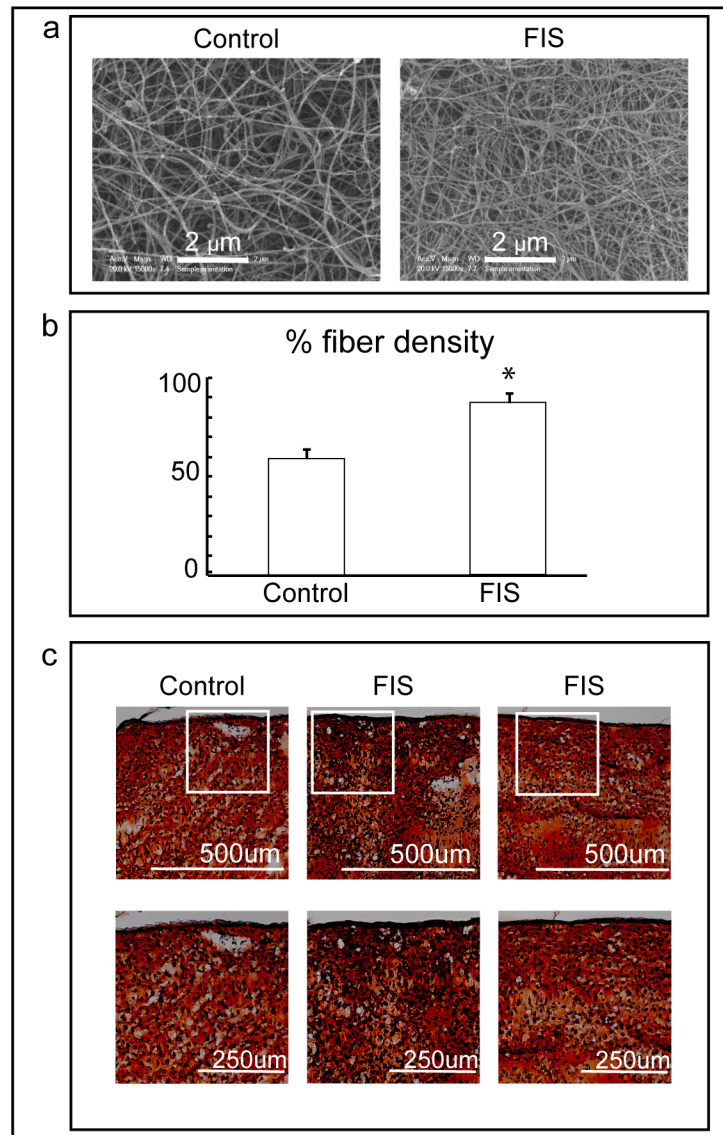
Figure 5- Neocartilage stimulated with FIS stress becomes more fibrous. a) Scanning electron microscopy images of neocartilage cultured with or without FIS stress showed an increase in the fiber density of the extracellular matrix of stimulated constructs. **b)** The fiber density of neocartilage as observed via scanning electron microscopy was quantified by processing scanning electron microscopy images through ImageJ software. **c)** Staining of proteoglycans in neocartilage constructs with a Safranin O stain.

<u>A combination of FIS stress and bioactive factors generated additive enhancements in mechanical properties, yielding 1.9- to 3.6-fold improvements over unstimulated controls.</u>

Once the optimal FIS stress loading regimen was identified, we investigated the effects of FIS stress stimulation in combination with growth factor TGF-β1, and matrix cross-linking agent, lysyl oxidase like 2 (LOXL2).[32-34] These bioactive factors, alone or in combination, have previously been shown to enhance tensile and compressive properties in both scaffold-based and scaffold-free neocartilages.[32] Thus, it was of interest to determine if FIS stress stimulation worked in tandem with bioactive factors to further enhance neocartilage properties.

When the bioactive factors were used in combination with FIS stress stimulation (0.05-0.21Pa for 12 days), both mechanical and biochemical properties of the neocartilage exhibited additive improvements (Supplementary Table 2A). In particular, collagen content of neocartilage stimulated with both FIS stress and bioactive factors was improved to 24±2%/DW compared to FIS stress only constructs, 14±2%/DW ($p < 0.001$), and to bioactive factors only constructs, 20±3%/DW ($p < 0.006$). Furthermore, FIS stress in combination with growth factors resulted in a 35% increase in aggregate modulus ($p < 0.002$) and a 56% increase in GAG content over bioactive factors alone ($p < 0.001$). Overall, FIS stress stimulation, combined with bioactive agents, yielded significant improvements in neocartilage properties over non-stimulated controls and significant increases over either form of stimulation alone.

We also assessed the stability of neocartilage properties *in vitro* for 8 weeks. We tissue-engineered constructs using the self-assembling process and after 7 days of initial culture, applied either FIS stress (0.05-0.21Pa for 12 days), FIS stress + bioactive factors, or no stimulation. In particular, the mechanical properties of constructs stimulated with FIS stress + bioactive factors were improved after 8 weeks *in vitro* with a 197% increase in aggregate modulus ($p < 0.001$), 194% increase in Young's modulus ($p < 0.001$), and a 361% improvement in

UTS (p<0.002) over unstimulated controls (Supplementary Table 2B). The consistent trends of elevated compressive and tensile properties in both 4- and 8-week models were encouraging for the application of FIS stress + bioactive factors in *in vivo* studies.

Implanted neocartilage treated with a combination of FIS stress and bioactive factors remodeled *in vivo*, yielding a 122% increase in collagen content and 168% increase in Young's modulus.

We assessed the stability of neocartilage properties *in vivo* by performing subcutaneous implantation of constructs stimulated 1) without FIS stress, 2) with FIS stress, or 3) with FIS stress + bioactive factors in athymic mice. The neocartilage was implanted for 4 weeks after initial *in vitro* culture duration of 4 weeks. Compared to those maintained *in vitro, in vivo* neocartilage exhibited significant histological, biochemical, and mechanical differences (Figure 6 a-d, Supplementary Table 3). Biochemical assays revealed the *in vivo* remodeling of extracellular matrix toward native tissue values across all construct groups, but particularly in neocartilage stimulated with FIS stress + bioactive factors. For example, constructs stimulated with FIS stress + bioactive factors exhibited a 122% increase in collagen content (p<0.001) and a 30% decrease in GAG content (p<0.001) compared to *in vitro* counterparts. Because the self-assembling process initially leads to higher GAG content and lower collagen content than native tissue, increased levels of collagen content and decreased levels of GAG content after implantation suggest that the neocartilage is remodeling and maturing (Figure 6d).[8, 35]

The mechanical characteristics of stimulated and unstimulated implanted tissues improved, suggesting that neocartilage undergoes *in vivo* maturation. This observation is in accordance with previous studies on implanting neocartilage.[7, 33, 36] In our study, the tensile Young's modulus of unstimulated constructs improved by 168% after implantation (p<0.002) but did not surpass the Young's modulus of implanted, treated groups. The UTS of control neocartilage and neocartilage stimulated with FIS stress improved after implantation, while the

neocartilage stimulated with both FIS and bioactive factors did not significantly change after implantation. The histology showed that the *in vivo* environment induced cellular organization and morphology changes in all construct groups; after implantation, chondrocytes oriented themselves in a columnar fashion and exhibited pronounced lacunae (Figure 6f). Collectively, these data show that the subcutaneous implantation of neocartilage constructs not only maintains and enhances the properties of neocartilage stimulated with FIS stress and FIS stress + bioactive factors toward those of native articular cartilage, but also results in neocartilage constructs that are morphologically reminiscent of native articular cartilage.

FIGURE 6
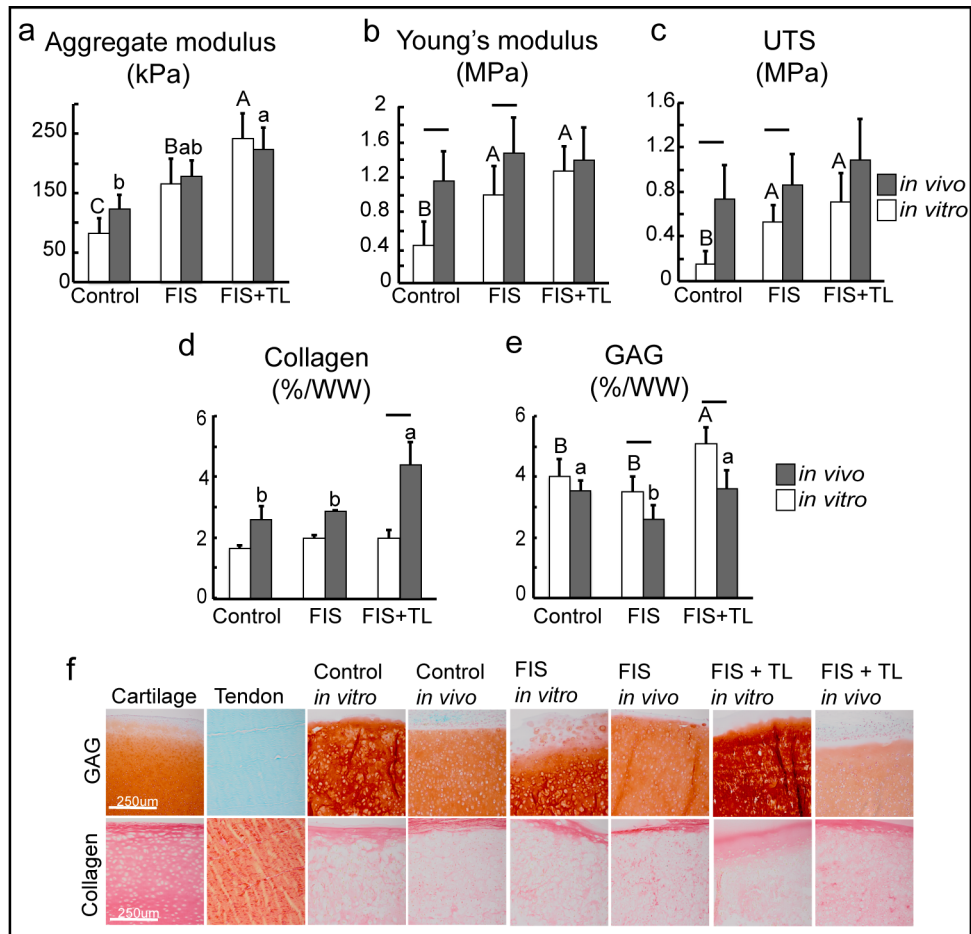
Figure 6- Neocartilage stimulated with FIS stress and implanted *in vivo* remodels and matures. Neocartilage was cultured *in vitro* for an initial 4 weeks and then either implanted for an additional 4 weeks or kept *in vitro* for an additional 4 weeks. Mechanical testing of neocartilage showed that both tensile and compressive characteristics either improved or remained the same after *in vivo* implantation. **a)** Aggregate modulus, **b)** Young's modulus, **c)** ultimate tensile strength (UTS). The biochemical properties of neocartilage showed that it remodels and matures *in vivo*. **d)** Collagen content, **e)** glycosaminoglycan (GAG) content. **a-e)** Lower-case letters placed on top of bar graphs indicate statistical significance amongst *in vivo* groups (one-way analysis of variance). Capital letters placed on top of bar graphs indicate statistical significance amongst *in vitro* groups (one-way analysis of variance). Line on top of bars denotes differences between *in vivo* and *in vitro* constructs (Student's t-test; p<0.05). **f)** Histological staining for collagen and GAG organization showed that after implantation, a more uniform distribution of collagen content was present, GAG density appeared more similar to native tissue, and chondrocytes were organized in a columnar fashion. All of these characteristics are reminiscent of native tissue.

Human neocartilage, stimulated with FIS stress, increased mechanical properties by 72-201% over unstimulated controls.

The ultimate goal of tissue engineering is to create tissues for use in human implantation, but improvements seen with bovine cells do not necessarily translate to passaged human chondrocytes. Furthermore, there are few studies, if any, where shear stress has been used to engineer human articular cartilage. When creating human neocartilage, bioactive factors, TGF-β1, LOXL2, and C-ABC, were used successfully during tissue culture.[15] It was, thus, of interest to determine if FIS stress stimulation would synergize with these bioactive factors to produce human neocartilage. Articular chondrocytes were harvested, expanded up to passage three, redifferentiated with aggregate culture, and both groups were placed into self-assembly with the addition of bioactive factors.[15] Neocartilage constructs were then separated into two groups, with or without FIS stress stimulation.

As in our bovine studies, the human neocartilage treated with FIS stress improved in mechanical functionality. In terms of compressive properties, the addition of FIS stress during tissue engineering yielded an aggregate modulus 72% larger (p<0.008) and a shear modulus

66% larger (p<0.05) than controls (Figure 7 a, b, Supplementary Table 4). FIS stress improved the tensile Young's modulus by 201% (p<0.02) and the UTS by 122% (p<0.008) over controls (Figure 7c, d, Supplementary Table 4). Although bovine neocartilage display much higher compressive properties than those of human neocartilage, these data are consistent with previous mechanical stimulation strategies applied to human neocartilage, [13] and illustrate the potential of using fluid-induced shear stress in engineering human neocartilage. Optimization of a FIS stress regimen is an effective method to drive human neocartilage toward native characteristics.

FIGURE 7
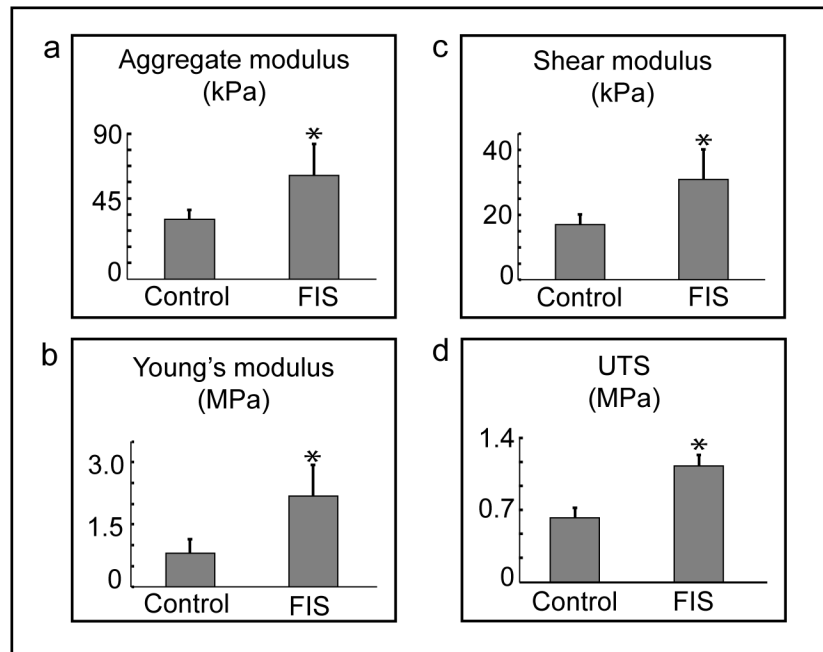
Figure 7- The mechanical properties of human neocartilage constructs stimulated with the optimized FIS stress regimen were improved over controls. The following properties of neocartilage constructs were tested and compared (Student's t-test, p<0.05): **a)** Aggregate modulus, **b)** shear modulus, **c)** Young's modulus, and **d)** ultimate tensile strength (UTS).

<u>FIS stress stimulation upregulated genes encoding a mechanosensitive complex of primary cilia.</u>

Toward elucidating the mechanism behind the improved properties of neocartilage stimulated with FIS stress, we performed RNA-Seq to capture genes that may be responsible. We hypothesized that FIS stress-induced improvements might not only be a result of increased nutrient perfusion and transport of waste, but also the result of complex cellular signaling events and matrix remodeling initiated by mechanotransduction. RNA-Seq and subsequent differential expression analysis revealed the upregulation of 694 genes and the downregulation of 613 genes in FIS stress-stimulated neocartilage compared to unstimulated controls (Figure 8a). Using the NIH's DAVID and Cytoscape to analyze the data obtained from RNA-Seq, we determined the major gene categories that appeared modified in response to FIS stress stimulation. These include mechano-regulated ion channels and complexes found on the primary cilia of cells, growth factors, extracellular matrix organization proteins, and extracellular matrix assembly proteins (Supplementary Figure 1).

From the genes that were shown to be altered by FIS stress using RNA-Seq, of particular interest was the upregulation of polycystin 1 (PC1) and 2 (PC2), which are encoded by PKD1 and PKD2 respectively, to form an ion-gated complex. RNA-Seq data were confirmed by RT-PCR for both bovine-derived and human-derived neocartilage constructs. We found that PKD1 and PKD2 were significantly upregulated in both bovine and human neocartilage stimulated with FIS stress (Figure 8b). This suggests that FIS stress induces the formation of more PC1/2 complexes on primary cilia, leading to increased sensitivity to fluid flow. Primary cilia are known to be necessary modulators of Indian Hedgehog (IHH) signaling in chondrocytes and other cell types.[37, 38] In chondrocytes, IHH is salient in regulating developmental features such as proliferation and maturation.[39] Therefore, we also investigated and verified the upregulation of IHH expression in the bovine-derived neocartilage constructs via RT-PCR

(Figure 8b). The activation of the PC1/2 complexes by fluid flow perturbation would result in a greater influx of Ca^{2+} ions, than unstimulated chondrocytes,[40, 41] initiating a cascade of upregulated extracellular matrix producing and remodeling genes and proteins in chondrocytes,[42-44] leading to the formation of mechanically robust neocartilage (Figure 8c).

FIGURE 8
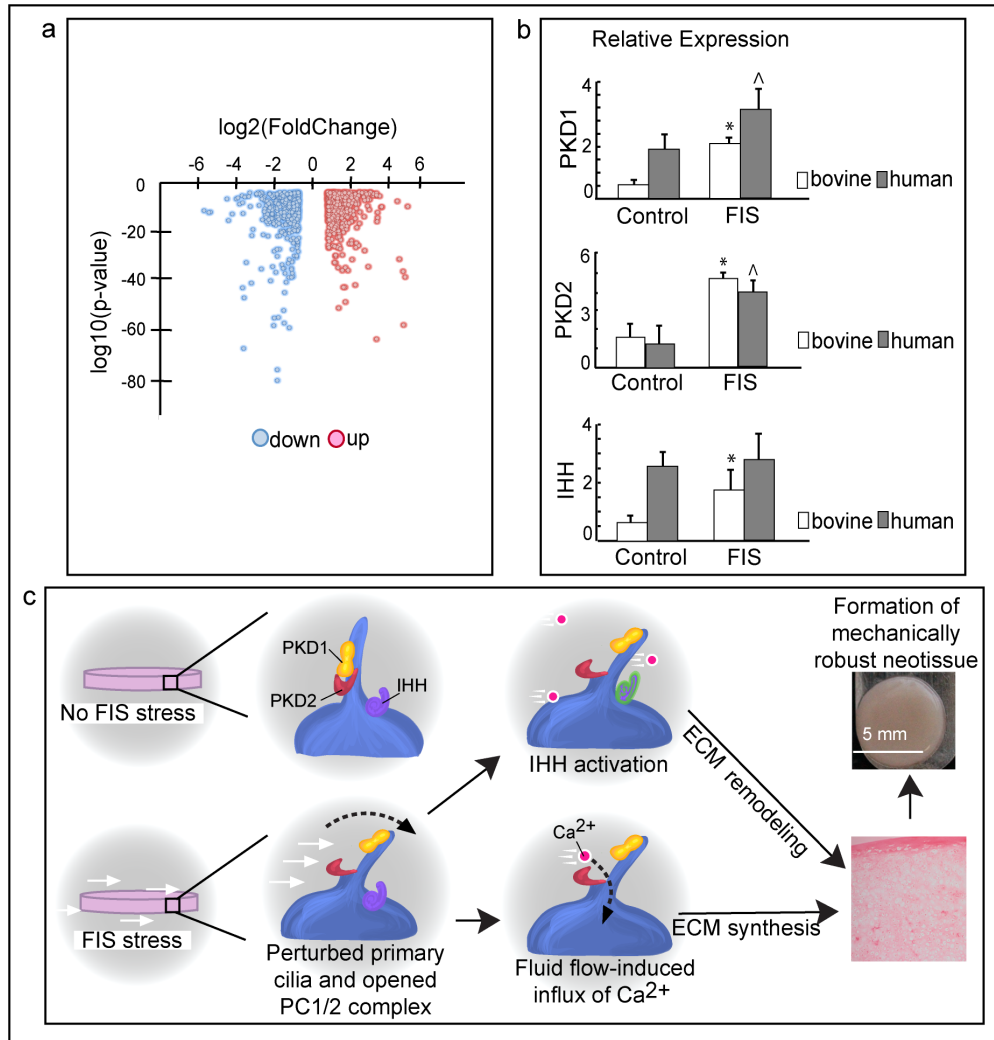
Figure 8- The modes of action of FIS stress a) A volcano plot generated from RNA-Seq and differential expression analysis is shown. Genes that were found to be upregulated in FIS stress-stimulated constructs are in red, and downregulated genes are in blue. Only genes that were found to have higher than a 2-fold change difference and a p-value < 0.05 are shown. **b)** The relative expressions of genes of interest IHH, PKD1, and PKD2 to the housekeeping gene are shown for control and FIS stress-stimulated constructs (Student's t-test, p<0.05, * shows significance for bovine, ^ shows significance for human). **c)** A schematic showing how FIS stress leads to robust neocartilage. When FIS stress is applied to the construct, the primary cilia of chondrocytes are perturbed and the PC1/2 complex is opened, allowing the influx of Ca^{2+} ions and an increase in IHH signaling. This leads to a cascade of signaling events that initiate extracellular matrix synthesis and remodeling which result in mechanically robust neocartilage constructs.

DISCUSSION

In this series of six studies, we investigated the use of fluid-induced shear stress to enhance the formation of tissue-engineered cartilage using the self-assembling process. In the first study, we designed a FIS stress device and performed computational fluid dynamics to predict the ranges of FIS stress produced in the device. We determined that the FIS stress device could impart separate ranges of shear stress on the neocartilage constructs, spanning multiple orders of magnitude: 0-0.01Pa, 0.07-0.15Pa, 0.05-0.21Pa, 0.37-0.70Pa, and 0.25-0.85Pa. For our second study, we found that neocartilage benefits from an optimal fluid-induced shear stress of 0.05-0.21Pa, improving mechanical and biochemical properties over control groups as well as other shear stress experimental groups. In the third study, we carried on the use of the optimal FIS stress loading conditions and combined with bioactive agents to yield additive improvements on the biochemical and mechanical properties of neocartilage. In the fourth study, we implanted the neocartilage constructs in athymic mice and found that they remodeled and matured *in vivo* toward native characteristics. In the fifth study, we successfully translated the optimal FIS stress stimulation loading conditions to human cartilage tissue culture. Finally, in the sixth study, we elucidated a complex on the primary cilia of both human and bovine chondrocytes that is sensitive to fluid flow and may be responsible for the observed improvements. This work is

significant because it presents a comprehensive examination of how fluid-induced shear stress improves neocartilage formation based on mechanotransduction through the primary cilia. Importantly, we showed that the magnitude of the applied fluid-induced shear stress can be tuned to elicit large improvements in mechanical, structural, and biochemical properties of tissue-engineered constructs.

There is a lack of clarity on the effects of fluid-induced shear stress on tissues. On one hand, fluid flow is known to increase nutrient perfusion and waste transport which is conducive to cellular health.[46] However, with fluid flow comes fluid-induced shear stress, which at high magnitudes may lead to pathologic tissue states in some cell types. For example in human chondrocytes, high-shear environments have been shown to cause apoptosis and increases in proinflammatory factors.[5, 45] Juxtaposed against these results, cartilage tissue culture that includes a shear stress regimen has been shown to lower coefficient of friction.[17, 18] Our work here shows that, during cartilage tissue culture, shear stress can be harmful at high shear stress levels (>0.21Pa), and beneficial for mechanical and biochemical properties within the range of 0.05-0.21Pa. This is in accordance with other tissue types such as vascular tissue, where shear stress less than 0.5Pa is conducive to angiogenesis[46], but at 20Pa, it leads to atherosclerosis.[47] This supports the hypothesis that the shear stress magnitude implemented during tissue culture can be optimized to provide improvements in neotissue properties.

When culturing neotissues and cells under physiologically relevant mechanical cues, it should be noted that native cells experience different magnitudes of mechanical stress compared to the surrounding tissue matrix. For native articular cartilage of the knee, biphasic models incorporating finite element analysis of interstitial fluid flux around chondrocytes show that the extracellular matrix experiences peak shear stresses of 55 kPa due to tissue deformation under physiological conditions. However, the chondrocytes dwelling in the tissue, which are protected by the pericellular and extracellular matrices, experience fluid-induced

shear stress at around 0.065Pa.[48] The shear stress experienced by native articular chondrocytes of the knee is comparable to the range of FIS stress found here to produce the most improved neocartilage constructs (0.05-0.21Pa), thus providing indirect validation of the computational model.[48] The self-assembled neocartilage constructs used in the studies presented are dense with chondrocytes in comparison to native articular cartilage and are not as well shielded by a collagenous matrix from fluid-induced shear stress. Therefore, we believe that the chondrocytes residing in the self-assembled neocartilage are experiencing similar shear stress magnitudes as they would in a native environment.

Histological staining showed that the fiber density of the neocartilage stimulated with FIS stress is uniform throughout. Because only the chondrocytes on the surface of the neocartilage constructs are exposed to the FIS stress imparted by the device, it is possible that the chondrocytes within the neocartilage are experiencing paracrine effects. Further experiments need to be performed under well-controlled shear regiments to fully understand the effects of paracrine signaling and to differentiate them from mechanotransduction. Additionally, it is possible that the improvements in neocartilage constructs stimulated with FIS stress may be partly attributed to increased nutrient diffusion and oxygen distribution. Previous studies have explored the use of spinner flasks and have found that neocartilage that remained in fluid flow for 6 weeks was inferior in terms of glycosaminoglycan content and collagen content when compared to neocartilage that experienced fluid flow for 2 weeks of culture.[53] A separate study showed that a continuous fluid flow applied on neocartilage for 3 days increased collagen type II deposition.[18] Interestingly, the shear stress applied in the previous study, 0.1Pa, is on the same order of magnitude as the optimal FIS stress found here, 0.05-0.21Pa. These studies further support the hypothesis that an optimal shear stress magnitude is important for the successful application of FIS stress on neotissues.

For other forms of mechanical stimulation on chondrocytes, mechanotransduction pathways, such as TRPV4 activation in tension, have been implicated.[13] To this list we now add the activation of the mechanically gated complex PC1/2 via fluid-induced shear stress. In osteoblasts and osteocytes, this mechanically gated complex allows for fluid flow-induced influx of Ca^{2+} ions.[49] For chondrocytes, it has been shown that the PC1/2 complex is involved in mechanotransducing compressive forces.[14] Because chondrocyte cilia have been previously observed,[14, 49] and because genomic data suggest that the PC1/2 complex exists on chondrocyte primary cilia,[38, 41, 49] our findings add to this body of work in implicating the PC1/2 complex in mechanotransducing fluid-induced shear stress in chondrocytes as well. Although further study, such as antagonizing primary cilia to show loss or gain of function, is necessary to fully confirm FIS stress modes of action on chondrocytes, this series of studies showed that shear stress stimulation acts via mechanotransduction to increase extracellular matrix content and to enhance mechanical properties.

In vivo, FIS stress-stimulated constructs were shown to outperform statically cultured constructs. There is a dearth of studies examining *in vivo* functionality of constructs stimulated with either direct shear stress or fluid-induced shear stress.[12] *In vitro* studies show that direct shear stress enhances *in vitro* integration,[50] as well as reduced friction coefficients.[51] Our work using fluid-induced shear stress showed its superior ability in cartilage to effect remodeling and maturation that carry over to the *in vivo* environment. These effects were manifested in increases in collagen content, chondrocyte organization, and pronounced lacunae of FIS stress-stimulated constructs. Although orthotopic *in vivo* implantation studies are necessary as a next step to validate functional superiority, this series of studies yielded promising results for the translational potential of neocartilage stimulated with FIS stress.

Here, we reported the design and use of a shear-loading device that successfully applies fluid flow-induced shear stress to tissue-engineer cartilage with enhanced compressive, shear,

tensile, structural, and biochemical properties. The device, capable of inducing FIS stresses spanning 0-0.85Pa, is potentially suitable for both scaffold-based and scaffold-free culture of neotissues, including tissue engineered bone, muscle, tendon, ligament, and fibrocartilage. For articular cartilage tissue engineering, we identified a FIS stress range, 0.05-0.21Pa, that improves mechanical properties by 1.9- to 3.6-fold via a primary cilia-based mechanosensitive complex. To implement this strategy for other tissue types in the future, one must identify optimal loading parameters for specific tissue culture conditions, including the use of scaffolds. In self-assembled neocartilage, this series of studies showed that the optimized regimen of FIS stress alone yields large enhancements in neocartilage properties. When a cocktail of bioactive agents was combined with FIS stress, further additive improvements in both mechanical and biochemical characteristics of neocartilage were noted. Toward translating these findings to human neocartilage, human articular chondrocytes exposed to FIS stress responded in a robust manner resulting in the formation of appropriately stiff and strong tissue-engineered cartilage, increasing mechanical properties by 0.7- to 2-fold. Together, these data demonstrated the beneficial contribution of fluid-induced shear stress to neocartilage tissue culture.

REFERENCES

[1] T.J. Goodwin, T.L. Prewett, D.A. Wolf, G.F. Spaulding, Reduced shear stress: A major component in the ability of mammalian tissues to form three-dimensional assemblies in simulated microgravity, Journal of Cellular Biochemistry 51(3) (1993) 301-311.

[2] Osteoarthritis Research Society International: OA as a serious disease, White Paper submited to U.S Food and Drug Administration, https://www.oarsi.org/sites/default/files/docs/2016/oarsi_white_paper_oa_serious_disease_121 416_1.pdf, 2016.

[3] J.M. Archambault, M.K. Elfervig-Wall, M. Tsuzaki, W. Herzog, A.J. Banes, Rabbit tendon cells produce MMP-3 in response to fluid flow without significant calcium transients, Journal of Biomechanics 35(3) (2002) 303-309.

[4] R.L. Smith, Trindade, M.C.D., Ikenoue, T. , Mohtai, M. , Das, P. , Carter, D.R., Goodman, S.B. , Schurman, D.J., Effects of shear stress on articular chondrocyte metabolism, Biorheology 37(1) (2000) 95-107.

[5] Z.R. Healy, F. Zhu, J.D. Stull, K. Konstantopoulos, Elucidation of the signaling network of COX-2 induction in sheared chondrocytes: COX-2 is induced via a Rac/MEKK1/MKK7/JNK2/c-Jun-C/EBPβ-dependent pathway, American Journal of Physiology-Cell Physiology 294(5) (2008) C1146-C1157.

[6] H. Kwon, N.K. Paschos, J.C. Hu, K.A. Athanasiou, Articular cartilage tissue engineering: the role of signaling molecules, Cellular and Molecular Life Sciences 73(6) (2016) 1173-1194.

[7] K.A. Athanasiou, R. Eswaramoorthy, P. Hadidi, J.C. Hu, Self-organization and the self-assembling process in tissue engineering, Annual Review of Biomedical Engineering 15 (2013) 115-136.

[8] J.C. Hu, K.A. Athanasiou, A self-assembling process in articular cartilage tissue engineering, Tissue Engineering 12(4) (2006) 969-979.

[9] K.A. Athanasiou, E.M. Darling, J.C. Hu, G.D. DuRaine, A.H. Reddi, Articular Cartilage, 2 ed., CRC Press, 2017.

[10] D.J. Huey, J.C. Hu, K.A. Athanasiou, Unlike bone, cartilage regeneration remains elusive, Science 338(6109) (2012) 917-921.

[11] R. Langer, J.P. Vacanti, Tissue engineering, Science 260(5110) (1993) 920.

[12] E.Y. Salinas, J.C. Hu, K.A. Athanasiou, A guide for using mechanical stimulation to enhance tissue-engineered articular cartilage properties, Tissue Engineering Part B: Reviews 24(5) (2018) 345-358.

[13] J.K. Lee, L.W. Huwe, N. Paschos, A. Aryaei, C.A. Gegg, J.C. Hu, K.A. Athanasiou, Tension stimulation drives tissue formation in scaffold-free systems, Nature Materials 16(8) (2017) 864.

[14] A.K. Wann, N. Zuo, C.J. Haycraft, C.G. Jensen, C.A. Poole, S.R. McGlashan, M.M. Knight, Primary cilia mediate mechanotransduction through control of ATP-induced Ca2+ signaling in compressed chondrocytes, The FASEB Journal 26(4) (2012) 1663-1671.

[15] H. Kwon, S.A. O'Leary, J.C. Hu, K.A. Athanasiou, Translating the application of transforming growth factor-β1, chondroitinase-ABC, and lysyl oxidase-like 2 for mechanically robust tissue-engineered human neocartilage, Journal of Tissue Engineering and Regenerative Medicine 13(2) (2019) 283-294.

[16] J.C. Bernhard, G. Vunjak-Novakovic, Should we use cells, biomaterials, or tissue engineering for cartilage regeneration?, Stem Cell Research & Therapy 7(1) (2016) 56.

[17] C.V. Gemmiti, R.E. Guldberg, Shear stress magnitude and duration modulates matrix composition and tensile mechanical properties in engineered cartilaginous tissue, Biotechnology and Bioengineering 104(4) (2009) 809-820.

[18] C.V. Gemmiti, R.E. Guldberg, Fluid flow increases type II collagen deposition and tensile mechanical properties in bioreactor-grown tissue-engineered cartilage, Tissue Engineering 12(3) (2006) 469-479.

[19] R.S. Cherry, E.T. Papoutsakis, Hydrodynamic effects on cells in agitated tissue culture reactors, Bioprocess Engineering 1(1) (1986) 29-41.

[20] C.M. Begley, S.J. Kleis, The fluid dynamic and shear environment in the NASA/JSC rotating-wall perfused-vessel bioreactor, Biotechnology and Bioengineering 70(1) (2000) 32-40.

[21] R.E. Berson, M.R. Purcell, M.K. Sharp, Computationally determined shear on cells grown in orbiting culture dishes, Oxygen Transport to Tissue XXIX, Springer2008, pp. 189-198.

[22] J.M.D. Thomas, A. Chakraborty, M.K. Sharp, R.E. Berson, Spatial and temporal resolution of shear in an orbiting petri dish, Biotechnology Progress 27(2) (2011) 460-465.

[23] A. Chakraborty, S. Chakraborty, V.R. Jala, J.M. Thomas, M.K. Sharp, R.E. Berson, B. Haribabu, Impact of bi-axial shear on atherogenic gene expression by endothelial cells, Annals of Biomedical Engineering 44(10) (2016) 3032-3045.

[24] V.C. Mow, S. Kuei, W.M. Lai, C.G. Armstrong, Biphasic creep and stress relaxation of articular cartilage in compression: theory and experiments, Journal of Biomechanical Engineering 102(1) (1980) 73-84.

[25] L.A. Setton, W. Zhu, V.C. Mow, The biphasic poroviscoelastic behavior of articular cartilage: role of the surface zone in governing the compressive behavior, Journal of Biomechanics 26(4-5) (1993) 581-592.

[26] V.C. Mow, M.C. Gibbs, W.M. Lai, W.B. Zhu, K.A. Athanasiou, Biphasic indentation of articular cartilage—II. A numerical algorithm and an experimental study, Journal of Biomechanics 22(8) (1989) 853-861.

[27] X. Lu, V. Mow, Biomechanics of articular cartilage and determination of material properties, Medicine and Science in Sports and Exercise 40(2) (2008) 193.

[28] D.D. Cissell, J.M. Link, J.C. Hu, K.A. Athanasiou, A modified hydroxyproline assay based on hydrochloric acid in Ehrlich's solution accurately measures tissue collagen content, Tissue Engineering Part C: Methods 23(4) (2017) 243-250.

[29] S. Heinz, C. Benner, N. Spann, E. Bertolino, Y.C. Lin, P. Laslo, J.X. Cheng, C. Murre, H. Singh, C.K. Glass, Simple combinations of lineage-determining transcription factors prime cis-regulatory elements required for macrophage and B cell identities, Molecular Cell 38(4) (2010) 576-589.

[30] R.L. Trevino, C.A. Pacione, A.-M. Malfait, S. Chubinskaya, M.A. Wimmer, Development of a Cartilage Shear-Damage Model to Investigate the Impact of Surface Injury on Chondrocytes and Extracellular Matrix Wear, Cartilage 8(4) (2016) 444-455.

[31] J.C. Bernhard, E. Hulphers, B. Rieder, J. Ferguson, D. Rünzler, T. Nau, H. Redl, G. Vunjak-Novakovic, Perfusion Enhances Hypertrophic Chondrocyte Matrix Deposition, But Not the Bone Formation, Tissue Engineering Part A 24(11-12) (2018) 1022-1033.

[32] E.A. Makris, R.F. MacBarb, N.K. Paschos, J.C. Hu, K.A. Athanasiou, Combined use of chondroitinase-ABC, TGF-β1, and collagen crosslinking agent lysyl oxidase to engineer functional neotissues for fibrocartilage repair, Biomaterials 35(25) (2014) 6787-6796.

[33] D.J. Huey, K.A. Athanasiou, Maturational growth of self-assembled, functional menisci as a result of TGF-β1 and enzymatic chondroitinase-ABC stimulation, Biomaterials 32(8) (2011) 2052-2058.

[34] D.R. Eyre, M.A. Weis, J.-J. Wu, Advances in collagen cross-link analysis, Methods 45(1) (2008) 65-74.

[35] J.K. Lee, J.C. Hu, S. Yamada, K.A. Athanasiou, Initiation of chondrocyte self-assembly requires an intact cytoskeletal network, Tissue Engineering Part A 22(3-4) (2016) 318-325.

[36] J. Jurvelin, M. Buschmann, E. Hunziker, Mechanical anisotropy of the human knee articular cartilage in compression, Proceedings of the Institution of Mechanical Engineers, Part H: Journal of Engineering in Medicine 217(3) (2003) 215-219.

[37] J.T. Eggenschwiler, K.V. Anderson, Cilia and Developmental Signaling, Annual Review of Cell and Developmental Biology 23(1) (2007) 345-373.

[38] Y. Rais, A. Reich, S. Simsa-Maziel, M. Moshe, A. Idelevich, T. Kfir, N. Miosge, E. Monsonego-Ornan, The growth plate's response to load is partially mediated by mechano-sensing via the chondrocytic primary cilium, Cellular and Molecular Life Sciences 72(3) (2015) 597-615.

[39] M.J. Hilton, X. Tu, J. Cook, H. Hu, F. Long, Ihh controls cartilage development by antagonizing Gli3, but requires additional effectors to regulate osteoblast and vascular development, Development 132(19) (2005) 4339.

[40] A.N. Gargalionis, E.K. Basdra, A.G. Papavassiliou, Polycystins in disease mechanobiology, Journal of Cellular Biochemistry 0(0) (2018).

[41] A. Mangolini, L. de Stephanis, G. Aguiari, Role of calcium in polycystic kidney disease: From signaling to pathology, World Journal of Nephrology 5(1) (2016) 76-83.

[42] S.-K. Han, W. Wouters, A. Clark, W. Herzog, Mechanically induced calcium signaling in chondrocytes in situ, Journal of Orthopaedic Research 30(3) (2012) 475-481.

[43] J.F. Weber, S.D. Waldman, Calcium signaling as a novel method to optimize the biosynthetic response of chondrocytes to dynamic mechanical loading, Biomech Model Mechanobiol 13(6) (2014) 1387-1397.

[44] A.J. Grodzinsky, M.E. Levenston, M. Jin, E.H. Frank, Cartilage Tissue Remodeling in Response to Mechanical Forces, Annual Review of Biomedical Engineering 2(1) (2000) 691-713.

[45] P. Wang, P.-P. Guan, C. Guo, F. Zhu, K. Konstantopoulos, Z.-Y. Wang, Fluid shear stress-induced osteoarthritis: roles of cyclooxygenase-2 and its metabolic products in inducing the expression of proinflammatory cytokines and matrix metalloproteinases, FASEB journal 27(12) (2013) 4664-4677.

[46] K.S. Cunningham, A.I. Gotlieb, The role of shear stress in the pathogenesis of atherosclerosis, Laboratory Investigation 85(1) (2005) 9-23.

[47] J.-J. Chiu, P.-L. Lee, C.-N. Chen, I. Lee Chih, S.-F. Chang, L.-J. Chen, S.-C. Lien, Y.-C. Ko, S. Usami, S. Chien, Shear Stress Increases ICAM-1 and Decreases VCAM-1 and E-selectin Expressions Induced by Tumor Necrosis Factor-α in Endothelial Cells, Arteriosclerosis, Thrombosis, and Vascular Biology 24(1) (2004) 73-79.

[48] G.A. Ateshian, K.D. Costa, C.T. Hung, A theoretical analysis of water transport through chondrocytes, Biomech Model Mechanobiol 6(1-2) (2007) 91-101.

[49] Z.S. Xiao, L.D. Quarles, Role of the polycytin-primary cilia complex in bone development and mechanosensing, Annals of the New York Academy of Sciences 1192(1) (2010) 410-421.

[50] J.S. Theodoropoulos, A.J. DeCroos, M. Petrera, S. Park, R.A. Kandel, Mechanical stimulation enhances integration in an in vitro model of cartilage repair, Knee Surgery, Sports Traumatology, Arthroscopy 24(6) (2016) 2055-2064.

[51] S. Grad, M. Loparic, R. Peter, M. Stolz, U. Aebi, M. Alini, Sliding motion modulates stiffness and friction coefficient at the surface of tissue engineered cartilage, Osteoarthritis and Cartilage 20(4) (2012) 288-295.

[52] J.M.D. Thomas, A. Chakraborty, R.E. Berson, M. Shakeri, M.K. Sharp, Validation of a CFD model of an orbiting culture dish with PIV and analytical solutions, AIChE Journal 63(9) (2017) 4233-4242.

[53] S.E. Carver, C.A. Heath, Influence of intermittent pressure, fluid flow, and mixing on the regenerative properties of articular chondrocytes, Biotechnology and Bioengineering 65(3) (1999) 274-281.

SUPPLEMENTAL DATA

Supplementary Table 1 | Optimizing FIS stress loading magnitudes in bovine constructs

S1A. Out Short

	Static	FIS 25	FIS 50	FIS 100
H_A (kPa) Average ± SD	133±50	44±21	379±76	95±36
E_Y (MPa) Average ± SD	0.78±0.26	0.76±0.32	1.34±0.35	0.52±0.14

UTS (MPa) Average ± SD	0.23±0.07	0.21±0.05	0.38±0.10	0.19±0.08
GAG (%/DW) Average ± SD	43±6	50±3	45±3	41±3
Col (%/DW) Average ± SD	12±1	12±1	13±1	10±1
DNA (ng/mg DW) Average ± SD	7687±1150	5862±1153	5510±1006	7951±1565

S1A. Out Short refers to constructs placed in the outer circle of the FIS stress device and cultured with 6 days of FIS stress stimulation. The column labeled "Static" refers to constructs that were not stimulated with FIS stress. The column labeled "FIS 25" refers to constructs that were cultured with the orbital shaker set at 25RPM. The column labeled "FIS 50" refers to constructs that were cultured with the orbital shaker set at 50RPM. The column labeled "FIS 100" refers to constructs that were cultured with the orbital shaker set at 100RPM.

S1B. In Short

	Static	FIS 25	FIS 50	FIS 100
H_A (kPa) Average ± SD	63±25	76±39	347±72	81±44
E_Y (MPa) Average ± SD	0.59±0.15	0.89±0.28	1.17±0.36	0.47±0.12
UTS (MPa) Average ± SD	0.18±0.05	0.19±0.05	0.42±0.14	0.14±0.03
GAG (%/DW) Average ± SD	44±8	50±2	43±2	46±5
Col (%/DW) Average ± SD	13±1	12±1	12±1	10±2
DNA (ng/mg DW) Average ± SD	4638±1724	7306±692	4463±1208	5985±2005

S1B. In Short refers to constructs placed in the inner circle of the FIS stress device and cultured with 6 days of FIS stress stimulation. The column labeled "Static" refers to constructs that were not stimulated with FIS stress. The column labeled "FIS 25" refers to constructs that were cultured with the orbital shaker set at 25RPM. The column labeled "FIS 50" refers to constructs that were cultured with the orbital shaker set at 50RPM. The column labeled "FIS 100" refers to constructs that were cultured with the orbital shaker set at 100RPM.

S1C. Out Long

	Static	FIS 50	FIS 100
H_A (kPa) Average ± SD	165±77	335±50	242±45
E_Y (MPa) Average ± SD	0.64±0.26	1.87±0.59	0.55±0.26
UTS (MPa) Average ± SD	0.22±0.05	0.60±0.15	0.21±0.05
GAG (%/DW) Average ± SD	44±4	42±4	42±2
Col (%/DW) Average ± SD	12±1	13±1	9±1
DNA (ng/mg DW) Average ± SD	7537±1791	6586±861	7375±807

S1C. Out Long refers to constructs placed in the outer circle of the FIS stress device and cultured with 12 days of FIS stress stimulation. The column labeled "Static" refers to constructs that were not stimulated with FIS stress. The column labeled "FIS 50" refers to constructs that were cultured with the orbital shaker set at 50RPM. The column labeled "FIS 100" refers to constructs that were cultured with the orbital shaker set at 100RPM.

S1D. In Long

	Static	FIS 50	FIS 100
H_A (kPa) Average ± SD	165±77	358±47	158±59
E_Y (MPa) Average ± SD	0.64±0.26	1.18±0.31	0.67±0.13
UTS (MPa) Average ± SD	0.22±0.05	0.54±0.08	0.23±0.03
GAG (%/DW) Average ± SD	44±4	45±3	40±5
Col (%/DW) Average ± SD	12±1	13±1	10±2
DNA (ng/mg DW) Average ± SD	5635±438	6259±1255	7854±832

S1D. In Long refers to constructs placed in the inner circle of the FIS stress device and cultured with 12 days of FIS stress stimulation. The column labeled "Static" refers to constructs that were not stimulated with FIS stress. The column labeled "FIS 50" refers to constructs that were cultured with the orbital shaker set at 50RPM. The column labeled "FIS 100" refers to constructs that were cultured with the orbital shaker set at 100RPM.

Supplementary Table 2 | Combining FIS stress with bioactive factors in bovine constructs

S2A. 4wks *in vitro*

	Static	FIS	BaF	FIS+BaF
H_A (kPa) Average ± SD	170±37	250±40	224±34	304±21
E_Y (MPa) Average ± SD	0.58±0.25	1.20±0.26	1.00±0.24	1.05±0.30
UTS (MPa) Average ± SD	0.26±0.11	0.49±0.09	0.45±0.11	0.42±0.13
GAG (%/DW) Average ± SD	39±2	29±3	20±2	31±1
Col (%/DW) Average ± SD	16±3	14±2	20±3	24±2

S2A. The column labeled "Static" refers to constructs that were not stimulated with FIS stress or bioactive factors. The column labeled "FIS" refers to constructs that were treated with FIS stress only. The column labeled "BaF" refers to constructs that were treated with bioactive factors only. The column labeled "FIS+BaF" refers to constructs that were treated with both FIS stress and bioactive factors.

S2B. 8wks *in vitro*

	Static	FIS	FIS+BaF
H_A (kPa) Average ± SD	82±27	166±42	243±41
E_Y (MPa) Average ± SD	0.43±0.26	1.00±0.33	1.28±0.28
UTS (MPa) Average ± SD	0.16±0.11	0.53±0.26	0.72±0.26

	Static	FIS	FIS+BaF
GAG (%/WW) Average ± SD	4±1	4±1	5±1
Col (%/WW) Average ± SD	2±1	2±1	2±1

S2B. The column labeled "Static" refers to constructs that were not stimulated with FIS stress or bioactive factors. The column labeled "FIS" refers to constructs that were treated with FIS stress only. The column labeled "FIS+BaF" refers to constructs that were treated with both FIS stress and bioactive factors.

Supplementary Table 3 | Neotissue properties after subcutaneous implantation into athymic mice

	Static	FIS	FIS+BaF
H_A (kPa) Average ± SD	124±23	178±28	224±36
E_Y (MPa) Average ± SD	1.16±0.33	1.48±0.41	1.39±0.37
UTS (MPa) Average ± SD	0.74±0.3	0.86±0.28	1.10±0.37
GAG (%/WW) Average ± SD	4±1	3±1	4±1
Col (%/WW) Average ± SD	3±1	3±0	5±1

S3. The column labeled "Static" refers to constructs that were not stimulated with FIS stress or bioactive factors. The column labeled "FIS" refers to constructs that were treated with FIS stress only. The column labeled "FIS+BaF" refers to constructs that were treated with both FIS stress and bioactive factors.

Supplementary Table 4 | Translating to human articular chondrocytes

	Static	FIS
H_A (kPa) Average ± SD	33±3	64±20

E_Y (MPa) Average ± SD	0.81±0.34	2.18±0.74
UTS (MPa) Average ± SD	0.53±0.25	1.19±0.16
GAG (%/DW) Average ± SD	15±3	13±3
Col (%/DW) Average ± SD	11±2	15±3

S4. The column labeled "Static" refers to constructs that were treated with only bioactive factors. The column labeled "FIS" refers to constructs that were treated with FIS stress and bioactive factors.

Supplementary Table 5 | Verifying upregulation of genes of interest via RT-PCR

S5A. Primers used in RT-PCR for bovine chondrocytes

Gene Name	Primer Direction	Sequence
PKD1	Forward	GGT GAG ACG GTC TTG GAA TTA G
	Reverse	GTC ACC CTT CCA GAA CAT ACA G
PKD2	Forward	CGG CAA CTC AGA GTC AGA AA
	Reverse	GCT GAC GGA GTA CAC ATC ATA G
IHH	Forward	CTT CAC CTG GGC TTC CTA AG
	Reverse	TGC CTT CCT CCC TAG TCT AAT
GAPDH (Housekeeping)	Forward	AAG TTC AAC GGC ACA GTC AA
	Reverse	GAT CTC GCT CCT GGA AGA TG

S5B. Primers used in RT-PCR for human chondrocytes

Gene Name	Primer Direction	Sequence

PKD1	Forward	CTG TGG GCT TCA GCA CTT TA
	Reverse	GAG GCT AGA AAC CGT CCA ATA C
PKD2	Forward	CTT TCC TTC CCA CTG TCC TAT G
	Reverse	GAG GGC TAA CAG AAG AGA GAA TG
IHH	Forward	CCA CAC TGA CCT CAC CAT TTA C
	Reverse	GAG CAC AAG GGC ATG GTT ATA G
B2M (Housekeeping)	Forward	CCA GCG TAC TCC AAA GAT TCA
	Reverse	TGG ATG AAA CCC AGA CAC ATA G

Supplementary Figure 1 | Pathway Enrichment Analysis

R-HSA-1640170: Cell Cycle
GO:0043408: regulation of MAPK cascade
GO:0006935: chemotaxis
M5885: NABA MATRISOME ASSOCIATED
GO:0043269: regulation of ion transport
GO:0030155: regulation of cell adhesion
R-HSA-109582: Hemostasis
GO:0043062: extracellular structure organization
GO:0045055: regulated exocytosis
GO:0051301: cell division
GO:0001568: blood vessel development
GO:0008285: negative regulation of cell proliferation
GO:0070482: response to oxygen levels
hsa04015: Rap1 signaling pathway
GO:0044772: mitotic cell cycle phase transition
GO:0097529: myeloid leukocyte migration
R-HSA-6785807: Interleukin-4 and Interleukin-13 signaling
GO:2001233: regulation of apoptotic signaling pathway
GO:0097435: supramolecular fiber organization
GO:0003013: circulatory system process
GO:0032787: monocarboxylic acid metabolic process
GO:0099536: synaptic signaling
GO:0051129: negative regulation of cellular component organization
GO:0007169: transmembrane receptor protein tyrosine kinase signaling pathway
M5884: NABA CORE MATRISOME
hsa04066: HIF-1 signaling pathway
GO:0001503: ossification
GO:0018209: peptidyl-serine modification
GO:0032963: collagen metabolic process
GO:0006979: response to oxidative stress
GO:0001101: response to acid chemical
GO:0032103: positive regulation of response to external stimulus
R-HSA-983189: Kinesins
M14: PID AURORA B PATHWAY
M129: PID PLK1 PATHWAY
hsa05200: Pathways in cancer
GO:0070848: response to growth factor
R-HSA-112316: Neuronal System
GO:0001817: regulation of cytokine production
GO:0009636: response to toxic substance
GO:0007610: behavior
GO:0048732: gland development
GO:0009612: response to mechanical stimulus
hsa04510: Focal adhesion
R-HSA-1280218: Adaptive Immune System
GO:0052547: regulation of peptidase activity
GO:0071248: cellular response to metal ion
GO:0045787: positive regulation of cell cycle
GO:0060627: regulation of vesicle-mediated transport
GO:0033002: muscle cell proliferation
M166: PID ATF2 PATHWAY
GO:0048017: inositol lipid-mediated signaling
hsa04611: Platelet activation
GO:1901841: regulation of high voltage-gated calcium channel activity
hsa04110: Cell cycle
GO:0007204: positive regulation of cytosolic calcium ion concentration
GO:0062013: positive regulation of small molecule metabolic process
GO:0009991: response to extracellular stimulus
M3468: NABA ECM REGULATORS
R-HSA-373760: L1CAM interactions
GO:0051051: negative regulation of transport
GO:0085029: extracellular matrix assembly
GO:0040008: regulation of growth
GO:0071396: cellular response to lipid
GO:0042326: negative regulation of phosphorylation
GO:0045981: positive regulation of nucleotide metabolic process
GO:0031099: regeneration
GO:0019216: regulation of lipid metabolic process
GO:0050866: negative regulation of cell activation
GO:0019932: second-messenger-mediated signaling
GO:0010876: lipid localization
GO:1904029: regulation of cyclin-dependent protein kinase activity
GO:0002237: response to molecule of bacterial origin
hsa04933: AGE-RAGE signaling pathway in diabetic complications
CORUM:310: Cell cycle kinase complex CDC2
hsa05323: Rheumatoid arthritis
GO:0031589: cell-substrate adhesion
GO:0002279: mast cell activation involved in immune response
GO:1903046: meiotic cell cycle process
GO:0048608: reproductive structure development
GO:0019233: sensory perception of pain
GO:0071459: protein localization to chromosome, centromeric region
GO:0051383: kinetochore organization
hsa04931: Insulin resistance
GO:0003018: vascular process in circulatory system
R-HSA-3928665: EPH-ephrin mediated repulsion of cells
CORUM:127: NDC80 kinetochore complex
GO:0007507: heart development
R-HSA-8957275: Post-translational protein phosphorylation
hsa04610: Complement and coagulation cascades
GO:0010952: positive regulation of peptidase activity
R-HSA-76002: Platelet activation, signaling and aggregation
GO:0061448: connective tissue development
GO:0060485: mesenchyme development
GO:0007264: small GTPase mediated signal transduction
GO:1900449: regulation of glutamate receptor signaling pathway
GO:0034756: regulation of iron ion transport
hsa05230: Central carbon metabolism in cancer
R-HSA-202733: Cell surface interactions at the vascular wall
GO:0072593: reactive oxygen species metabolic process

-log10(P)

CHAPTER 3- THE EFFECTS OF SHEAR STRESS STIMULATION ACROSS THE DEVELOPMENTAL STAGES OF SELF-ASSEMBLED NEOCARTILAGE

ABSTRACT

Cartilage degradation develops in about 27 million Americans each year, and current treatment options are inefficient long-term solutions. An emerging treatment is the fabrication of replacement cartilage using tissue engineering. Mechanical stimulation during culture has been shown to improve the properties of neocartilage constructs, yet shear stress stimulation has not been fully studied. An optimal fluid-induced shear stress magnitude has previously been identified, and the purpose of these experiments was to determine if it is most beneficial to apply shear stress during an earlier time (synthesis) or a later time (maturation) in the tissue development of neocartilage culture. Because the tissue matrix of neocartilage changes as tissue culture progresses, we hypothesize that if we apply fluid-induced shear stress stimulation during different time intervals of development, the tissue will present different mechanical and biochemical properties. Mechanical testing and biochemical analysis revealed that neocartilage stimulated during the later time point, also known as the maturation stage, was significantly higher in mechanical stiffness and collagen content compared to unstimulated controls by 3-fold and 2-fold, respectively. These results indicate that when fluid-induced shear stress stimulation is implemented during the maturation stage, neocartilage constructs with properties that are more similar to those of native cartilage are produced. Consequently, we can get closer to providing a better treatment option for those who suffer from cartilage degradation.

Authors: Salinas EY, Herrera JM, Hu JC, Athanasiou KA

Manuscript Prepared for Submission

INTRODUCTION

Articular cartilage is a smooth, white tissue covering the ends of bones that distributes forces during movement. Trauma and wear can cause defects in articular cartilage, which lead to uneven loading distributions and concentrated stress at the edges of the defect. This uneven concentration of stress leads to further deterioration, and ultimately, osteoarthritis. According to the Center for Disease Control and Prevention, osteoarthritis is estimated to develop in about 67.2 million Americans by the year 2025.[1] Currently, the most common clinical solutions for treating articular cartilage lesions are chondroplasty and microfracture, neither of which is considered effective for more than 5 years post-treatment.[2-4] An emerging solution for articular cartilage defects is the tissue engineering of scaffold-less neocartilage constructs for implantation. Scaffold-less techniques, including the self-assembling process, remove the need for exogenous materials that have disadvantages, such as inadequate degradation rates and the obstruction of mechanotransduction.[5-7] There is a need to develop a long-term solution for the treatment of articular cartilage lesions, and tissue-engineering neocartilage using the self-assembling process is a promising option.

A favorable cell source and species for the *in vitro* experimentation of neocartilage constructs are chondrocytes from the costal cartilage of the Yucatan minipig. Costal chondrocytes allow for autologous chondrocyte harvest without the need to further damage the affected joint. Although costal cartilage does not articulate, costal chondrocytes produce hyaline cartilage when self-assembled to form neocartilage, and they are advantageous over other alternative cell sources because they regain their chondrogenic phenotype via aggregate redifferentiation after expansion.[8] Costal chondrocytes from Yucatan minipigs can be considered an effective and efficient cell source to use in the laboratory to form neocartilage because of their chondrogenic phenotype and translatable potential.

The signals generated from the mechanical forces imparted during motion help maintain articular cartilage health, and may be replicated *in vitro* with the use of bioreactors to create neocartilage with robust mechanical properties and extracellular matrix.[9, 10] Because articular cartilage is avascular, native chondrocytes depend on mechanical movement for nutrient transport, signaling, and cellular waste removal.[11-13] In native articular cartilage, mechanical forces, such as compression, tension, shear, and hydrostatic pressure are generated during motion. *In vitro*, compressive stimulation has been shown to lead to the synthesis of extracellular matrix and to improve compressive properties,[9, 14-16] and tensile stimulation has been shown to increase tensile stiffness and glycosaminoglycan content in neocartilage.[17, 18] Of particular interest to this study is shear stress, which has been shown to mechano-regulate ion channels on the primary cilia of chondrocytes, and to improve extracellular matrix content and mechanical properties.[19-22] Collectively, these studies show the importance of using mechanical stimulation to improve neocartilage properties toward those of native articular cartilage.

During development there is an important interplay between mechanical stimuli, signaling factors, and cell-to-cell signaling.[13, 23] These signals and stimuli are essential in providing cues to create the complex structure of articular cartilage. Chondrocytes need mechanical loading during embryonic development to produce and maintain the extracellular matrix. [24, 25] Subsequently, during postnatal development, mechanical loading regulates cartilage thickness for proper function.[13, 26] Self-assembled neocartilage has been shown to follow similar developmental steps as native tissue.[5, 27] First, the cells are seeded in a nonadherent substrate such as a hydrogel, and after four hours, the cells interact and undergo minimization of free energy.[28] Next, the neocartilage undergoes stages of synthesis and maturation. During the synthesis stage, the chondrocytes begin to produce extracellular matrix. Next, in the maturation stage neocartilage produces more glycosaminoglycans and decreases

its collagen content (Figure 1).[14, 27] In particular, previous studies on self-assembled neocartilage have shown that the application of compressive stimulation during the synthesis stage leads to an improved aggregate modulus over neocartilage stimulated during the maturation stage. [14] This information indicates that when creating neocartilage, mechanical stimulation should be included, and that it is important to determine the stage of cartilage development during which mechanical stimulation should be applied. [29]

The experiments presented here focus on the application of fluid-induced shear stress across the stages of neocartilage self-assembly. Fluid-induced shear stress stimulation has shown to improve the properties of self-assembled neocartilage constructs,[21, 22] and in this article when shear stress is mentioned, fluid-induced shear stress is being referred. Although an optimal shear stress magnitude has previously been identified (0.05-0.21Pa), it is unknown when its application during tissue culture is most effective. Therefore, the first objective of these studies was to determine if it is most beneficial to apply shear stress during the synthesis stage or during the maturation stage of the neocartilage self-assembling process (Figure 1). This was done with bovine articular chondrocytes, as they are inexpensive and widely available. The second objective of this study was to determine the translatability of this shear stress stimulation regimen to a more clinically relevant animal model and cell source, i.e., costal chondrocytes from the Yucatan minipig.[30, 31] To assess these two objectives, mechanical properties and extracellular matrix content are measured in every study. The hypotheses are that the application of shear stress stimulation during one of the stages of self-assembly will better enhance the mechanical properties and extracellular matrix content of neocartilage than the other stage and also over nonstimulated controls, and that this stage of application will also be useful for improving neocartilage created with minipig costal chondrocytes.
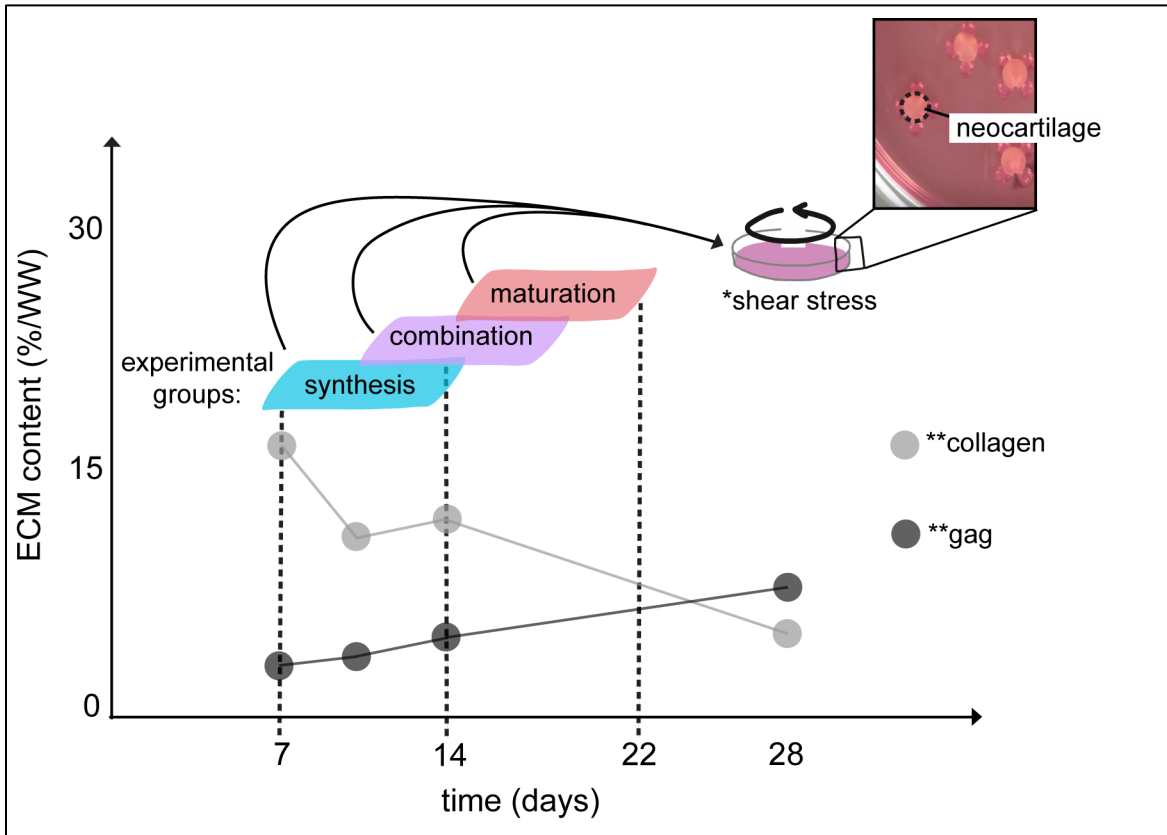
FIGURE 1

Figure 1 – The design of the experimental groups of this study follow the stages of the self-assembling process of neocartilage. The synthesis stage occurs from day 7 to day 14 of culture when glycosaminoglycan content increases slowly and collagen content decreases slowly. During the maturation stage, from day 14 to day 28, glycosaminoglycan content continues to increase and collagen content continues to decrease, but the total turnover of extracellular matrix increases. The neocartilage constructs were either nonstimulated controls or stimulated with shear stress during the synthesis stage, the maturation stage, or a combination stage (day 11 to day 18). *shear stress refers to fluid-induced shear stress, the application of which is described previously in Salinas et al. 2020. **data obtained from Ofek et al. 2008. Abbreviations: extracellular matrix (ECM), glycosaminoglycan (GAG)

MATERIALS AND METHODS

Overview of experimental phases

Phase I - To determine the optimal fluid-induced shear stress application time interval, neocartilage constructs that were created with bovine articular chondrocytes were stimulated with shear stress during the synthesis stage (d7-14), maturation stage (d14-21), or a combination of both stages (d11-17). (Figure 1) There were three experimental groups (n=6 for each group) in phase I, which were based on the different stages of neocartilage growth under self-assembly, and a nonstimulated control group served as a control. Previously, the effects of shear stress stimulation on self-assembled neocartilage was examined at different magnitudes; it was determined that shear stress stimulation within a range of 0.05-0.21Pa (50RPM) yielded the most mechanically robust neocartilage constructs out of other stimulated groups, and non-stimulated controls.[32] Therefore, fluid-induced shear stress stimulation was always applied within a range of 0.05-0.21Pa (50RPM) in this experiment. All neocartilage constructs were cultured as described previously for a total of 28 days.[33]

Phase II - After conducting phase I, it was determined that the group stimulated with shear stress during the maturation stage possessed better mechanical and biochemical properties compared to the other experimental groups and to the nonstimulated control. To assess the reproducibility of the results obtained in phase I, bovine articular chondrocytes were used to create nonstimulated neocartilage constructs and neocartilage constructs stimulated during the maturation stage. Each group had a total of six neocartilage constructs created from bovine articular cartilage chondrocytes that were cultured for a total of 28 days as in phase I.

Phase III - To explore the translatability of the optimized shear stress stimulation protocol to a different species and chondrocyte source, minipig costal chondrocytes were expanded to passage 3 and used to create neocartilage constructs. In this phase, the information obtained in phases I and II was carried forth, and neocartilage was either

99

nonstimulated or stimulated with shear stress only during the maturation stage. Each group had a total of six neocartilage constructs, and the neocartilage was cultured for a total of 28 days as in phase I and phase II.

Isolation of bovine articular chondrocytes

For phases I and II of this study, bovine articular cartilage chondrocytes were isolated by mincing cartilage from the condyles and trochlear groove of the knees of \two-month old Jersey calves, and storing the minced pieces from each leg in approximately 30ml wash medium, which consisted of Dulbecco's Modified Eagle's Medium (DMEM). 1% penicillin-streptomycin-fungizone (PSF). The minced tissue from each leg was washed 2-3 times with wash medium and then digested for 18hr using 0.2% (w/v) Collagenase type II in chondrogenic medium, 1% PSF, and 3% fetal bovine serum (FBS). The tissue in the collagenase solution was placed in a petri dish and incubated for 18hr on the orbital shaker at 37°C at 60rpm. Following the 18hr time period, the collagenase solution with the chondrocytes was filtered through 70μm cell strainers into 50ml tubes. The chondrocytes were washed and centrifuged for 5 minutes at 400G to remove the collagenase. The chondrocytes were then sterile filtered and washed with red blood cell lysis buffer.[34] Finally, chondrocytes were counted and frozen in chondrogenic medium with 90% FBS and 10% dimethyl sulfoxide.

Isolation of minipig costal chondrocytes

For phase III, minipig costal cartilage was obtained from 6-month old minipigs. Costal cartilage was minced into ~1mm^3 pieces. The cartilage pieces were digested for 18hr in 0.2% w/v (2mg/ml) collagenase type II and 3% fetal bovine serum (FBS) on an orbital shaker. Finally, the cells were strained, counted, and frozen in 90% FBS and 10% dimethyl sulfoxide, as previously described.[35]

Passaging and aggregate differentiation of minipig costal chondrocytes

First, cell vials were thawed by being placed in a 37°C water bath. Wash medium was aliquoted into 50ml tubes and 4 vials/tube were added in a drop-wise technique to ensure cell viability. The tubes were spun down at 400g for 5 minutes, and resuspended in volume of warmed chondrogenic media with 2% FBS. The cells were counted and brought to 1e6 cells /ml in CHG+2% FBS plus growth factors (1 ng/ml TGF-β1 +5ng/ml bFGF+10ng/ml PDGF). The cells were seeded at 27ml per flask, and the flasks were placed in 10% CO_2 incubator. Finally, the flasks were checked for confluence every 1-2 days and the cells were fed every 3-4 days with CHG+2% FBS and growth factors (1ng/ml TGF-β1 + 5ng/ml bFGF + 10ng/ml PDGF).

The cells were passaged every two weeks or until the cells were confluent. First, old medium was removed from the flask using an aspirating pipet carefully to prevent lifting any cells. Wash medium was added to each and was then removed carefully to rinse the flask. Next, 0.05% Trypsin-EDTA was added to each flask's growth surface and placed in an incubator for ~8-9 minutes to lift the cells. Wash medium+10% FBS was added to the growth surface of the flask, and the cell suspension was collected into a tube to neutralize the Trypsin-EDTA. The tubes were spun down, and the supernatant was poured into another 50ml tube. A 0.2% w/v (2mg/ml) Collagenase II solution was prepared and sterile filtered. The pellet was resuspended in appropriate amount of the Collagenase II solution in tubes and placed in a 37°C water bath. The cell suspension was pipet up and down every 10-15 minutes for 20-30 minutes. The cell suspension was spun down to remove the Collagenase II, and resuspended into another 50ml tube not use an aspirating pipet. Spin down and seed into flask as described above.

Finally, the cells were then placed into aggregate differentiation, which allowed the cells to recover their chondrogenic phenotype.[36] In order to seed the aggregates, we made 1% agarose, added 1 agarose to a petri dish, rotated plate to ensure coating, and added ~5ml of wash medium. The cells were removed from the flasks, resuspended, and counted as descried in the passaging protocol. They were then brought to 10e6 cells/ml in CHG plus growth factors

101

(10 ng/ml TGF-β1+100ng/ml GDF5+100ng/ml BMP-2). For one petri dish, 27.75ml of CHG plus 30µl TGF-β1, 30µl GDF5, 30µl BMP-2 were added. The cells suspension was then to each petri dish by adding drop-wise from 5ml pipet in a circular motion around the plate. In a slow motion, the plate was given a swirl circular motion to bring all the cells together in the center of the plate. The petri dishes were placed on an orbital shaker for 24hrs at 50RPM in a 10% CO_2 incubator. The orbital shaker is stopped after 24hrs, and the aggregates were fed every 3-4 days for 11 days.

Self-assembly of neocartilage constructs

5-mm-diameter stainless steel well-makers were used to make 2% agarose wells in a 48-well plate, and once the agarose solidified, chondrogenic media was added. The media was changed at least twice before seeding chondrocytes. Chondrocytes were seeded into the 2% agarose wells (4M bovine chondrocytes per well, 2M minipig chondrocytes per well) to begin the self-assembling process. Four hours after seeding, 0.5ml of chondrogenic media was added to each well. Seven days after seeding, the self-assembled neocartilage constructs were unconfined from the agarose wells and cultured in 24-well plates. The neocartilage constructs received 1ml of media every day of the first week and 2ml on alternating days for the continuation of the 28-day culture period.

Shear stress stimulation and device

Fluid-induced shear (FIS) stress was applied to the treatment groups by placing the neocartilage constructs in a FIS stress device at the previously specified stages. The device was created by adding 25ml of 3% agarose to a petri dish, placing the device mold to create small protruding agarose poles, and removing the mold once the agarose solidified as described previously.[32] Each of the neocartilage constructs were positioned between four surrounding poles to keep the constructs in place, and 15ml of chondrogenic media were added to the

102

device. The FIS stress device was then placed on an orbital shaker at 50RPM, and as the orbital shaker rotated, it allowed the media in the FIS stress device to flow over the neocartilage constructs. Media was changed every 2-3 days. After stimulation with FIS stress, the neocartilage constructs were returned to regular 24-well plates and received 2ml of media on alternating days.

Analysis of mechanical properties

After 28 days, mechanical testing of the neocartilage constructs was performed. To analyze the gross morphology of the neocartilage constructs sample thickness and diameter were measured with ImageJ software. To determine the compressive properties, a cylindrical 1mm punch was taken from the center of the construct, and a creep indentation analysis test was performed as described previously to determine aggregate modulus, permeability, and Poisson's ratio.[37]

Tensile testing was conducted using a uniaxial material testing machine, Instron model 5565, as previously described.[38] Neocartilage constructs were cut into dog bone-shaped samples and were glued to paper rectangles with a gauge length of 1.55mm. The sample thickness, width of the dog bones, and sample cross-sectional areas were measured using ImageJ. A uniaxial strain until failure test was conducted with a strain rate of 1% per second. Load–displacement curves were normalized to the cross-sectional area of each sample. Finally, the apparent Young's modulus and ultimate tensile strength were calculated using MATLAB software.

Analysis of biochemical properties

For extracellular matrix content, wet weight and dry weight of the samples were measured, and specific assays were used to quantify DNA, collagen content, and glycosaminoglycan content. First, the samples were frozen to allow for sublimation during a 72hr lyophilization cycle. After lyophilization, dry weights were measured and the tissue was digested in a 1ml/1mg buffered

papain solution for 18hr at 65°C. The measured DNA, glycosaminoglycans, and collagen amounts were normalized by the tissue per wet weight.

DNA content was quantified using PicoGreen assay. Pico green reagents were added to 8ml of the digested sample and fluorescence was measured at 485/528nm excitation/emission with a Magellan plate reader. Glycosaminoglycan content was measured using a Blyscan glycosaminoglycan assay kit. In short, 8µl of the digested sample reacted with 500ml dye reagent for a total of 30min, vertexing every 5min. The samples were then centrifuged to create a precipitate, which was then dissolved in 500uL of dissociated reagent, and the absorbance was measured at 650nm. The total collagen content was measured using a chloramine-T hydroxyproline assay and a SIRCOL collagen standard.[39] 100µl of the bovine digested sample was used for phase I and phase II, and 70ml of the minipig digested sample was used for phase III. In summary, 200µl of 4N NaOH was added to the samples, they were autoclaved, and then 200ml 4N HCl was added. Samples were then incubated with 1.25ml of 0.062M chloramine T for 20min at room temperature. Subsequently, they were incubated with 1.25ml of 1.2M Ehrlich's reagent for 20min at 65°C. The samples developed color and absorbance was measured at 550nm.

Statistics

For phase I one-way analysis of variance (ANOVA) and Tukey's *post hoc* tests were performed using $p < 0.05$ to determine statistically significant differences among groups. Groups deemed significantly different by the Tukey's post hoc tests were denoted using alphabetical letters. For phases II and III, a students t-test was used at $p<0.05$ to determine statistically significant differences amongst groups.

RESULTS

<u>Phase I</u>

To determine which time of stimulation would lead to the most mechanically robust neocartilage constructs, in phase I, fluid-induced shear stress was applied at the magnitude described previously, at the different stages of neocartilage development mentioned above. When stimulated with shear stress, collagen content was improved over the collagen content of nonstimulated neocartilage, showing a 2.2-fold increase. For the compressive stiffness, the neocartilage constructs stimulated during the maturation stage had improved aggregate modulus values over the unstimulated control by 2.6-fold, and they also trended higher than the neocartilage constructs stimulated during the combination stage. (Figure 2a) When considering tensile properties, neocartilage stimulated during the maturation and combination stages saw improvements in UTS over nonstimulated controls showing about a 2-fold increase. (Figure 2b) Combined, these data showed that to most effectively improve the mechanical properties of neocartilage constructs with shear stress, the stimulus should be applied during the maturation stage.
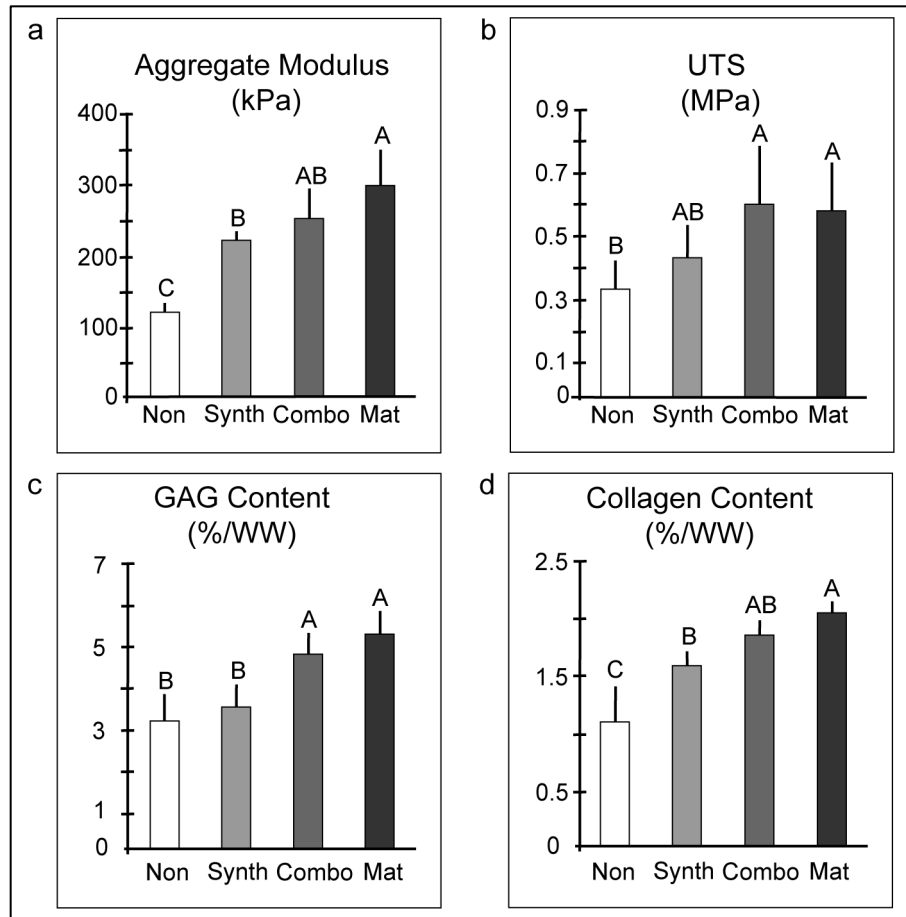
FIGURE 2

Figure 2 – Phase I study results for neocartilage created from bovine articular chondrocytes and either nonstimulated, or stimulated during the synthesis stage, the maturation stage, or a combination of these stages to determine an optimal shear stress stimulation stage. **a)** The aggregate modulus, **b)** the ultimate tensile strength, **c)** the glycosaminoglycan content, and **d)** the collagen content of neocartilage constructs are shown. Bars not sharing the same letter are statistically different evaluated at a $p<0.05$ using a one-way ANOVA and Tukey's post hoc test. Abbreviations: nonstimulated \(Non), synthesis (Synth), combination (Combo), maturation (Mat), ultimate tensile strength (UTS), glycosaminoglycan (GAG), percent per wet weight (%/WW), kilopascals (kPa), megapascals (MPa)

Phase II

For phase II, extracellular matrix content was compared between nonstimulated and neocartilage stimulated with shear stress during the maturation stage. As in phase I, glycosaminoglycan content in shear stress stimulated neocartilage was higher than in nonstimulated controls, which showed a 2.25-fold increase. (Figure 3a) Collagen content was

improved when stimulated with shear stress over nonstimulated neocartilage, showing a 2-fold increase. (Figure 3b) All together, the reproducibility of the results from phase I is verified in phase II, and it can be concluded that shear stress stimulation applied during the maturation stage of neocartilage development leads to neocartilage constructs with extracellular matrix content that is more similar to native tissue than nonstimulated controls.

To assess the reproducibility of the mechanical properties resulting from in phase I, the neocartilage constructs in phase II were also tested for compressive and tensile properties. As in phase I, neocartilage constructs stimulated with shear stress during the maturation stage showed a nearly 3.3-fold improvement in aggregate modulus over nonstimulated controls (Figure 3c). In terms of tensile properties, only the UTS value of stimulated samples improved over nonstimulated controls, an increase of 2.5-fold (Figure 3d). As with phase I, the Young's modulus value of shear-stimulated neocartilage constructs was not statistically different from nonstimulated controls (Figure 3e). These data show that the results from phase I were reproducible in terms of mechanical properties, and that neocartilage stimulated with shear stress during the maturation phase out-performs nonstimulated neocartilage in aggregate modulus and UTS.
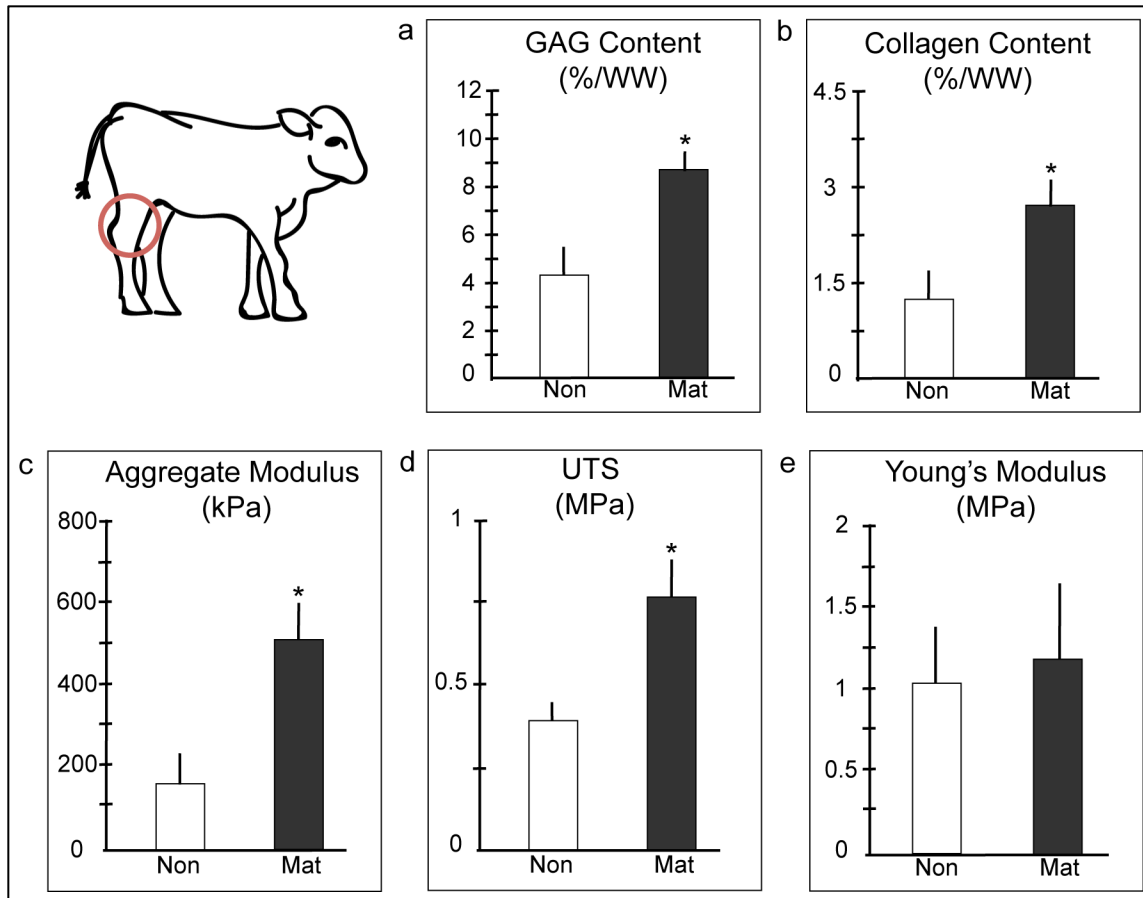
FIGURE 3

Figure 3 – Phase II study results for neocartilage created from bovine articular chondrocytes and either nonstimulated or stimulated during the maturation stage to asses the reproducibility of phase I results. **a)** The glycosaminoglycan content, **b)** the collagen content, **c)** the aggregate modulus, **d)** the ultimate tensile strength, and **e)** the Young's modulus of neocartilage constructs are shown. An asterisk (*) above a bar indicates that the value is statistically different from the nonstimulated control, evaluated at a $p<0.05$ using a Student's t-test. Abbreviations: nonstimulated (Non), maturation (Mat), ultimate tensile strength (UTS), glycosaminoglycan (GAG), percent per wet weight (%/WW), kilopascals (kPa), megapascals (MPa)

Phase III

To evaluate the translatability of fluid-induced shear stress stimulation across chondrocytes from different sources and species, phase III explored the use of minipig costal chondrocytes to produce neocartilage constructs. As in neocartilage created with bovine neocartilage constructs, an increase in glycosaminoglycan content was observed in minipig neocartilage stimulated during the maturation stage compared to the stimulated control (Figure 4a). Specifically, a 2.7-

fold increase in glycosaminoglycan content was observed in stimulated over nonstimulated neocartilage. Interestingly, although collagen content trended higher, a significant increase in collagen content was not observed in the shear stress stimulated neocartilage created with minipig costal chondrocytes (Figure 4b). Overall, however, it can be said that for neocartilage created with minipig costal chondrocytes, shear stress stimulation during the maturation stage improves extracellular matrix properties toward those of native tissue, just as it was observed for bovine chondrocytes derived from the knee.

As in previous phases, it was also of interest to determine the effects that shear stress applied during the maturation stage would have on the mechanical properties of neocartilage created with minipig costal chondrocytes. Compressive and tensile properties were examined as described previously, and it was found that the aggregate modulus value of neocartilage stimulated with shear stress during the maturation phase was 1.5-fold higher than nonstimulated neocartilage (Figure 4c). Furthermore, tensile properties were also improved. The UTS of neocartilage stimulated with shear stress during the maturation phase was 2-fold higher than that of nonstimulated neocartilage. Similarly, the Young's modulus of neocartilage stimulated with shear stress during the maturation phase was 1.8-fold higher than nonstimulated neocartilage (Figure 4d, e). An improvement in Young's modulus had not been seen previously in neocartilage constructs made with bovine articular chondrocytes. These data show that shear stress applied during the maturation stage significantly improves the mechanical properties of neocartilage constructs created with minipig costal chondrocytes.
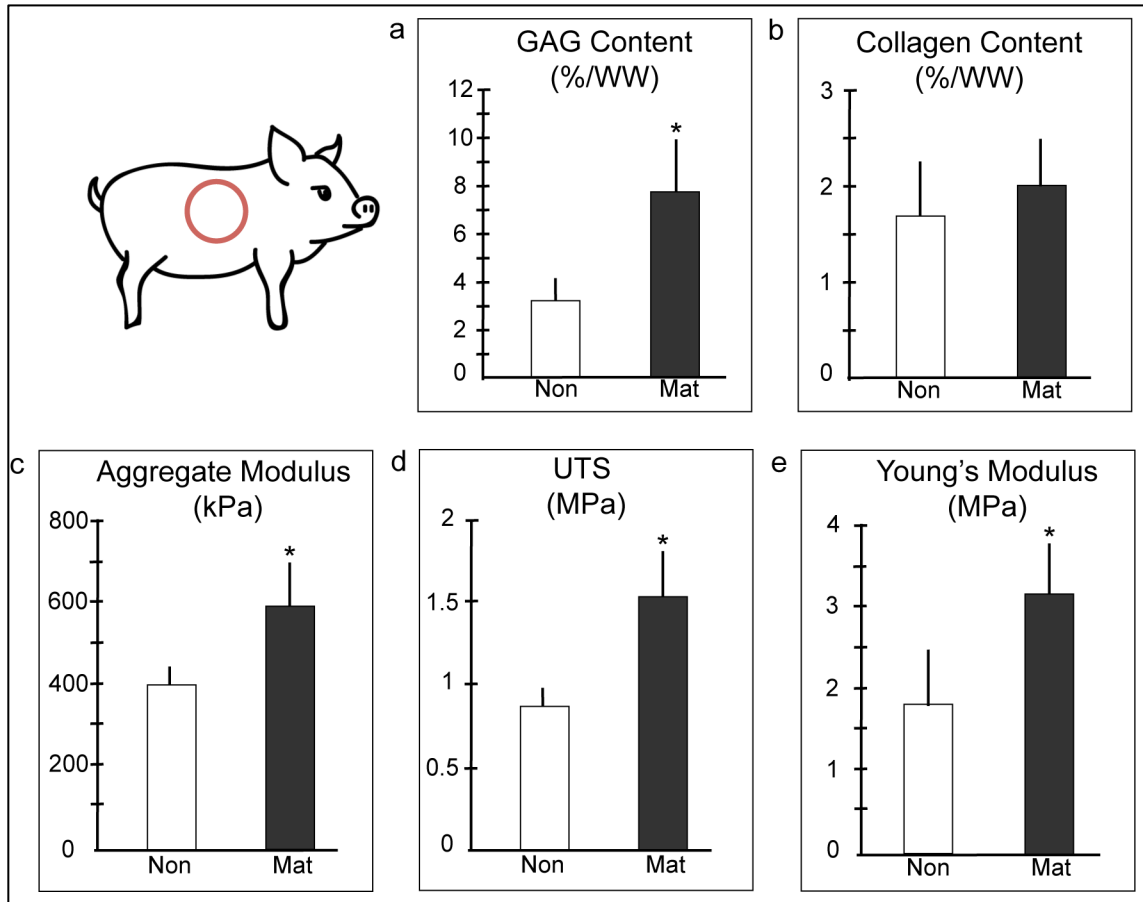
FIGURE 4

Figure 4 – Phase III study results for neocartilage created from minipig costal chondrocytes and either nonstimulated or stimulated during the maturation stage to asses the translatability of the shear stress stimulation regimen. **a)** The glycosaminoglycan content, **b)** the collagen content, **c)** the aggregate modulus, **d)** the ultimate tensile strength, and **e)** the Young's modulus of neocartilage constructs are shown. The asterisk (*) floating above the bars indicate statistically different groups evaluated at a $p < 0.05$ using a students t-test. Abbreviations: nonstimulated (Non), maturation (Mat), ultimate tensile strength (UTS), glycosaminoglycan (GAG), percent per wet weight (%/WW), kilopascals (kPa), megapascals (MPa)

DISCUSSION

Toward addressing the current need to determine the optimal time of application of fluid-induced shear stress, the objectives of the study were: 1) to identify the most efficient developmental stage of self-assembled neocartilage development to apply fluid-induced shear stress and 2) to determine if this stage of shear stress stimulation translates from a bovine to a minipig animal model. The hypothesis was that the time of application of shear stress stimulation would have an effect on the mechanical properties and extracellular matrix content of the self-assembled neocartilage for both species. The results of these studies indicated that, for neocartilage created with bovine articular chondrocytes, shear stress stimulation during the maturation stage yielded the most superior mechanical properties of compressive stiffness and tensile strength, as well as the extracellular matrix content of collagen and glycosaminoglycans. Furthermore, when the shear stress stimulation protocol was translated to neocartilage created with minipig costal chondrocytes, mechanical properties across the board were improved, as well as glycosaminoglycan content. Altogether, the results of these studies indicate that neocartilage stimulated with shear stress applied during the maturation stage demonstrate the best qualities for *in vivo* implantation because they are the closest to native tissue.

During the synthesis stage, nonstimulated neocartilage constructs initiate the production of extracellular matrix and start out with high levels of collagen and low levels of glycosaminoglycan.[27, 40] When the constructs enter the maturation stage, the nonstimulated neocartilage constructs ramp up the production of glycosaminoglycan, and collagen levels show a stark decrease.[27] Previous studies indicate that MAPK has a significant role in signaling chondrocyte mechanotransduction pathways and regulating catabolic and anabolic activities of chondrocytes.[15, 41-43] For instance, p38 MAPK signaling promotes chondrocyte proliferation and chondrocytes that are stimulated by TGF produced the proteoglycans.[15, 44, 45] Previous studies on shear stress have also shown that primary cilia in chondrocytes may be the

mechanically gated actors that are triggered by shear stress allowing an induction of calcium ions that results in an increase in extracellular matrix density and, consequently, mechanical properties.[19, 20, 32] The increased levels of collagen content in the neocartilage stimulated during the maturation stage indicate that shear stress is either reactivating collagen producing protein pathways or preventing the deterioration of collagen. Similarly, the increased levels of glycosaminoglycans in the neocartilage indicate an upregulation in the activity of glycosaminoglycan producing pathways. Although further study is necessary to determine the precise pathways leading to these results, it can be concluded that shear stress stimulation during the maturation stage of neocartilage self-assembly is the most effective for producing improved extracellular matrix levels.

In previous studies using bovine articular chondrocytes, the use of fluid-induced shear stress during the synthesis stage led to improved neocartilage construct compressive properties, but tensile properties saw no enhancements when compared to nonstimulated controls. In the study presented here, bovine neocartilage stimulated with shear stress during the combination of synthesis and maturation stages and during the maturation stage saw improvements in the UTS but not the Young's modulus value. This observation further supports the rationale that there is a time-specific dependency for the efficaciousness of shear stress stimulation. Previous studies have shown that, in nonstimulated neocartilage, a decrease in collagen content, which is generally attributed to lower tensile strength and stiffness, is presented during the maturation stage.[27, 46] However, when neocartilage is stimulated with shear stress during the maturation stage, neocartilage shows an increase in collagen content and, subsequently, an increase in UTS. Interestingly, when creating minipig neocartilage, shear stress stimulation applied during the maturation stage improved both UTS and Young's modulus, yet, collagen content was not improved. This indicates that pyridinoline crosslinks, which bind collagen fibers, are also likely increased when shear stress is applied during the

maturation stage.[46, 47] The results accumulated from these studies show that application of shear stress is useful for improving not only compressive properties, as was shown previously, but, when applied during the maturation stage, can also be effective for improving tensile properties.

The results of these studies hold value for future studies in neocartilage tissue engineering. For example, in the clinic, articular cartilage lesions can run larger than the 5mm diameter constructs presented in this study and would need larger neocartilage implants for treatment. Another potential study stemming from this would be to couple shear stress with other mechanical stimulation strategies that are best implemented on self-assembled neocartilage during the synthesis stage, such as compression or tension.[14, 17] Although the addition of a cocktail of bioactive factors to improve neocartilage properties is straightforward, they are typically expensive and have pleiotropic effects, which can complicate their use in clinical translation.[48-51] A properly timed combination of mechanical stimulation techniques may lead to synergistic improvements in neocartilage properties and could potentially eliminate the need for bioactive factors.

Tissue-engineering strategies show the potential to overcome the disadvantages of current articular cartilage lesion treatment options. However, it is necessary to create neocartilage constructs with mechanical properties and extracellular matrix content akin to native tissue before they are ready for implantation *in vivo*. With the use of an optimized application regimen of shear stress for neocartilage, we can get closer to providing a better treatment option for the repair of focal cartilage defects. As shown in phase III, shear stress is effective across different species and cell types including expanded cells. Previous to this experiment, no research had been conducted to determine when during tissue culture shear stress stimulation is most effective on self-assembled neocartilage. The studies presented here

demonstrate that if used at the right magnitude and time of application shear stress can be optimized to improve the mechanical properties and extracellular matrix content of neocartilage.

REFERENCES

[1] J.M. Hootman, C.G. Helmick, K.E. Barbour, K.A. Theis, M.A. Boring, Updated Projected Prevalence of Self-Reported Doctor-Diagnosed Arthritis and Arthritis-Attributable Activity Limitation Among US Adults, 2015-2040, Arthritis Rheumatol 68(7) (2016) 1582-1587.

[2] B.J. Huang, J.C. Hu, K.A. Athanasiou, Cell-based tissue engineering strategies used in the clinical repair of articular cartilage, Biomaterials 98 (2016) 1-22.

[3] F. McCormick, J.D. Harris, G.D. Abrams, R. Frank, A. Gupta, K. Hussey, H. Wilson, B. Bach, Jr., B. Cole, Trends in the surgical treatment of articular cartilage lesions in the United States: an analysis of a large private-payer database over a period of 8 years, Arthroscopy 30(2) (2014) 222-6.

[4] S.R. Montgomery, B.D. Foster, S.S. Ngo, R.D. Terrell, J.C. Wang, F.A. Petrigliano, D.R. McAllister, Trends in the surgical treatment of articular cartilage defects of the knee in the United States, Knee Surgery, Sports Traumatology, Arthroscopy 22(9) (2014) 2070-2075.

[5] K.A. Athanasiou, R. Eswaramoorthy, P. Hadidi, J.C. Hu, Self-organization and the self-assembling process in tissue engineering, Annual Review of Biomedical Engineering 15 (2013) 115-136.

[6] H. Wang, Y. Li, Y. Zuo, J. Li, S. Ma, L. Cheng, Biocompatibility and osteogenesis of biomimetic nano-hydroxyapatite/polyamide composite scaffolds for bone tissue engineering, Biomaterials 28(22) (2007) 3338-3348.

[7] S. Prasadh, R.C.W. Wong, Unraveling the mechanical strength of biomaterials used as a bone scaffold in oral and maxillofacial defects, Oral Science International 15(2) (2018) 48-55.

[8] L.W. Huwe, W.E. Brown, J.C. Hu, K.A. Athanasiou, Characterization of costal cartilage and its suitability as a cell source for articular cartilage tissue engineering, Journal of tissue engineering and regenerative medicine 12(5) (2018) 1163-1176.

[9] A.J. Grodzinsky, M.E. Levenston, M. Jin, E.H. Frank, Cartilage Tissue Remodeling in Response to Mechanical Forces, Annual Review of Biomedical Engineering 2(1) (2000) 691-713.

[10] A.M. Gharravi, M. Orazizadeh, K. Ansari-Asl, S. Banoni, S. Izadi, M. Hashemitabar, Design and fabrication of anatomical bioreactor systems containing alginate scaffolds for cartilage tissue engineering, Avicenna Journal of Medical Biotechnology 4(2) (2012) 65.

[11] J. Klompmaker, R. Veth, H. Jansen, H. Nielsen, J. De Groot, A. Pennings, R. Kuijer, Meniscal repair by fibrocartilage in the dog: characterization of the repair tissue and the role of vascularity, Biomaterials 17(17) (1996) 1685-1691.

[12] I.G. Otterness, J.D. Eskra, M.L. Bliven, A.K. Shay, J.P. Pelletier, A. Milici, Exercise protects against articular cartilage degeneration in the hamster, Arthritis & Rheumatism: Official Journal of the American College of Rheumatology 41(11) (1998) 2068-2076.

[13] K.A. Athanasiou, E.M. Darling, J.C. Hu, G.D. DuRaine, A.H. Reddi, Articular Cartilage, 2 ed., CRC Press, 2017.

[14] L.W. Huwe, G.K. Sullan, J.C. Hu, K.A. Athanasiou, Using Costal Chondrocytes to Engineer Articular Cartilage with Applications of Passive Axial Compression and Bioactive Stimuli, Tissue Eng Part A 24(5-6) (2018) 516-526.

[15] J.B. Fitzgerald, M. Jin, D.H. Chai, P. Siparsky, P. Fanning, A.J. Grodzinsky, Shear- and Compression-induced Chondrocyte Transcription Requires MAPK Activation in Cartilage Explants, Journal of Biological Chemistry 283(11) (2008) 6735-6743.

[16] S.C. Tran, A.J. Cooley, S.H. Elder, Effect of a mechanical stimulation bioreactor on tissue engineered, scaffold-free cartilage, Biotechnology and Bioengineering 108(6) (2011) 1421-1429.

[17] J.K. Lee, L.W. Huwe, N. Paschos, A. Aryaei, C.A. Gegg, J.C. Hu, K.A. Athanasiou, Tension stimulation drives tissue formation in scaffold-free systems, Nature Materials 16(8) (2017) 864.

[18] E.J. Vanderploeg, C.G. Wilson, M.E. Levenston, Articular chondrocytes derived from distinct tissue zones differentially respond to in vitro oscillatory tensile loading, Osteoarthritis and cartilage 16(10) (2008) 1228-1236.

[19] A.K. Wann, N. Zuo, C.J. Haycraft, C.G. Jensen, C.A. Poole, S.R. McGlashan, M.M. Knight, Primary cilia mediate mechanotransduction through control of ATP-induced Ca2+ signaling in compressed chondrocytes, The FASEB Journal 26(4) (2012) 1663-1671.

[20] R. Ruhlen, K. Marberry, The chondrocyte primary cilium, Osteoarthritis and Cartilage 22(8) (2014) 1071-1076.

[21] C.V. Gemmiti, R.E. Guldberg, Shear stress magnitude and duration modulates matrix composition and tensile mechanical properties in engineered cartilaginous tissue, Biotechnology and Bioengineering 104(4) (2009) 809-820.

[22] C.V. Gemmiti, R.E. Guldberg, Fluid flow increases type II collagen deposition and tensile mechanical properties in bioreactor-grown tissue-engineered cartilage, Tissue Engineering 12(3) (2006) 469-479.

[23] H. Kwon, N.K. Paschos, J.C. Hu, K.A. Athanasiou, Articular cartilage tissue engineering: the role of signaling molecules, Cellular and Molecular Life Sciences 73(6) (2016) 1173-1194.

[24] E.R. Bastow, K.J. Lamb, J.C. Lewthwaite, A.C. Osborne, E. Kavanagh, C.P. Wheeler-Jones, A.A. Pitsillides, Selective activation of the MEK-ERK pathway is regulated by mechanical stimuli in forming joints and promotes pericellular matrix formation, J Biol Chem 280(12) (2005) 11749-58.

[25] G. Dowthwaite, C. Flannery, J. Flannelly, J. Lewthwaite, C. Archer, A. Pitsillides, A mechanism underlying the movement requirement for synovial joint cavitation, Matrix Biology 22(4) (2003) 311-322.

[26] P.A.J. Brama, J.M. TeKoppele, B. Beekman, B. van El, A. Barneveld, P.R. van Weeren, Influence of development and joint pathology on stromelysin enzyme activity in equine synovial fluid, Annals of the Rheumatic Diseases 59(2) (2000) 155.

[27] G. Ofek, C.M. Revell, J.C. Hu, D.D. Allison, K.J. Grande-Allen, K.A. Athanasiou, Matrix development in self-assembly of articular cartilage, PloS one 3(7) (2008) e2795-e2795.

[28] J.K. Lee, J.C. Hu, S. Yamada, K.A. Athanasiou, Initiation of chondrocyte self-assembly requires an intact cytoskeletal network, Tissue Engineering Part A 22(3-4) (2016) 318-325.

[29] E.Y. Salinas, J.C. Hu, K.A. Athanasiou, A guide for using mechanical stimulation to enhance tissue-engineered articular cartilage properties, Tissue Engineering Part B: Reviews 24(5) (2018) 345-358.

[30] C.G. Pfeifer, M.B. Fisher, V. Saxena, M. Kim, E.A. Henning, D.A. Steinberg, G.R. Dodge, R.L. Mauck, Age-Dependent Subchondral Bone Remodeling and Cartilage Repair in a Minipig Defect Model, Tissue Eng Part C Methods 23(11) (2017) 745-753.

[31] N. Vapniarsky, A. Aryaei, B. Arzi, D.C. Hatcher, J.C. Hu, K.A. Athanasiou, The Yucatan Minipig Temporomandibular Joint Disc Structure-Function Relationships Support Its Suitability for Human Comparative Studies, Tissue Eng Part C Methods 23(11) (2017) 700-709.

[32] E.Y. Salinas, A. Aryaei, N. Paschos, R.E. Berson, H. Kwon, J.C. Hu, K.A. Athanasiou, Fluid-induced shear stress on tissue-engineered cartilage, Biofabrication (2020).

[33] J.C. Hu, K.A. Athanasiou, A self-assembling process in articular cartilage tissue engineering, Tissue Engineering 12(4) (2006) 969-979.

[34] W.E. Brown, J.C. Hu, K.A. Athanasiou, Ammonium-Chloride-Potassium Lysing Buffer Treatment of Fully Differentiated Cells Increases Cell Purity and Resulting Neotissue Functional Properties, Tissue Eng Part C Methods 22(9) (2016) 895-903.

[35] N. Vapniarsky, L.W. Huwe, B. Arzi, M.K. Houghton, M.E. Wong, J.W. Wilson, D.C. Hatcher, J.C. Hu, K.A. Athanasiou, Tissue engineering toward temporomandibular joint disc regeneration, Sci Transl Med 10(446) (2018) eaaq1802.

[36] K.A. Athanasiou, J.C. Hu, H. Kwon, Methods and systems for conserving highly expanded cells, in: U.S.P. Office (Ed.) 2018.

[37] K.D. Allen, K.A. Athanasiou, Viscoelastic characterization of the porcine temporomandibular joint disc under unconfined compression, J Biomech 39(2) (2006) 312-322.

[38] E.A. Makris, R.F. MacBarb, D.J. Responte, J.C. Hu, K.A. Athanasiou, A copper sulfate and hydroxylysine treatment regimen for enhancing collagen cross-linking and biomechanical properties in engineered neocartilage, The FASEB Journal 27(6) (2013) 2421-2430.

[39] D.D. Cissell, J.M. Link, J.C. Hu, K.A. Athanasiou, A modified hydroxyproline assay based on hydrochloric acid in Ehrlich's solution accurately measures tissue collagen content, Tissue Engineering Part C: Methods 23(4) (2017) 243-250.

[40] A.J. Hayes, A. Hall, L. Brown, R. Tubo, B. Caterson, Macromolecular organization and in vitro growth characteristics of scaffold-free neocartilage grafts, Journal of Histochemistry & Cytochemistry 55(8) (2007) 853-866.

[41] S. Ashraf, B.-H. Cha, J.-S. Kim, J. Ahn, I. Han, H. Park, S.-H. Lee, Regulation of senescence associated signaling mechanisms in chondrocytes for cartilage tissue regeneration, Osteoarthritis and cartilage 24(2) (2016) 196-205.

[42] E. Mariani, L. Pulsatelli, A. Facchini, Signaling pathways in cartilage repair, International journal of molecular sciences 15(5) (2014) 8667-8698.

[43] Y. Zhang, T. Pizzute, M. Pei, A review of crosstalk between MAPK and Wnt signals and its impact on cartilage regeneration, Cell and tissue research 358(3) (2014) 633-649.

[44] R.K. Studer, R. Bergman, T. Stubbs, K. Decker, Chondrocyte response to growth factors is modulated by p38 mitogen-activated protein kinase inhibition, Arthritis Res Ther 6(1) (2004) R56-R64.

[45] X. Wang, F. Li, C. Fan, C. Wang, H. Ruan, Effects and relationship of ERK1 and ERK2 in interleukin-1β-induced alterations in MMP3, MMP13, type II collagen and aggrecan expression in human chondrocytes, International journal of molecular medicine 27(4) (2011) 583-589.

[46] A.K. Williamson, A.C. Chen, K. Masuda, E.J.-M.A. Thonar, R.L. Sah, Tensile mechanical properties of bovine articular cartilage: Variations with growth and relationships to collagen network components, Journal of Orthopaedic Research 21(5) (2003) 872-880.

[47] D.R. Eyre, M.A. Paz, P.M. Gallop, Cross-linking in collagen and elastin, Annual review of biochemistry 53(1) (1984) 717-748.

[48] Y.M. Farhat, A.A. Al-Maliki, T. Chen, S.C. Juneja, E.M. Schwarz, R.J. O'Keefe, H.A. Awad, Gene expression analysis of the pleiotropic effects of TGF-β1 in an in vitro model of flexor tendon healing, PloS one 7(12) (2012) e51411.

[49] M.C. Fleisch, C.A. Maxwell, M.-H. Barcellos-Hoff, The pleiotropic roles of transforming growth factor beta in homeostasis and carcinogenesis of endocrine organs, Endocrine-related cancer 13(2) (2006) 379-400.

[50] L. Bian, K.M. Crivello, K.W. Ng, D. Xu, D.Y. Williams, G.A. Ateshian, C.T. Hung, Influence of temporary chondroitinase ABC-induced glycosaminoglycan suppression on maturation of tissue-engineered cartilage, Tissue Engineering Part A 15(8) (2009) 2065-2072.

[51] R. Lin, J.C. Kwok, D. Crespo, J.W. Fawcett, Chondroitinase ABC has a long-lasting effect on chondroitin sulphate glycosaminoglycan content in the injured rat brain, Journal of neurochemistry 104(2) (2008) 400-408.

CHAPTER 4- COMBINING COMPRESSION AND SHEAR STRESS STIMULATION IN NEOCARTILAGE TISSUE CULTURE

ABSTRACT

Mechanically stimulating neocartilage constructs has been shown to drive mechanical properties toward native tissue values. Fluid-induced shear stress and passive axial compression stress have been used separately to improve compressive stiffness, collagen content, and fiber density. The objective of this work was to determine if shear stress and compression stress could be used in combination to further enhance the mechanical properties of neocartilage constructs. Two separate cell lines (bovine articular chondrocytes and minipig costal chondrocytes), and neocartilage geometries (5mm diameter and 8x13mm) were used to test the combination of mechanical stimuli. It was found that the combination of shear stress and compression stress yielded bovine neocartilage constructs with compressive stiffness (625kPa) at native tissue levels (450-1100kPa). It was also found that when the combination of mechanical stimuli was applied to minipig neocartilage constructs, both compressive and tensile stiffness improved over nonstimulated controls. Separately, previous strategies have provided incremental progression toward effective neocartilage implants, but a combination of both mechanical stimulation and bioactive factors has now been found to deliver neocartilage that may be able to withstand native tissue environments.

Authors: Salinas EY, Herrera JM, Hu JC, Athanasiou KA

INTRODUCTION

The most mobile joint type in the body is the synovial joint, in which a fibrous synovial membrane envelops a lubricating synovial fluid and articular cartilage.[1] Articular cartilage is an avascular tissue, sparsely populated by cells, that lines the ends of long bones and cushions and distributes forces generated during locomotion.[2, 3] Unfortunately, cumulative and progressive degenerative changes in articular cartilage ultimately produce osteoarthritis in about 27 million Americans each year.[4] Currently, to mitigate the progression of articular cartilage degeneration, chondroplasty and microfracture are used.[5-9] These clinical treatment options are not considered effective for more than 5 years after their implementation.[5] However, the self-assembling process, which only uses cells, has emerged as a promising tissue engineering strategy to create neocartilage implants for the regeneration of articular cartilage lesions. [10]

Passive compression stress stimulation has been shown to enhance mechanical and biochemical properties in both self-assembled and scaffold-containing neocartilage.[11-16] Specifically, passive compression stimulation has been shown to improve compressive modulus values in self-assembled neocartilage when compared to nonstimulated controls.[12] Passive compression stress stimulation is applied to self-assembled neocartilage by placing a weight on top of the tissue, and this method has been found to be most effective when applied at 5kPa during the synthesis stage of the self-assembling process.[12] Generally, to create these types of biomechanical improvements in neocartilage, bioactive factors, such as TGF-β1, are used.[17-24] However, previous studies exploring the use of passive compression and other types of mechanical stimulation suggest that bioactive factors could be replaced with mechanical stimulation strategies to achieve mechanically robust neocartilage for implantation.[12, 13, 25, 26]

Another type of mechanical stimulation that has recently been shown to improve self-assembled neocartilage properties is fluid-induced pulsatile shear stress.[27] In particular, shear stress has been found to improve the compressive modulus and extracellular matrix density.[28-31] Shear stress stimulation is imparted on self-assembled neocartilage by applying fluid-flow over the tissue, and has been found to be most effective when applied at a range of 0.05-0.21Pa during the maturation stage of the self-assembling process.[28, 32] Shear stress acts to improve neocartilage properties by activating a mechanically-gated ion channel on the primary cilia of chondrocytes that allows the influx of calcium ions into the cell.[28, 33-37] Shear stress, like compression stress, has the potential to be used in lieu of bioactive factors for eliciting improvements in neocartilage mechanical properties.

The vast majority of prior studies have examined a single mechanical stimulus at a time, and have shown substantial evidence of improving neocartilage properties. [12, 14, 15, 27, 38] Implementing a combination of mechanical stimulation strategies during one culture period may elicit synergistic improvements. When bioactive factors, such as TGF-β1 or LOXL2, are used, they are typically applied in combination to improve several properties of neocartilage.[17, 39] Like bioactive factors, mechanical stimulation strategies can be used in combination. Previous studies have explored the combination of compression stress and shear stress on neocartilage constructs and native tissues.[15, 16, 40] Several of these studies have focused on applying compression stress and shear stress on scaffold-containing neocartilage using a single bioreactor that mimics a dynamic native environment via a metal platen.[16, 40] In particular, it was found that there were significant enhancements in the mechanical stiffness of scaffold-containing neocartilage that was stimulated with dynamic compression and shear stress, but extracellular matrix content was not improved. Previous studies suggest that combining compression stress and shear stress on self-assembled neocartilage may be beneficial to improving mechanical properties and extracellular matrix content.

In the following experiments the combination of compression stress and shear stress is investigated in self-assembled neocartilage created from either bovine articular chondrocytes or Yucatan minipig costal chondrocytes (which are more expensive to procure but more amenable to translation). First, a small (5mm diameter), round neocartilage geometry made with bovine articular chondrocytes was used to compare a nonstimulated culture, a compression stress only culture, a shear stress only culture, and a combined culture regimen. In the subsequent experiment, a combined culture regimen of compression stress and shear stress was applied to larger (8x13mm), rectangular neocartilages created from minipig costal chondrocytes.[41] It was hypothesized that the combination of compression stress and shear stress would yield neocartilage constructs with improved mechanical properties and extracellular matrix content when compared to nonstimulated controls or neocartilage stimulated with only one mechanical stimulation type.
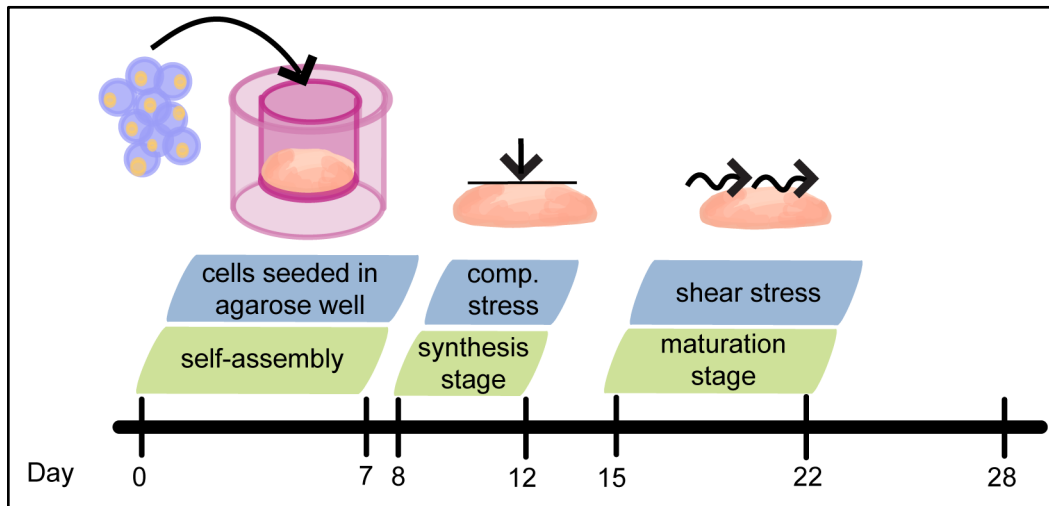
FIGURE 1

Figure 1 – Tissue culture timeline of a self-assembled neocartilage construct stimulated with compression stress and shear stress. On day 0, chondrocytes are seeded in a non-adherent agarose well that was previously saturated with chondrogenic media. On day 7, neocartilage is removed from the agarose well. From day 8 to day 12, the neocartilage undergoes compressive stress stimulation in the compression bioreactor. On day 12 the neocartilage constructs are removed from the compression stress bioreactor and placed in a 24-well plate. On day 15 shear stress is applied on the neocartilage via the fluid-induced pulsatile shear stress bioreactor and remains there until day 22. Finally, on day 22 the neocartilage is removed from shear stress stimulation and is placed in a 24-well plate until the end of culture on day

MATERIALS AND METHODS

Phase I

In the first phase of this study, small (5mm diameter), circular, neocartilage constructs were created using bovine articular chondrocytes to explore the effects of combining compression and shear stress. There were four groups, one receiving only shear, one receiving only compression, one receiving both shear and compression, and one receiving no stimulation. Each group had a total of six constructs, which were cultured using sterile culture techniques for a total of 28 days.

Phase II

In the second phase, large (8 x13mm), rectangular constructs were created from minipig costal cartilage chondrocytes to explore the combination of compression and shear stress in neocartilage culture. Two groups were examined: the treatment group identified in phase 1 of the study, and a control receiving no stimulation.

Chondrocyte harvest

For phase I, bovine articular cartilage chondrocytes were isolated from the condyles and trochlear groove of the knees of two-month old calves. The cartilage was minced from each leg and were stored in approximately 30ml wash medium, i.e., Dulbecco's Modified Eagle's Medium

(DMEM), 1% Penicillin-Streptomycin-Fungizone (PSF). The minced tissue was washed 2-3 times with wash medium and then digested for 18hr using 0.2% (w/v) collagenase type II in chondrogenic medium, 1% PSF, and 3% fetal bovine serum (FBS). The tissue in the collagenase and medium solution was placed in a petri dish and incubated for 18hr at 37° C. The shear stress device was placed on top of an orbital shaker at 60rpm for 18hr. After the 18hr time period, the collagenase solution with the chondrocytes was filtered using 70µm cell strainers into 50ml tubes. The chondrocytes were washed and centrifuged to remove the collagenase for 5 minutes at 400G (1500rpm). Next, the chondrocytes were sterile filtered and washed with a red blood cell lysis buffer.[42] Finally, chondrocytes were counted and frozen in a chondrogenic medium with 90% FBS and 10% dimethyl sulfoxide.

For phase II, minipig costal chondrocytes were obtained from the ribs of 6-month old minipigs. Costal cartilage was minced into ~1 mm^3 pieces and were digested for 18hr using 0.2% w/v (2mg/ml) collagenase type II and 3% FBS. The tissue was placed in the collagenase solution into a petri dish in an incubator. Finally, the cells were strained, counted, and frozen in a chondrogenic medium with 90% FBS and 10% DMSO.

Expansion of minipig costal cartilage chondrocytes

 First, cell vials were thawed in a 37°C water bath. Four vials per tube were added in a drop-wise technique to 30mls of wash medium, spun down at 400G for 5 minutes, and resuspended in volume of 37°C CHG+2% FBS. The cells were counted and brought to 1e6 cells/ml in CHG+2% FBS plus growth factors (1ng/ml TGF-β1 + 5ng/ml bFGF + 10ng/ml PDGF). The cells were seeded at 27ml per flask, and the flasks were placed in a 10% CO_2 incubator. Finally, the flasks were checked for confluence every 1-2 days, and the cells were fed every 3-4 days with CHG+2% FBS and growth factors (1ng/ml TGF-β1 + 5ng/ml bFGF + 10ng/ml PDGF).

The cells were passaged every two weeks or until the cells were confluent. For passaging, first, the old medium was removed from the flask, wash medium was added, and was then removed. Next, 15mls of 0.05% Trypsin-EDTA was added to each T225 flask's growth surface. The flasks were placed in an incubator for ~8-9 minutes to lift the cells. Wash medium+10% FBS was added to the growth surface of the flask to neutralize the Trypsin-EDTA. The tubes were spun down, and the supernatant was poured into another 50ml tube. The pellet was resuspended in 0.2% w/v (2mg/ml) Collagenase II solution in tubes and placed in a 37°C water bath. The cell suspension was agitated using a 10ml serological pipette every 10-15 minutes for 1hr. The cell suspension was spun down to remove the Collagenase type II, and resuspended into another 50ml tube. The cells were counted, resuspended into media, and seeded into flasks. Finally, the cells were placed into aggregate differentiation, which allowed the cells to recover their chondrogenic phenotype as previously described in detail. [43]

Self-assembly of neocartilage

For phase I, 5mm diameter circular wells were used to create 2% agarose wells in a 48-well plate. Once the agarose solidified, chondrogenic medium was changed at least twice to saturate the agarose with medium before seeding. The cells were seeded at 4M cells per construct, and were left in an incubator for 4hrs. After 4hrs, 0.5ml of chondrogenic media with DMEM supplemented with 1%/vol PSF, 1%/vol ITS+ Premix Universal Culture Supplement, 1%/vol nonessential amino acids, and 10nM dexamethasone was added to each well carefully, as not to disturb the newly formed constructs. Media was changed daily for the first week. The neocartilage constructs were unconfined from their agarose beds on day 7 and were placed in well-plates with 2ml of media. The media was changed every other day until the completion of the 28-day culture period.

In phase II, rectangular well-makers with a hole at each of the four corners were used to make 2% agarose wells in a 24-well plate. Once the agarose solidified, chondrogenic medium was changed at least twice before cell seeding. Chondrocytes were seeded into the 2% agarose wells using 7M cells per construct to begin the self-assembling process. Four hours after seeding, 0.5ml of chondrogenic medium with DMEM supplemented with 1%/vol PSF, 1%/vol ITS+ premix, 1%/vol nonessential amino acids, and 10 nM dexamethasone was added to each well. Two days after seeding, they were unconfined from the agarose wells and cultured in 24-well plates. The constructs received 2ml of chondrogenic medium each on alternating days for the continuation of the 28-day culture period.

Compression stimulation

In phase I, the compression chamber was created making circular agarose beds in 6-well plates. The constructs were placed in the agarose beds and were covered with a layer of agarose to protect the construct from the stainless steel weights. After placing the agarose, 8ml of media was added into the wells, and the second layer of the well plate was added. The weights, calculated to apply a 5kPa strain, were carefully placed through the hole of the top lid and on top of the construct (Figure 2). The top layer of the well-plate was necessary to stabilize the weight in place. The chamber was then placed in an incubator at 36°C from days 8 -12 of development.

For phase II, compression was applied in a compression chamber on days 8 to 12 of development as described previously.[12] A six-well plate was first coated with 3ml of agarose, and a well-maker was used to create an agarose bed to encase the constructs. The well-maker was removed once the agarose solidified, and it created four thin walls of agarose on four sides. Then, 1ml of agarose was placed inside a petri dish and small rectangular flaps of agarose were cut from the dish. The constructs were placed inside each of the wells on top of the agarose

bed. The flaps were placed on top of the constructs so that the constructs were surrounded and protected by agarose on all sides. The compression chamber was placed on top of the 6-well plate, which helps stabilize the weights directly on top of the constructs (Figure 2). 10ml of media was added into each well, and weights were placed on top of the constructs, causing a 5kPa compressive stress, as described previously.[12] The chamber was closed with a lid, placed in an incubator at 37°C, and were left undisturbed until day 12 of development. The chamber was removed and the constructs were placed, free-floating, on regular six-well plates.

FIGURE 2

Compression stress stimulation bioreactors for neocartilage

a) Rectangular geometry

top
bottom

8mm
13mm

side view

weight
6-well plate
media
agarose
neocartilage

b) Circular geometry

top
bottom

5mm

side view

weight
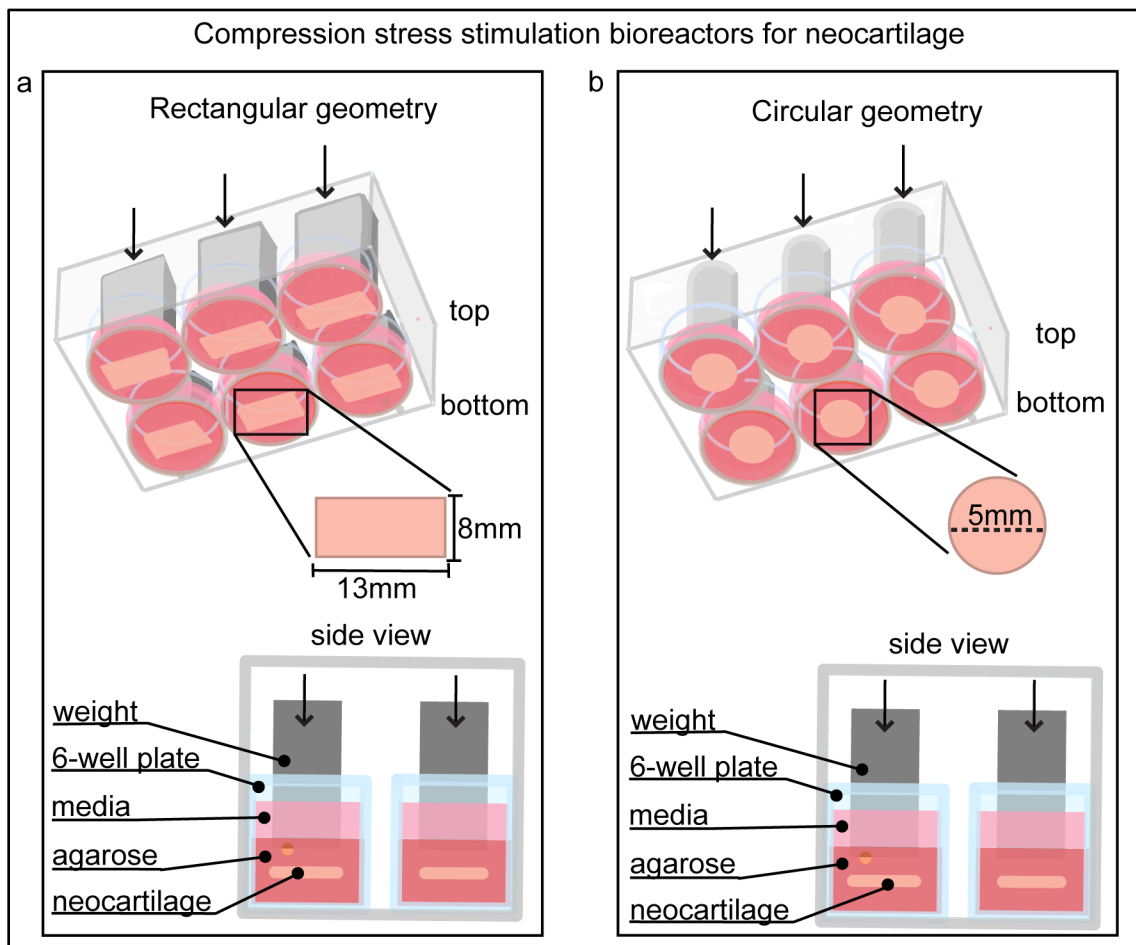6-well plate
media
agarose
neocartilage

Figure 2 – Compression stress stimulation bioreactors. A reverse axis isometric view and a side view of the compression stress stimulation bioreactors are shown. In both **a)** the rectangular geometry and **b)** the circular geometry, the neocartilage is encased in agarose saturated with chondrogenic medium and placed under a weight that exerts 5.5kPa of compressive stress on the neocartilage. The agarose encased neocartilage constructs sit in a 6-well plate that is topped off with 4ml of chondrogenic medium. The neocartilage remains in the compression stress bioreactor from day 8 to day 12 of tissue culture.

Shear stress stimulation

Previously, the effects of shear stress stimulation in engineered neocartilage was examined at different magnitudes; it was determined that stimulation within a range of 0.045-0.21Pa (50RPM) applied at days 15 to 22 yielded the most mechanically robust constructs out of other examined stimulus levels and also as compared to non-stimulated controls.[28]

For phase I, the shear stress device was created as described previously.[28] Each of the constructs were positioned between four poles to keep the constructs in place, and 15ml of chondrogenic media was added into the bioreactor. The fluid-induced shear stress device was then placed on an orbital shaker at 50RPM, and as the orbital shaker rotated, it allowed the media in the FIPS device to flow over the constructs and apply a cyclical pressure that ranged from 0.05Pa to 0.21Pa, as described previously.[28] Media was changed every 2-3 days. After stimulation with shear stress, the constructs were returned to regular 24-well plates and received 2ml of media on alternating days (Figure 3).

For phase II, a new bioreactor was fabricated using a petri dish, an acrylic base with holes, and small rods that were placed into the holes (Figure 3). The rods were placed into groups of four around the circumference of the base. These rods kept the constructs in place because the constructs were rectangular and had a hole in each of the four corners. The constructs were placed into the bioreactor, and 15ml of media was added. The bioreactor was placed in an orbital shaker days 15 to 22, and the constructs were fed every other day.
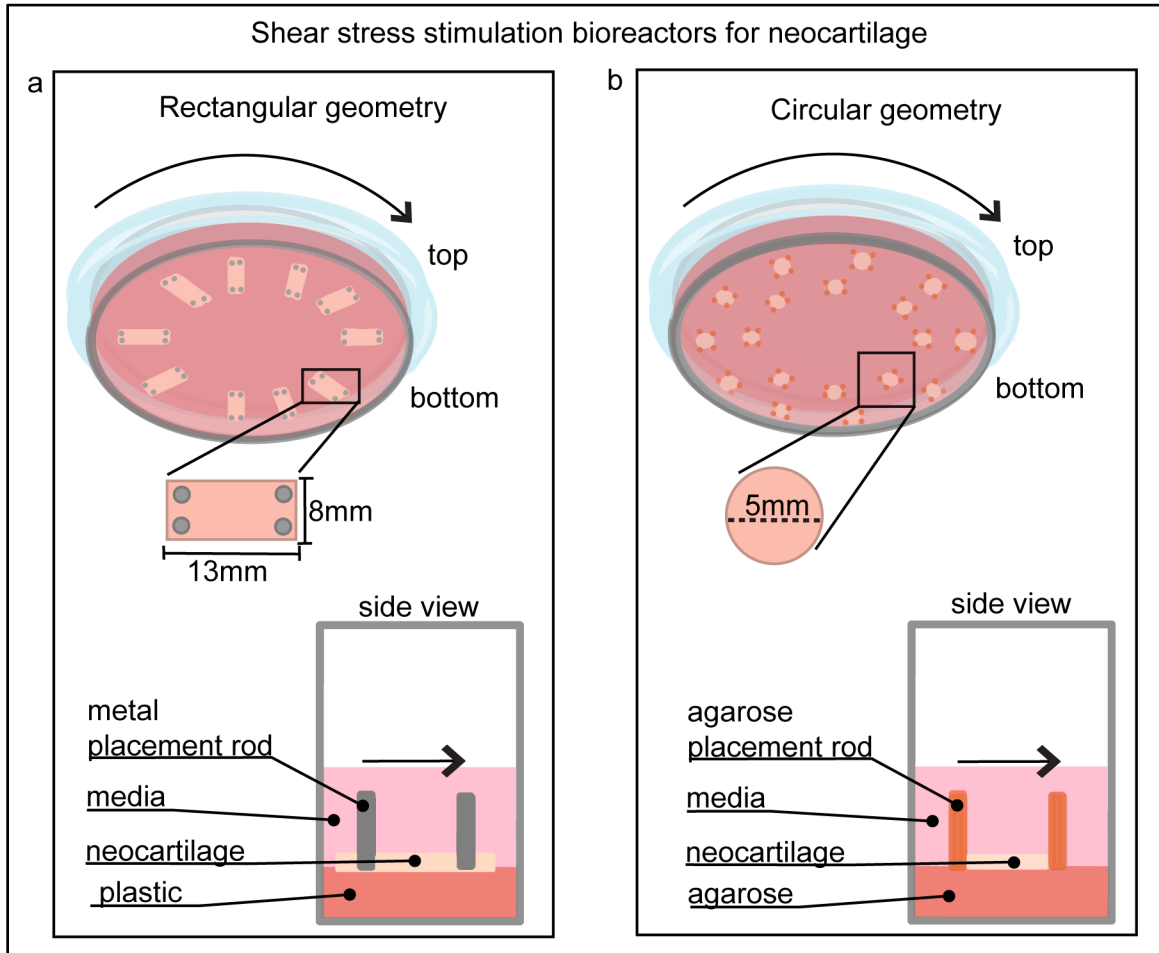
FIGURE 3

Figure 3 – Fluid induced pulsatile shear stress stimulation bioreactors. A reverse axis isometric view and a side view of the shear stress stimulation bioreactors are shown. Both bioreactors are created in a 90mm diameter petri dish, and the petri dish is filled with 15ml of chondrogenic medium. The bioreactor is then placed on an orbital shaker, which creates fluid flow in the bioreactor and, in turn, induces fluid-induced pulsatile shear stress on the neocartilage constructs. In **a)** the shear stress bioreactor for neocartilage of a rectangular geometry, the 8 x13 mm constructs are held in place by four 1mm diameter stainless steel rods located at the corners of the neocartilage. In **b)** the shear stress bioreactor for neocartilage of a circular geometry (5mm in diameter), the neocartilage constructs sit in the middle of four agarose posts.

Biomechanical analysis

To analyze the gross morphology, ImageJ software was used to calculate the constructs' sample thickness and diameter. To determine the compressive properties, a cylindrical 1mm punch was taken from the center of the construct, and a creep indentation test was administered. The aggregate modulus value was calculated using the biphasic model with MATLAB.

Tensile testing was conducted using Instron model 5565, a uniaxial material testing machine. Cartilage constructs were cut into dog bone-shaped samples and were glued to paper rectangles. ImageJ was used to measure the sample thickness, width of the dog bones, and sample cross-sectional areas. A uniaxial strain until failure test was conducted with a strain rate of 1% per second. Load–displacement curves were normalized to the cross-sectional area of each sample, and the Young's modulus and ultimate tensile strength values were calculated with MATLAB.

Biochemical Assessment

To analyze the biochemical content, wet weight and dry weight of the samples were measured. The measured DNA, GAG, and collagen amounts were normalized to both wet weight and dry weight. First, the samples were lyophilized and digested in a 1ml papain solution in a phosphate buffer at 65°C for 18hr. DNA content was quantified using PicoGreen assay. PicoGreen reagents were added to 8ml of the digested sample, and fluorescence was measured at 485/528nm Ex/Em with a Magellan plate reader. A modified chloramine-T hydroxyproline assay and a SIRCOL collagen standard were used to calculate collagen content.[44] 200uL of 4N NaOH was added to the samples, autoclaved, and then 200ml 4N HCl was added. Samples were then incubated with 1.25ml of 0.062M chloramine T for 20min at room temperature, and then they were incubated in 1.25ml of 1.2M Ehrlich's reagent for 20min at 65°C. Absorbance

was measured at 550nm. Finally, GAG content was measured using a Blyscan Glycosaminoglycan Assay kit. 8μl of the digested sample was placed into 500ml dye reagent and set to vortex every 5min for 30 min. The samples were centrifuged, the precipitate as then dissolved in 500ul of dissociated reagent, and the absorbance was measured at 650nm.

<u>Statistics</u>

For phase 1, one-way analysis of variance (ANOVA), and Tukey's *post hoc* tests were performed using $p < 0.05$ to determine statistical significance. For phase 2, a *t*-test was used to compare the two groups. Groups that determined to be statistically different are denoted by different alphabetical letters in the figures.

<div align="center">RESULTS</div>

<u>Phase I</u>

Phase I of this study was conducted with neocartilage derived from bovine articular chondrocytes to determine if a combination of compression stress and shear stress stimulation improved neocartilage mechanical properties beyond compression stress or shear stress alone. As has been seen in previous studies, the addition of only compression stress stimulation improved aggregate modulus and Young's modulus values over nonstimulated controls (Figure 4a, b). Neocartilage stimulated with only shear stress also showed enhanced aggregate modulus values and Young's modulus values over nonstimulated controls (Figure 4a, b). When compared against each other, neocartilage stimulated with only shear stress and neocartilage stimulated with only compression stress did not show any significant differences in terms of compressive and tensile moduli. However, when neocartilage was stimulated with a combination of compression stress and shear stress, the aggregate modulus was significantly improved over nonstimulated controls and compression stress only controls. Neocartilage

stimulated with a combination of compression stress and shear stress also trended higher in aggregate modulus when compared to neocartilage stimulated with only shear stress. Although this trend was not replicated in tensile properties, this data show that including both shear stress and compression stress to a neocartilage tissue culture regimen enhances the compressive moduli of neocartilage over the use of either compression or shear stress alone.

The extracellular matrix content of all neocartilage constructs were also investigated in phase I of this study. Interestingly, neither compression stress nor shear stress alone significantly improved glycosaminoglycan content over nonstimulated controls (Figure 4c). Similarly, collagen content was not significantly improved in neocartilage stimulated with either compression stress or shear stress alone (Figure 4d). When compression stress and shear stress were combined, however, a significant improvement was seen in levels of both glycosaminoglycan content and collagen content over nonstimulated controls. These data show that a combination of compression stress and shear stress is effective for enhancing levels of extracellular matrix in neocartilage constructs created with bovine articular chondrocytes.
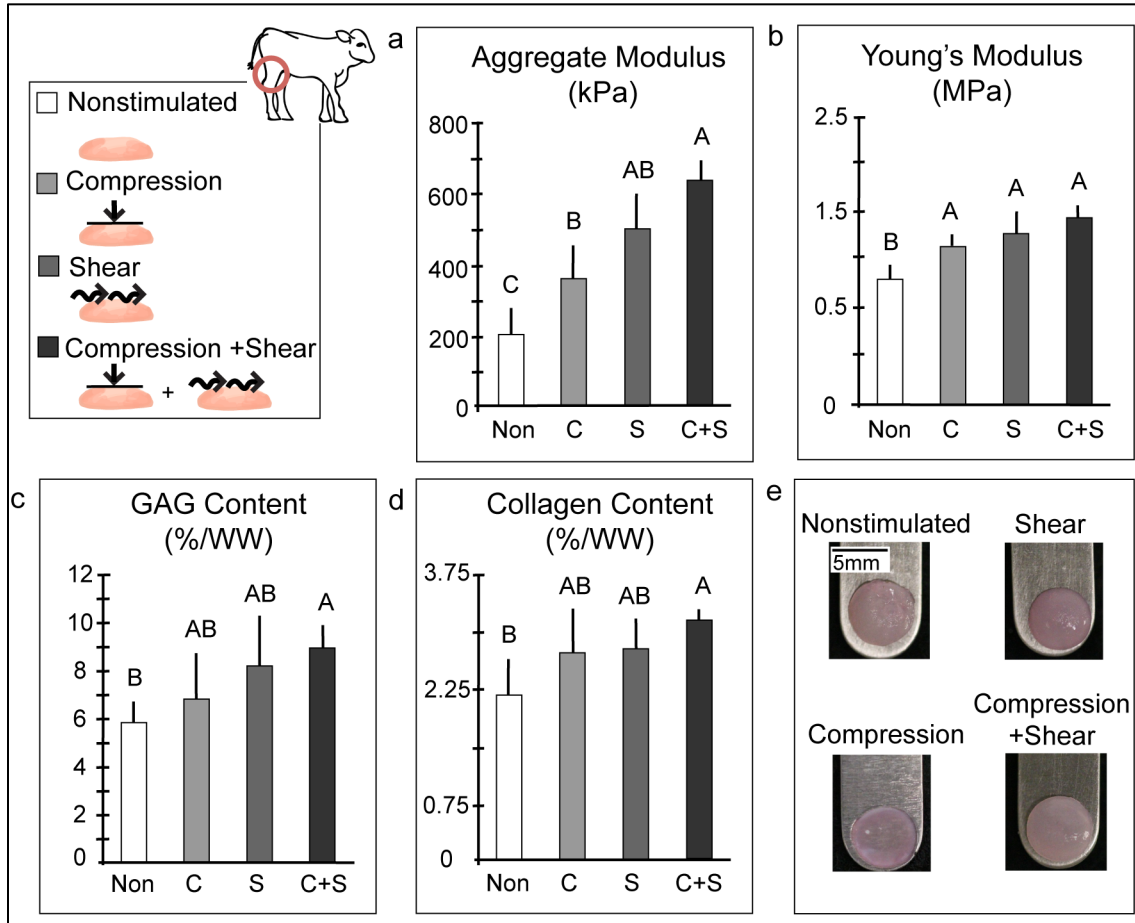
FIGURE 4

Figure 4 – Phase I study results for neocartilage created from bovine articular chondrocytes and either nonstimulated or stimulated with compression stress only, shear stress only, or a combination of both. **a)** The aggregate modulus, **b)** the ultimate tensile strength, **c)** the glycosaminoglycan content, and **d)** the collagen content of neocartilage constructs are shown. **e)** The representative gross morphology of constructs. The capital letters floating above the bars indicate statistically different groups evaluated at a $p < 0.05$ using a one-way ANOVA and Tukey's *post hoc* test. Abbreviations: nonstimulated (Non), shear stress only (S), compression stress only (C), combination of compression and shear stress (C+S), glycosaminoglycan (GAG), percent per wet weight (%/WW), kilopascals (kPa), megapascals (MPa).

Phase II

In phase II, minipig costal cartilage chondrocytes were used to create large neocartilage constructs to determine the translatability of using a combination of compression and shear stress. When a combination of compression stress and shear stress was used in neocartilage culture, the aggregate modulus was significantly improved over nonstimulated control constructs

(Figure 5a). Similarly, the Young's modulus of neocartilage stimulated with both compression stress and shear stress was enhanced over nonstimulated controls (Figure 5b). These data show that using a combination of compression stress and shear stress during neocartilage tissue culture improves mechanical properties in large constructs made from minipig costal chondrocytes.

As in phase I, extracellular matrix content was also examined in phase II for all neocartilage constructs. A lack of significant improvements was seen when comparing constructs that were stimulated with a combination of compression stress and shear stress stimulation (Figure 5c, d). The glycosaminoglycan content of stimulated neocartilage was not improved over nonstimulated controls. Similarly, the collagen content of stimulated neocartilage was not improved over nonstimulated controls. This indicates that this particular combination of mechanical stimulation does not cause significant differences in extracellular matrix levels in neocartilage constructs created with minipig costal chondrocytes.
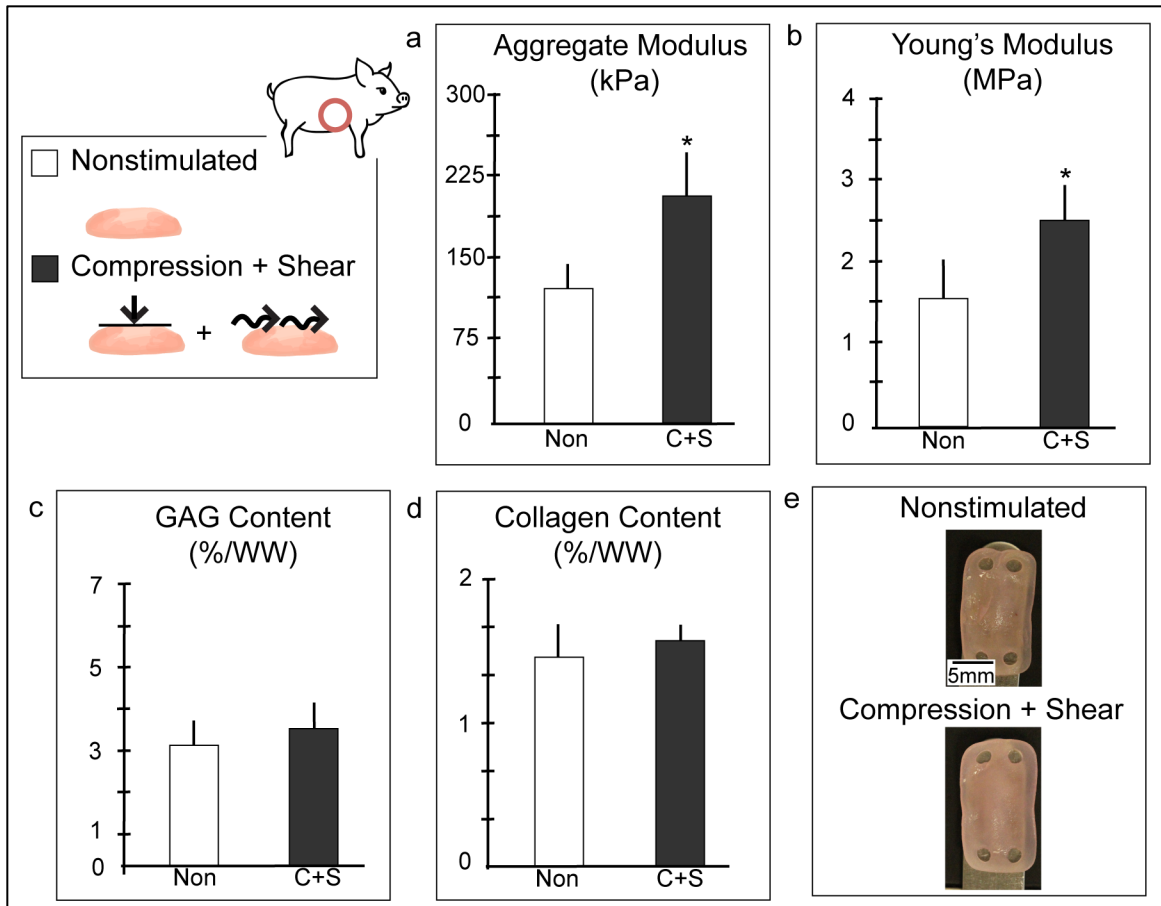
FIGURE 5

Figure 5 – Phase II study results for large neocartilage constructs created from minipig costal chondrocytes and either not stimulated or stimulated with a combination of compression stress and shear stress. **a)** The aggregate modulus, **b)** the ultimate tensile strength, **c)** the glycosaminoglycan content, and **d)** the collagen content of neocartilage constructs are shown. **e)** representative gross morphology of constructs An asterisk (*) above a bar indicates that the group is statistically different at a $p<0.05$ using a students t-test. Abbreviations: nonstimulated (non), combination of compression and shear stress (C+S), glycosaminoglycan (GAG), percent per wet weight (%/WW), kilopascals (kPa), megapascals (MPa)

DISCUSSION

To determine if the combination of compression stress and shear stress stimulation is an efficient strategy to improve neocartilage construct mechanical properties and extracellular matrix levels, the objectives of this study were: 1) to create neocartilage constructs with bovine articular chondrocytes and compare the mechanical and biochemical outcomes of culturing

them under compression stress, shear stress, or both, and 2) to translate the combination of compression and shear stress stimulation to large neocartilage constructs created with minipig costal chondrocytes. Previous to this study, compression stimulation had not been attempted on self-assembled neocartilage constructs created with bovine articular chondrocytes. Furthermore, the development of a bioreactor was necessary for applying compression stimulation on circular 5mm diameter neocartilage constructs. It was hypothesized that neocartilage cultured under the combination of compression stress and shear stress would outperform nonstimulated neocartilage and in terms of mechanical properties and extracellular matrix content of both minipig and bovine constructs. The results of this study showed that a combination of compression and shear stress improved the mechanical properties of neocartilage constructs over nonstimulated constructs and constructs stimulated with only compression stress. In terms of extracellular matrix content, neocartilage stimulated with both compression and shear stress improved over nonstimulated controls. Although these results show that neocartilage cultured under both compression and shear stress improve mechanical properties over controls, the lack of improvements in extracellular matrix content suggest that improvements in crosslinks or extracellular matrix organization may be at play. [45-47]

Previous studies in self-assembled neocartilage have investigated the most effective times of application for both compression stress and shear stress stimulation.[12] For compression stress, it was found that stimulation during the synthesis stage of neocartilage development is the most effective when compared to the maturation stage and no stimulation.[11, 12] Specifically, glycosaminoglycan content, Young's modulus, and ultimate tensile stress values all trended higher when compression stimulation was applied during the synthesis stage. For shear stress, it was found that stimulation during the maturation stage of neocartilage development is most effective when compared to the synthesis stage and no stimulation. Specifically, aggregate modulus, ultimate tensile strength, and collagen content

were all significantly improved when shear stress was implemented during the maturation stage of neocartilage development.[28] The present study aimed to combine the application timelines of compression stress and shear stress stimulation to create further improved neocartilage constructs.

As in previous studies, the addition of compression stress during the culture of neocartilage created from bovine articular chondrocytes improved aggregate modulus, a compressive property.[12] The addition of shear stress has also been shown to improve neocartilage aggregate modulus.[28] When combined, the implementation of both compression and shear stress improved the aggregate modulus of neocartilage over nonstimulated controls and neocartilage stimulated with only compression stress. When comparing against the neocartilage stimulated with only shear stress, the neocartilage stimulated with both compression and shear stress trended higher in aggregate modulus, but was not significantly improved. This indicates that shear stress stimulation boosts aggregate modulus properties when used in combination with compression stress stimulation, but this combination was not enough to create a significant difference from neocartilage stimulated with only shear stress. There are nutrient diffusion limitations presented in using compression stimulation because the neocartilage must be encased in agarose [48, 49]; these limitations are not present when implementing only shear stress.[50] It is possible that the addition of shear stress stimulation is overcoming the nutrient diffusion limitations of a compression stress only culture regimen. According to the results presented here, the addition of compression stimulation does not upgrade a shear stress stimulation only culture to produce neocartilage constructs with improved compressive properties.

The Young's modulus, a tensile property, was improved over nonstimulated neocartilage in all groups that implemented mechanical stimulation. As in previous studies, the neocartilage that was stimulated with only shear stress displayed improved Young's modulus values,[51] and

the neocartilage that was stimulated with only compression stress also showed improvements in neocartilage Young's moduli. When compression stress and shear stress were used in combination, however, the Young's modulus of the neocartilage constructs did not improve over either form of stimulus alone. Because the creation of neocartilage requires mechanical properties that hold up to native tissue environments, a different form of stimulus, either biochemical or mechanical, may be necessary to further improve tensile properties. For example, the addition of the growth factor TGF-β1 has previously been shown to drastically improve tensile properties in neocartilage, such as ultimate tensile strength and Young's modulus.[52] Another bioactive factor known for improving tensile properties is LOXL2, which increases the amount of pyridinoline crosslinks between collagen fibers.[53] When trying to improve tensile properties of neocartilage without the use of bioactive factors, it may be possible to use uniaxial tension stimulation as it has been shown to improve Young's modulus 10-fold over nonstimulated controls.[38] The caveat of using uniaxial tensile stimulation is that it does not improve compressive properties. However, because the use of shear stress or compression stress improves neocartilage compressive properties, the combination of either of these stimuli with uniaxial tensile stress has the potential to yield neocartilage with enhanced mechanical properties all around.

This study explored the translatability and flexibility of using a combination of compression stress and shear stress on different cell types and different neocartilage geometries. Specifically, bovine articular chondrocytes were used to create 5mm diameter neocartilage constructs, and minipig costal chondrocytes were used to create large, 8x13mm, rectangular constructs. Bovine articular chondrocytes are widely available and economically feasible for exploratory experiments, but are not amenable for allogeneic implantation in pre-clinical large animal studies. On the other hand, minipig costal chondrocytes are suitable for allogeneic implantation in pre-clinical large animal studies because of the minipigs docile nature

and similar anatomy to humans.[54-56] However, minipig costal chondrocytes are not widely available and are typically more expensive to acquire than bovine articular chondrocytes. In this study it was shown that a combination of compression stress and shear stress elicit similar positive responses in both bovine articular chondrocytes and minipig costal chondrocytes and in both large and small neocartilage geometries.

This set of studies contributes to the progression of tissue engineering in creating mechanically robust neocartilage constructs for implantation. In terms of using mechanical stimulation, future studies should investigate the use of other combinations of mechanical stimulation such as compression stress and uniaxial tensile stress. Another option would be implementing uniaxial tensile stress and shear stress in combination to improve neocartilage mechanical properties. The use of a combination of mechanical stimulation alongside a cocktail of bioactive factors has yet to be investigated and has the potential to improve neocartilage properties to the level of native articular cartilage. Separately, previous strategies have provided incremental progression toward effective neocartilage implants, but a combination of both mechanical stimulation and bioactive factors has the potential to deliver neocartilage that can be used successfully in vivo to treat articular cartilage lesions.

REFERENCES

[1] M.W. Ropes, E.C. Rossmeisl, W. Bauer, THE ORIGIN AND NATURE OF NORMAL HUMAN SYNOVIAL FLUID, J Clin Invest 19(6) (1940) 795-799.

[2] C.W. Archer, J. McDowell, M.T. Bayliss, M.D. Stephens, G. Bentley, Phenotypic modulation in sub-populations of human articular chondrocytes in vitro, Journal of Cell Science 97(2) (1990) 361.

[3] J. Klompmaker, R. Veth, H. Jansen, H. Nielsen, J. De Groot, A. Pennings, R. Kuijer, Meniscal repair by fibrocartilage in the dog: characterization of the repair tissue and the role of vascularity, Biomaterials 17(17) (1996) 1685-1691.

[4] J.M. Hootman, C.G. Helmick, K.E. Barbour, K.A. Theis, M.A. Boring, Updated Projected Prevalence of Self-Reported Doctor-Diagnosed Arthritis and Arthritis-Attributable Activity Limitation Among US Adults, 2015-2040, Arthritis Rheumatol 68(7) (2016) 1582-1587.

[5] B.J. Huang, J.C. Hu, K.A. Athanasiou, Cell-based tissue engineering strategies used in the clinical repair of articular cartilage, Biomaterials 98 (2016) 1-22.

[6] F. McCormick, J.D. Harris, G.D. Abrams, R. Frank, A. Gupta, K. Hussey, H. Wilson, B. Bach, Jr., B. Cole, Trends in the surgical treatment of articular cartilage lesions in the United States: an analysis of a large private-payer database over a period of 8 years, Arthroscopy 30(2) (2014) 222-6.

[7] S.R. Montgomery, B.D. Foster, S.S. Ngo, R.D. Terrell, J.C. Wang, F.A. Petrigliano, D.R. McAllister, Trends in the surgical treatment of articular cartilage defects of the knee in the United States, Knee Surg Sports Traumatol Arthrosc 22(9) (2014) 2070-5.

[8] A. Gobbi, G. Karnatzikos, A. Kumar, Long-term results after microfracture treatment for full-thickness knee chondral lesions in athletes, Knee Surg Sports Traumatol Arthrosc 22(9) (2014) 1986-96.

[9] P.C. Kreuz, M.R. Steinwachs, C. Erggelet, S.J. Krause, G. Konrad, M. Uhl, N. Südkamp, Results after microfracture of full-thickness chondral defects in different compartments in the knee, Osteoarthritis Cartilage 14(11) (2006) 1119-25.

[10] J.C. Hu, K.A. Athanasiou, A self-assembling process in articular cartilage tissue engineering, Tissue Engineering 12(4) (2006) 969-979.

[11] S.D. Waldman, D.C. Couto, M.D. Grynpas, R.M. Pilliar, R.A. Kandel, A single application of cyclic loading can accelerate matrix deposition and enhance the properties of tissue-engineered cartilage, Osteoarthritis and Cartilage 14(4) (2006) 323-330.

[12] L.W. Huwe, G.K. Sullan, J.C. Hu, K.A. Athanasiou, Using Costal Chondrocytes to Engineer Articular Cartilage with Applications of Passive Axial Compression and Bioactive Stimuli, Tissue Eng Part A 24(5-6) (2018) 516-526.

[13] J.B. Fitzgerald, M. Jin, D.H. Chai, P. Siparsky, P. Fanning, A.J. Grodzinsky, Shear- and Compression-induced Chondrocyte Transcription Requires MAPK Activation in Cartilage Explants, Journal of Biological Chemistry 283(11) (2008) 6735-6743.

[14] A.J. Grodzinsky, M.E. Levenston, M. Jin, E.H. Frank, Cartilage Tissue Remodeling in Response to Mechanical Forces, Annual Review of Biomedical Engineering 2(1) (2000) 691-713.

[15] S.C. Tran, A.J. Cooley, S.H. Elder, Effect of a mechanical stimulation bioreactor on tissue engineered, scaffold-free cartilage, Biotechnology and Bioengineering 108(6) (2011) 1421-1429.

[16] N. Yusoff, N.A. Abu Osman, B. Pingguan-Murphy, Design and validation of a bi-axial loading bioreactor for mechanical stimulation of engineered cartilage, Medical Engineering & Physics 33(6) (2011) 782-788.

[17] H. Kwon, N.K. Paschos, J.C. Hu, K.A. Athanasiou, Articular cartilage tissue engineering: the role of signaling molecules, Cellular and Molecular Life Sciences 73(6) (2016) 1173-1194.

[18] D.J. Huey, K.A. Athanasiou, Maturational growth of self-assembled, functional menisci as a result of TGF-β1 and enzymatic chondroitinase-ABC stimulation, Biomaterials 32(8) (2011) 2052-2058.

[19] E.A. Makris, R.F. MacBarb, N.K. Paschos, J.C. Hu, K.A. Athanasiou, Combined use of chondroitinase-ABC, TGF-β1, and collagen crosslinking agent lysyl oxidase to engineer functional neotissues for fibrocartilage repair, Biomaterials 35(25) (2014) 6787-6796.

[20] T. Ito, R. Sawada, Y. Fujiwara, T. Tsuchiya, FGF-2 increases osteogenic and chondrogenic differentiation potentials of human mesenchymal stem cells by inactivation of TGF-β signaling, Cytotechnology 56(1) (2008) 1-7.

[21] H. Liu, Z. Zhao, R.B. Clarke, J. Gao, I.R. Garrett, E.E.C. Margerrison, Enhanced Tissue Regeneration Potential of Juvenile Articular Cartilage, The American Journal of Sports Medicine 41(11) (2013) 2658-2667.

[22] J.E. Babensee, L.V. McIntire, A.G. Mikos, Growth Factor Delivery for Tissue Engineering, Pharmaceutical Research 17(5) (2000) 497-504.

[23] L.A. Fortier, J.U. Barker, E.J. Strauss, T.M. McCarrel, B.J. Cole, The Role of Growth Factors in Cartilage Repair, Clinical Orthopaedics and Related Research® 469(10) (2011) 2706-2715.

[24] A.M. Handorf, C.S. Chamberlain, W.-J. Li, Endogenously Produced Indian Hedgehog Regulates TGFβ-Driven Chondrogenesis of Human Bone Marrow Stromal/Stem Cells, Stem Cells and Development 24(8) (2014) 995-1007.

[25] K.D. Allen, K.A. Athanasiou, Viscoelastic characterization of the porcine temporomandibular joint disc under unconfined compression, J Biomech 39(2) (2006) 312-322.

[26] K.A. Wartella, J.S. Wayne, Bioreactor for biaxial mechanical stimulation to tissue engineered constructs, Journal of biomechanical engineering 131(4) (2009).

[27] S. Evelia, A. Ashkan, P. Nikolaos, B. Eric, K. Heenam, H. Jerry, A. Kyriacos, Shear stress induced by fluid flow produces improvements in tissue-engineered cartilage, Biofabrication (2020).

[28] E.Y. Salinas, A. Aryaei, N. Paschos, R.E. Berson, H. Kwon, J.C. Hu, K.A. Athanasiou, Fluid-induced pulsatile shear stress on tissue-engineered cartilage, Biofabrication (2020).

[29] C.V. Gemmiti, R.E. Guldberg, Shear stress magnitude and duration modulates matrix composition and tensile mechanical properties in engineered cartilaginous tissue, Biotechnology and Bioengineering 104(4) (2009) 809-820.

[30] C.V. Gemmiti, R.E. Guldberg, Fluid flow increases type II collagen deposition and tensile mechanical properties in bioreactor-grown tissue-engineered cartilage, Tissue Engineering 12(3) (2006) 469-479.

[31] S.E. Carver, C.A. Heath, Influence of intermittent pressure, fluid flow, and mixing on the regenerative properties of articular chondrocytes, Biotechnology and Bioengineering 65(3) (1999) 274-281.

[32] J.M.D. Thomas, A. Chakraborty, M.K. Sharp, R.E. Berson, Spatial and temporal resolution of shear in an orbiting petri dish, Biotechnology Progress 27(2) (2011) 460-465.

[33] A.K. Wann, N. Zuo, C.J. Haycraft, C.G. Jensen, C.A. Poole, S.R. McGlashan, M.M. Knight, Primary cilia mediate mechanotransduction through control of ATP-induced Ca2+ signaling in compressed chondrocytes, The FASEB Journal 26(4) (2012) 1663-1671.

[34] J.T. Eggenschwiler, K.V. Anderson, Cilia and Developmental Signaling, Annual Review of Cell and Developmental Biology 23(1) (2007) 345-373.

[35] D. Maggiorani, R. Dissard, M. Belloy, J.-S. Saulnier-Blache, A. Casemayou, L. Ducasse, S. Grès, J. Bellière, C. Caubet, J.-L. Bascands, J.P. Schanstra, B. Buffin-Meyer, Shear Stress-Induced Alteration of Epithelial Organization in Human Renal Tubular Cells, PLOS ONE 10(7) (2015) e0131416.

[36] R. Ruhlen, K. Marberry, The chondrocyte primary cilium, Osteoarthritis and Cartilage 22(8) (2014) 1071-1076.

[37] Z.S. Xiao, L.D. Quarles, Role of the polycytin-primary cilia complex in bone development and mechanosensing, Annals of the New York Academy of Sciences 1192(1) (2010) 410-421.

[38] J.K. Lee, L.W. Huwe, N. Paschos, A. Aryaei, C.A. Gegg, J.C. Hu, K.A. Athanasiou, Tension stimulation drives tissue formation in scaffold-free systems, Nature Materials 16(8) (2017) 864.

[39] E.A. Makris, R.F. MacBarb, D.J. Responte, J.C. Hu, K.A. Athanasiou, A copper sulfate and hydroxylysine treatment regimen for enhancing collagen cross-linking and biomechanical properties in engineered neocartilage, The FASEB Journal 27(6) (2013) 2421-2430.

[40] L. Bian, J.V. Fong, E.G. Lima, A.M. Stoker, G.A. Ateshian, J.L. Cook, C.T. Hung, Dynamic mechanical loading enhances functional properties of tissue-engineered cartilage using mature canine chondrocytes, Tissue Eng Part A 16(5) (2010) 1781-1790.

[41] L.W. Huwe, W.E. Brown, J.C. Hu, K.A. Athanasiou, Characterization of costal cartilage and its suitability as a cell source for articular cartilage tissue engineering, Journal of tissue engineering and regenerative medicine 12(5) (2018) 1163-1176.

[42] W.E. Brown, J.C. Hu, K.A. Athanasiou, Ammonium-Chloride-Potassium Lysing Buffer Treatment of Fully Differentiated Cells Increases Cell Purity and Resulting Neotissue Functional Properties, Tissue Eng Part C Methods 22(9) (2016) 895-903.

[43] K.A. Athanasiou, J.C. Hu, H. Kwon, Methods and systems for conserving highly expanded cells, in: U.S.P. Office (Ed.) 2018.

[44] D.D. Cissell, J.M. Link, J.C. Hu, K.A. Athanasiou, A modified hydroxyproline assay based on hydrochloric acid in Ehrlich's solution accurately measures tissue collagen content, Tissue Engineering Part C: Methods 23(4) (2017) 243-250.

[45] C.J. Little, N.K. Bawolin, X. Chen, Mechanical properties of natural cartilage and tissue-engineered constructs, Tissue Eng Part B Rev 17(4) (2011) 213-27.

[46] A.K. Williamson, A.C. Chen, K. Masuda, E.J.-M.A. Thonar, R.L. Sah, Tensile mechanical properties of bovine articular cartilage: Variations with growth and relationships to collagen network components, Journal of Orthopaedic Research 21(5) (2003) 872-880.

[47] A.K. Williamson, K. Masuda, E.J.M.A. Thonar, R.L. Sah, Growth of Immature Articular Cartilage in Vitro: Correlated Variation in Tensile Biomechanical and Collagen Network Properties, Tissue Engineering 9(4) (2003) 625-634.

[48] J. Liu, J. Hilderink, T.A. Groothuis, C. Otto, C.A. Van Blitterswijk, J. de Boer, Monitoring nutrient transport in tissue‑engineered grafts, Journal of tissue engineering and regenerative medicine 9(8) (2015) 952-960.

[49] L. Bian, S. Angione, K. Ng, E. Lima, D. Williams, D. Mao, G. Ateshian, C. Hung, Influence of decreasing nutrient path length on the development of engineered cartilage, Osteoarthritis and cartilage 17(5) (2009) 677-685.

[50] G.A. Ateshian, K.D. Costa, C.T. Hung, A theoretical analysis of water transport through chondrocytes, Biomech Model Mechanobiol 6(1-2) (2007) 91-101.

[51] A.H. Huang, B.M. Baker, G.A. Ateshian, R.L. Mauck, Sliding contact loading enhances the tensile properties of mesenchymal stem cell-seeded hydrogels, Eur Cell Mater 24 (2012) 29-45.

[52] A.H. Huang, A. Stein, R.S. Tuan, R.L. Mauck, Transient exposure to transforming growth factor beta 3 improves the mechanical properties of mesenchymal stem cell–laden cartilage constructs in a density-dependent manner, Tissue Engineering Part A 15(11) (2009) 3461-3472.

[53] E.A. Makris, D.J. Responte, N.K. Paschos, J.C. Hu, K.A. Athanasiou, Developing functional musculoskeletal tissues through hypoxia and lysyl oxidase-induced collagen cross-linking, Proceedings of the National Academy of Sciences 111(45) (2014) E4832-E4841.

[54] N. Vapniarsky, A. Aryaei, B. Arzi, D.C. Hatcher, J.C. Hu, K.A. Athanasiou, The Yucatan Minipig Temporomandibular Joint Disc Structure-Function Relationships Support Its Suitability for Human Comparative Studies, Tissue Eng Part C Methods 23(11) (2017) 700-709.

[55] L.M. Panepinto, R.W. Phillips, The Yucatan miniature pig: characterization and utilization in biomedical research, Lab Anim Sci 36(4) (1986) 344-7.

[56] C.G. Pfeifer, M.B. Fisher, V. Saxena, M. Kim, E.A. Henning, D.A. Steinberg, G.R. Dodge, R.L. Mauck, Age-Dependent Subchondral Bone Remodeling and Cartilage Repair in a Minipig Defect Model, Tissue Eng Part C Methods 23(11) (2017) 745-753.

CHAPTER 5- IMPROVING MECHANICAL PROPERTIES OF NEOCARTILAGE WITH A COMBINATION OF TENSION AND SHEAR STRESS STIMULATION DURING TISSUE CULTURE

ABSTRACT

The manipulation of neocartilage construct mechanical properties toward native tissue values is typically achieved with bioactive factors. With self-assembled neocartilage in particular, a cocktail of bioactive agents (TGF-β1, C-ABC, and LOXL2) is used to improve tensile properties. Mechanical stimulation strategies, however, have only been used separately to improve self-assembled neocartilage. Uniaxial tension stress has been found to improve tensile stiffness and strength, while fluid-induced shear stress has yielded neocartilage with improved compressive stiffness. Thus, the objective of this research was to use a combination of mechanical stimulation strategies to improve multiple neocartilage mechanical properties. It was found that the combination of shear stress and tensile stress led to synergistic improvements, not only in tensile properties, but compressive stiffness as well. Furthermore, the extracellular matrix content of neocartilage constructs stimulated with combined treatments was additively improved over nonstimulated controls. Overall, the combination of uniaxial tension stress and fluid-induced shear stress yielded improvements in extracellular matrix properties that were not seen in neocartilage constructs stimulated with only one form of mechanical stimulus.

Authors: Salinas EY, Herrera JM, Hu JC, Athanasiou KA

INTRODUCTION

Every tissue in the body has a few common necessities: nutrient transport, waste transport, and signal transmission. In the body, these necessities are largely achieved by vasculature, which transport soluble factors and deliver mechanical signals via fluid-induced shear stress. Conversely, when looking at *in vitro* tissue engineering, the transfer of nutrients and soluble factors, along with fluid-induced mechanical signals, are limited, if not completely lacking, because the tissue being cultured typically sits in a stationary well of culture medium. Although static cultures are customary in tissue engineering, numerous studies have shown the benefits of using mechanical stimulation to enhance a variety of tissues. [1-6] For example, vascular endothelial cells and cardiomyocytes have been shown to respond positively to shear stress. [7-9] Additionally, neocartilage has been shown to benefit from certain levels of hydrostatic pressure, and separately to tensile stress.[10-14] Motivated by the necessity of mechanical stimulation in the body, and by the benefits of mechanical stimulation in tissue culture, this study aimed to explore the combination of two types of mechanical stress to improve engineered tissue properties.

Articular cartilage, in particular, relies heavily on mechanical movement and synovial fluid flow to attain nutrients and transmit signals because it is avascular. [15] Because articular cartilage is avascular, it does not have access to circulating progenitor cells and does not posses the ability to repair. [16] For the 250,000 Americans a year that seek clinical treatment for articular cartilage damage and degradation, tissue engineered neocartilage has the potential to provide a long-term repair option. [17] Robust mechanical properties are salient for neocartilage implants because in the body, articular cartilage experiences constant and repetitive shear stress, hydrostatic pressure, compressive stress, and tensile stress. [15, 18-21] The self-assembling process is a developing tissue engineering strategy for the creation of neocartilage that does not rely on scaffolds to provide robust mechanical properties. [22]

Instead, the self-assembling process utilizes bioactive factors or mechanical stimulation to enhance neocartilage properties. When mechanical stimulation, such as tension, compression, or shear stress is applied during neocartilage self-assembly, the results are improved mechanical properties and extracellular matrix content. [19, 23-25] In particular, fluid-induced shear stress has been shown to improve the compressive moduli of self-assembled neocartilage, and continuous tensile stress has been shown to improve tensile stiffness and strength.

Shear stress stimulation during tissue culture, implemented at low frequencies (<1 Hz) and low magnitudes (<0.5 Pa), has been utilized to improve neocartilage construct properties. [1, 25-28] In particular, the application of direct shear stress via a parallel plate improved scaffold-free neocartilage tensile properties. [29, 30] In a separate study it was found that when a chondrocyte-seeded polyurethane scaffold was stimulated with shear stress, boundary lubrication friction coefficients were lowered toward native tissue values. [28] For self-assembled neocartilage in particular, it was found that the inclusion of fluid-induced shear stress during tissue culture improved neocartilage compressive properties and collagen content. [25] Furthermore, it was been found that fluid-induced shear stress upregulated genes encoding mechanically gated ion channels in primary cilia, suggesting that this is the initial actor in a cascade of events that culminates in improved extracellular matrix content and mechanical properties. Although it is still not widely used, overall, the application of low levels of shear stress has revealed itself to be a valuable addition in neocartilage tissue culture.

Axial tensile strain of engineered tissues results from tensile forces being applied by directly pulling the tissue outward along the edges.[24, 31] Although there are very few studies that have investigated the use of tensile stimulation on neocartilage, its effectiveness in yielding stiff and strong tensile properties has been shown. [24, 32-34] Specifically, when combined with a cocktail of bioactive factors, continuous uniaxial tension produced neocartilage reaching 94%

of native articular cartilage tensile stiffness. [24] Additionally, uniaxial tensile stimulation has been the only form of treatment that has developed anisotropy in neocartilage constructs. [24] Overall, uniaxial tensile stress has shown evidence of being a useful tool for driving the morphology and mechanical properties of neocartilage toward those of native articular cartilage.

In this study, the application of constant uniaxial tension stress was combined with fluid-induced shear stress on neocartilage constructs during tissue culture. The neocartilage constructs used in this study were created with the self-assembling process from expanded costochondrocytes of Yucatan minipigs, and formed into 8x13mm rectangular constructs. This investigation compared the combination of tension and shear stress stimulation on neocartilage constructs against neocartilage that was stimulated with only tension, with only shear, or nonstimulated control constructs. All neocartilage constructs were evaluated in terms of extracellular matrix content (glycosaminoglycans and collagen content), as well as mechanical properties (aggregate modulus, Young's modulus, and ultimate tensile strength). It was hypothesized that the neocartilage constructs that received both continuous uniaxial tensile stress and fluid-induced shear stress would yield improved properties over constructs that only received one form of mechanical stimulus or no stimulus at all.

MATERIALS AND METHODS

<u>Study design</u>

Neocartilage constructs were created with expanded and redifferentiated minipig costal chondrocytes via the self-assembling process. After an initial 7 days of culture, the neocartilage constructs were treated according to four different experimental groups: 1) Nonstimulated control, 2) Uniaxial tensile stress, 3) Fluid-induced shear stress, 4) Uniaxial tensile stress and fluid-induced shear stress. Figure 1 shows the times of application for the mechanical stimulation strategies.
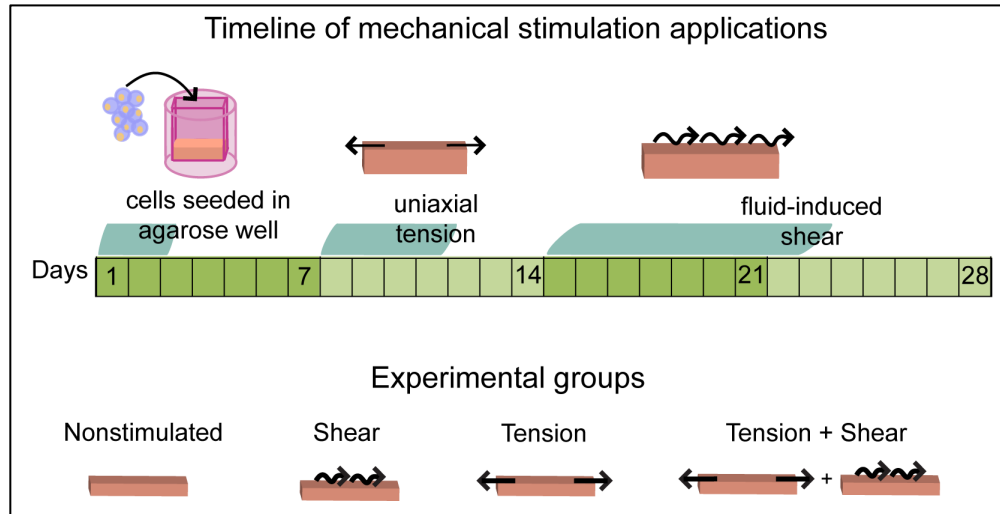
FIGURE 1

Figure 1 – Tissue culture timeline of a self-assembled neocartilage construct stimulated with uniaxial tension stress and fluid-induced shear stress. On day 0, chondrocytes are seeded in a non-adherent agarose well that was previously saturated with chondrogenic media. On day 7, neocartilage is removed from the agarose well. From day 8 to day 12, the neocartilage undergoes uniaxial tension stress stimulation in the tension bioreactor. On day 12 the neocartilage constructs are no longer stretched, but remain in the tension stress bioreactor. On day 15, shear stress is applied on the neocartilage via the fluid-induced shear stress bioreactor and remains there until day 22. Finally on day 22, the neocartilage is removed from shear stress stimulation and is placed in a 24-well plate until the end of culture on day 28. A schematic of the experimental groups is shown in the bottom half of the figure.

Mini pig costal chondrocyte harvest

Mini pig costal chondrocytes were harvested from the costal cartilage of juvenile (6-8 months) Yucatan minipigs obtained from (S&S Farms, California, USA). The perichondrium was removed from the costal cartilage and minced. Next, the minced cartilage was digested in a solution of 0.2% w/v collagenase and 3% fetal bovine serum (FBS) for 18hr. The chondrocytes that were extracted during digestion were then strained, counted, and frozen in a solution of 90% FBS and 10% dimethyl sulfoxide.

<u>Expansion and aggregate redifferentiation</u>

Mini pig costal chondrocytes were thawed in a water bath at 37°C, rinsed in wash media, centrifuged at 400g, and resuspended in warm chondrogenic media with 2%FBS. The cells were counted and brought to 1e6 cells/ml in CHG+2% FBS plus growth factors (1ng/ml TGF-β1 + 5ng/ml bFGF + 10ng/ml PDGF). Finally 2.5ml of the cell solution plus 27.5 ml of CHG+2% FBS were seeded per T225 flask, and the flasks were placed in an incubator set to 10% CO_2. The chondrogenic media + growth factors in the flasks were changed every 3-4 days. When the cells expanded to fill about 95% of the bottom of the flask, they were ready to be passaged as described previously. [35]

The cells were ready for passage about 2 weeks after being seeded. The cells were lifted using 0.05% Trypsin-EDTA, and then rinsed in chondrogenic media. Cells were then resuspended in a solution of 2% collagenase and 3% FBS for 2 hours at 37°C. The cells were then seeded onto a T225 flask as specified above.

Once the cells were expanded to passage 3, they were placed into aggregate redifferentiation, as described previously.[36] Briefly, the cells were lifted from expansion and placed in a 1% agarose coated petri dish at 10e6 cell/mL of chondrogenic media and growth factors (10ng/mL TGF-β1 + 100ng/mL GDF5 + 100ng/mL BMP-2). The petri dish was placed on an orbital shaker at 50RPM for the first 24 hours after seeding. Next the petri dish was moved to a shelf and fed every 3-4 days for 11 days. The aggregates are then digested using 0.05% trypsin-EDTA solution and a subsequent 2% collagenase solution (with 3% FBS) to liberate the chondrocytes that were used to make the neocartilage.

<u>Neocartilage self-assembly</u>

First, 8x13mm agarose wells (2%) were created using an acrylic well-maker as described previously. [23] Chondrocytes were suspended in chondrogenic media and seeded in the wells.

Each well was seeded with 7 million chondrocytes suspended in 250µl of chondrogenic media. After 4 hours, the cells were fed chondrogenic media. The chondrogenic media in the wells was replaced every day for the first 2 days. On day 3, the neocartilage was removed from the wells, placed in 6-well plates, and the chondrogenic media was replaced every other day. The total culture duration time was 28 days.
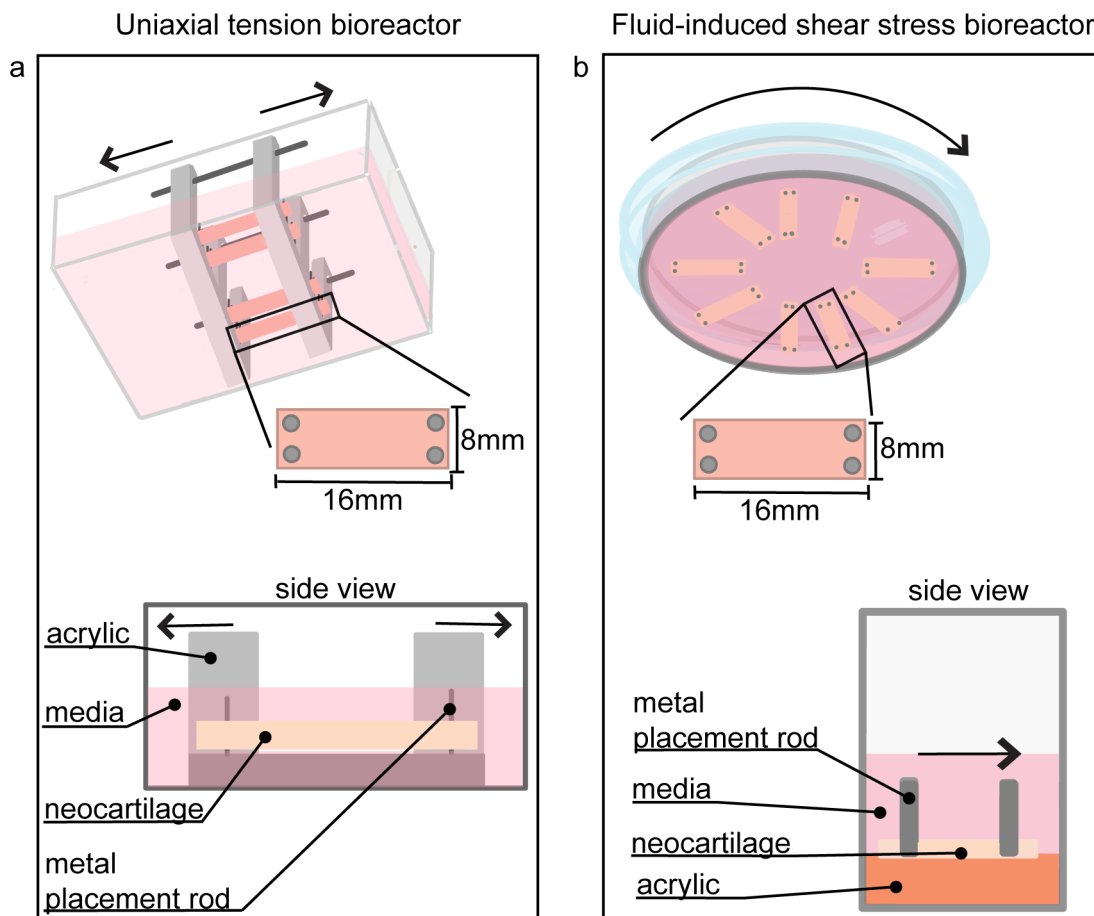
FIGURE 2

Figure 2 – Mechanical stimulation bioreactors. A reverse axis isometric view and a side view of both **a)** constant uniaxial tension bioreactor, and **b)** shear stress bioreactor are shown. **a)** In the tension stress bioreactor, 8x13mm neocartilage constructs are held in place with stainless steel placement rods running through the pre-made holes, and stretched over 4 days to reach 16 mm in length. **b)** In the shear stress bioreactor, the constructs are also held in place with stainless steel placement rods. The shear stress bioreactor is then placed on an orbital shaker at 50 RPM to apply the fluid-induced shear stress in the direction shown by the arrow.

Mechanical stimulation

Continuous uniaxial tension regimen described previously by Lee et al. was implemented. The application of tensile strain was as follows: 18% on day 7, followed by approximately 4.9-6.5% additional strain applied each day from days 8-12 and then held constant in the tension bioreactor until day 15. (Figure 2a) On day 15, the neocartilage constructs were transferred to the shear stress bioreactor. (Figure 2b) Fluid induced shear stress was applied from day 15 to day 22. The constructs were not stimulated mechanically from day 22 to day 28.

Mechanical Testing

To analyze the gross morphology of neocartilage constructs, ImageJ software was used to calculate sample thickness, diameter, and cross sectional area. To determine the compressive properties, a cylindrical 2mm punch was taken from the center of the construct, and a creep indentation test was administered. Aggregate modulus (H_A), permeability (k), and Poisson's ratio (nu) were calculated as described previously. [37]

Tensile testing was conducted using, Instron model 5565, a uniaxial material testing machine. Cartilage constructs were cut into dog bone-shaped samples, as per ASTM standards, and were glued to paper rectangles. ImageJ was used to measure the sample thickness, width of the dog bones, and sample cross-sectional areas. A uniaxial strain until failure test was conducted with a strain rate of 1% per second. Load–displacement curves were normalized to the cross-sectional area of each sample and the Young's Modulus and Ultimate Tensile Strength were calculated with MATLAB.

Extracellular matrix content analysis

To analyze the biochemical content, first wet weight of the samples were measured. The measured DNA, GAG, and collagen amounts were normalized by the tissue wet weight. First,

the samples were lyophilized, their wet weight was measured, and the tissue was digested in a 1ml/mg papain solution in a phosphate buffer at 65°C for 18hr. DNA content was quantified using PicoGreen assay. Pico green reagents were added to 8ml of the digested sample and fluorescence was measured at 485/528nm Ex/Em with a Magellan plate reader. Chloramine-T hydroxyproline assay and a SIRCOL collagen standard were used to calculate collagen content. 200µl of 4N NaOH was added to the samples, they were autoclaved, and then 200mL 4N HCl was added. Samples were then incubated with 1.25ml of 0.062M chloramine T for 20min at room temperature, and then they were incubated in 1.25ml of 1.2M Ehrlich's reagent for 20min at 65°C. Absorbance was measured at 550nm. [38] Finally, GAG content was measured using a Blyscan Glycosaminoglycan Assay kit. 8µl of the digested sample was placed into 500ml dye reagent, and vortexed every 5min for 30min. The samples were centrifuged, the precipitate was then dissolved in 500µl of dissociated reagent, and the absorbance was measured at 650nm.

Statistics

One-way analysis of variance (ANOVA) and Tukey's *post hoc* tests were used to compare biochemical and mechanical data for multiple group comparisons. Data are presented as mean + standard deviation. Six constructs were used per experimental group. All six constructs were used for biochemical analysis and mechanical testing.

RESULTS

Compressive Stiffness

The aggregate moduli of the neocartilage constructs were measured using a creep indentation test and analysis, as described previously. [37] In terms of compressive properties, neocartilage constructs that were treated with only tensile stimulation elicited an average aggregate modulus were not statistically different from neocartilage constructs that did not receive any form of mechanical stimulation. (Figure 3a) Neocartilage constructs that received only shear stress

stimulation comprised of an average aggregate modulus that was significantly more stiff than neocartilage constructs that only received tension and also significantly more stiff than nonstimulated control constructs. (Figure 3a) These trends in compressive properties mirror the trends seen in previous studies. [24, 25] When both tension and shear stimulation were implemented during tissue culture, the aggregate modulus of neocartilage constructs was significantly improved over all other groups to an average of. (Figure 3a) The combination of tension and shear stress stimulation in neocartilage tissue culture resulted in a synergistic increase in neocartilage compressive stiffness.
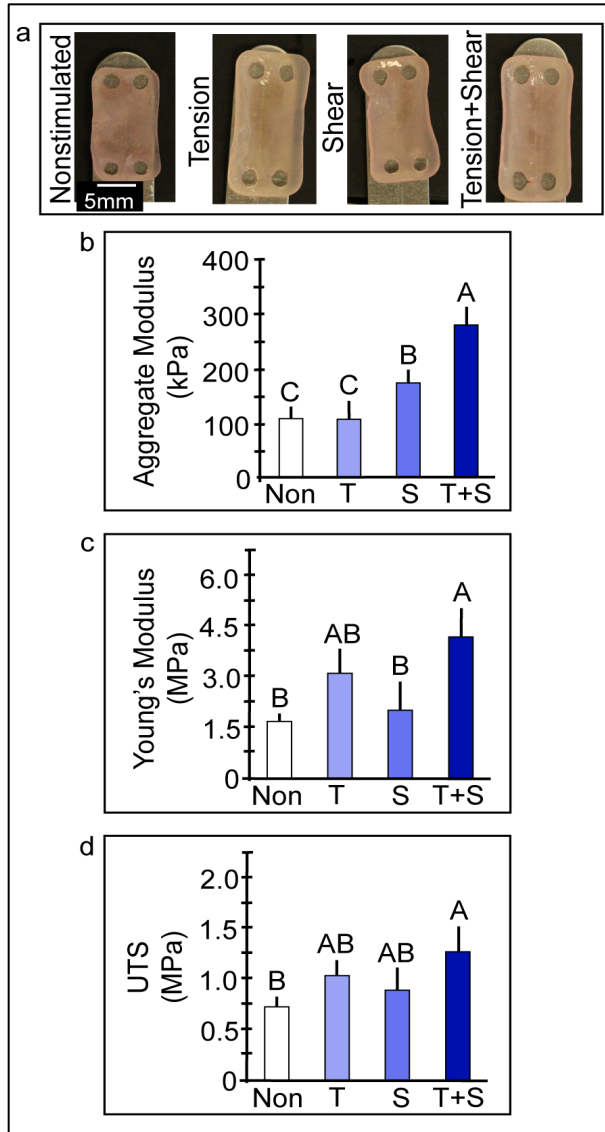
FIGURE 3

Figure 3 – Mechanical properties of neocartilage constructs created from minipig costal chondrocytes and either not stimulated, or stimulated with only shear stress, only tension stress, or a combination of tension stress and shear stress. **a)** The gross morphology of neocartilage constructs **b)** the aggregate modulus, **c)** the Young's modulus, **d)** the ultimate tensile strength are shown. The capital letters floating above the bars indicate statistically different groups evaluated at a $p<0.05$ using a one-way ANOVA and post-hoc Tukey's test. Abbreviations: nonstimulated (Non), shear stress only (S), tension stress only (C), combination of tension and shear stress (T+S)

Tensile Strength and Stiffness

The ultimate tensile strength (UTS) of the neocartilage constructs were measured using a uniaxial strain until failure test and analyzed as described previously. In terms of tensile strength, tension-only neocartilage constructs were not significantly different in UTS from nonstimulated control constructs. (Figure 3c) Similarly, neocartilage constructs that were stimulated with only shear stress (Figure 3c) were not significantly different in UTS from nonstimulated control constructs. Both of these results are consistent with those of previous studies conducted on the effects of tensile stress stimulation and shear stress stimulation. [24, 25] Interestingly, neocartilage constructs that were treated with both shear stress and tensile stress were significantly improved in UTS over neocartilage constructs that were not treated with any form of mechanical stimulation. (Figure 3c) The combination of tension and shear stress stimulation in neocartilage tissue culture resulted in an improvement in tensile strength that had not previously been accomplished with either form of stimulus alone.

To assess the Young's modulus of the neocartilage constructs a uniaxial strain until failure test and analysis was used as described previously. Neocartilage constructs stimulated with tensile stress only trended higher but were not significantly different in Young's modulus than neocartilage constructs that received no mechanical stimulation. (Figure 3b) When stimulated with only shear stress, neocartilage constructs did not show improved Young's modulus over neocartilage constructs that received no mechanical stimulation. (Figure 3b) However, when the shear stress and tensile stress stimulation were combined, neocartilage constructs exhibited Young's moduli that were significantly higher than shear stress-only contstructs and also significantly higher than nonstimulated control constructs. (Figure 3b) These results show that the addition of tension stimulation to a shear stress only culture regimen improves the tensile stiffness of neocartilage constructs.

Collagen Content

Collagen content of the neocartilage implants was assessed using a modified hydroxyproline assay as described previously. [38] Comparisons amongst experimental groups were made by normalizing the collagen content values to wet weight. (Figure 4a) Neocartilage constructs that were stimulated with only tensile stress trended higher but did not contain a significantly different amount of collagen than constructs that were not stimulated with any form of mechanical stimulation. Neocartilage constructs that were only stimulated with shear stress were significantly different from nonstimulated controls, but not statistically different to those that were stimulated with only tensile stress. When shear stress stimulation was combined with tension stimulation during culture, the resulting neocartilage constructs contained a significantly higher amount of collagen content than the neocartilage constructs that did not receive any form of mechanical stimulus. Additionally, the combination of mechanical stimuli resulted in neocartilage with significantly higher amounts of collagen than those stimulated with tensile stress. These results show that the combination of shear stress and tensile stress improve neocartilage collagen content over either form of mechanical stimulus applied alone.
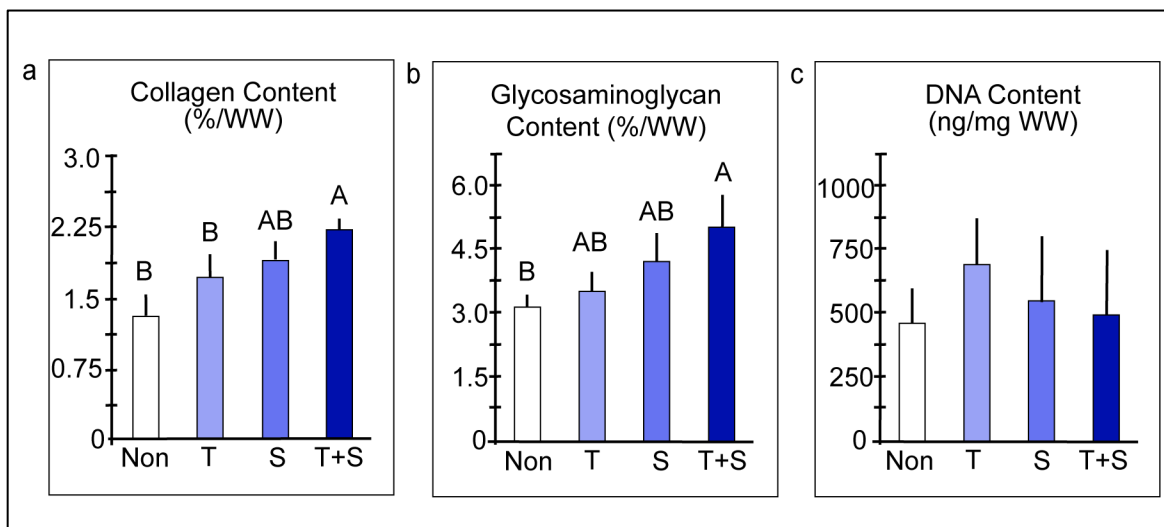
FIGURE 4

161

Figure 4 – Biochemical properties of neocartilage constructs created from mini pig costal chondrocytes and either not stimulated, or stimulated with only shear stress, only tension stress, or a combination of tension stress and shear stress. **a)** The collagen content percent per wet weight, **b)** the glycosaminoglycan content percent per wet weight, **c)** the DNA content ng/mg of wet weight are shown. The capital letters floating above the bars indicate statistically different groups evaluated at a $p<0.05$ using a one-way ANOVA and post-hoc Tukey's test. Abbreviations: nonstimulated (Non), shear stress only (S), tension stress only (C), combination of tension and shear stress (T+S)

Glycosaminoglycan content

To assess the glycosaminoglycan content of the neocartilage implants, a Blyscan Glycosaminoglycan Assay kit was used, and comparisons amongst experimental groups were made by normalizing the glycosaminoglycan values to wet weight. (Figure 4b) Neocartilage constructs that were stimulated with only tensile stress trended higher but did not contain a significantly different amount of glycosaminoglycan than constructs that were not stimulated with any form of mechanical stimulation. Similarly, neocartilage constructs that were only stimulated with shear stress also trended higher in glycosaminoglycan content, but were not significantly different from those that were not stimulated with any form of mechanical stimulus. When shear stress stimulation was combined with tension stimulation during culture, the resulting neocartilage constructs contained a significantly higher amount of glycosaminoglycan than the neocartilage constructs that did not receive any form of mechanical stimulus. These results show that the combination of shear stress and tensile stress enhance glycosaminoglycan content in neocartilage constructs over either form of mechanical stimulus applied alone.

DISCUSSION

The main objective of this work was to determine if a combination of mechanical stimulation tactics could improve neocartilage construct properties over either form of stimulus alone. The mechanical stimulation tactics that were investigated here were uniaxial tension stress and fluid-

induced shear stress. Previously, the application of uniaxial tension stress over four days of culture was found to improve tensile stiffness and strength to 94% of native articular values. [24] However, the improvements in tensile properties were not replicated in compressive stiffness. [24] Conversely, the application of fluid-induced shear stress was found to improve compressive stiffness, but not tensile properties. [25] Thus, it was hypothesized that applying both uniaxial tension and shear stress would lead to improvements in tensile and compressive stiffness, as well as ultimate tensile strength.

In this study, neocartilage constructs were divided into four experimental groups: 1) nonstimulated control, 2) uniaxial tension stress only, 3) fluid-induced shear stress only, and 4) a combination of uniaxial tension stress and fluid-induced shear stress. This full factorial design allowed for the comparison of a combined mechanical stimulation regimen over either form of stimulus alone. The results of this study indicated that a combination of uniaxial tension stress and fluid-induced shear stress improves not only neocartilage tensile stiffness and strength, but also compressive stiffness. These results were not previously attainable with only one form of mechanical stimulus, where either only tensile properties or compressive properties were improved. In particular, the combination of uniaxial tension stress and fluid-induced shear stress elicited synergistic results in both tensile and compressive stiffness. This is significant because it indicates that mechanical stimulation tactics can be used in combination to drive a multitude of neocartilage mechanical properties toward those of native tissue.

Neocartilage extracellular matrix content reflected the trends seen in mechanical properties. The glycosaminoglycan and collagen levels of neocartilage constructs trended the highest when a combination of uniaxial tension stress and fluid-induced shear stress was applied. In terms of extracellular matrix levels, the neocartilage constructs that received combined treatments trended higher, but were not significantly different from constructs that only received shear stress. However, the significant and synergistic improvements observed in

mechanical properties indicate that uniaxial tension stress may be contributing to neocartilage extracellular matrix in ways that were not investigated here. For example, previous studies have demonstrated elevated levels of pyridinoline crosslinks in neocartilage constructs stimulated with uniaxial tension stress. [24, 39-41] Furthermore, aside from elevated crosslinks among collagen fibers, uniaxial tension has also been shown to physically orient extracellular matrix fibers in the direction of applied tension, leading to anisotropy and enhancements in directional tensile properties. [24] Overall, the combination of uniaxial tension stress and fluid-induced shear stress yielded improvements in extracellular matrix properties that were not seen in neocartilage constructs stimulated with only one form of mechanical stimulus.

When tissue-engineering articular cartilage, bioactive factors are more commonly used in tissue culture than mechanical stimulation. Previous studies have even found that bioactive factors can be used in combination to improve a myriad of neocartilage properties. [42-45] For example, the use of TGF-β1, C-ABC, and LOXL2 has been found to improve collagen content, pyridinoline crosslink levels, and subsequently tensile properties. [42, 46] Although the ease of applying soluble bioactive factors, such as growth factors and enzymes, is appealing there are several drawbacks when translating their use to preclinical studies. Mainly, the use of transforming growth factors elicit pleiotropic effects that could potentially lead to mutations, and further, the use of enzymes risks increased degradation of tissue in the body. [47-50] Mechanical stimulus, on the other hand, does not pose such risks for translation and has been shown to improve neocartilage properties. Furthermore, this study provided evidence that, like bioactive factors, different forms of mechanical stimulation tactics can be tailored and used in combination to improve multiple neocartilage properties.

There is still much to be studied in terms of using of mechanical stimulation in neocartilage tissue engineering. In particular, a study comparing the outcomes of using only bioactive factors to the use of only mechanical stimulation could demonstrate which is more

efficient in improving neocartilage properties. Alternatively, combining the use of both mechanical stimulus and bioactive factors may be useful in attaining native tissue properties. Manipulating neocartilage constructs with mechanical stimulation can provide mechanically robust, and potentially safer options, for implantation in pre-clinical studies bringing tissue engineered articular cartilage closer to the clinic.

REFERENCES

[1] E.Y. Salinas, J.C. Hu, K.A. Athanasiou, A Guide for Using Mechanical Stimulation to Enhance Tissue-Engineered Articular Cartilage Properties, Tissue Engineering Part B: Review 5(24) (2018) 345-358.

[2] K. Li, C. Zhang, L. Qiu, L. Gao, X. Zhang, Advances in application of mechanical stimuli in bioreactors for cartilage tissue engineering, Tissue Engineering Part B: Reviews 23(4) (2017) 399-411.

[3] S. Park, C. Hung, G. Ateshian, Mechanical response of bovine articular cartilage under dynamic unconfined compression loading at physiological stress levels, Osteoarthritis and cartilage 12(1) (2004) 65-73.

[4] W.-Y. Lin, Y.-H. Chang, H.-Y. Wang, T.-C. Yang, T.-K. Chiu, S.-B. Huang, M.-H. Wu, The study of the frequency effect of dynamic compressive loading on primary articular chondrocyte functions using a microcell culture system, BioMed research international 2014 (2014).

[5] J. Natenstedt, A.C. Kok, J. Dankelman, G.J. Tuijthof, What quantitative mechanical loading stimulates in vitro cultivation best?, Journal of experimental orthopaedics 2(1) (2015) 15.

[6] R. El-Ayoubi, C. DeGrandpré, R. DiRaddo, A.-M. Yousefi, P. Lavigne, Design and dynamic culture of 3D-scaffolds for cartilage tissue engineering, Journal of biomaterials applications 25(5) (2011) 429-444.

[7] C.F. Dewey, Jr., S.R. Bussolari, M.A. Gimbrone, Jr., P.F. Davies, The Dynamic Response of Vascular Endothelial Cells to Fluid Shear Stress, Journal of Biomechanical Engineering 103(3) (1981) 177-185.

[8] K.S. Cunningham, A.I. Gotlieb, The role of shear stress in the pathogenesis of atherosclerosis, Laboratory Investigation 85(1) (2005) 9-23.

[9] J.-J. Chiu, P.-L. Lee, C.-N. Chen, I. Lee Chih, S.-F. Chang, L.-J. Chen, S.-C. Lien, Y.-C. Ko, S. Usami, S. Chien, Shear Stress Increases ICAM-1 and Decreases VCAM-1 and E-selectin Expressions Induced by Tumor Necrosis Factor-α in Endothelial Cells, Arteriosclerosis, Thrombosis, and Vascular Biology 24(1) (2004) 73-79.

[10] S. Park, R. Krishnan, S.B. Nicoll, G.A. Ateshian, Cartilage interstitial fluid load support in unconfined compression, Journal of Biomechanics 36(12) (2003) 1785-1796.

[11] C. Correia, A.L. Pereira, A.R. Duarte, A.M. Frias, A.J. Pedro, J.T. Oliveira, R.A. Sousa, R.L. Reis, Dynamic culturing of cartilage tissue: the significance of hydrostatic pressure, Tissue Engineering Part A 18(19-20) (2012) 1979-1991.

[12] B.D. Elder, K.A. Athanasiou, Effects of temporal hydrostatic pressure on tissue-engineered bovine articular cartilage constructs, Tissue engineering Part A 15(5) (2009) 1151-1158.

[13] B.D. Elder, K.A. Athanasiou, Synergistic and additive effects of hydrostatic pressure and growth factors on tissue formation, PloS one 3(6) (2008) e2341.

[14] R.L. Smith, M. Trindade, J. Shida, G. Kajiyama, T. Vu, Time-dependent effects of intermittent hydrostatic pressure on articular c on rocyte type II collagen and aggrecan mRNA expression, J. Rehabil. Res. Dev 37 (2000) 153-161.

[15] K.A. Athanasiou, E.M. Darling, J.C. Hu, G.D. DuRaine, A.H. Reddi, Articular Cartilage, 2 ed., CRC Press, 2017.

[16] D.J. Huey, J.C. Hu, K.A. Athanasiou, Unlike bone, cartilage regeneration remains elusive, Science 338(6109) (2012) 917-921.

[17] F. McCormick, J.D. Harris, G.D. Abrams, R. Frank, A. Gupta, K. Hussey, H. Wilson, B. Bach, Jr., B. Cole, Trends in the surgical treatment of articular cartilage lesions in the United States: an analysis of a large private-payer database over a period of 8 years, Arthroscopy 30(2) (2014) 222-6.

[18] B. Martinac, Mechanosensitive ion channels: molecules of mechanotransduction, J Cell Sci 117(Pt 12) (2004) 2449-60.

[19] N. Wang, J.D. Tytell, D.E. Ingber, Mechanotransduction at a distance: mechanically coupling the extracellular matrix with the nucleus, Nature reviews Molecular cell biology 10(1) (2009) 75-82.

[20] A. Katsumi, A.W. Orr, E. Tzima, M.A. Schwartz, Integrins in mechanotransduction, Journal of Biological Chemistry 279(13) (2004) 12001-12004.

[21] K.N. Dahl, A.J. Ribeiro, J. Lammerding, Nuclear shape, mechanics, and mechanotransduction, Circulation research 102(11) (2008) 1307-1318.

[22] J.C. Hu, K.A. Athanasiou, A self-assembling process in articular cartilage tissue engineering, Tissue Engineering 12(4) (2006) 969-979.

[23] L.W. Huwe, G.K. Sullan, J.C. Hu, K.A. Athanasiou, Using Costal Chondrocytes to Engineer Articular Cartilage with Applications of Passive Axial Compression and Bioactive Stimuli, Tissue Eng Part A 24(5-6) (2018) 516-526.

[24] J.K. Lee, L.W. Huwe, N. Paschos, A. Aryaei, C.A. Gegg, J.C. Hu, K.A. Athanasiou, Tension stimulation drives tissue formation in scaffold-free systems, Nature Materials 16(8) (2017) 864.

[25] S. Evelia, A. Ashkan, P. Nikolaos, B. Eric, K. Heenam, H. Jerry, A. Kyriacos, Shear stress induced by fluid flow produces improvements in tissue-engineered cartilage, Biofabrication (2020).

[26] C.V. Gemmiti, R.E. Guldberg, Shear stress magnitude and duration modulates matrix composition and tensile mechanical properties in engineered cartilaginous tissue, Biotechnology and Bioengineering 104(4) (2009) 809-820.

[27] C.V. Gemmiti, R.E. Guldberg, Fluid flow increases type II collagen deposition and tensile mechanical properties in bioreactor-grown tissue-engineered cartilage, Tissue Engineering 12(3) (2006) 469-479.

[28] S. Grad, M. Loparic, R. Peter, M. Stolz, U. Aebi, M. Alini, Sliding motion modulates stiffness and friction coefficient at the surface of tissue engineered cartilage, Osteoarthritis and Cartilage 20(4) (2012) 288-295.

[29] A.J. Grodzinsky, M.E. Levenston, M. Jin, E.H. Frank, Cartilage Tissue Remodeling in Response to Mechanical Forces, Annual Review of Biomedical Engineering 2(1) (2000) 691-713.

[30] A.M. Gharravi, M. Orazizadeh, K. Ansari-Asl, S. Banoni, S. Izadi, M. Hashemitabar, Design and fabrication of anatomical bioreactor systems containing alginate scaffolds for cartilage tissue engineering, Avicenna Journal of Medical Biotechnology 4(2) (2012) 65.

[31] S. Wu, Y. Wang, P.N. Streubel, B. Duan, Living nanofiber yarn-based woven biotextiles for tendon tissue engineering using cell tri-culture and mechanical stimulation, Acta biomaterialia 62 (2017) 102-115.

[32] E.J. Vanderploeg, C.G. Wilson, M.E. Levenston, Articular chondrocytes derived from distinct tissue zones differentially respond to in vitro oscillatory tensile loading, Osteoarthritis and cartilage 16(10) (2008) 1228-1236.

[33] K.A. Wartella, J.S. Wayne, Bioreactor for biaxial mechanical stimulation to tissue engineered constructs, Journal of biomechanical engineering 131(4) (2009).

[34] F. Bieler, C. Ott, M. Thompson, R. Seidel, S. Ahrens, D.R. Epari, U. Wilkening, K. Schaser, S. Mundlos, G. Duda, Biaxial cell stimulation: A mechanical validation, J Biomech 42(11) (2009) 1692-1696.

[35] N. Vapniarsky, L.W. Huwe, B. Arzi, M.K. Houghton, M.E. Wong, J.W. Wilson, D.C. Hatcher, J.C. Hu, K.A. Athanasiou, Tissue engineering toward temporomandibular joint disc regeneration, Sci Transl Med 10(446) (2018) eaaq1802.

[36] M.K. Murphy, T.E. Masters, J.C. Hu, K.A. Athanasiou, Engineering a fibrocartilage spectrum through modulation of aggregate redifferentiation, Cell Transplant 24(2) (2015) 235-45.

[37] V.C. Mow, M.C. Gibbs, W.M. Lai, W.B. Zhu, K.A. Athanasiou, Biphasic indentation of articular cartilage—II. A numerical algorithm and an experimental study, Journal of Biomechanics 22(8) (1989) 853-861.

[38] D.D. Cissell, J.M. Link, J.C. Hu, K.A. Athanasiou, A modified hydroxyproline assay based on hydrochloric acid in Ehrlich's solution accurately measures tissue collagen content, Tissue Engineering Part C: Methods 23(4) (2017) 243-250.

[39] E.A. Makris, R.F. MacBarb, D.J. Responte, J.C. Hu, K.A. Athanasiou, A copper sulfate and hydroxylysine treatment regimen for enhancing collagen cross-linking and biomechanical properties in engineered neocartilage, The FASEB Journal 27(6) (2013) 2421-2430.

[40] A.K. Williamson, A.C. Chen, K. Masuda, E.J.-M.A. Thonar, R.L. Sah, Tensile mechanical properties of bovine articular cartilage: Variations with growth and relationships to collagen network components, Journal of Orthopaedic Research 21(5) (2003) 872-880.

[41] A.K. Williamson, K. Masuda, E.J.M.A. Thonar, R.L. Sah, Growth of Immature Articular Cartilage in Vitro: Correlated Variation in Tensile Biomechanical and Collagen Network Properties, Tissue Engineering 9(4) (2003) 625-634.

[42] E.A. Makris, R.F. MacBarb, N.K. Paschos, J.C. Hu, K.A. Athanasiou, Combined use of chondroitinase-ABC, TGF-β1, and collagen crosslinking agent lysyl oxidase to engineer functional neotissues for fibrocartilage repair, Biomaterials 35(25) (2014) 6787-96.

[43] B.D. Elder, K.A. Athanasiou, Systematic assessment of growth factor treatment on biochemical and biomechanical properties of engineered articular cartilage constructs, Osteoarthritis and cartilage 17(1) (2009) 114-123.

[44] A.H. Huang, A. Stein, R.S. Tuan, R.L. Mauck, Transient exposure to transforming growth factor beta 3 improves the mechanical properties of mesenchymal stem cell–laden cartilage constructs in a density-dependent manner, Tissue Engineering Part A 15(11) (2009) 3461-3472.

[45] R.K. Studer, R. Bergman, T. Stubbs, K. Decker, Chondrocyte response to growth factors is modulated by p38 mitogen-activated protein kinase inhibition, Arthritis Res Ther 6(1) (2004) R56-R64.

[46] H. Kwon, S.A. O'Leary, J.C. Hu, K.A. Athanasiou, Translating the application of transforming growth factor-β1, chondroitinase-ABC, and lysyl oxidase-like 2 for mechanically

robust tissue-engineered human neocartilage, Journal of Tissue Engineering and Regenerative Medicine 13(2) (2019) 283-294.

[47] L. Bian, K.M. Crivello, K.W. Ng, D. Xu, D.Y. Williams, G.A. Ateshian, C.T. Hung, Influence of temporary chondroitinase ABC-induced glycosaminoglycan suppression on maturation of tissue-engineered cartilage, Tissue Engineering Part A 15(8) (2009) 2065-2072.

[48] R. Lin, J.C. Kwok, D. Crespo, J.W. Fawcett, Chondroitinase ABC has a long-lasting effect on chondroitin sulphate glycosaminoglycan content in the injured rat brain, Journal of neurochemistry 104(2) (2008) 400-408.

[49] M.C. Fleisch, C.A. Maxwell, M.-H. Barcellos-Hoff, The pleiotropic roles of transforming growth factor beta in homeostasis and carcinogenesis of endocrine organs, Endocrine-related cancer 13(2) (2006) 379-400.

[50] Y.M. Farhat, A.A. Al-Maliki, T. Chen, S.C. Juneja, E.M. Schwarz, R.J. O'Keefe, H.A. Awad, Gene expression analysis of the pleiotropic effects of TGF-β1 in an in vitro model of flexor tendon healing, PloS one 7(12) (2012) e51411.

CHAPTER 6- INVESTIGATING THE USE OF TENSION AND SHEAR STRESS STIMULATION COMBINED WITH BIOACTIVE FACTORS TO ENHANCE NEOCARTILAGE CONSTRUCT PROPERTIES

ABSTRACT

Tissue-engineered neocartilage has the potential to transform the clinical treatment options available to patients with focal articular cartilage defects. Self-assembled neocartilage in particular is manipulated with bioactive factors and mechanical stimulation to achieve properties, such as compressive stiffness and glycosaminoglycan content, near native tissue values. The aim of this study was to combine the use of bioactive factors and mechanical stimulation strategies to improve all neocartilage construct properties toward those of native values. Three different combinations of stimulation were investigated: neocartilage treated with bioactive factors only, neocartilage treated with bioactive factors and fluid-induced shear stress, and neocartilage treated with bioactive factors, fluid-induced shear stress, and uniaxial tension. It was found that the neocartilage constructs that were treated with bioactive factors and shear stress exhibited the highest compressive aggregate moduli and glycosaminoglycan content, reaching native tissue levels. This study indicates that neocartilage should be treated with bioactive factors and fluid-induced shear stress prior to orthotopic implantation in order to provide the most mechanically robust constructs. Although the results from this study present neocartilage with compressive stress reaching levels near native articular tissue compressive stiffness, biomimetic native articular properties in terms of both compressive and tensile stiffness has yet to be achieved.

Authors: Salinas EY, Hu JC, Athanasiou KA

INTRODUCTION

After a focal articular cartilage defect emerges from trauma and over use, the degradation of surrounding articular cartilage ensues, creating a vexing clinical problem affecting 250,000 Americans every year. [1] Articular cartilage tissue engineering has the potential to transform the way patients are treated for focal articular cartilage lesions by providing neocartilage implants. However, before tissue-engineering technologies can be translated to the clinic to repair focal articular cartilage defects, neocartilage implants should be designed to be as mechanically robust as native articular cartilage. Typically, neocartilage implant mechanical properties are enhanced with the use of bioactive factors. [2] These bioactive factors typically include growth factors, such as TGF-β1, FGF-2, BMP-2, and GDF-5, as well as enzymes, such as C-ABC and LOXL2. [3-9]In general, the uses of certain bioactive factors, either alone or in combination, at the correct dosage, drive neocartilage properties to be closer to native articular cartilage.

The self-assembling process has been used for over a decade to create neocartilage constructs without the use of scaffolds. [10]Chondrocytes are seeded in a non-adherent agarose well, and intrinsic minimization of free energy drives cell-to-cell interactions and, subsequently, extracellular matrix formation. [11] The resulting neocartilage tissue is not as mechanically robust as native articular cartilage, but the inclusion of bioactive factors, and separately, mechanical stimulation, during tissue culture has yielded neocartilage that is getting closer and closer to being biomimetic.[5, 12, 13] In particular, a cocktail of bioactive factors (TGF-β1, C-ABC, and LOXL2) has improved self-assembled neocartilage tissue Young's modulus and ultimate tensile strength by 245% and 186%, respectively.[5] Separately, the use fluid-induced shear stress has improved the aggregate modulus of self-assembled neocartilage constructs by 450%.[13] When fluid-induced shear stress was combined with uniaxial tension stress, self-assembled neocartilage mechanical properties improved across the board with

synergistic improvements in Young's modulus, ultimate tensile strength, and compressive aggregate modulus. Overall, these stimulation tactics have been incrementally improving different properties of neocartilage constructs, and the combination of all these treatments has the potential to finally result in biomimetic neocartilage.

In this study, the combination of several bioactive factors (TGF-β1, C-ABC, and LOXL2) and two forms of mechanical stimulation (fluid-induced shear stress and uniaxial tension) were investigated in self-assembled neocartilage. The main objective of this work was to determine which combination of mechanical stimulation and bioactive factors yielded the most biomimetic neocartilage constructs in terms of Young's modulus, ultimate tensile strength, compressive aggregate modulus, collagen content, and glycosaminoglycan content. This investigation consisted of three experimental groups: 1) neocartilage treated with only bioactive factors (BF), 2) neocartilage treated with bioactive factors and fluid-induced shear stress (BF+S), and 3) neocartilage treated with bioactive factors, fluid-induced shear stress and uniaxial tension (BF+S+T). It was hypothesized that neocartilage treated with bioactive factors, fluid-induced shear stress, and uniaxial tension would elicit the most improved neocartilage properties overall.

MATERIALS AND METHODS

Study design

This study aimed to determine which of three combinations of bioactive factors and mechanical stimulation strategies would result in the most mechanically robust neocartilage constructs. The bioactive factors used were TGF-β1, C-ABC, and LOXL2, and the mechanical stimulation strategies investigated were fluid-induced shear stress and uniaxial tension. The times of application of these neocartilage treatments are shown in Figure 1. This study consisted of three experimental groups, also shown in Figure 1. The neocartilage construct properties that were

used to evaluate the neocartilage tissue were compressive aggregate modulus, Young's modulus, ultimate tensile strength, glycosaminoglycan content, and collagen content.
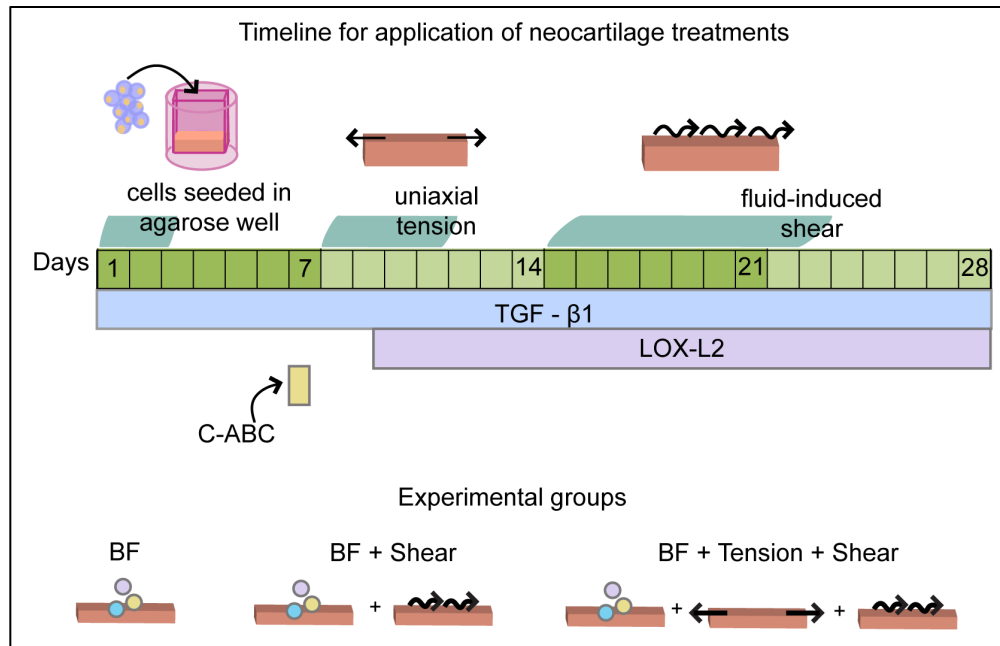
FIGURE 1

Figure 1 - A schematic timeline for the application of neocartilage treatments is shown. Chondrocytes are first seeded in an agarose well, at day 2 the neocartilage is removed from the agarose well. Uniaxial tension stimulation begins at day 8 and is continued until day 12. Fluid-induced shear stress stimulation begins at day 15 and continues until day 21. The application of bioactive factors is also shown. TGF-β1 is applied through the entire duration of tissue culture. C-ABC is applied for 4 hours on day 7. Finally, LOXL2 is applied from day 10 through the duration of tissue culture. In the bottom half of the figure, experimental groups are shown. Abbreviations: TGF-β1 (transforming growth factor beta 1), C-ABC (chondroitinase ABC), LOXL2 (lysyloxidase like 2), BF (bioactive factors)

Neocartilage self-assembly

Rectangular well makers were used to make 2% agarose wells with a hole at each corner in a 24-well plate. Chondrogenic media was changed at least twice before cell seeding to saturate the wells. Expanded and redifferentiated minipig costal chondrocytes were seeded into the agarose wells using 7M cells per construct. [14, 15] Four hours after seeding, 0.5ml of

chondrogenic media (DMEM supplemented with 1%/vol PSF, 1%/vol ITS+ premix, 1%/vol nonessential amino acids, and 10nM dexamethasone) was added to each well. Two days after seeding, the self-assembled neocartilage constructs were unconfined from the agarose wells and placed in 24-well plates until day 8.

Mechanical stimulation

The constant uniaxial tension regimen was implemented as described previously.[12] The application of tensile strain was as follows: 18% on day 7, followed by approximately 4.9-6.5% additional strain applied each day from days 8-12 and then held constant in the tension bioreactor until day 15. On day 15, the neocartilage constructs were transferred to the shear stress bioreactor. Fluid induced shear stress was applied from day 15 to day 22. The constructs were not stimulated mechanically from day 22 to day 28. The shear stress device was created as described previously, in chapter 4. Each of the constructs were draped over four poles to keep the constructs in place, and 15ml of chondrogenic media were added into the bioreactor. The fluid-induced shear stress device was then placed on an orbital shaker at 50RPM, and as the orbital shaker rotated, it allowed the media in the device to flow over the constructs and apply a pressure of about 0.1Pa. Media was changed every 2-3 days. After stimulation with shear stress, the constructs were returned to regular 24-well plates and received 2ml of media on alternating days.

Mechanical testing

The gross morphology of neocartilage constructs was documented and ImageJ software was used to calculate sample thickness and cross sectional area. To determine the compressive properties, a cylindrical 3mm punch was taken from the center of the construct, and a creep indentation test was administered. Aggregate modulus was calculated as described previously. [16]

Tensile testing was conducted using a uniaxial material testing machine (Instron model 5565). Neocartilage constructs were cut into dog bone-shaped samples, as per ASTM standards, and glued to paper rectangles with a precut gauge length of 1.55mm. ImageJ was used to measure the sample thickness, width of the dog bones, and sample cross-sectional areas. A uniaxial strain until failure test was conducted with a strain rate of 1% per second. Load–displacement curves were normalized to the cross-sectional area of each sample and the Young's modulus and ultimate tensile strength were calculated with MATLAB.

Extracellular matrix content analysis

To analyze the extracellular matrix content, first wet weight of the samples were measured, frozen, lyophilized, and digested in papain solution. The measured GAG, and collagen amounts were normalized to the tissue wet weight. A Chloramine-T hydroxyproline assay and a SIRCOL collagen standard were used to calculate collagen content as described previously.[17] Briefly, 200µl of 4N NaOH was added to the samples, they were autoclaved, and then 200ml 4N HCl was added. Samples were then incubated with 1.25ml of 0.062M chloramine T for 20min at room temperature, and then they were incubated in 1.25ml of 1.2M Ehrlich's reagent for 20min at 65°C. Absorbance was measured at 550nm. Finally, GAG content was measured using a Blyscan Glycosaminoglycan Assay kit. Briefly, 8ul of the digested sample was placed into 500ml dye reagent, and vortexed every 5min for 30min. The samples were centrifuged, the precipitate was then dissolved in 500µl of dissociated reagent, and the absorbance was measured at 650nm.

Statistical analysis

One-way analysis of variance (ANOVA) and Tukey's *post hoc* tests were used to compare biochemical and mechanical data for multiple group comparisons. Data are presented as mean

+ standard deviation. Six constructs were used per experimental group. All six constructs were used for biochemical analysis and mechanical testing.

RESULTS

Gross morphology

The gross morphology of neocartilage constructs was observed and documented. Representative images of neocartilage from each group are shown in Figure 2a. Neocartilage constructs that were stimulated with BF did not show any distinct morphological differences from neocartilage constructs that were stimulated with BF+S. Neocartilage constructs that were stimulated with BF+S+T obtained a curled morphology and appeared thinner than constructs stimulated with BF and BF+S.

Mechanical properties

The compressive aggregate modulus, Young's modulus and ultimate tensile strength of all neocartilage constructs were evaluated. When looking at compressive aggregate modulus, the neocartilage stimulated with BF+S elicited a significant increase over neocartilage that was stimulated with BF and neocartilage that was stimulated with BF+S+T. (Figure 2b) Neocartilage that was stimulated with BF+S+T was not significantly different in terms of compressive aggregate modulus from neocartilage that was stimulated with only BF. When looking at tensile properties, Young's modulus and ultimate tensile strength were evaluated. There were no significant differences amongst any of the experimental groups in terms of Young's modulus (Figure 2c); the evaluation of ultimate tensile strength also did not show any significant differences amongst groups. (Figure 2d) In terms of mechanical properties, the results of this study indicate that the inclusion of BF+S during the tissue culture of neocartilage lead to significant improvements in compressive stiffness.
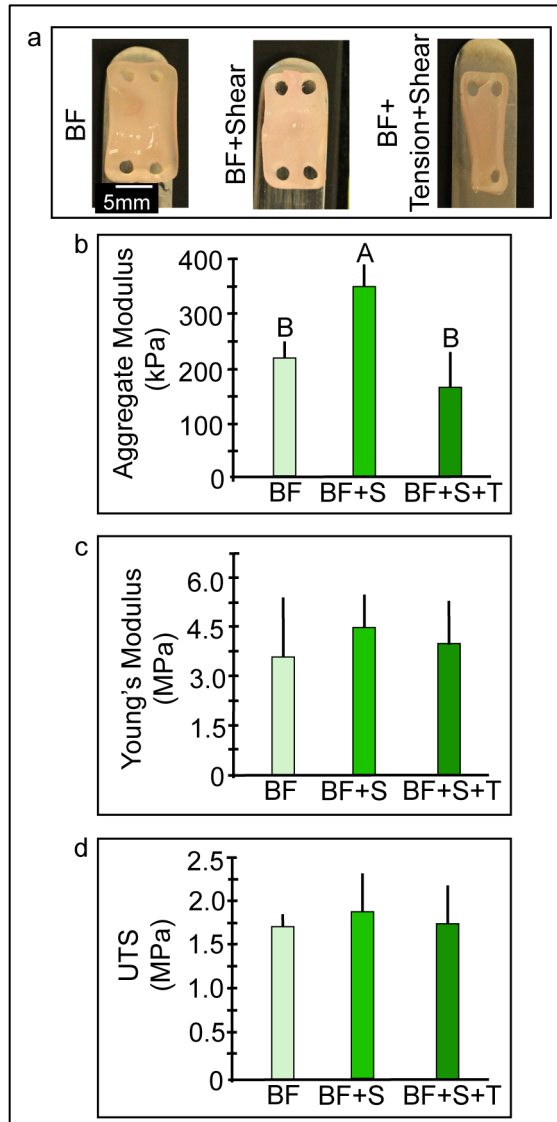
FIGURE 2

Figure 2 - The gross morphology and mechanical properties of neocartilage constructs are shown. **a)** The representative gross morphology of neocartilage constructs for each experimental group. **b)** The aggregate modulus of neocartilage constructs. **c)** The Young's modulus of neocartilage constructs. **d)** The ultimate tensile strength of neocartilage constructs. The capital letters floating above the bars indicate statistically different groups evaluated at a p<0.05 using a one-way ANOVA and post-hoc Tukey's test. Abbreviations: BF (bioactive factors), BF+S (bioactive factors + shear stress), BF+S+T (bioactive factors + shear stress + tension stress), UTS (ultimate tensile strength).

Extracellular matrix content

The glycosaminoglycan content and collagen content of neocartilage constructs was evaluated as described previously via a DMMB assay and a hydroxyproline assay, respectively. The glycosaminoglycan content of neocartilage constructs stimulated with BF+S was significantly different from the glycosaminoglycan content of neocartilage stimulated with only BF and BF+S+T. (Figure 3a) The collagen content was not significantly different among any groups. These results indicate that the use of BF+S during tissue culture yield neocartilage constructs that are more similar to native articular cartilage in terms of extracellular matrix content.
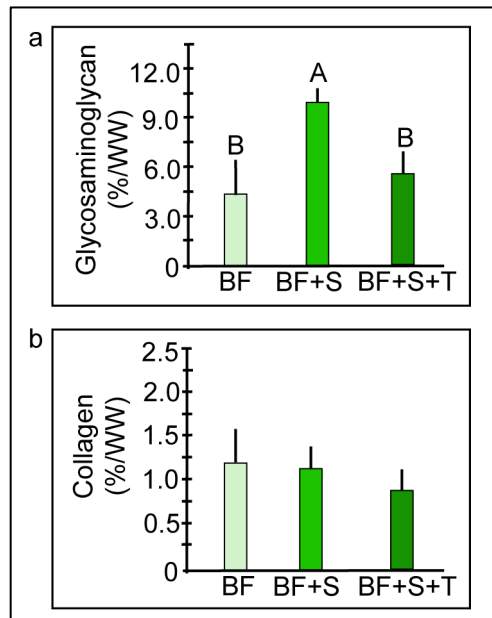
FIGURE 3

Figure 3- The extracellular matrix content of neocartilage constructs was evaluated in terms of a) percentage of glycosaminoglycan content normalized to wet weight, and b) percentage of collagen content normalized to wet weight. The capital letters floating above the bars indicate statistically different groups evaluated at a p<0.05 using a one-way ANOVA and post-hoc Tukey's test. Abbreviations: BF (bioactive factors), BF+S (bioactive factors + shear stress), BF+S+T (bioactive factors + shear stress + tension stress), WW (wet weight)

DISCUSSION AND FUTURE DIRECTIONS

In this study, the combination of bioactive factors and mechanical stimulation was investigated. The overall objective of this work was to determine which combination of bioactive factors and mechanical stimulation would lead to neocartilage with the most improved mechanical and biochemical properties. The three experimental groups tested were neocartilage treated with only bioactive factors (BF), neocartilage treated with bioactive factors and fluid-induced shear stress (BF+S), and neocartilage treated with bioactive factors, fluid-induced shear stress, and uniaxial tension (BF+S+T). Based on previous studies investigating combinations of bioactive factors and combinations of mechanical stimulation, it was hypothesized that neocartilage stimulated with BF+S+T would lead to the most biomimetic neocartilage constructs.

Interestingly, the results of this study indicated that the most mechanically robust neocartilage constructs in terms of compressive aggregate modulus were obtained from stimulation with BF+S. Additionally, there were no differences in tensile stiffness and strength among the experimental groups. In terms of extracellular matrix content, neocartilage stimulated with BF+S possessed the highest amount of glycosaminoglycan content compared to other groups. Currently, neocartilage tissue engineering aims to provide the most mechanically robust constructs for implantation in preclinical studies. Although further investigation is needed to determine the cause of these *in vitro* results, this study indicates that neocartilage should be treated with BF+S prior to orthotopic implantation in order to provide the most mechanically robust constructs.

The results of this study suggest that neocartilage constructs treated with bioactive factors, shear stress, and uniaxial tension stress (BF+S+T) are being over-stimulated. In particular, it is possible that the neocartilage constructs treated with BF+S+T experienced a deleterious amount of mechanical stimulation when used in combination with bioactive factors. In previous studies, fluid-induced shear stress and uniaxial tension were optimized in

neocartilage that was not treated with bioactive factors. This means that the optimized mechanical stimulation regimens were for neocartilage that is not as stiff as neocartilage that is treated with bioactive factors. The decrease in neocartilage properties after stimulation with BF+S+T could also be a result of neocartilage being over-saturated with calcium ions. In particular, it has been found that uniaxial tension activates TRPV4 pathways known to increase intracellular calcium, and fluid-induced shear stress has been found to activate PKD1 and PKD2 ion channels that also lead to increased levels of intracellular calcium. [12, 13, 18, 19] Although this has not been tested in self-assembled neocartilage, previous studies show that increasing levels of calcium ions in media can cause increasing levels of chondrocyte death.[20] Furthermore, it has also been shown that variations in intracellular calcium content are associated with cartilage matrix degradation. [21] With this information, it is clear that more stimulation is not always better in terms of improving neocartilage mechanical properties, and further studies need to focus on optimizing mechanical stimulation tactics for use in combination with bioactive factors.

Although the results from this study present neocartilage reaching levels near native articular cartilage compressive stiffness, there is still much left to uncover and achieve. For example, neocartilage with biomimetic native articular properties in terms of both compressive and tensile stiffness has yet to be achieved. Future iterations of this study may consider a full factorial experimental design to better understand the cause of diminishing mechanical properties when BF+S+T are used. It would also be of value to determine if combined mechanical stimulation strategies lead to constructs as mechanically robust as those obtained by using only bioactive factors. Finally, implantation of neocartilage stimulated with BF+S in an orthotopic location in a large animal model is salient for confirming the safety of translating neocartilage stimulated with bioactive factors and mechanical stimulation to the clinic. Overall,

the results of this study move tissue-engineered cartilage closer to the clinic by providing a feasible stimulation tactic for producing mechanically robust neocartilage implants.

REFERENCES

[1] F. McCormick, J.D. Harris, G.D. Abrams, R. Frank, A. Gupta, K. Hussey, H. Wilson, B. Bach, Jr., B. Cole, Trends in the surgical treatment of articular cartilage lesions in the United States: an analysis of a large private-payer database over a period of 8 years, Arthroscopy 30(2) (2014) 222-6.

[2] H. Kwon, N.K. Paschos, J.C. Hu, K.A. Athanasiou, Articular cartilage tissue engineering: the role of signaling molecules, Cellular and Molecular Life Sciences 73(6) (2016) 1173-1194.

[3] B.D. Elder, K.A. Athanasiou, Systematic assessment of growth factor treatment on biochemical and biomechanical properties of engineered articular cartilage constructs, Osteoarthritis and cartilage 17(1) (2009) 114-123.

[4] H. Kwon, S.A. O'Leary, J.C. Hu, K.A. Athanasiou, Translating the application of transforming growth factor-β1, chondroitinase-ABC, and lysyl oxidase-like 2 for mechanically robust tissue-engineered human neocartilage, Journal of Tissue Engineering and Regenerative Medicine 13(2) (2019) 283-294.

[5] E.A. Makris, R.F. MacBarb, N.K. Paschos, J.C. Hu, K.A. Athanasiou, Combined use of chondroitinase-ABC, TGF-β1, and collagen crosslinking agent lysyl oxidase to engineer functional neotissues for fibrocartilage repair, Biomaterials 35(25) (2014) 6787-6796.

[6] H. Liu, Z. Zhao, R.B. Clarke, J. Gao, I.R. Garrett, E.E.C. Margerrison, Enhanced Tissue Regeneration Potential of Juvenile Articular Cartilage, The American Journal of Sports Medicine 41(11) (2013) 2658-2667.

[7] T. Ito, R. Sawada, Y. Fujiwara, T. Tsuchiya, FGF-2 increases osteogenic and chondrogenic differentiation potentials of human mesenchymal stem cells by inactivation of TGF-β signaling, Cytotechnology 56(1) (2008) 1-7.

[8] M.K. Murphy, D.J. Huey, A.J. Reimer, J.C. Hu, K.A. Athanasiou, Enhancing Post-Expansion Chondrogenic Potential of Costochondral Cells in Self-Assembled Neocartilage, PLOS ONE 8(2) (2013) e56983.

[9] N. Tsumaki, K. Tanaka, E. Arikawa-Hirasawa, T. Nakase, T. Kimura, J.T. Thomas, T. Ochi, F.P. Luyten, Y. Yamada, Role of CDMP-1 in skeletal morphogenesis: promotion of mesenchymal cell recruitment and chondrocyte differentiation, The Journal of cell biology 144(1) (1999) 161-173.

[10] J.C. Hu, K.A. Athanasiou, A self-assembling process in articular cartilage tissue engineering, Tissue Engineering 12(4) (2006) 969-979.

[11] J.K. Lee, J.C. Hu, S. Yamada, K.A. Athanasiou, Initiation of chondrocyte self-assembly requires an intact cytoskeletal network, Tissue Engineering Part A 22(3-4) (2016) 318-325.

[12] J.K. Lee, L.W. Huwe, N. Paschos, A. Aryaei, C.A. Gegg, J.C. Hu, K.A. Athanasiou, Tension stimulation drives tissue formation in scaffold-free systems, Nature Materials 16(8) (2017) 864.

[13] S. Evelia, A. Ashkan, P. Nikolaos, B. Eric, K. Heenam, H. Jerry, A. Kyriacos, Shear stress induced by fluid flow produces improvements in tissue-engineered cartilage, Biofabrication (2020).

[14] M.K. Murphy, T.E. Masters, J.C. Hu, K.A. Athanasiou, Engineering a fibrocartilage spectrum through modulation of aggregate redifferentiation, Cell Transplant 24(2) (2015) 235-45.

[15] L.W. Huwe, G.K. Sullan, J.C. Hu, K.A. Athanasiou, Using Costal Chondrocytes to Engineer Articular Cartilage with Applications of Passive Axial Compression and Bioactive Stimuli, Tissue Eng Part A 24(5-6) (2018) 516-526.

[16] V.C. Mow, M.C. Gibbs, W.M. Lai, W.B. Zhu, K.A. Athanasiou, Biphasic indentation of articular cartilage—II. A numerical algorithm and an experimental study, Journal of Biomechanics 22(8) (1989) 853-861.

[17] D.D. Cissell, J.M. Link, J.C. Hu, K.A. Athanasiou, A modified hydroxyproline assay based on hydrochloric acid in Ehrlich's solution accurately measures tissue collagen content, Tissue Engineering Part C: Methods 23(4) (2017) 243-250.

[18] A.K. Wann, N. Zuo, C.J. Haycraft, C.G. Jensen, C.A. Poole, S.R. McGlashan, M.M. Knight, Primary cilia mediate mechanotransduction through control of ATP-induced Ca2+ signaling in compressed chondrocytes, The FASEB Journal 26(4) (2012) 1663-1671.

[19] M.N. Phan, H.A. Leddy, B.J. Votta, S. Kumar, D.S. Levy, D.B. Lipshutz, S.H. Lee, W. Liedtke, F. Guilak, Functional characterization of TRPV4 as an osmotically sensitive ion channel in porcine articular chondrocytes, Arthritis & Rheumatism 60(10) (2009) 3028-3037.

[20] A.K. Amin, J.S. Huntley, P.G. Bush, A.H.R.W. Simpson, A.C. Hall, Chondrocyte death in mechanically injured articular cartilage—the influence of extracellular calcium, Journal of Orthopaedic Research 27(6) (2009) 778-784.

[21] C. Nguyen, M. Lieberherr, C. Bordat, F. Velard, D. Côme, F. Lioté, H.K. Ea, Intracellular calcium oscillations in articular chondrocytes induced by basic calcium phosphate crystals lead to cartilage degradation, Osteoarthritis and Cartilage 20(11) (2012) 1399-1408.

CHAPTER 7- ESTABLISHING THE SAFETY OF SELF-ASSEMBLED ARTICULAR CARTILAGE IMPLANTS IN THE YUCATAN MINIPIG

ABSTRACT

For 250,000 Americans every year, the only clinical options for articular cartilage lesion repairs are microfracture, chondroplasty, mosaicplasty, and autologous chondrocyte implantation, which are unreliable and produce inconsistent results. The translation of tissue-engineered neocartilage is a significant clinical need that has the potential to provide consistent and long-term articular cartilage repair. However, before the translation of efficacious tissue-engineered technologies can be conceived, the FDA requires that preclinical studies demonstrate both local and systemic safety. Therefore, the objective of this study was to evaluate the preclinical safety of allogeneic, neocartilage implants using the Yucatan minipig as an animal model. The allogeneic, neocartilage implants were created using the scaffold-free, self-assembling process, which does not have the typical detriments associated with scaffold-based approaches, such as scaffold degradation byproducts. It was hypothesized that the self-assembled, allogeneic, neocartilage implants would not cause adverse local or systemic responses in minipigs. The local immune response was investigated in Surgical Set #1, where every minipig received multiple implants that were fixed within cartilage defects using three different strategies (microfracture, fibrin, or superficial fibrin). In Surgical Set #2, the systemic immune response was examined using three minipigs which received neocartilage implants, and two minipigs which served as empty defect, negative control animals. The results of this study indicate that allogeneic, self-assembled, neocartilage implants are safe for use in the Yucatan minipig model, suggesting that an analogous approach in the human would also be safe.

Authors: Salinas EY, Link JM, Hu JC, and Athanasiou KA

INTRODUCTION

Of the issues facing articular cartilage tissue engineering, one of the most pressing is the translation of these technologies into the clinic. Annually in the U.S., about 250,000 articular cartilage repair surgeries (i.e., microfracture, chondroplasty, mosaicplasty, and autologous chondrocyte implantation) are performed, indicating a significant clinical need for a reliable repair strategy.[1] The current treatment options for articular cartilage lesions are inadequate because of their inconsistency in producing hyaline cartilage, integrating with native tissue, and even filling the entire lesion.[2] Articular cartilage tissue-engineered constructs are a promising option for the repair of cartilage lesions because they can be designed and manipulated *in vitro* to enhance biochemical and biomechanical properties, completely fill cartilage lesions, and integrate with surrounding native tissue. However, even before the translation of efficacious technologies can be conceived, the safety of implanting allogeneic, tissue-engineered implants should be demonstrated.

Although articular cartilage is largely considered to be immune-privileged because of its avascularity and isolated encapsulation by the synovial membrane,[3-5] the FDA still requires that preclinical studies demonstrate both local and systemic safety.[6] The local safety of a neocartilage implant may first be assessed by looking at resulting gross morphological changes, such as the deterioration of native tissue surrounding the implant. Locally, the safety of a neocartilage implant may also be determined at the microscopic level by using histological staining to evaluate the level of tissue fibrosis and cellular infiltration. Determining the local response to an implant may be done with a small number of animals by also including an empty defect control in the same synovial joint. On the other hand, the evaluation of a systemic response necessitates control specimens that do not receive implants. Assessing a systemic response to neocartilage implants may involve the collection of hematology samples for the completion of complete blood counts and blood phenotyping chemistry panels. In this study,

both local and systemic responses were investigated to determine the safety of allogeneic, tissue-engineered, neocartilage implants.

Using the self-assembling process, the creation of robust, scaffold-free, neocartilage implants has been achieved.[7-9] The self-assembling process has several advantages over traditional tissue engineering systems in that it does not rely on the use of scaffolds for robust biomechanical properties, which have been shown to contribute to an immune response following implantation.[10] Conversely, scaffold-free, self-assembled neocartilage, formed via cell-to-cell interactions to recapitulate the native developmental conditions of cartilage,[11] does not have the typical detriments associated with scaffold-based approaches, such as scaffold degradation byproducts.[10] Additionally, the use of biochemical and biomechanical stimuli during the tissue culture process results in neocartilage with functional properties on par with native tissue.[12-16] In particular, for this study, bioactive factors (TGF-β1, LOXL2, C-ABC, and C-ABC$_{int}$) and mechanical stimulation (fluid-induced shear stress) were used to create self-assembled neocartilage with robust mechanical properties for implantation in a Yucatan minipig animal model.

Yucatan minipig costal cartilage cells present a favorable cell source and species for preclinical studies of neocartilage implants. Costal cartilage cells allow for autologous and allogeneic chondrocyte harvest without further damaging the affected joint. Although costal cartilage does not articulate, costal cartilage cells produce hyaline cartilage when used in the self-assembling process to create neocartilage implants.[17] Additionally, costal cartilage cells are advantageous over other alternative cell sources, such as stem cells, because they are able to regain their chondrogenic phenotype after expansion and aggregate redifferentiation, and they generate a more stable, homogeneous cell population.[18, 19] The Yucatan minipig in particular, is considered a suitable animal model for most preclinical work geared toward safety because of its similarity to humans in terms of anatomy, weight, immunology, physiology, and

188

bone biology.[20-24] When considering Yucatan minipigs specifically for use in articular cartilage repair, they also have similar histologic features in terms of glycosaminoglycans and collagen type II.[17, 24, 25] Because of these advantages, costal cartilage cells from Yucatan minipigs present a feasible and efficient cell source and species for use in the laboratory and in translational articular cartilage repair studies.

The objective of this study was to evaluate the preclinical safety of allogeneic, neocartilage implants using the Yucatan minipig as an animal model. The neocartilage implants were created according to the self-assembling process using allogeneic, passaged costal cartilage cells, then enhanced with bioactive factors and mechanical stimulation, and, finally, primed for integration with the native tissue using C-ABC$_{int}$. To assess both the local and systemic safety profiles of the minipig response to neocartilage implants, two separate surgical sets were conducted. In Surgical Set #1, every minipig received multiple implants that were engineered in the same fashion, but were fixed within cartilage defects using three different strategies (microfracture, fibrin, or superficial fibrin). It was hypothesized that implants that remain in place for the duration of the study would not lead to a local immune or inflammatory response. In Surgical Set #2, three minipigs received neocartilage implants (implant group), while two minipigs served as empty defect, negative control animals (empty defect group). For Surgical Set #2, it was hypothesized that the animals that received implants would not present with a systemic immune response different to that of the negative control animals. Overall, the results from these two surgical sets should provide evidence to support the notion that self-assembled, allogeneic, neocartilage implants are safe and do not lead to adverse local or systemic reactions.

MATERIALS AND METHODS

<u>Fabrication of tissue engineered implants</u>

Chondrocyte procurement and expansion: Costal chondrocytes were obtained from 6-month-old Yucatan mini pigs. The costal cartilage was removed from the rib cage and the perichondrium was removed. The remaining cartilage was minced into pieces about $1mm^3$, and subsequently digested in a 0.2% weight/volume collagenase solution with 3% FBS for 18hr. The liberated cells were then strained, washed, and plated in tissue culture flasks. The chondrocytes were seeded at 2 million cells per T225 flasks with 30ml of expansion media consisting of chondrogenic media at 2% FBS and additional growth factors growth factors (1ng/ml TGF-β1, 10ng/ml PDGF, and 5ng/ml bFGF).

The chondrocytes were passaged every two weeks or until cells were confluent as described previously.[8, 9] To passage, chondrocytes were lifted from the flask using 0.05% Trypsin-EDTA. After quelling the Trypsin-EDTA reaction with wash media at 10% FBS, the cells were spun down and resuspended in a 0.2% weight/volume collagenase solution at 3% FBS for about 2hr at 37°C. This cell suspension was agitated with a serological 25ml pipette every 15 minutes. Finally, the cell suspension was spun down, washed, and resuspended in expansion media to be plated again.

After the chondrocytes were expanded to passage 3, they were placed into aggregate redifferentiation as described previously. [9] The aggregates were seeded in a dropwise fashion into an agarose coated petri dish at a density of 22.5 million cells per 30ml of redifferentiation media. Redifferentiation media consisted of chondrogenic media and growth factors (10ng/ml TGF-β1, 100ng/ml GDF5, and 100ng/ml BMP-2). The petri dishes were then placed on an orbital shaker at a speed of 50 RPM for 24hr. After 24hr the cell suspension was removed from the orbital shaker and fed redifferentiation media every 3-4 days for 2 weeks. After 2 weeks, the cell suspension was resuspended in 0.05% Trypsin for 45 minutes, washed and resuspended in

0.2% w/v collagenase for 2hr, and strained. The remaining cells were used to create the neocartilage constructs.

Self-assembling process: Neocartilage implants were created using the self-assembling method as described previously. [7, 15] Briefly, 5mm diameter molds were used to create 2% agarose wells in a 48-well plate. Chondrogenic media was exchanged 2-3 times to saturate the wells before cell seeding. Chondrocytes were seeded at 2 million cells per well in 100µl of chondrogenic media. After 4 hr, the cells were fed with 500µl of chondrogenic media and additional growth factors (10ng/ml TGF-β1). 3 days after seeding, the neocartilage constructs were removed from the wells, and after 7 days they were treated with C-ABC as described previously.[15] Finally, the constructs were treated with LOXL2 as described previously.[26]

Shear stress stimulation: Neocartilage constructs were stimulated with fluid-induced shear stress from days 14-21 of tissue culture as described previously.[27] Briefly, the fluid-induced shear stress device was created using a mold, 3% agarose, and a petri dish. The mold was placed into the petri dish containing 3% agarose, producing small protruding agarose poles that hold the neocartilage in place. The neocartilage constructs were placed in the fluid-induced shear stress device, and 15ml of chondrogenic media and additional growth factors were added. The device was then placed on an orbital shaker and set to 50RPM. As the orbital shaker rotated, the chondrogenic media flowed over the constructs subjecting them to a fluid induced shear stress range of 0.05-0.021Pa. Chondrogenic media was replaced every 2-3 days, and after day 21 of culture, the neocartilage constructs were removed from the device and placed into 24-well plates until the end of culture.

C-ABC integration treatment: Directly prior to surgical implantation, using a sterile dermal biopsy punch, 4- and 5-mm discs were taken from implants, which were then treated with chondroitinase ABC for integration (C-ABC$_{int}$; 0.15U/ml for 2hr).[28] Following treatment, C-

ABC$_{int}$ activity was quenched with zinc sulfate (1mM) for 10 minutes, and elimination of residual, inactive enzyme was achieved by sequentially washing constructs with medium. Subsequently, implants were placed in CHG containing HEPES buffer (25mM) for transport to UCI medical center.

Quality control of engineered implants

Mechanical testing of engineered constructs: Constructs were mechanically tested prior to implantation to generate a baseline of properties and were also tested at the end of the study to provide in vitro control data. Tensile testing was conducted on dog-bone-shaped specimens as previously described.[17] Briefly, these samples were glued to paper tabs, which were then gripped by a uniaxial testing machine (Instron 5565, Norwood, MA), and a pull-to-failure test was conducted at a rate of 1% strain per second. From these experimental data, Young's modulus and ultimate tensile strength values were determined for the constructs. Creep indentation compressive tests were conducted on constructs using a flat, porous indenter tip and a constant load as previously described.[29] A linear biphasic model and finite element analysis were used to obtain the aggregate modulus, permeability, and Poisson's ratio from the experimental creep curves.[29] These data can be found in the supplementary material (Figure S1).

In vitro toxicology: On the day of implantation for both surgery sets, media samples were taken from tissue culture wells containing constructs to be implanted and stored at -20°C for subsequent analysis. For each surgery set, aliquots were taken from each sample, pooled, and sent to the UC Davis Comparative Pathology Lab (CPL), where they were tested for mycoplasma, bacterial, and fungal contamination.

Acquisition of Yucatan Minipigs: Skeletally-mature (~18 months old) Yucatan minipigs were obtained from LoneStar Laboratory Swine, a commercial provider of laboratory-grade

swine (LoneStar Laboratory Swine, Exemplar Genetics, Sioux Center, IA, USA). These minipigs came from a closed herd, and their health was verified prior to shipment to the UCI Medical Center (UCIMC) University Laboratory Animal Resources (ULAR) facility.

<u>Surgical Set #1</u>

Surgical approach: The surgical preparation, which included the administration of anesthesia, was performed with assistance by ULAR Veterinary Services. The initial induction was performed with an intramuscular (IM) injection of Telazol (Tiletamine + Zolazapam at 10mg/kg) and xylazine (2mg/kg). Dosages were subject to the discretion of the veterinarian. An intravenous (IV) catheter was placed in the ear vein for the administration of intravenous fluids (LRS 5–10ml/kg/hr), and a mask was used to deliver isoflurane during this induction period. Once the minipig was sufficiently unconscious, they were intubated, and general anesthesia was maintained with isoflurane (1–3%) accompanied with mechanical ventilation. Preemptive analgesia was delivered with meloxicam 0.4mg/kg IM as well as buprenorphine at 0.2mg/kg subcutaneously. Vitals monitoring was achieved with capnography, a thermometer, and pulse oximeter, and the pigs were kept at a temperature of 37–38°C with heated water blankets.

Under general anesthesia, the knees were surgically prepared and draped. With the minipig in dorsal recumbency, a craniolateral parapatellar approach was taken to access the knee joint. The patella and patellar tendon were not distracted and cruciate ligaments, and joint surface cartilage integrity was maintained. The digital extensor tendon that runs along the lateral condyle was removed in 2 out of 3 of the mini pigs to better access the condyles (the minipig that received superficial fibrin glue treatment did not have the digital extensor tendon removed). A 5mm diameter biopsy punch was used to uniformly mark circular defects on the femoral condyles. A map of the defects created and their corresponding treatments is found in Figure 1. A ring curette and Midex Rex drill were used to delicately remove all of the articular

cartilage in the defect until a full thickness chondral defect with perpendicular walls was created. Implants were placed and fixed according to the defect maps shown in Figure 1, and then fixation was tested by articulating the knee joint multiple times and ensuring the implants were still in place. To conclude the procedure, the joint capsule, subcutaneous tissue, and skin were individually sutured in a simple interrupted fashion.

Post-operative animal care: Post-operative analgesia included the administration of Meloxicam 0.4 mg/kg IM or Banamine (Flunixin) 2.2mg/kg once daily for 3 days and then as needed per ULAR vet services' recommendation. An additional dosage of buprenorphine was given 2–3 days postoperatively if needed.

Euthanasia: The minipigs in Surgical Set #1 were euthanized 4 weeks after implantation with an IM injection of Telazol/Xylazine followed by an IV injection of pentobarbital (Euthazol) at a dose of 1 ml (390mg/4.5kg). Both knee joints were removed en bloc and transported to the lab to be processed for safety assessments.
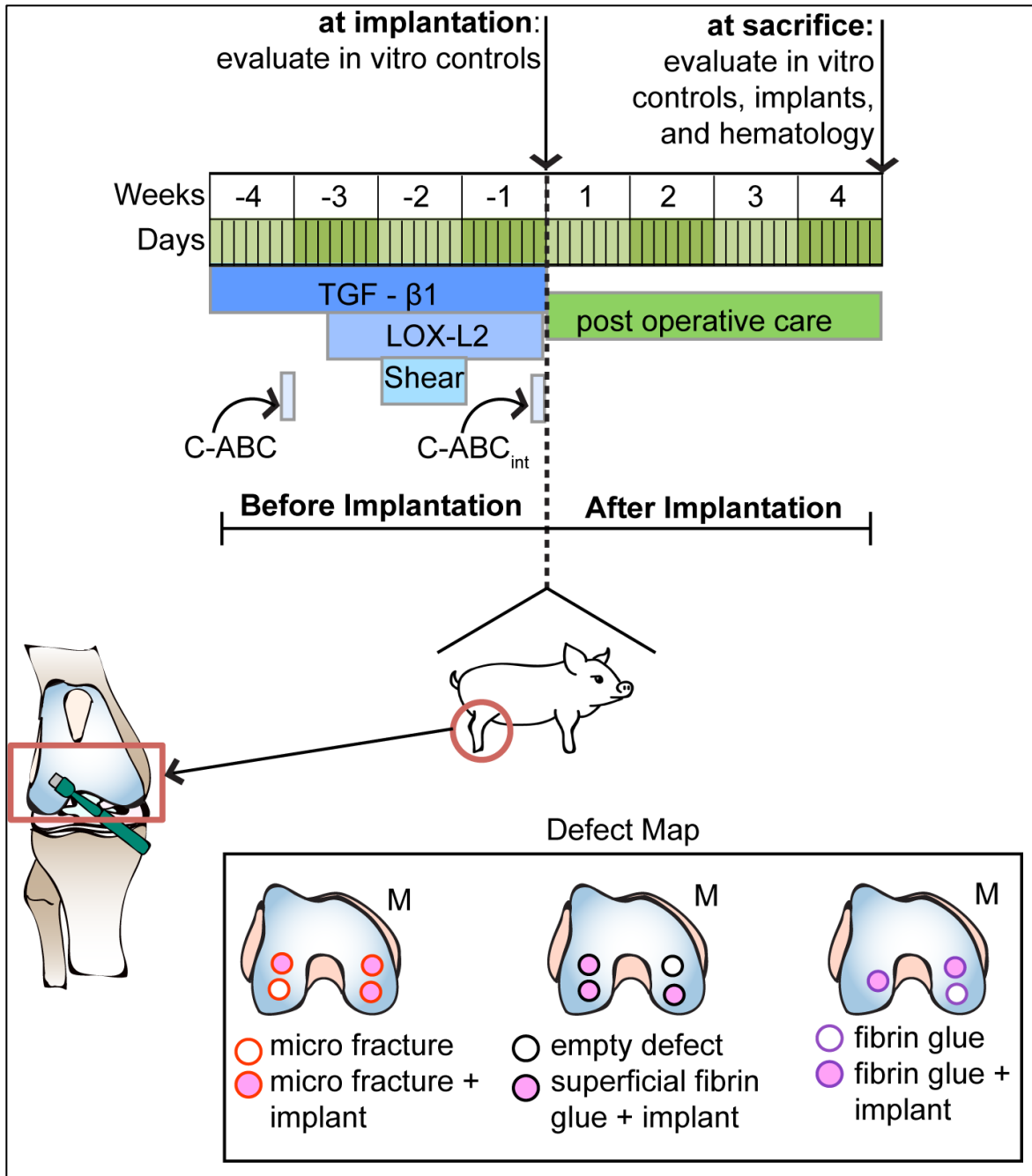
FIGURE 1

Figure 1 - Surgical Set #1 timeline and surgical approach: A schematic depicting a timeline for the creation of the tissue engineered neocartilage implants, to implantation and sacrifice. The timeline at the top of the figure shows the tissue engineering strategy used to create the implants. Neocartilage implants were treated with TGF-β1 for the entire duration of culture, C-ABC for 4hr at day 7, LOX-L2 from days 10-28, and shear stress from days 14-21. Finally, on the day before surgery, C-ABC$_{int}$ treatment was applied. The day of the surgery, *in vitro* control constructs were evaluated. The implants remained in the minipigs for 4 wks, at which point they were sacrificed. On the day of sacrifice, the implants were evaluated, and blood was collected for hematology assays. The bottom half of the figure depicts the surgical approach for Surgical Set #1. A total of 3 minipigs were operated on, all on their right knee, and a biopsy punch was used to create all defects (shown in the defect map).

Surgical Set #2

Surgical approach: Preparation for surgery, including the administration of anesthesia, was performed with assistance by ULAR Veterinary Services. Initial induction was with Telazol 10mg/kg IM injection with addition of xylazine 2mg/kg IM. Dosages were subject to the discretion of the veterinarian An IV catheter was placed in the ear vein and was used for administration of IV fluids (LRS 5–10ml/kg/hr). In addition, isoflurane delivered by mask was used during the IV catheter and induction period. Once in the appropriate depth of anesthesia, the minipig was intubated; general anesthesia was maintained with isoflurane (1–3%) accompanied with mechanical ventilation. Pre–emptive analgesia was delivered with Meloxicam 0.4mg/kg IM as well as sustained release buprenorphine at 0.2mg/kg subcutaneously. Vitals monitoring was achieved with capnography, a thermometer, and pulse oximetry. A heated water pad was used to keep the pigs at a temperature of 37–38 degree Celsius. Once the minipig was anesthetized, 2–4ml of blood was collected for analysis of complete blood count (CBC) and blood phenotyping chemistry panel (BPCP) to establish a baseline of properties for all minipigs. Additional blood samples for CBC and the BPCP were collected for each animal directly prior to euthanasia in order to determine the possible systemic effect of the implant.

Under general anesthesia, the animals had their knees surgically prepared and draped. A craniolateral parapatellar approach to the knee joint with a scalpel blade was performed with the minipig in dorsal recumbency. The patella or patellar tendon was not distracted, and the digital extensor tendon that runs along the lateral condyle was preserved in all cases. Additionally, cruciate ligaments and joint surface cartilage integrity were maintained. A 5mm diameter biopsy punch was used to uniformly mark two circular sections on the medial femoral condyle. A map of the defects created and their corresponding treatments is found in Figure 2. A ring curette and Midex Rex drill were used to delicately remove all of the articular cartilage in the defect until a full thickness chondral defect with perpendicular walls was created. Then, for three minipigs, tissue-engineered constructs were placed in the defect sites and secured with fibrin glue. Implant fixation was tested by articulating the knee joint multiple times and ensuring the implants were still in place. For the other two minipigs, the defect sites were left empty. To conclude the procedure, the joint capsule, subcutaneous tissue, and skin were individually sutured in a simple interrupted fashion.

Postoperative animal care: For Surgical Set #2, minipigs were placed in a custom-made, IACUC-approved, sling immediately after surgery to prevent the minipig from injuring itself while coming out of anesthesia, as well as to prevent the immediate loading of the operated knee joint (Figure 3). The sling was made of vinyl fabric and had four holes for the limbs, which were equipped with padding. Double-layer reinforcements were included to support the weight of the mini pigs. Plywood was used to transport the sling while holding the minipig. Rotation of the plywood unrolled the sling, giving it an adjustable height feature and allowing the minipig to be gently placed on the bottom of the cage 3-4 hr after surgery, once the minipig was sufficiently awake to walk and load the knee joint normally. The cage in which the minipigs were placed while in the sling was also equipped with additional cage padding to prevent the minipig from injuring itself in its semi-conscious postoperative state.

In terms of postoperative analgesia, animals received Meloxicam 0.4 mg/kg IM or Banamine (Flunixin) 2.2 mg/kg once daily for 3 days and then as needed per ULAR vet services' recommendation. An additional dosage of buprenorphine was given 2–3 days postoperatively if needed. Also, two minipigs were selected for midpoint arthroscopy at 4 weeks to ensure that there was no synovial tissue damage or gross evidence of an immune response.

Euthanasia: The mini pigs in Surgical Set #2 were euthanized 8 weeks after implantation with an intramuscular injection of Telazol/Xylazine followed by an IV injection of pentobarbital (Euthazol) at a dose of 1ml (390 mg/4.5 kg). Both knee joints were removed en bloc and transported to the lab to be processed for safety assessments.

<u>Safety Assessments</u>

Gross morphology: Immediately after euthanasia, the hind limbs were removed at the hip joint, keeping the knee joint intact, and transported to the laboratory for dissection. The hind limbs were then dissected to expose the knee joint, and the femur was separated from the tibia and patella. All femoral condyles, including non-operated joints and condyles were measured, and their appearance was documented via photographs.

FIGURE 2

Weeks: -5 -4 -3 -2 -1 1 2 3 4 5 6 7 8

Days

at implantation: evaluate in vitro controls and hematology

at midpoint: arthroscopy and hematology

at sacrifice: evaluate in vitro controls, implants, and hematology

TGF - β1

LOX-L2

Shear

C-ABC

C-ABC$_{int}$

post operative care

Before Implantation

After Implantation

Defect Map

M

M

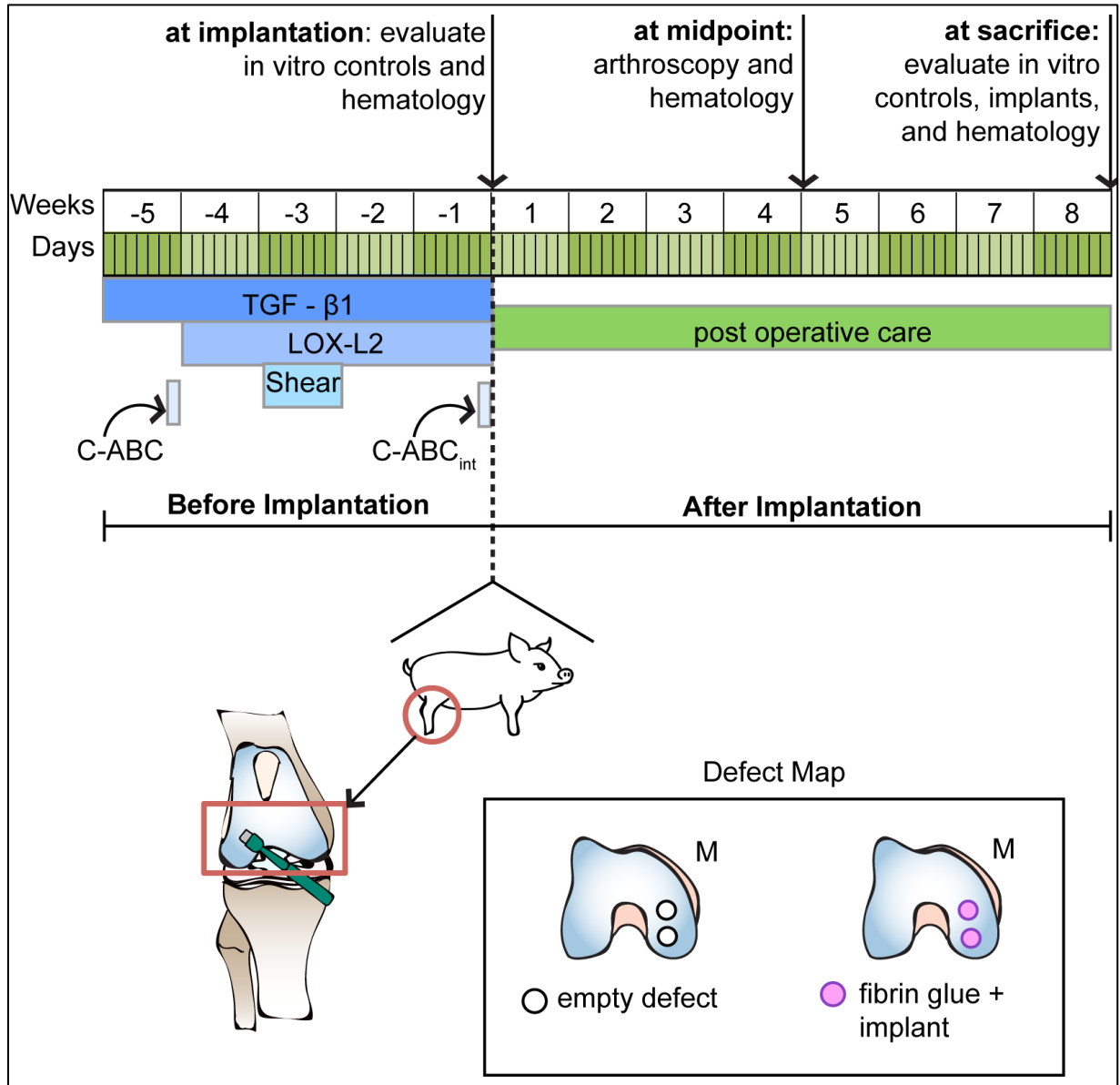○ empty defect

○ fibrin glue + implant

Figure 2- Surgical Set #2 timeline and surgical approach: A schematic depicting a timeline from the creation of the tissue engineered neocartilage implants, implantation, and sacrifice. The timeline at the top of the figure shows the tissue engineering strategy used to create the implants. Neocartilage implants were treated with TGF-β1 for the entire duration of culture, C-ABC for 4h at day 7, LOX-L2 from days 10-28, and shear stress from days 14-21. Finally, on the day before surgery C-ABC$_{int}$ treatment was applied. The bottom half of the figure depicts the surgical approach for Surgical Set #2. A total of 5 minipigs were operated on the right knee. 3 of these minipigs received implants, and 2 did not. At implantation, *in vitro* control constructs were evaluated for their mechanical properties, and a sample of blood was collected from each minipig for hematology assays. At 4 wks post-operatively, 2 of the minipigs that had neocartilage implanted underwent arthroscopy, and a sample of their blood was collected for hematology assays. At sacrifice, control constructs that were left in *in vitro* culture for 8 weeks were evaluated for their mechanical properties, the condyles of the minipigs were processed, and blood samples and synovial fluid were collected from all minipigs for hematology and cytology assays, respectively.

Lameness scale and animal wellness observations: The minipigs were evaluated for lameness 2 weeks after undergoing surgery. The stance and gait of the minipigs was graded using a scale from 0 to 5.[30] Minipigs were given grades as follows: 0 - full weight bearing stance with no apparent lameness while walking; 1 - mild lameness while walking; 2 - mid weight bearing stance with apparent lameness; 3 - stands toe-touching only with significant lameness while walking; 4 - stands holding leg up with significant lameness; and 5 - non weight bearing. Additionally, animal wellness was observed with the help from veterinary staff and animal husbandry at ULAR on a daily basis. The minipigs were monitored for their activity, eating, weight-gain, and engagement with the staff and researchers.
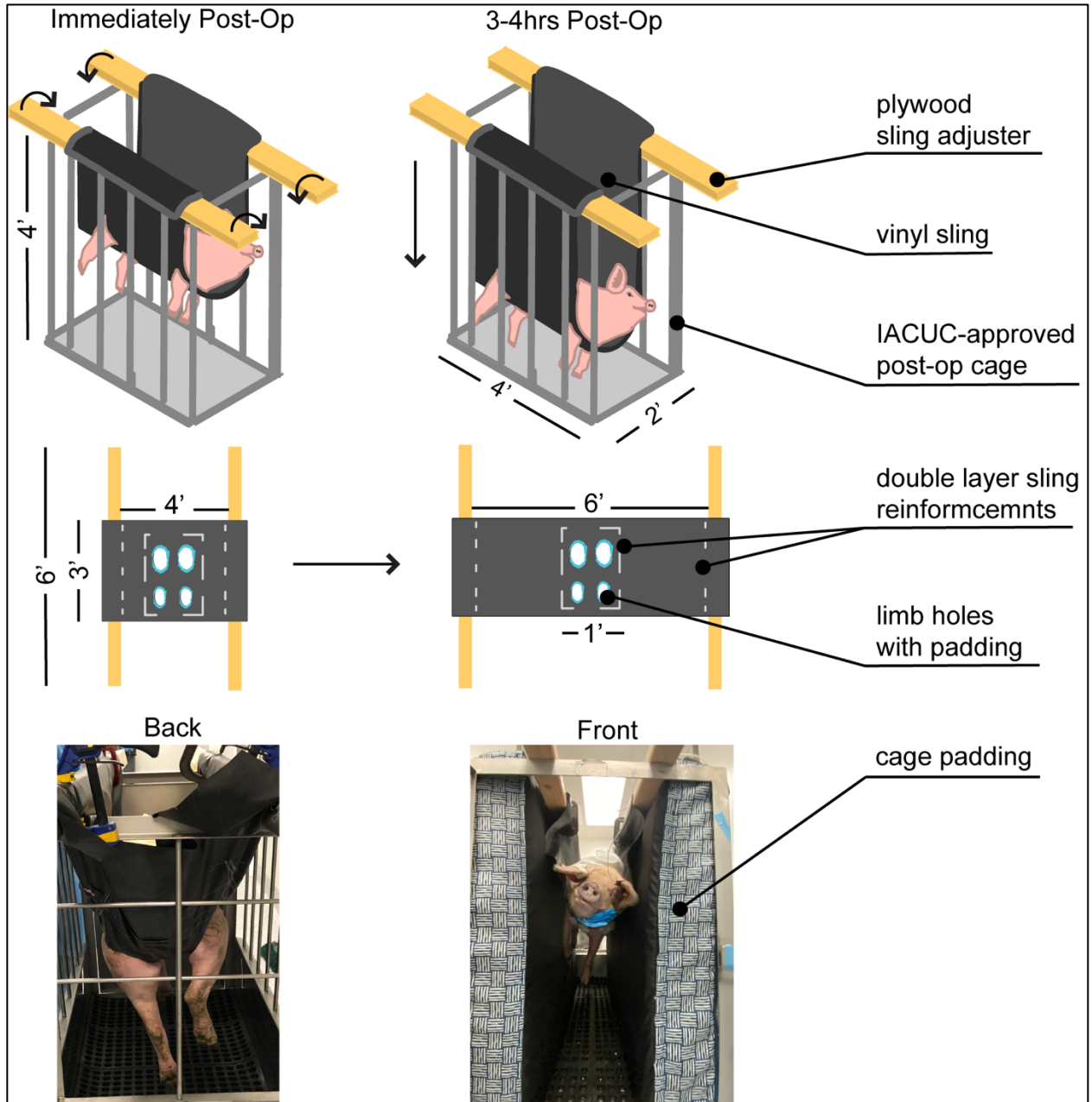
FIGURE 3

Immediately Post-Op

3-4hrs Post-Op

plywood
sling adjuster

vinyl sling

IACUC-approved
post-op cage

double layer sling
reinformcemnts

limb holes
with padding

Back

Front

cage padding

Figure 3- Surgical Set #2 post-operative care: Immediately after surgery, minipigs were placed in a custom-made, IACUC-approved, sling. The sling is made of vinyl and has 4 holes for the limbs, which were equipped with padding. Double-layer reinforcements were included to support the weight of the minipigs. Plywood was used to transport the sling while holding the minipig. Rotation of the plywood unrolls the sling, giving it an adjustable height feature and allowing the minipig to be gently placed on the bottom of the cage 3-4 hrs post-operatively. The cage was also equipped with additional cage padding to prevent the minipig from injuring itself in its semi-conscious post-op state.

Histopathology: Condyles were removed from the distal femur using an oscillating saw and then fixed in 10% neutral-buffered formalin for ~1 month. Subsequently, the condyles were decalcified in a 10-20% EDTA solution for ~1 month.[31] Decalcification solution was changed 2-3 times per week. Once samples were fully decalcified, the condyles were trimmed to contain only the defect site and 1-2mm of adjacent, native tissue. Then, these samples were processed, embedded in paraffin, and sectioned at a thickness of 5μm. Finally, these sections were stained with hematoxylin and eosin (H&E) as previously described and evaluated for evidence of a local immune response and tissue abnormality.[32]

UC Davis CPL Assays: Blood samples taken from minipigs pre- and post-operatively were shipped overnight to the UC Davis Comparative Pathology Laboratory (UCD CPL), where they were subjected to a CBC and a BPCP. Additionally, synovial fluid was collected post-mortem from each minipig and subjected to a synovial fluid cytology exam performed by a trained veterinary pathologist. Finally, cell-culture media samples that contained constructs that were implanted were collected from each surgical set, pooled, and sent to the UCD CPL for microbial contamination testing (e.g., mycoplasma and bacterial).

Statistics: Using Graphpad Prism, a Student's t-test was run for each CBC and BPCP output. Data was grouped in two ways. First, data were grouped according to treatment (i.e., empty defect or implant) and compared to assess differences between the treatments. Second, within treatment groups, presurgical values were compared to endpoint values to assess change within groups over time.

RESULTS

Lameness scale and animal wellness observations: Two weeks after the surgery, the stance and gait of the minipigs were evaluated using a scale from 0 to 5. A score of 0 was given to minipigs that did not exhibit lameness and a score of 5 was given to minipigs that were non-weight bearing. The minipig that received 4 defects and treated with implants fixed with superficial fibrin glue was given a score of 1, indicating a full-weight bearing stance and mild lameness while walking. The minipig that received the microfracture treatment was evaluated as a 2, meaning that the minipig stood with mild weight-bearing and there was lameness noted while walking. The minipig that received 3 defects and was treated with fibrin glue was also evaluated as a 2.

Animal wellness throughout the implantation period was also documented. The ULAR staff determined that eating, drinking water, and weight gain was normal in all minipigs. The minipigs were moderately subdued for 24-48 hr immediately after the surgery. Once recovered from the immediate effects of surgery, the minipigs regained a keen engagement in their surroundings. Additionally, the ULAR veterinary and husbandry staff noted moderate interest and normal interaction with the minipigs.

Gross morphology: The gross morphology of the condyles was observed and documented about 6 hr after sacrifice. The photos in Figure 4 show the gross morphology of the constructs and the corresponding defect maps. All defects were created with a biopsy punch, and one control defect was included in each operated knee in which no implants were placed. In the minipig that received the microfracture treatment, the resulting gross morphology at 4 weeks post-op shows little to no repair tissue in all of the defects and no implant retention. In the minipig that received implants held in place with fibrin glue covering the top of the defect, the resulting gross morphology at 4 weeks post-op showed no repair tissue and no implant retention

in the anterior-lateral and posterior-medial defects. Some repair tissue was evident in the posterior-lateral defect as well as in the anterior-medial defect. In the minipig that received implants fixed with fibrin glue along the bottom, sides, and top of the defect, the gross morphology at 4 weeks post op showed implant retention and repair in the anterior-medial defect. The posterior-medial defect and the defect on the lateral condyle showed the formation of repair tissue. These results indicate that the use of microfracture and an implant are not an effective option for tissue repair and implant retention. Fibrin glue is a more effective tool for implant retention; thus, this treatment strategy was carried into Surgical Set #2.

Histopathology: Hematoxylin and eosin staining of the implant that remained in place for the duration of the study demonstrated hematoxylin staining that appeared similar in intensity to the adjacent native tissue (Figure 5). Cells were retained within the implant and exhibited chondrocyte morphology (e.g., rounded shape and lacunae structure) (Figure 5, inset A). Some cells near a portion of the surface of the implant, which stained less intensely for hematoxylin, appeared to be more fibroblastic (Figure 5, inset B). However, there was no indication of the presence of immune cells such as macrophages or foreign body giant cells, nor did a fibrous, collagen capsule form around the periphery of the implant. Within the bone, which appears to have undergone some remodelling, osteocytes were visible within trabeculae, while osteoclasts and osteoblasts appeared to have occupied the space between trabeculae (Figure 5, inset C).
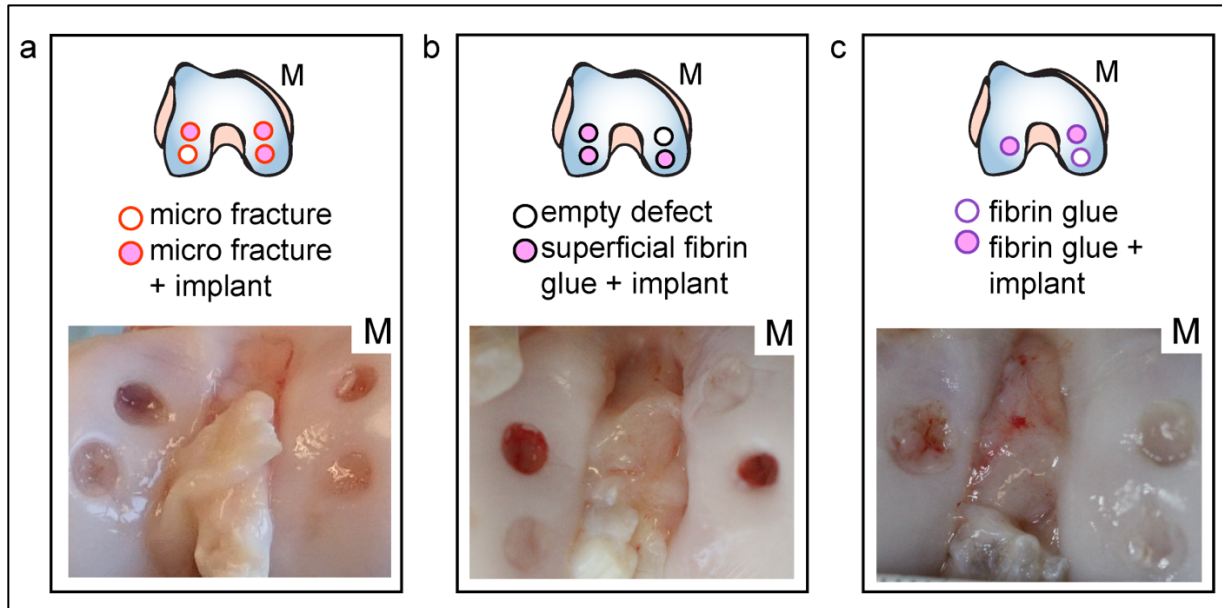
FIGURE 4

Figure 4- Surgical Set #1 defect maps and resulting gross morphology: Defect maps for all three minipigs are presented at the top of each panel and depict the location of defects made and their corresponding conditions. All defects were created with a biopsy punch. 1 control defect was included in each operated knee in which no implants were placed. **a)** All 4 defects created were treated with microfracture, 3 of which also received an implant. The resulting gross morphology at 4 weeks following surgery shows little to no repair tissue in all of the defects and no implant retention. **b)** 4 defects were created, and 3 of these received an implant. The implants were held in place with fibrin glue covering the top of the defect. The fourth defect was left empty. The resulting gross morphology at 4 weeks after surgery shows no repair tissue and no implant retention in the anterior lateral and posterior medial defects. Some repair tissue is evident in the posterior lateral defect, as well as in the anterior medial defect. **c)** 3 defects were created, 2 of which received an implant. The implants were held in place with fibrin glue along the bottom, sides, and top of the defect. The third defect was filled with fibrin glue only. The gross morphology at 4 weeks following surgery shows implant retention and repair in the anterior medial defect. The posterior medial defect and the defect on the lateral condyle show the formation of repair tissue.

Cell culture media contamination testing: The pooled cell culture media sample was negative for all testable contaminants including fungus, bacteria, and mycoplasma.
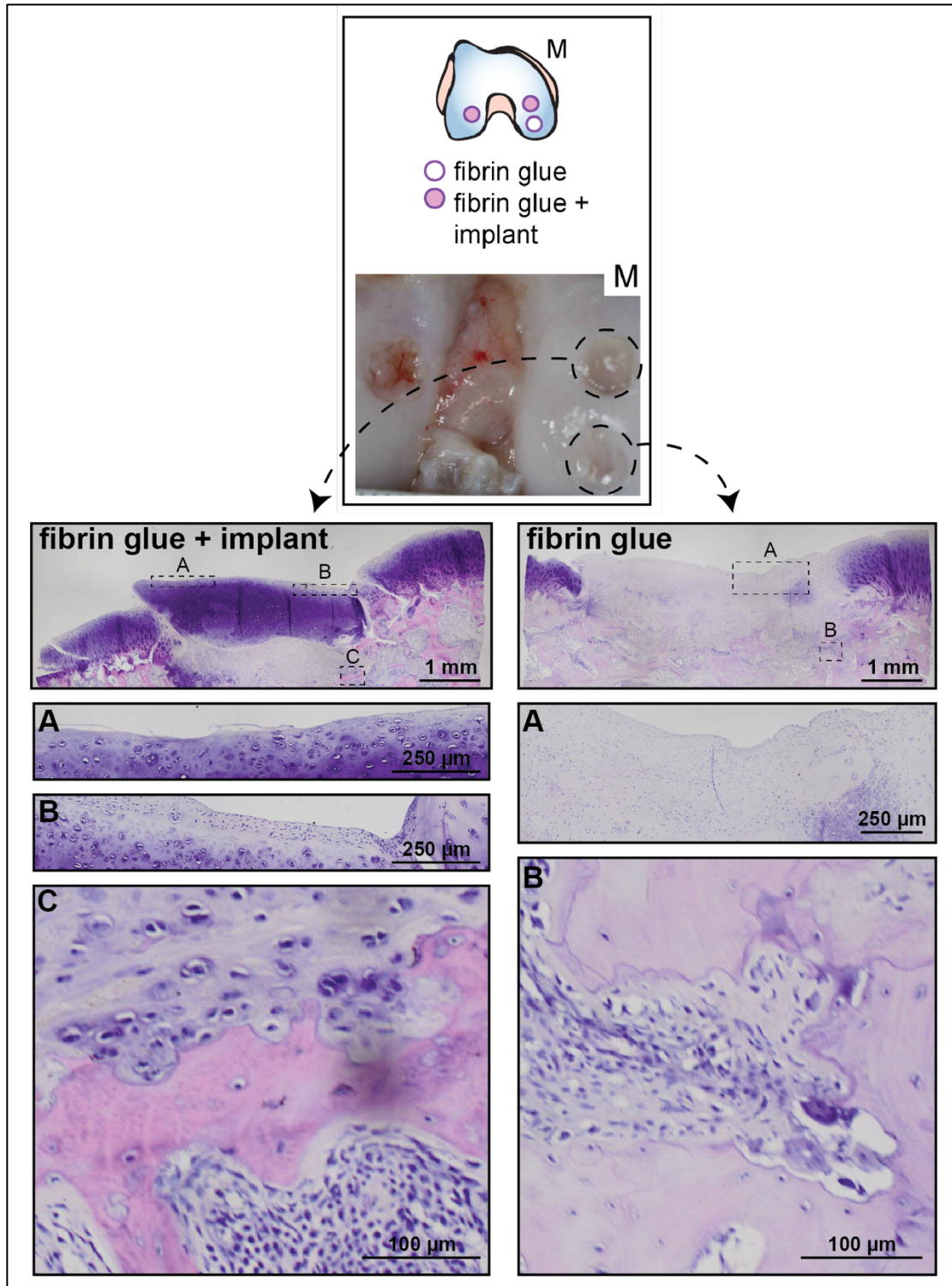
FIGURE 5

Figure 5- Histopathology of graft sites from the fibrin minipig. The fibrin glue + implant graft site did not illustrate any evidence of a local immune response to the implant at the surface (A and B) or in the bone (C). In general, chondrocyte phenotype and matrix integrity were retained at the surface of the implant (A), but some cells took on a more fibroblastic phenotype (B). Basic multicellular units, bone remodeling compartments, and osteocytes within lacunae were present in the bone (C). The fibrin glue graft site filled with what appears to be fibrous repair tissue (A), while the bone also exhibited signs of remodeling and healthy osteocyte structure (B).

Surgical Set #2

Lameness scale and animal wellness observations: As in Surgical Set #1, the stance and gait of the minipigs were evaluated using a scale from 0 to 5 about 1 week after the surgery. A score of 0 was given to minipigs that did not exhibit lameness and a score of 5 was given to mini pigs that were non-weight bearing. The three minipigs that received two defects each and were treated with implants were given scores of 1, 1, and 2. The two minipigs that received two defects each, but were not treated with implants were given scores of 1. A score of 1 indicated a normal stance with mild lameness while walking, and a score of 2 indicated that the minipig stood with mild weight-bearing and there was lameness noted while walking.

Animal wellness throughout the implantation period was also documented. The ULAR staff determined that eating, drinking water, and weight gain was normal in all minipigs. The minipigs were moderately subdued for 24-48 hr immediately after the surgery. Once recovered from the immediate effects of surgery, the minipigs regained a keen engagement and interest in their surroundings, as well as normal interaction.

Gross morphology: As in Surgical Set #1, the gross morphology of the condyles was observed and documented about 6 hr after sacrifice. The photos in Figure 6 show the gross morphology of the constructs and the corresponding defect maps from surgical set 2. All defects were created with a biopsy punch. The defects were left empty in 2 minipigs, whereas 3

minipigs received 2 implants each. The gross morphology of the mini pigs that received no

implants demonstrated little to no repair tissue in the defects at 8 wks postoperatively. The

gross morphology of the mini pigs that received implants showed repair tissue in 2 of the 3 mini

pigs, but no implant retention. This indicates that a fixation strategy with only the use of fibrin

glue is not effective in keeping the implants in the defect after surgery. The repair tissue and

lack of gross pathology, however, provides evidence that the implants are safe to use and don't

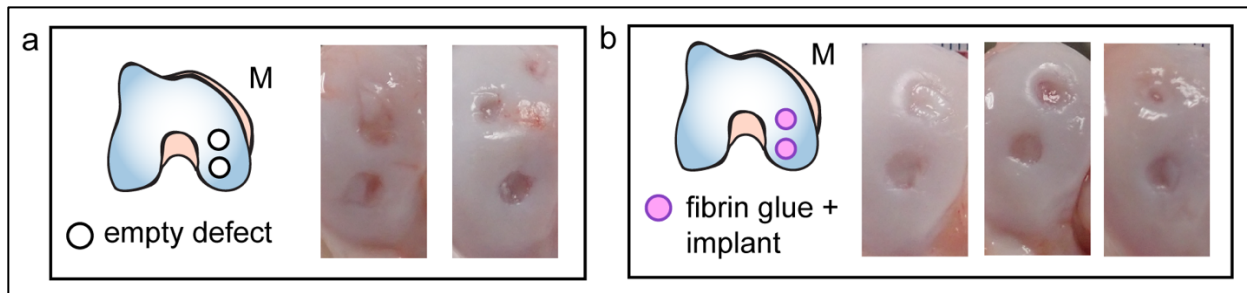produce a local immune response.

FIGURE 6

Figure 6- Surgical Set #2 results: Defect maps for control (a) and treated (b) minipigs are presented and depict the location of defects made and their corresponding treatment. All defects were created with a biopsy punch. **a)** The gross morphology of the minipigs that received no implants show little to no repair tissue in the defects at 8 weeks following surgery. **b)** The gross morphology of the minipigs that received implants show no implant retention in all three minipigs 8 weeks after surgery. However, repair tissue was evident in 2 of the 3 minipigs.

Complete Blood Count (CBC): For comparison between the implant and empty defect

groups, all endpoint CBC values were normalized to their corresponding presurgical values. No

CBC values for the implant group were significantly different from the empty defect group

(Figure 7). For assessment of changes within groups over time, absolute CBC values at t=0 and

t=8 weeks were compared using a student's t-test. 18 out of 20 CBC values remained stable

throughout the duration of the study for the implant group. Red blood cell count was significantly

higher (5.40 ± 0.49 M/µL vs. 4.24 ± 0.26 M/µL; p = 0.02) at t=8 wks than t=0 for the implant group, as was the red blood cell distribution width (RDW) (18.20 ± 0.10% vs. 17.57 ± 0.25%; p = 0.02). One minipig demonstrated substantially elevated monocyte levels, but this was due to a skin infection unrelated to the experimental treatment. All CBC values remained stable over the course of the study for the empty defect group.

Blood phenotyping chemistry panel (BPCP): For comparison between the implant and empty defect groups, all endpoint BPCP values were normalized to their corresponding presurgical values. No BPCP values for the implant group were significantly different from the empty defect group (Figure 8). For assessment of changes within groups over time, absolute BPCP values at t=0 and t=8 weeks were compared using a student's t-test. 14 out of 15 BPCP values remained stable for the duration of the study in the implant group. Alkaline phosphatase significantly increased from t=0 to t=8 weeks (43.70 ± 4.77 U/L vs. 56.00 ± 4.93 U/L; p = 0.04). 14 out of 15 values were unchanged for the empty defect group. Blood urea nitrogen significantly increased from t=0 to t=8 weeks (14.15 ± 0.64 mg/dl vs. 19.70 ± 1.24 mg/dl; p = 0.03).
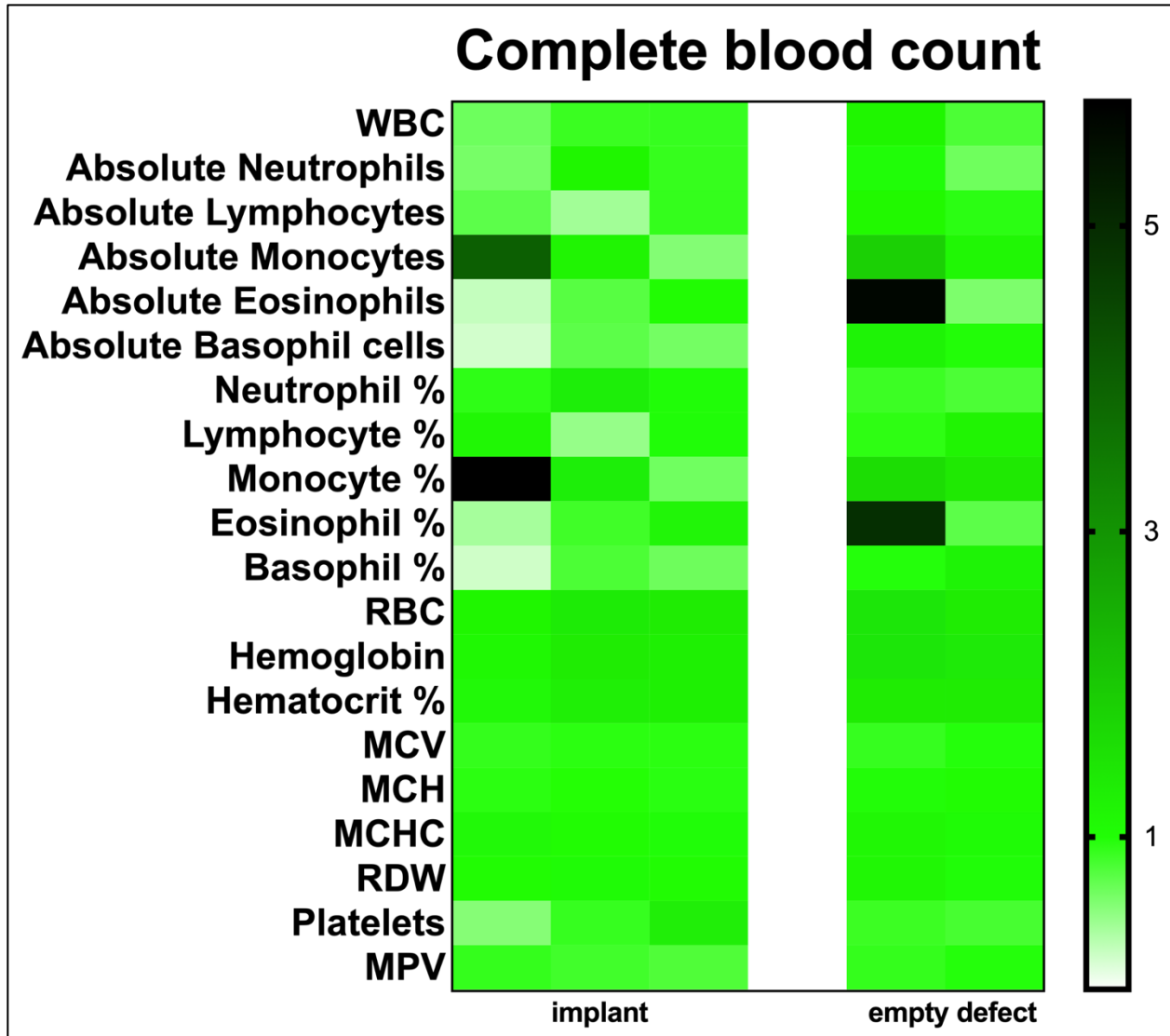
FIGURE 7

Figure 7 - Surgical Set #2 8-week endpoint complete blood count normalized to presurgical values. For each complete blood count measure, there were no significant differences between the implant group and the empty defect group. Abbreviations: WBC, white blood cells; RBC, red blood cells; MCV, mean corpuscular volume, mean corpuscular hemoglobin; MCHC, mean corpuscular hemoglobin concentration; RDW, red cell distribution width; MPV, mean platelet volume
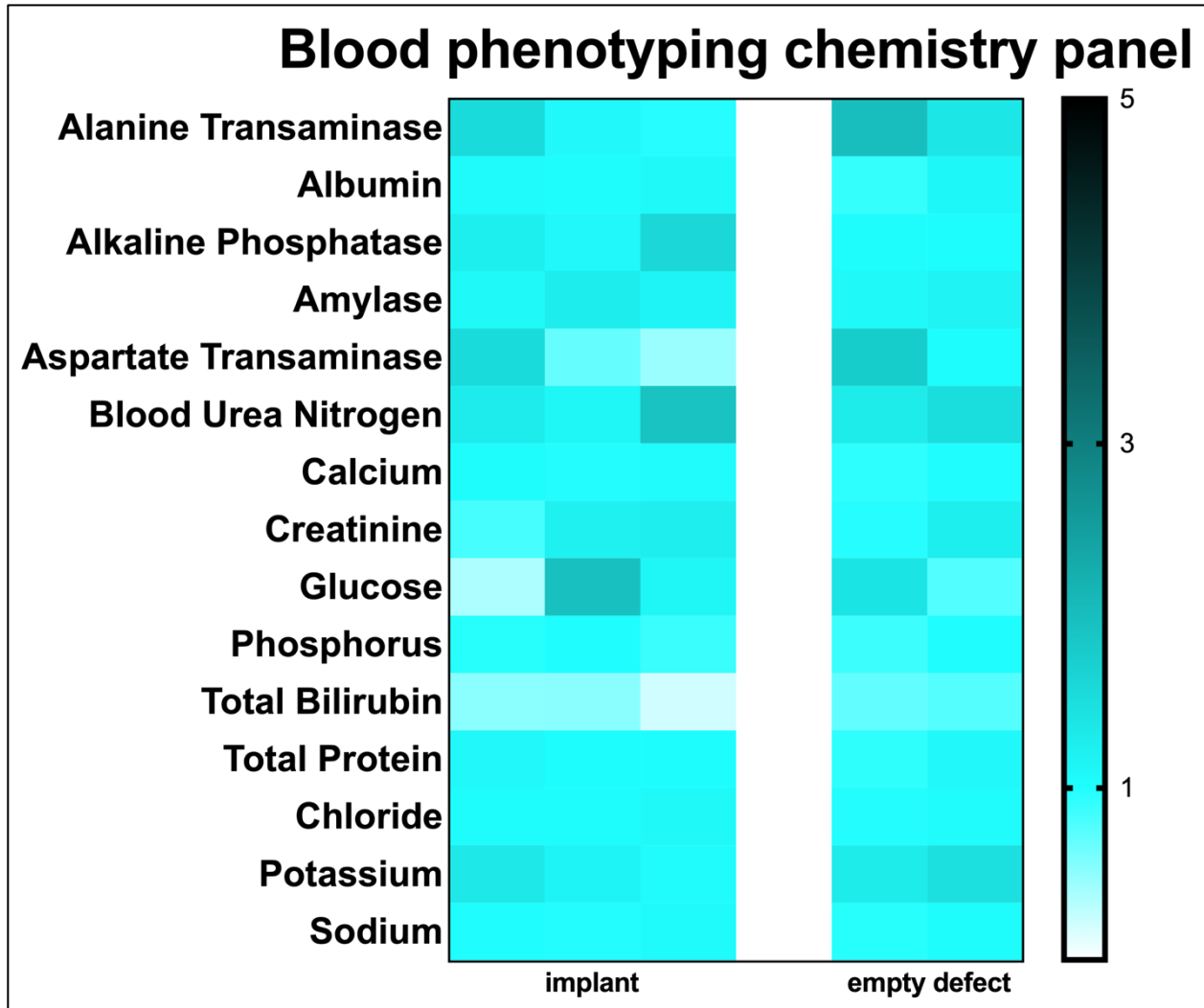
FIGURE 8

Figure 8- Surgical set #2 8-week endpoint blood phenotyping chemistry panel normalized to presurgical values. For each blood phenotyping chemistry measure, there were no differences between the implant group and the empty defect group.

Synovial fluid cytology: Qualitative synovial fluid cytology detected slightly elevated numbers of large non-reactive macrophages and erythrocytes in both implant and empty defect groups. A small number of lymphocytes were also detected in both groups. One minipig in the implant group presented with markedly elevated numbers of large non-reactive macrophages and neutrophils, but this was not observed in the other two minipigs from this group.

Cell culture media contamination testing: The pooled cell culture media sample was negative for all testable contaminants including fungus, bacteria, and mycoplasma.

DISCUSSION

Toward the clinical translation of allogeneic, tissue-engineered neocartilage implants, it is imperative to demonstrate their biocompatibility and safety in preclinical animal models. While it is generally accepted that articular cartilage is an immune-privileged tissue,[3-5] rigorous, preclinical evaluation of the both the local and systemic safety profiles of allogeneic, biologic implants is required by the FDA before proceeding with human clinical trials.[6] Since the ultimate goal of our laboratory is clinical translation of neocartilage implants, the objective of this study was to evaluate the preclinical safety of allogeneic, self-assembled neocartilage implants using the Yucatan minipig animal model. The study was conducted in two separate surgical sets. In Surgical Set #1, all minipigs received multiple implants that were engineered in the same fashion, but were fixed within cartilage defects using three different strategies (microfracture, fibrin, or superficial fibrin). For this set, the hypothesis that implants that remain in place for the duration of the study would not lead to a local immune or inflammatory response was supported by gross morphologic and histopathologic evaluation. In Surgical Set #2, three minipigs received cartilage implants (implant group), while two minipigs served as empty defect, negative control animals (empty defect group). The implant group did not experience a systemic immune response that developed over time, and measures of systemic health did not differ from the empty defect group. The results from these two surgical sets support the notion that self-assembled neocartilage implants are safe and do not lead to adverse local or systemic immune reactions.

The allogeneic neocartilage implants used in this study did not appear to lead to a local immune response in the distal femur articular cartilage of the Yucatan minipig. The integrity of

extracellular matrix (ECM) in the implant was retained, suggesting that there was no degradation of ECM by an immune response and associated catabolic inflammation.[33] The chondrocytic phenotype of cells within the implant was largely maintained, indicating that cells had not dedifferentiated, a process that can be initiated by cytokines released during an immune response.[34, 35] While it appears as though there are some fibroblastic cells on the surface of the implant, the change in phenotype of these cells was likely caused by the presence of fibrin glue used to initially fix this implant in place. Fibrin glue has been shown to lead to dedifferentiation of chondrocytes *in vivo*.[36] Additionally, since these fibroblastic cells were not present around the entirety of the implant, there is no indication of fibrous capsule or foreign body giant cell formation, suggesting that there was no foreign body response.[33, 35] Cells in bone between trabeculae appear to be "basic multicellular units" (BMUs) of osteoclasts and osteoblasts within bone remodeling compartments. This is indicative of normal remodeling following bone injury,[37] which was likely caused during the initial formation of the defect and not by the implant, since BMUs and bone remodeling compartments are visible near the fibrin-only defect site as well as the implant site. Future preclinical work should consider limiting defect depth to the chondral layer to mitigate subchondral bone remodeling. Osteocyte nuclei within lacunae are also clearly visible in trabeculae near both defect sites, suggesting that these cells have not apoptosed nor has the tissue necrosed.[38, 39] Altogether, the integrity of the implant ECM and lack of evidence of a foreign body response suggest that the implants used in this study are safe and do not cause a local immune response.

The implants in this study did not cause a systemic immune response that negatively impacted the health and well-being of the minipigs. In addition to there being no notable differences between the implant and empty defect groups in terms of gait and wellness as evaluated by ULAR veterinary and husbandry staff, there were no significant differences between these two groups for any CBC or BPCP output value. This suggests that the implants

did not cause a chronic, adverse condition in the minipigs. 18 out of 20 complete blood count outcome measures did not significantly change over time for the implant group. For both the implant group and empty defect group, red blood cell content (RBC) and red blood cell distribution width (RDW) increased. For the implant group, RBC and RDW significantly increased by 1.27-fold and 1.04-fold, respectively, while for the empty defect group, RBC and RDW also trended higher by 1.40-fold and 1.06-fold, respectively. This comparable trend suggests that consistent environmental factors that affected both groups of pigs, rather than the implants, were responsible for these changes. In terms of the BPCP results, 14 out of 15 output values did not significantly change over time for the implant group. Alkaline phosphatase levels in the blood did significantly increase by 1.28-fold from t=0 to t=8 wks, but at both timepoints, alkaline phosphatase levels were below the reference value range provided by Exemplar Genetics (43.70 ± 4.77U/L at t=0, 56.00 ± 4.93U/L at t= 8 wks, reference range: 75-167U/L). Since low alkaline phosphatase levels can be caused by malnutrition,[40, 41] it is possible that the observed temporal increase can be attributed to a recovery following the multiple day transportation time from LoneStar Laboratory Swine to UCIMC. In a similar fashion to the CBC and BPCP, the synovial fluid cytology exam did not demonstrate any appreciable, consistent differences between synovial fluid samples from each group, which would have been present in the case of an adverse response within the joint.[42] Ultimately, minipigs that received implants exhibited no concerning systemic changes over time or relative to the empty defect control group.

In conclusion, allogeneic, self-assembled neocartilage implants appear to be safe for use in the Yucatan minipig model, suggesting that an analogous approach in the human would also be safe. Therefore, future preclinical studies conducted by our lab should focus on the efficacy of this approach. First and foremost, a reliable implant fixation strategy is crucial to assessing the efficacy of engineered cartilage implants and must be carefully developed.

Secondarily, while the sling immobilization strategy deployed for Surgical Set #2 seemed to improve minipig recovery from anesthesia, a longer-duration immobilization strategy could work in conjunction with a cartilage fixation strategy to ensure implant retention. Securely fixing the implant and protecting it from mechanical stimuli initially could also allow the C-ABC$_{int}$ treatment to promote long-term integration, stability, and durability.[28] In the end, a study confirming the safety of allogeneic neocartilage implants such as this one was necessary to serve as a foundation for efficacy studies moving forward.

REFERENCES

[1] F. McCormick, J.D. Harris, G.D. Abrams, R. Frank, A. Gupta, K. Hussey, H. Wilson, B. Bach, Jr., B. Cole, Trends in the surgical treatment of articular cartilage lesions in the United States: an analysis of a large private-payer database over a period of 8 years, Arthroscopy 30(2) (2014) 222-6.

[2] B.J. Huang, J.C. Hu, K.A. Athanasiou, Cell-based tissue engineering strategies used in the clinical repair of articular cartilage, Biomaterials 98 (2016) 1-22.

[3] B. Arzi, G.D. DuRaine, C.A. Lee, D.J. Huey, D.L. Borjesson, B.G. Murphy, J.C. Hu, N. Baumgarth, K.A. Athanasiou, Cartilage immunoprivilege depends on donor source and lesion location, Acta Biomater 23 (2015) 72-81.

[4] H.D. Adkisson, C. Milliman, X. Zhang, K. Mauch, R.T. Maziarz, P.R. Streeter, Immune evasion by neocartilage-derived chondrocytes: Implications for biologic repair of joint articular cartilage, Stem Cell Research 4(1) (2010) 57-68.

[5] D.J. Huey, J. Sanchez-Adams, V.P. Willard, K.A. Athanasiou, Immunogenicity of bovine and leporine articular chondrocytes and meniscus cells, Tissue Eng Part A 18(5-6) (2012) 568-75.

[6] Guidance for Industry: Preparation of Investigational Device Exemptions and Investigational New Drug Applications for Products Intended To Repair or Replace Knee Cartilage; Availability, DataStream Content Solutions, LLC, 2012.

[7] J.C. Hu, K.A. Athanasiou, A self-assembling process in articular cartilage tissue engineering, Tissue Eng 12(4) (2006) 969-79.

[8] M.K. Murphy, D.J. Huey, J.C. Hu, K.A. Athanasiou, TGF-beta1, GDF-5, and BMP-2 stimulation induces chondrogenesis in expanded human articular chondrocytes and marrow-derived stromal cells, Stem Cells 33(3) (2015) 762-73.

[9] M.K. Murphy, G.D. DuRaine, A. Reddi, J.C. Hu, K.A. Athanasiou, Inducing articular cartilage phenotype in costochondral cells, Arthritis Res Ther 15(6) (2013) R214.

[10] K.A. Athanasiou, R. Eswaramoorthy, P. Hadidi, J.C. Hu, Self-organization and the self-assembling process in tissue engineering, Annu Rev Biomed Eng 15 (2013) 115-36.

[11] G. Ofek, C.M. Revell, J.C. Hu, D.D. Allison, K.J. Grande-Allen, K.A. Athanasiou, Matrix development in self-assembly of articular cartilage, PLoS One 3(7) (2008) e2795.

[12] B.D. Elder, K.A. Athanasiou, Systematic assessment of growth factor treatment on biochemical and biomechanical properties of engineered articular cartilage constructs, Osteoarthritis and cartilage 17(1) (2009) 114-123.

[13] C.J. Little, N.K. Bawolin, X. Chen, Mechanical properties of natural cartilage and tissue-engineered constructs, Tissue Eng Part B Rev 17(4) (2011) 213-27.

[14] N.J. Gunja, R.K. Uthamanthil, K.A. Athanasiou, Effects of TGF-β1 and hydrostatic pressure on meniscus cell-seeded scaffolds, Biomaterials 30(4) (2009) 565-573.

[15] E.A. Makris, R.F. MacBarb, N.K. Paschos, J.C. Hu, K.A. Athanasiou, Combined use of chondroitinase-ABC, TGF-beta1, and collagen crosslinking agent lysyl oxidase to engineer functional neotissues for fibrocartilage repair, Biomaterials 35(25) (2014) 6787-96.

[16] J.K. Lee, L.W. Huwe, N. Paschos, A. Aryaei, C.A. Gegg, J.C. Hu, K.A. Athanasiou, Tension stimulation drives tissue formation in scaffold-free systems, Nature Materials 16 (2017) 864.

[17] L.W. Huwe, G.K. Sullan, J.C. Hu, K.A. Athanasiou, Using Costal Chondrocytes to Engineer Articular Cartilage with Applications of Passive Axial Compression and Bioactive Stimuli, Tissue Engineering Part A 24(5-6) (2017) 516-526.

[18] M.K. Murphy, D.J. Huey, A.J. Reimer, J.C. Hu, K.A. Athanasiou, Enhancing Post-Expansion Chondrogenic Potential of Costochondral Cells in Self-Assembled Neocartilage, PLOS ONE 8(2) (2013) e56983.

[19] M.K. Murphy, T.E. Masters, J.C. Hu, K.A. Athanasiou, Engineering a fibrocartilage spectrum through modulation of aggregate redifferentiation, Cell transplantation 24(2) (2015) 235-245.

[20] L.M. Panepinto, R.W. Phillips, The Yucatan miniature pig: characterization and utilization in biomedical research, Lab Anim Sci 36(4) (1986) 344-7.

[21] K. Gutierrez, N. Dicks, W.G. Glanzner, L.B. Agellon, V. Bordignon, Efficacy of the porcine species in biomedical research, Front Genet 6 (2015) 293-293.

[22] C.G. Pfeifer, M.B. Fisher, V. Saxena, M. Kim, E.A. Henning, D.A. Steinberg, G.R. Dodge, R.L. Mauck, Age-Dependent Subchondral Bone Remodeling and Cartilage Repair in a Minipig Defect Model, Tissue Eng Part C Methods 23(11) (2017) 745-753.

[23] T. Gotterbarm, S.J. Breusch, U. Schneider, M. Jung, The minipig model for experimental chondral and osteochondral defect repair in tissue engineering: retrospective analysis of 180 defects, Lab Anim 42(1) (2008) 71-82.

[24] N. Vapniarsky, A. Aryaei, B. Arzi, D.C. Hatcher, J.C. Hu, K.A. Athanasiou, The Yucatan Minipig Temporomandibular Joint Disc Structure-Function Relationships Support Its Suitability for Human Comparative Studies, Tissue Eng Part C Methods 23(11) (2017) 700-709.

[25] K.D. Allen, K.A. Athanasiou, Tissue engineering of the TMJ disc: a review, Tissue Eng 12(5) (2006) 1183-96.

[26] E.A. Makris, R.F. MacBarb, D.J. Responte, J.C. Hu, K.A. Athanasiou, A copper sulfate and hydroxylysine treatment regimen for enhancing collagen cross-linking and biomechanical properties in engineered neocartilage, FASEB J 27(6) (2013) 2421-30.

[27] S. Evelia, A. Ashkan, P. Nikolaos, B. Eric, K. Heenam, H. Jerry, A. Kyriacos, Shear stress induced by fluid flow produces improvements in tissue-engineered cartilage, Biofabrication (2020).

[28] J.M. Link, J.C. Hu, K.A. Athanasiou, Chondroitinase ABC Enhances Integration of Self-Assembled Articular Cartilage, but Its Dosage Needs to Be Moderated Based on Neocartilage Maturity, Cartilage (2020) 1947603520918653.

[29] V.C. Mow, S.C. Kuei, W.M. Lai, C.G. Armstrong, Biphasic creep and stress relaxation of articular cartilage in compression? Theory and experiments, J Biomech Eng 102(1) (1980) 73-84.

[30] Animal physiotherapy; assessment, treatment and rehabilitation of animals, Scitech Book News 31(3) (2007).

[31] E. Miquelestorena-Standley, M.L. Jourdan, C. Collin, C. Bouvier, F. Larousserie, S. Aubert, A. Gomez-Brouchet, J.M. Guinebretière, M. Tallegas, B. Brulin, L.R. Le Nail, A. Tallet, F. Le Loarer, J. Massiere, C. Galant, G. de Pinieux, Effect of decalcification protocols on immunohistochemistry and molecular analyses of bone samples, Mod Pathol (2020).

[32] N. Vapniarsky, L.W. Huwe, B. Arzi, M.K. Houghton, M.E. Wong, J.W. Wilson, D.C. Hatcher, J.C. Hu, K.A. Athanasiou, Tissue engineering toward temporomandibular joint disc regeneration, Sci Transl Med 10(446) (2018).

[33] Z. Sheikh, P.J. Brooks, O. Barzilay, N. Fine, M. Glogauer, Macrophages, Foreign Body Giant Cells and Their Response to Implantable Biomaterials, Materials (Basel, Switzerland) 8(9) (2015) 5671-5701.

[34] L. Duan, B. Ma, Y. Liang, J. Chen, W. Zhu, M. Li, D. Wang, Cytokine networking of chondrocyte dedifferentiation in vitro and its implications for cell-based cartilage therapy, American journal of translational research 7(2) (2015) 194-208.

[35] J.M. Anderson, A. Rodriguez, D.T. Chang, Foreign body reaction to biomaterials, Semin Immunol 20(2) (2008) 86-100.

[36] V.J. Bianchi, A. Lee, J. Anderson, J. Parreno, J. Theodoropoulos, D. Backstein, R. Kandel, Redifferentiated Chondrocytes in Fibrin Gel for the Repair of Articular Cartilage Lesions, Am J Sports Med 47(10) (2019) 2348-2359.

[37] L.J. Raggatt, N.C. Partridge, Cellular and molecular mechanisms of bone remodeling, Journal of Biological Chemistry 285(33) (2010) 25103-25108.

[38] X. Feng, J.M. McDonald, Disorders of Bone Remodeling, Annual Review of Pathology: Mechanisms of Disease 6(1) (2011) 121-145.

[39] R.L. Jilka, B. Noble, R.S. Weinstein, Osteocyte apoptosis, Bone 54(2) (2013) 264-71.

[40] D. Lackeyram, C. Yang, T. Archbold, K.C. Swanson, M.Z. Fan, Early Weaning Reduces Small Intestinal Alkaline Phosphatase Expression in Pigs, The Journal of Nutrition 140(3) (2010) 461-468.

[41] J.C. Waterlow, Enzyme changes in malnutrition, Journal of clinical pathology. Supplement (Association of Clinical Pathologists) 4 (1970) 75-79.

[42] E. Gibon, L.A. Córdova, L. Lu, T.-H. Lin, Z. Yao, M. Hamadouche, S.B. Goodman, The biological response to orthopedic implants for joint replacement. II: Polyethylene, ceramics, PMMA, and the foreign body reaction, Journal of biomedical materials research. Part B, Applied biomaterials 105(6) (2017) 1685-1691.
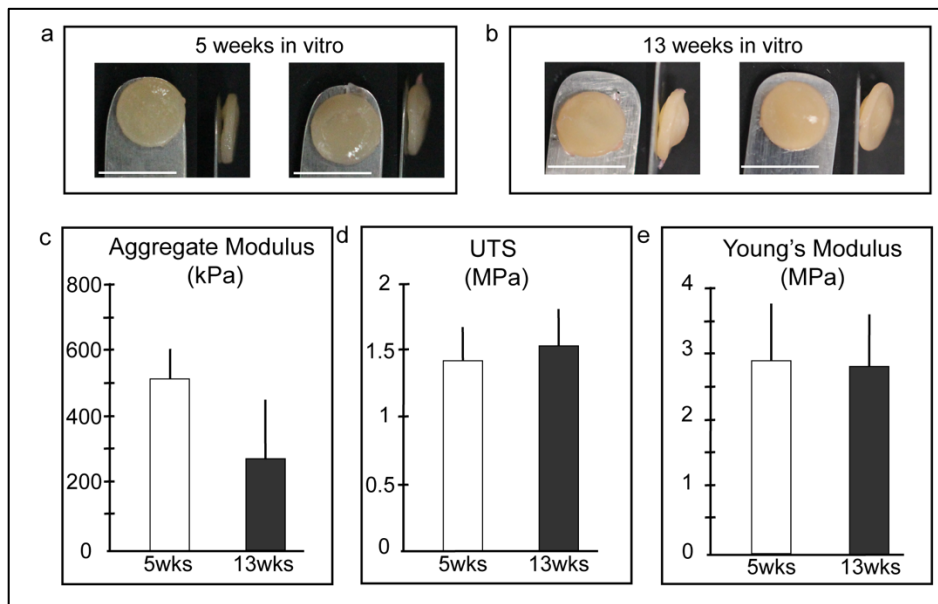
SUPPLEMENTAL DATA

Figure S1- Gross morphology and mechanical properties of self-assembled articular cartilage constructs after 5 weeks and 13 weeks of *in vitro* culture are depicted from Surgical Set #2. **a)** Thick, robust constructs had formed by 5 weeks of *in vitro* culture. **b)** Constructs had developed cysts and abnormal shape by 13 weeks of *in vitro* culture. **c)** Directly prior to implantation (i.e., after 5 weeks of *in vitro* culture), constructs had robust aggregate moduli, but that diminished during further *in vitro* culture. **d,e)** Tensile properties did not change during prolonged *in vitro* culture.

CONCLUSION

This research focuses on driving the translation of neocartilage tissue engineering technologies to clinical applications. Articular cartilage defects and degradation commonly affect the knee joint, and the current clinical treatment options are insufficient in terms of success rate or long-term repair. Tissue engineering of articular cartilage has the potential to transform the current clinical options available to patients suffering from articular cartilage defects and degeneration. Currently, however, the neocartilage constructs being created in laboratories are not as mechanically robust as native articular cartilage in the knee. Although several forms of bioactive factors and mechanical stimulation tactics are used to improve neocartilage extracellular matrix content and mechanical properties, no form of stimulus has improved both compressive and tensile properties to the levels of native articular cartilage. In this work, to achieve neocartilage constructs with robust compressive and tensile properties, the use of fluid-induced shear stress was developed, optimized, and then combined with other strategies proven to increase compressive and tensile properties. The safety of these neocartilage constructs was then assessed *in vivo,* focusing on local and systemic immune responses to neocartilage implantation in the knee of a large animal. Overall, this work takes a tissue engineering strategy for developing robust neocartilage tissue from the laboratory bench to preclinical safety assessments.

To address the issue of creating mechanically robust neocartilage constructs, the use of fluid-induced shear stress on self-assembled neocartilage was developed and optimized. First, a bioreactor capable of administering fluid-induced shear stress was designed. With the use of computational fluid dynamics, it was found that the fluid-induced shear stress bioreactor applied shear stress ranging from 0-0.85Pa on neocartilage constructs, depending on the parameters set. Next, an optimal range of fluid-induced shear stress, 0.05-0.21Pa, was shown to recapitulate native articular cartilage fiber density and improved the compressive modulus

values of neocartilage created from bovine articular chondrocytes by 450%. The exploration of the modes of action of fluid-induced shear stress revealed a mechanosensitive complex on the primary cilia of chondrocytes that is genetically upregulated in neocartilage stimulated with shear stress. Thus, it was determined that fluid-induced shear stress was an effective mechanical stimulation strategy for improving the compressive moduli of neocartilage constructs created with bovine articular chondrocytes.

The translatability of this newly developed fluid-induced shear stress strategy was examined by treating neocartilage made with minipig costal chondrocytes and, separately, human articular chondrocytes. Additionally, neocartilage translatability was investigated via subcutaneous implantation in nude mice. The improvements seen in neocartilage created with bovine articular chondrocytes were replicated when neocartilage created with minipig costal chondrocytes. Mini pig neocartilage yielded improvements in both compressive and tensile stiffness when treated fluid-induced shear stress. Human neocartilage was also found to benefit from the addition of fluid-induced shear stress, with mechanical properties increasing by 72-201% over unstimulated control constructs. Finally, when neocartilage stimulated with fluid-induced shear stress was subcutaneously implanted in mice, the constructs were found to mature *in vivo* and elicited improved in tensile stiffness. These studies determined that fluid-induced shear stress is a mechanical stimulation strategy that can be used to improve neocartilage created with a variety of cell types and can drive neocartilage maturation when implanted *in vivo.*

Fluid-induced shear stress was found to improve compressive moduli to values similar to native articular cartilage (~450-1100kPa). Tensile stiffness and strength was also improved in minipig and human neocartilage, but not near native articular cartilage levels. Thus, the combination of fluid-induced shear stress with other forms of mechanical stimulation and bioactive factors was explored in attempts to achieve neocartilage with both compressive and

tensile properties reaching native articular cartilage values. First, the combination of compression and shear stress yielded enhanced compressive stiffness, but not tensile stiffness or strength. Next, the combination of shear stress and uniaxial tension was investigated. The results from this study revealed that neocartilage stimulated with both shear stress and uniaxial tension produced synergistic enhancements in compressive and tensile stiffness, as well as improved tensile strength. When mechanical stimulation was combined with bioactive factors, it was found that the combination of bioactive factors and fluid-induced shear stress yielded the most mechanically robust neocartilage constructs compared to other groups. Thus, it was determined that prior to implantation, neocartilage should be stimulated with a combination of bioactive factors and fluid-induced shear stress.

This work culminated in the orthotopic implantation of mechanically robust neocartilage created with minipig costal chondrocytes and treated with bioactive factors and fluid-induced shear stress. As per FDA requirements, the large animal, preclinical study presented here intended to assess the local and systemic safety of neocartilage implanted in the femoral condyles of Yucatan minipigs. The neocartilage implants did not elicit local or systemic inflammatory responses in minipigs. In particular, the gross morphology of the native articular cartilage tissue surrounding the surgical defects did not present evidence of degradation or tissue fibrosis. Furthermore, histological staining also did not show evidence of fibrosis or infiltrating immune cells. The systemic immune response was evaluated using complete blood count and blood phenotyping chemistry panels, and did not show differences between animals that received implants and animals that did not receive implants. Overall, the results from the large animal *in vivo* studies lead to the conclusion that there are no adverse local or systemic safety effects of neocartilage implants that are treated with mechanical stimulation and bioactive factors.

Future studies should determine if neocartilage cultured with combined mechanical stimulation strategies will yield mechanical properties that are similar to those cultured with combinations of only bioactive factors. Additionally, a full factorial experimental design involving the combination of bioactive factors, tension stress, and shear stress could lead to a better understanding of diminishing mechanical properties when bioactive factors, tension stress, and shear stress are used. It would also be of value to determine efficient fixation strategies for implants placed in the femoral condyles of large animals, so that the efficacy of neocartilage implants in repairing defects can also be assessed.

Overall, this research is significant because it has elucidated strategies to improve the properties of neocartilage toward native articular cartilage, as well as demonstrated the safety of neocartilage implants in a clinically relevant location in a large animal model. This work is foundational for future preclinical studies because it has presented evidence of both the local and systemic safety of self-assembled, mechanically stimulated, neocartilage implants. With further research, tissue-engineered neocartilage implants have the potential to transform clinical treatment options for patients suffering from articular cartilage defects and degeneration.

APPENDIX A- THE TRIBOLOGY OF CARTILAGE: MECHANISMS, EXPERIMENTAL TECHNIQUES, AND RELEVANCE TO TRANSLATIONAL TISSUE ENGINEERING

ABSTRACT

Diarthrodial joints, found at the ends of long bones, function to dissipate load and allow for effortless articulation. Essential to these functions are cartilages, soft hydrated tissues such as hyaline articular cartilage and the knee meniscus, as well as lubricating synovial fluid. Maintaining adequate lubrication protects cartilages from wear, but a decrease in this function leads to tissue degeneration and pathologies such as osteoarthritis. To study cartilage physiology, articular cartilage researchers have employed tribology, the study of lubrication and wear between two opposing surfaces, to characterize both native and engineered tissues. The biochemical components of synovial fluid allow it to function as an effective lubricant that exhibits shear-thinning behavior. Although tribological properties are recognized to be essential to native tissue function and a critical characteristic for translational tissue engineering, tribology is vastly understudied when compared to other mechanical properties such as compressive moduli. Further, tribometer configurations and testing modalities vary greatly across laboratories. This review aims to define commonly examined tribological characteristics and discuss the structure-function relationships of biochemical constituents known to contribute to tribological properties in native tissue, address the variations in experimental set-ups by suggesting a move toward standard testing practices, and describe how tissue-engineered cartilages may be augmented to improve their tribological properties.

INTRODUCTION

226

Diarthrodial joints, such as the knee, contain hyaline articular cartilage, fibrocartilage, and intra-articular space filled with synovial fluid. Hyaline articular cartilage is a highly hydrated, anisotropic tissue composed primarily of collagen II, proteoglycans, and chondrocytes that covers the ends of long bones and acts as a load-bearing, lubricated surface during joint articulation.(Athanasiou et al., 2017) Fibrocartilage structures, such as the meniscus in the knee, confine motion, dissipate loads, and contribute to essentially frictionless articulation of diarthrodial joints as well. Synovial fluid is confined to the joint space by the articular capsule and contains macromolecular components, such as superficial zone protein (SZP) and hyaluronan, which are essential to joint lubrication.(Jay and Waller, 2014; Noyori et al., 1998) This review will focus on the articular surfaces of hyaline articular cartilage and the knee meniscus, as well as synovial fluid, since they are the components responsible for maintaining low-friction motion and lubrication, or tribological functions, in diarthrodial joints.

Tribology is the study of the interactions between two surfaces moving relative to one another. While it traditionally refers to the study of non-biological materials, tribological principles have been extended to understand the loading environment of diarthrodial joints. The quantitative properties when studying the tribology of diarthrodial joints are surface roughness, R_a, and coefficient of friction, μ. This review will utilize both of these properties for evaluation of tribological properties of the native and engineered tissues described in subsequent sections. A crucial characteristic of native hyaline articular cartilage is its ability to exhibit minimal friction at joint-gliding speeds between 0-0.03m/s when subjected to loads that are five times bodyweight.(Bergmann et al., 1993; Morrell et al., 2005) The replication of tribological properties is crucial to the translation of tissue-engineered articular cartilages, yet they remain under-characterized in tissue-engineered constructs. For instance, a PubMed search for "articular cartilage lubrication" yielded 422 results, but a search for "articular cartilage mechanical properties" produced 1,789 references. Building on some of the tissue-engineering strategies

described in this review to improve the tribological properties of engineered constructs could decrease this discrepancy.

It is predicted that by the year 2050 osteoarthritis, an articular cartilage degeneration disease, will affect at least 130 million people world-wide.(Maiese, 2016) Articular cartilage degeneration causes pain and inflammation of the joint, loss in mechanical function, as well as loss in tribological function. As health care technologies expand and life expectancy in the United States consequently increases, incidences of articular cartilage degeneration will also increase, necessitating viable treatment options such as implantable tissue-engineered articular cartilage constructs with adequate mechanical and tribological properties.

In this review, the components, such as SZP and hyaluronan, and mechanisms, such as shear-thinning of synovial fluid, known to contribute to the tribological properties of articular cartilages will be described. The pathologies that compromise articular cartilage tribological function will also be discussed. Specifically, this review will delve into how surface roughness, coefficient of friction, and lubrication regimes affect and are affected by the state of biochemical components known to regulate tribological function. Tribological properties will be compared quantitatively by looking at the spread of the coefficient of friction obtained across laboratories using a variety of tribometer modalities. Although there is a consensus toward testing articular cartilages under boundary lubrication regimes, variations exist from laboratory to laboratory in terms of tribometer configurations, testing substrates, and lubricants. A recommendation will be made toward reconciling and standardizing tribological measurements for articular cartilages. Therapeutic targeting of tribological properties will be presented and discussed, including the current state of recapitulating tribological properties in tissue-engineered articular cartilages for translation. Finally, the areas of articular cartilage tribology that remain understudied will be presented.

COMMONLY EXAMINED TRIBOLOGICAL CHARACTERISTICS IN CARTILAGE

The two quantitative tribological characteristics measured in both native and engineered articular cartilage are surface roughness and coefficient of friction. In this section, surface roughness and coefficient of friction are defined, and the values of native articular cartilage are presented. Finally, the coefficient of friction and surface roughness of synthetic materials are juxtaposed to native cartilage tribological properties for added context and perspective.

Surface roughness

A common measure of surface roughness, R_a, quantifies asperities on the articulating surface. Surface roughness is derived by measuring the average height deviation from the surface midline and is typically reported in nanometers.(Zappone et al., 2008) Surface roughness ranges from 1-150 nm in native hyaline articular cartilage across the body. In comparison, the femoral head components of total hip replacements typically range from 40-200 nm in surface roughness.(Ghosh and Abanteriba, 2016; Ghosh et al., 2013; Moa-Anderson BJ, 2003)

Coefficient of friction

Coefficient of friction, μ, refers to the ratio of the horizontal force needed to move two surfaces across each other relative to the normal force. Coefficient of friction is the tribological property most studied in the field of articular cartilage. In both native and experimental settings, coefficient of friction is dependent on the articular surface roughness, normal load, lubrication mode, as well as experimental conditions such as testing modality. Coefficient of friction may be determined under static or kinetic conditions. Furthermore, the initial and equilibrium coefficient of friction can also be measured. The coefficients of friction that will be examined in this review were obtained under kinetic, equilibrium conditions in the boundary lubrication regime. The coefficient of friction of native articular cartilage has been reported to range broadly from 0.001-0.45 (Table 1).(Athanasiou et al., 2017; McCutchen, 1962; Middendorf et al., 2017). For

comparison, typical new and cleaned rolling bearings offer a coefficient of friction of 0.005, indicating that articular cartilage can be more frictionless than a man-made bearing under certain conditions.(Woydt and Wäsche, 2010)

TRIBOLOGICAL STRUCTURE-FUNCTION RELATIONSHIPS IN DIARTHRODIAL JOINTS

In this section, the cartilage components that are essential for tribological function are identified. The capacity of lubricin and hyaluronan to modify the tribological characteristics of a diarthrodial joint is described. The importance of the interaction between lubricin and hyaluronan in the synovial fluid is also described and further discussed in the context of different lubrication modes. Lubrication modes, including boundary, mixed, elastohydrodynamic, and hydrodynamic, are defined, and the loading conditions that yield these lubrication modes are also established.

Cartilage components essential for tribological function

Among the components of diarthrodial joints, synovial fluid and the articular cartilage surface, or lamina splendens, play particularly important roles in cartilage lubrication.(Athanasiou et al., 2017) Two key synovial fluid constituents are hyaluronan and SZP.(Majd et al., 2014). Hyaluronan, among other roles, gives rise to the shear-thinning properties of synovial fluid, critical to fluid film lubrication in articulating joints.(Tamer, 2013) Matrix molecules present at the articular cartilage surface, primarily collagen II, can form molecular associations with SZP and hyaluronan in synovial fluid.(Flowers et al., 2017; Majd et al., 2014) These complexes at the cartilage surface create a "sacrificial layer" vital in mediating boundary lubrication.(Chan et al., 2012) Due to their vital functions in mediating cartilage lubrication, SZP and hyaluronan are discussed in more detail below.

Lubricin/SZP/proteoglycan 4: Lubricin, SZP, and proteoglycan 4 (PRG4) are terms often used interchangeably throughout the literature to describe one of the critical lubricants in diarthrodial joints. While each is a product of the *PRG4* gene, they are distinct macromolecules of varying sizes (SZP: 345 kDa, lubricin: 227 kDa, PRG4: 460 kDa).(Peng et al., 2015) However, because it is difficult to distinguish unique functions among them, this review will refer to the products of the *PRG4* gene collectively as SZP. This is a mucinous glycoprotein secreted into synovial fluid by superficial zone chondrocytes and synoviocytes, shown to mitigate superficial zone cartilage damage and chondrocyte death.(Jay and Waller, 2014)

The globular N- and C- termini of SZP can interact with a variety of molecules at the cartilage surface, such as collagen II, fibronectin, and cartilage oligomeric protein to form a lubricating boundary layer.(Flowers et al., 2017; Jay and Waller, 2014) SZP has also demonstrated strong adsorption to denatured, amorphous, and fibrillar collagen II, suggesting its adsorption is not dependent on the conformation of collagen.(Chang et al., 2014) Meniscus surfaces can also benefit from this lubricating layer, because SZP localization at its surface has been observed.(Warnecke et al., 2017) In general, SZP has been shown to reduce coefficients of friction across a variety of tissues and materials.(Chang et al., 2014; Jay and Waller, 2014; Peng et al., 2015) Its function can be further enhanced in the presence of hyaluronan, with which it can interact to form complexes.(Greene et al., 2011)

Hyaluronan: The non-sulfated glycosaminoglycan (GAG) hyaluronan is a large polysaccharide (2000 kDa in diarthrodial joints) that is found both floating freely in synovial fluid and as part of the extracellular matrix of articular cartilage.(Cowman et al., 2015) GAGs are thought to be responsible for interstitial fluid pressurization in articular cartilage, and the depletion of GAGs, in particular hyaluronan, has adverse effects on its frictional and lubricating properties. (Comper and Laurent, 1978; Higaki et al., 1998) For example, gradually removing hyaluronan from a lubricating solution was shown to increase the coefficient of friction of the

native articular cartilage surfaces being examined.(Higaki et al., 1998) Hyaluronan in a matrix is known to act as a viscoelastic material, and, because of its large size, hyaluronan induces steric hindrance that attenuates fluid flow within a solution.(Comper and Laurent, 1978; Šimkovic et al., 2000; Tamer, 2013) Since these properties of hyaluronan contribute to joint tribology, several hyaluronan-based clinical products have been developed to mitigate the symptoms of osteoarthritis.(Sun et al., 2017; Tamer, 2013)

In experimental laboratory settings, hyaluronan has been studied as a joint lubricating agent using cartilage-cartilage, cartilage-steel, and cartilage-glass interactions.(Bell et al., 2006; Higaki et al., 1998; Murakami et al., 1998) Furthermore, hyaluronan alone, and its complexing with SZP, contribute greatly to the shear-thinning behavior of synovial fluid, suggesting that a healthy joint necessitates both hyaluronan and SZP for tribological function.(Greene et al., 2011) Therefore, when studying and characterizing the tribology of diarthrodial joint tissues, both hyaluronan and SZP should be present in the testing solution if one is to expect coefficients of friction approximating *in vivo* values.

Regulation of lubrication modes in diarthrodial joints

The shear-thinning properties of synovial fluid allow it to act as a viscous fluid at low shear rates or sliding speeds.(Ambrosio et al., 1999; Hyun et al., 2002) The loading and shear rates that affect the viscosity of synovial fluid also influence the lubrication mode (boundary or fluid-film) and tribological properties of articulating joints. Because of the inherent porosity of articular cartilage, it is theorized that the articular cartilage "weeps" interstitial fluid into the intra-articular space when pressurized. When in fluid-film lubrication, pressure on the fluid in the intra-articular space drives fluid into the tissue, theoretically "boosting" its mechanical properties.(Lewis and McCutchen, 1959; McCutchen, 1959; Walker et al., 1968) Stribeck curves, such as the one shown in Figure 1, are used to plot the dependence of the coefficient of friction on sliding speed,

applied normal load, and viscosity of the fluid between the sliding surfaces, and illustrate how these parameters determine the mode (i.e., boundary or fluid-film) and regime of lubrication. These lubrication regimes are boundary (Figure 1A), mixed (Figure 1B), elastohydrodynamic (Figure 1C), and hydrodynamic lubrication (Figure 1D), which will be discussed in greater detail below.

Boundary lubrication plays a crucial role in articular cartilage tribology and mediates frictional properties of articular cartilages if the joint is functioning under high loads, low sliding speeds, or high fluid viscosity.(Chan et al., 2010; Gleghorn and Bonassar, 2008) *In vivo* and cadaveric studies have shown that under physiological loads, the pressure distribution and lubrication regimes across the articular cartilage surface are not uniform, and, in areas of high load, articular cartilage surfaces experience boundary lubrication.(McCutchen, 1959) Most studies examining the tribological properties of articular cartilage surfaces conduct measurements under a boundary lubrication regime because of its translational relevance, since this regime interrogates sample properties rather than lubricant properties (Table 1 and Table 2). In the boundary lubrication regime, articular cartilage surfaces are separated by only one or two molecules, known as a sacrificial layer.(Chan et al., 2012) The primary molecules responsible for forming the layer of separation are hyaluronan and SZP, which shelter the articular cartilage surface from high friction.(Neu et al., 2008) Other molecules involved in forming the sacrificial layer are aggrecans and surface-activated phospholipids.(Jahn et al., 2016) This sacrificial layer of molecules lining articular cartilage in boundary lubrication mode is replenished at an equal or higher rate than it is depleted, which maintains a low coefficient of friction on the articular cartilage surface. Studies have shown that in healthy articular cartilage, the boundary lubrication layer would be replenished at least 10 times faster than the development of wear caused by an increase in friction coefficient.(Chan et al., 2012)

Fluid-film lubrication occurs at high articulation speeds or low loads. Fluid-film lubrication can be either elastohydrodynamic or hydrodynamic depending on these loading conditions, but is classified as fluid film lubrication if the interacting articular cartilage surfaces are fully separated by a fluid-film distance larger than the surface roughness of the tissue.(McNary et al., 2012) If the articular cartilage surface is deformed by the fluid-film, then lubrication is considered to be in the elastohydrodynamic regime. Under the elastohydrodynamic regime, joint physiological loads are initially borne by the synovial fluid; the corresponding fluid pressure is then transferred onto the articulating surfaces. In fluid-film mode, the complex formed by SZP and hyaluronan is disassembled because of their weak physical interaction.(Zappone et al., 2008) This allows SZP to float freely in the synovial fluid and disperse evenly throughout the intra-articular space.(Greene et al., 2011)

Pathologies affecting diarthrodial joint tribology

Conditions that can induce cartilage degeneration and, consequently, a reduction in tribological properties, include congenital disorders, wear and tear, traumatic injury, and inflammation. One congenital disease with particular relevance to cartilage lubrication is camptodactyly-arthropathy-coxa vara-pericarditis (CACP) syndrome, caused by a mutation in the *PRG4* gene.(Jay and Waller, 2014) Inherited in an autosomal recessive fashion, affected patients exhibit non-inflammatory, juvenile-onset joint failure, suggesting SZP is necessary for joint health and function.(Marcelino et al., 1999) The ability of SZP to rescue function in tissues affected by CACP has been tested *in vitro* using bovine articular cartilage.(Waller et al., 2013) These explants demonstrated a boundary mode friction coefficient of 0.04 when lubricated with synovial fluid taken from patients with CACP (i.e., lacking functional SZP). When SZP was added to the CACP synovial fluid, however, the coefficient of friction dropped to 0.005. Thus, functional SZP appears to be a critical regulator of cartilage lubrication.

In addition to genetic conditions, general wear and tear of the articular surface can lead to local collagen depletion, one of the first stages of osteoarthritis.(Grenier et al., 2014) Superficial collagen loss likely depletes the cartilage surface of key boundary lubrication components, such as SZP, hyaluronan, and binding domains, and can increase surface roughness, potentially furthering the progression of osteoarthritis.(Coles et al., 2010; Jay et al., 2007) Differences in gross morphology, biochemical content, and mechanical properties between healthy and diseased cartilages are depicted in Figure 2. Healthy human femoral head articular cartilage has demonstrated a boundary mode coefficient of friction of 0.119, whereas early osteoarthritic tissue and advanced osteoarthritic tissue had friction coefficients of 0.151 and 0.409, respectively.(Park et al., 2014) Values were determined using atomic force microscopy (AFM), thus surface roughness was simultaneously measured. The increase in friction coefficients with osteoarthritis progression correlated with higher tissue surface roughness, as it was determined healthy, early osteoarthritic, and advanced osteoarthritic tissue each had a surface roughness of 104, 382, and 537 nm, respectively. These findings indicate osteoarthritis progression is closely related to deteriorating cartilage lubrication.

Traumatic injury often induces post-traumatic osteoarthritis, a condition that can inhibit the lubrication of articular cartilages. For example, in an equine injury model, synovial fluid hyaluronan concentration and molecular weight decreased following the injury, which impacted the fluid's lubrication abilities. The boundary mode friction coefficient of bovine articular cartilage tested in healthy equine synovial fluid was 0.026, whereas it was 0.036 when tested with synovial fluid from injured horses.(Antonacci et al., 2012)

Inflammatory pathways can also be activated by traumatic injury and osteoarthritis, leading to the upregulation of inflammatory cytokines such as interleukin-1β (IL-1β), known to adversely affect lubrication of articular cartilage.(Gleghorn et al., 2009) In an *in vitro* study, 48-hour IL-1β treatment of bovine cartilage explants increased the boundary mode equilibrium

coefficient of friction from 0.26 to 0.36. It has also been shown that an important regulator of cartilage lubrication and superficial zone maintenance is epidermal growth factor receptor (EGFR). In an animal study, EGFR-deficient mice developed early cartilage degeneration and demonstrated little to no hyaluronan and SZP localization at the cartilage surface.(Jia et al., 2016) In bovine articular cartilage explants, transforming growth factor alpha (TGF-α), known to activate EGFR-signaling, led to nearly a six-fold increase in *PRG4* mRNA and a 28% reduction in the explant friction coefficient. Thus, if EGFR-signaling is disrupted in articular cartilage, for instance through upregulation of IL-1β, key lubrication components, tissue tribological properties, and overall tissue health can be damaged.(Jia et al., 2016; Sanchez-Guerrero et al., 2012) In general, regardless of the mechanism of depletion, a lack of boundary lubricant will increase frictional forces in the superficial zone of articular cartilage, potentially leading to deregulated chondrocyte metabolism, apoptosis, and degeneration.(Waller et al., 2013)

METHODS FOR QUANTIFYING TRIBOLOGICAL PROPERTIES

In this section, methods for quantifying tribological properties are listed and discussed. The most commonly used tribometer configurations, pin-on-disc, pin-on-plate, and rolling-ball-on-disc, for articular cartilage are described and compared. The use of atomic force microscopy to quantify surface roughness is also included. Because different testing configurations can lead to disparities in coefficient of friction and surface roughness values, suggestions for standardized practices are also presented.

Tribometers

A tribometer quantifies tribological properties, such as coefficient of friction. There are many different tribometer configurations across engineering, but the most popular in articular cartilage research are pin-on-disc, pin-on-plate, and rolling-ball-on-disc (Figure 3). Regardless of the configuration, all tribometers aim to measure the properties of two materials rubbing against each other and the effectiveness of lubricants between them. Usually, articular cartilages are

tested against a substrate of either stainless steel or glass, with lubricants ranging from phosphate buffered saline (PBS) solution to fetal bovine serum. To showcase the multitude of ways tribological properties are studied, Table 1 and Table 2 compare recent tribology studies on hyaline articular cartilage, as well as the knee meniscus, by describing sample types, tribometer configurations, substrates, and lubricants. In particular, Table 1 demonstrates how these experimental methodological variations yield large discrepancies in the coefficient of friction of native articular cartilages. For example, quantifying coefficient of friction by using cartilage-on-cartilage will yield lower values compared to using glass-on-cartilage.(Warnecke et al. 2017) Furthermore, the testing solution also has an effect on coefficient of friction, such as BSF yielding lower values compared to PBS.(Schmidt et al. 2007) It is emerging that having a standard practice of quantifying coefficient of friction of native and engineered articular cartilage would be useful in facilitating comparisons between laboratories. For instance, this standard method could involve a pin-on-plate or pin-on-disc tribometer configuration with the tissue submerged in PBS under boundary lubrication.

Pin-on-disc/plate: The pin-on-disc and pin-on-plate tribometer configurations are the most popular amongst articular cartilage research groups. Usually, they contain an acrylic pin to which articular cartilage samples may be glued and then placed in contact with a substrate (Figure 3A and Figure 3B).(Bonnevie et al., 2014; Kanca et al., 2018a; Shi et al., 2011) The disc or plate substrate, generally made of glass or stainless steel, is completely submerged in a lubricating fluid, such as PBS, for testing. Adjustable weights are used to apply a known normal force on the articulating surfaces. A strain gauge, or other force sensor types, is used to measure the friction force of the sample as the disc or plate rubs against it. Boundary lubrication mode should be the lubrication modality used for this tribometer configuration to ensure that the properties that are observed reflect the properties of the sample against the substrate. If

identification of the lubrication properties of a solution is desired, both boundary and fluid-film lubrication studies should be performed to fully characterize the lubricant.

Rolling-ball-on-disc: Tribometers may also take the form of a rolling-ball-on-disc (Figure 3C). In this configuration, both the ball and the disc can be driven independently allowing for a variety of kinematic conditions.(Nečas et al., 2018) This configuration is generally used to test the interaction of substrates used in total knee replacements and is useful for testing the wear characteristics of plastic inserts and metal components in synthetic joint replacements over time. Although useful for certain applications, the rolling-ball-on-disc tribometer does not feasibly allow the testing of a small articular cartilage tissue sample. Ball-on-disc tribometers, although rarely used, also exist and differ from rolling-ball-on-disc tribometers in that the ball is used to translate against a sample without rolling.(Blum and Ovaert, 2013; Grad et al., 2012)

Atomic force microscopy

AFM is capable of surface imaging and force measurements at the nanoscale, making this approach valuable for measuring tribological properties such as surface roughness and "microscale" coefficient of friction.(Park et al., 2004) Through the use of AFM, it has been found that the surface roughness, R_a, of immature bovine articular cartilage is around 72 nm.(Moa-Anderson BJ, 2003) AFM is particularly useful for testing tribological properties occurring under boundary lubrication because of its ability to operate at single asperity, high pressure contact.(Chan et al., 2010) However, studies have shown that AFM tip size and scan size affect surface roughness measurements.(Sedin and Rowlen, 2001) Therefore, when presenting AFM measurements for surface roughness, it is also important to report the tip size and scan size, as well as a native tissue measurement with the same tip size and scan size, for comparison.

TOWARD ENGINEERING NATIVE TRIBOLOGICAL PROPERTIES

Because adequate lubrication is vital for diarthrodial joint health and function, various strategies to engineer biomimetic tribological properties for both native tissue and engineered constructs have been explored. Approaches include the development of biolubricants to alter both fluid-film and boundary lubrication, low-friction scaffolds, as well as bioactive factors and mechanical stimulation regimens that promote endogenous lubrication mechanisms.

Biolubricants

Biolubricants can augment boundary lubrication properties by binding to articular cartilage to replace components often depleted in damaged or degenerated articular cartilage, such as GAGs. For example, hyaluronan-binding peptides were attached to cartilage via heterobifunctional polyethylene glycol (PEG) chains to recruit hyaluronan from solution to the cartilage surface.(Singh et al., 2014) This strategy significantly decreased coefficients of friction in both healthy and osteoarthritic cartilage explants by ~50% relative to control conditions (i.e., PBS as the lubricant) and could be retained in the rat joint for at least 72 hours, much longer than hyaluronan alone. Importantly, in osteoarthritic cartilage explants, high concentration of hyaluronan in the testing solution did not reduce friction coefficients relative to the hyaluronan-binding system applied to the same tissue type, indicating that even low levels of hyaluronan, when bound to a surface, can improve lubrication properties.(Singh et al., 2014) Samples in this study were tested in a pin-on-disc (in this case, tissue-on-tissue) configuration within the boundary lubrication regime.

There are already clinically available hyaluronan-based biolubricants, or viscosupplements, such as Artz®, Healon®, Hyalgan®, Opegan®, Opelead®, Orthovisc®, and Synvisc-One®.(Sun et al., 2017; Tamer, 2013) While some patients experience a transient improvement in their osteoarthritis symptoms after treatment, evidence is lacking to demonstrate the clinical efficacy and disease-modifying ability of these injections.(Henrotin et

al., 2018) In a similar context, modified, recombinant SZP as an intra-articular injection has been investigated preclinically in a rat osteoarthritis model.(Flannery et al., 2009) 1 week following osteoarthritis induction, SZP injections were administered for 4 weeks before animal sacrifice, significantly improving total joint scores and reducing cartilage degeneration. Like hyaluronan viscosupplementation, however, the long-term clinical efficacy of SZP injections remains to be elucidated.

In another study, a poly(glutamic acid) backbone (PGA) was modified with poly(2-methyl-2 oxazoline) (PMOXA) and hydroxybenzaldehyde (HBA) to create a graft copolymer (PGA-PMOXA-HBA) that mimics the boundary lubrication properties of SZP and hyaluronan.(Morgese et al., 2018) PGA-PMOXA-HBA is designed to bind to damaged articular cartilage to provide a boundary lubrication layer and prevent cytokine penetration into the tissue. Tested in a rolling-ball-on-disc configuration within the boundary lubrication regime, certain PGA-PMOXA-HBA formulations were able to reduce friction coefficients of damaged articular cartilage (around 0.14) to levels exhibited by healthy articular cartilage (less than 0.06).(Morgese et al., 2017) Furthermore, PGA-CPMOXA-HBA prevented chondroitinase ABC-mediated and collagenase-mediated digestion of GAGs and collagen, respectively.(Morgese et al., 2018) Another technique involved an interpenetrating polymer network (IPN) designed to mimic GAGs lost during osteoarthritis progression. IPN includes a GAG-inspired zwitterionic polymer 2-methacryloyloxyethyl phos-phorylcholine (pMPC) that is photopolymerized *in situ* and decreased friction coefficients in bovine articular cartilage by 24% relative to untreated controls in a pin-on-disc configuration under fluid-film lubrication mode.(Cooper et al., 2017) These and other lubricants can reduce friction at the cartilage interface, however comparing absolute values from each study is difficult because the testing modality and lubrication mode vary broadly. Furthermore, it is possible that achieving a clinically effective strategy may require an approach that focuses more specifically on boundary lubrication of articular cartilage.

<u>Scaffolds</u>

Articular cartilage synthetic scaffold design criteria tend to focus on mechanical properties; however, some scaffolds have been developed with greater emphasis on improving tribological properties (Table 2). In one study, biodegradable polyvinyl alcohol (PVA) polymer hydrogels were functionalized with a carboxylic acid derivative boundary lubricant molecule and reduced friction coefficients up to 70% relative to unfunctionalized PVA scaffolds.(Blum and Ovaert, 2013) Furthermore, functionalized PVA hydrogels demonstrated friction coefficients that resembled those of native cartilage. Friction tests were conducted in a ball-on-disc configuration within the boundary lubrication mode. PVA/polyvinyl pyrrolidone (PVP) blend hydrogels have also been tested against articular cartilage across lubrication modes and demonstrated average coefficients of friction between 0.12 and 0.14, which were close to cartilage-on-cartilage interaction (0.03) and much lower than cartilage-on-stainless steel articulation (0.46).(Kanca et al., 2018b) Interestingly, increasing hydrogel compressive modulus was highly correlated to coefficient of friction, likely due to lower congruence in stiffer hydrogels.

In a combinatorial approach, infiltration of a 3D-woven polycaprolactone scaffold with an alginate/polyacrylamide hydrogel created a composite scaffold that significantly reduced the boundary lubrication coefficient of friction from 0.64 for the scaffold alone to 0.28.(Liao et al., 2013) A tissue-engineered cartilage implant that replicates NeoCart® demonstrated a decreasing boundary mode coefficient of friction throughout 7 weeks of culture (0.40 at week 0 to 0.24 at week 7).(Middendorf et al., 2017) The coefficient of friction of constructs from week 3 of culture onward was not statistically different than healthy human cartilage (0.22) tested in the same pin-on-plate configuration using PBS as the test solution. This study is one of the first to assess the *in vitro* boundary lubrication tribological properties of an engineered articular cartilage product that has been investigated in a clinical trial. These characterizations are imperative for articular cartilage scaffolds that will be used *in vivo*.

Studying tribological properties for meniscal replacements is also of paramount importance. While hyaline articular cartilage has generally been a focus for scaffold strategies to improve diarthrodial joint lubrication, some scaffolds for meniscus replacement have also incorporated tribological properties as design criteria. Toward engineering lubrication in menisci, a silk fibroin scaffold that could potentially be used for meniscus replacement was developed. The friction coefficients of the scaffold tested against femoral cartilage (0.056) were significantly higher than native articular cartilage (0.014) and meniscus (0.021) controls tested against femoral articular cartilage.(Warnecke et al., 2017)

According to requirements for meniscus replacements described previously,(Rongen et al., 2014) a coefficient of friction of 0.056 for the scaffold against femoral articular cartilage could be within the range of acceptable tribological properties for meniscus replacements.(Warnecke et al., 2017) It should be noted that these values are dependent upon many factors such as the experimental setup, thus any comparisons to native tissue should only be made within the same testing modality, lubrication mode, and tissue type.

One meniscus replacement that was tested *in vivo* consisted of a porous polyurethane scaffold implanted into sheep to augment meniscus repair after partial meniscectomy. After 6 months *in vivo*, the boundary lubrication mode coefficient of friction of engineered meniscus (~0.35), tested in a pin-on-plate configuration, was not significantly different from either contralateral or adjacent healthy meniscus tissue, suggesting that the polyurethane scaffold was able to promote biomimetic neotissue formation.(Galley et al., 2011) Biomaterial scaffolds have been developed with coefficient of friction as a design criterion, but it is difficult to compare them to each other due to varying testing modalities. In general, the lack of meniscus tribology research is even more acute than for hyaline articular cartilage.

Bioactive factors

Bioactive factors, or molecules with an effect on cell behavior or extracellular matrix structure, that can enhance the tribological properties of native and engineered articular cartilages have been explored. Synoviocytes and superficial zone chondrocytes are known to endogenously produce SZP.(Peng et al., 2014) It has been demonstrated that TGF-β1 increased SZP secretion in superficial zone chondrocytes seeded in monolayer, identifying it as a bioactive factor of interest.(Iwasa and Reddi, 2017) Combined treatment of synovium explants with TGF-β1 and bone morphogenetic protein 7 (BMP-7) further improved SZP secretion.(Iwakura et al., 2013)

An increase in SZP secretion does not always cause a decrease in tissue friction coefficients, as SZP must be retained at the cartilage surface to improve boundary lubrication.(Peng et al., 2016) To improve retention of SZP in engineered cartilage, native superficial zone cartilage extract, which likely contains binding macromolecules for SZP, was added to the culture media of self-assembled articular cartilage. Groups treated with a low concentration of extract demonstrated greater SZP staining and a boundary mode coefficient of friction of 0.03, which was significantly lower than the coefficient of friction of self-assembled cartilage cultured in the absence of superficial zone cartilage extracts (0.10).(Peng et al., 2016) Combining superficial zone extract with growth factors such as TGF-β1 and BMP-7 could further enhance tribological properties.

Another growth factor of interest is insulin-like growth factor I (IGF-1). IGF-1 led to SZP localization at the surface of a collagen I gel seeded with meniscal fibrochondrocytes after 20 days in culture. This treatment resulted in a boundary friction coefficient of 0.22, which was not statistically different from the native tissue value of 0.2. Gels not stimulated with IGF-1, however, had a coefficient of friction of 0.29, which was significantly greater than the native

tissue value.(Bonnevie et al., 2014) In another study, increasing the proportion of mesenchymal stem cells seeded with fibrochondrocytes led to a dose-dependent increase in SZP deposition on collagen I gels, which was matched by a decrease in coefficients of friction.(Bonnevie et al., 2016) The correlation between SZP deposition and coefficient of friction had an R^2 value of 0.80.

This suggests that MSCs not only produce SZP, but could produce SZP-binding factors that could be further investigated to improve SZP retention in native and engineered tissues. Bioactive factors to improve cartilage lubrication remain largely unexplored compared to bioactive factors used to improve other mechanical properties such as compressive moduli.

Mechanical stimulation

Mechanical stimulation, when applied at physiologic levels, has led to improvements in tissue-engineered cartilage lubrication. For example, a joint-mimicking loading system was applied to cell-seeded fibrin/hyaluronan composite gels. This biomimetic load increased SZP surface localization, suggesting enhancement of the construct surface, but quantitative tribological properties were not reported in this study.(Park et al., 2018) In a separate study, chondrocyte-seeded polyurethane scaffolds were subjected to dynamic compression and sliding surface motion by a ceramic ball, which also led to SZP localization at the surface of the construct. Additionally, constructs subjected to both sliding and compression exhibited a reduced coefficient of friction (0.251), compared to unloaded controls (0.681) and constructs only stimulated in compression (0.427).(Grad et al., 2012)

Hydrostatic pressure, known to increase collagen synthesis and tensile properties in self-assembled articular cartilage, has also been investigated as a mechanical stimulus to enhance cartilage tribological properties.(Murphy et al., 2013) Self-assembled constructs treated with TGF-β1 and chondroitinase-ABC (C-ABC) were subjected to 10 MPa of continuous

hydrostatic pressure from days 10 to 14 of culture for 1 hr per day. These constructs demonstrated increased SZP staining compared to constructs stimulated with TGF-β1 and C-ABC alone. Since coefficient of friction was not examined in this study, hydrostatic pressure as a method to improve tribological properties merits further investigation.

Supplementing culture media with factors found in synovial fluid, such as hyaluronan, can further replicate physiologic conditions during loading and have an impact on tribological properties. Indeed, mechanically stimulated, chondrocyte-seeded polyurethane scaffolds produced significantly more *PRG4* mRNA and SZP when culture medium was supplemented with hyaluronan.(Wu et al., 2017) This indicates that not only does hyaluronan have lubricating properties, but it also can regulate cellular behavior to promote better tribological properties. However, this study did not examine the functional impact of greater SZP content on construct tribological properties. These studies suggest that mechanical stimulation techniques should be further investigated toward improving lubrication of engineered constructs.

PERSPECTIVES

When articular cartilages are described, load-bearing capacity and nearly frictionless surfaces are presented as key characteristics. However, in many studies of tissue-engineered cartilages, mechanical properties are investigated while tribological properties are rarely explored. To augment the translatability of tissue-engineered cartilages, both mechanical and tribological functions should be considered as release criteria for cartilage implants. Because the FDA has guidelines for mechanical testing of engineered articular cartilages, we suggest that analogous guidelines be created for tribological properties.

Tissue-engineered articular cartilages must exhibit biomimetic mechanical properties, otherwise they will likely fail under repeated loads. *In vivo* durability is also of concern; therefore, tribological properties of engineered articular cartilages are also crucial because poor lubrication

contributes to tissue degeneration.(Coles et al., 2010; Jay et al., 2007; Jia et al., 2016; Park et al., 2014) Indeed, if gross morphology, biochemical content, or mechanical properties are negatively impacted by insufficient lubrication, articular cartilages could degenerate in each of these aspects.

The tribological properties of native articular cartilages have yet to be defined, due to variability in testing conditions. A standardized tribological testing protocol, such as testing tissue bathed in PBS in a pin-on-plate configuration within the boundary lubrication regime, would be ideal to facilitate interlaboratory comparisons. If limitations exist that prevent adoption of this standardized assay, incorporating native tissue controls when performing tribological testing of engineered cartilages would provide a better indication of translational potential.

Of the two articular cartilages discussed in this review, the tribological properties of the knee meniscus remain relatively understudied, even though meniscus lubrication is vital for diarthrodial joint health. For example, a PubMed search for "knee meniscus tribology" returned 8 results, whereas a PubMed search for "articular cartilage tribology" returned 47 references. While this disparity is stark, both fields would benefit from increased research.

A well-defined understanding of the tribology of native cartilages can provide design criteria for tissue-engineering efforts. Using that understanding to engineer clinically applicable implants should be the aim of cartilage researchers. Achieving biomimetic tribological properties in engineered articular cartilages will be crucial to the translational success of these approaches.

TABLES

TABLE 1

Coefficients of friction (μ) for native articular cartilage and meniscus in the boundary lubrication regime

Tissue type	Species	Modality	Substrate	Lubricant	μ*	Reference
AC	ovine	pin-on-plate	stainless steel	FBS	0.46	(Kanca et al., 2018b)
AC	ovine	pin-on-plate	AC	FBS	0.03	(Kanca et al., 2018b)
AC	human	pin-on-plate	glass	PBS	0.22	(Middendorf et al., 2017)
AC	porcine	pin-on-plate	glass	SF	0.001-0.11	(McCutchen, 1962)
AC	bovine	ball-on-disc	glass	N/A	0.19	(Blum and Ovaert, 2013)
AC	bovine	rolling-ball-on-disc	glass	PBS	0.12-0.16	(Jia et al., 2016)
AC	bovine	ball-on-disc	glass	N/A	0.121	(Grad et al., 2012)
AC	bovine	pin-on-plate	stainless steel	PBS	0.025	(Moore and Burris, 2015)
AC	bovine	pin-on-plate	glass	PBS	0.13	(Oungoulian et al.,

AC	bovine	pin-on-plate	CoCr HC	PBS	0.15	(Ougoulian et al., 2015)
AC	bovine	pin-on-plate	CoCr LC	PBS	0.13	(Ougoulian et al., 2015)
AC	bovine	pin-on-plate	stainless steel	PBS	0.24	(Ougoulian et al., 2015)
AC	bovine	pin-on-disc	glass	PBS	0.069-0.13	(Peng et al., 2015)
AC	bovine	annulus-on-disc[+]	AC	PBS	0.24	(Schmidt et al., 2007)
AC	bovine	annulus-on-disc[+]	AC	BSF	0.028	(Schmidt et al., 2007)
AC	bovine	disc-on-disc[+]	AC	PBS	0.08	(Waller et al., 2013)
AC	bovine	disc-on-disc[+]	AC	CACP-SF	0.04	(Waller et al., 2013)
AC	bovine	disc-on-disc[+]	AC	HSL	0.03	(Waller et al., 2013)
AC	bovine	disc-on-disc[+]	AC	HSF	0.01	(Waller et al., 2013)
AC	bovine	disc-on-disc[+]	AC	CACP-	0.005	(Waller et al.,

				SF+HSL		2013)
AC	bovine	pin-on-plate	AC	BSF	0.014	(Warnecke et al., 2017)
AC	bovine	pin-on-plate	glass	BSF	0.215	(Warnecke et al., 2017)
meniscus	bovine	pin-on-plate	glass	PBS	0.17-0.24	(Bonnevie et al., 2014)
meniscus	bovine	pin-on-plate	glass	PBS	0.20	(Bonnevie et al., 2016)
meniscus	bovine	pin-on-plate	glass	PBS	0.032	(Peng et al., 2015)
meniscus	bovine	pin-on-plate	AC	BSF	0.021	(Warnecke et al., 2017)
meniscus	bovine	pin-on-plate	glass	BSF	0.10	(Warnecke et al., 2017)
meniscus	ovine	pin-on-plate	glass	PBS	0.25-0.3	(Galley et al., 2011)
meniscus	ovine	pin-on-plate	glass	ESF	0.09-0.14	(Galley et al., 2011)

Abbreviations. AC: articular cartilage; BSF: bovine synovial fluid; CACP-SF: camptodactyly-arthropathy-coxa vara-pericarditis syndrome synovial fluid; CoCr LC: cobalt chromium low carbon; CoCr HC: cobalt chromium high carbon; ESF: equine synovial fluid; FBS: fetal bovine

serum; HSF: human synovial fluid; HSL: human superficial zone protein; PBS: phosphate buffered saline; SF: synovial fluid;

*Boundary lubrication, average, equilibrium, kinetic coefficient of friction (µ) Tribological testing modalities analogous to pin-on-disc

TABLE 2

Coefficients of friction (µ) for engineered articular cartilage and meniscus in the boundary lubrication regime

Construct type	Species	Modality	Substrate	Lubricant	µ*	Reference
cell-seeded AC scaffold (polyurethane)	bovine	ball-on-disc	glass	N/A	0.251-0.681	(Grad et al., 2012)
scaffold-free AC	bovine	pin-on-disc	glass	PBS	0.08-0.17	(Peng et al., 2014)
scaffold-free AC	bovine	pin-on-disc	glass	PBS	0.02-0.10	(Peng et al., 2016)
cell-seeded AC scaffold (collagen I)	human	pin-on-plate	glass	PBS	0.24	(Middendorf et al., 2017)
scaffold-free AC	leporine	pin-on-plate	glass	PBS	0.05-0.1	(Whitney et al., 2015)
scaffold-free AC	leporine	pin-on-plate	glass	PBS	0.05-0.38	(Whitney et al., 2017)
acellular AC construct (PCL scaffold with Alg/PAAm IPN	synthetic	pin-on-plate	stainless steel	PBS	0.28	(Liao et al., 2013)

hydrogel)

acellular AC hydrogel (PVA/PVP)	synthetic	pin-on-plate	AC	FBS	0.12-0.14	(Kanca et al., 2018b)
acellular AC hydrogel (PVA)	synthetic	ball-on-disc	glass	N/A	0.27-0.93	(Blum and Ovaert, 2013)
cell-seeded meniscus scaffold (collagen I)	bovine	pin-on-plate	glass	PBS	0.21-0.48	(Bonnevie et al., 2014)
cell-seeded meniscus scaffold (collagen I)	bovine	pin-on-plate	glass	PBS	0.15-0.33	(Bonnevie et al., 2016)
Acellular meniscus scaffold (collagen I)	synthetic	pin-on-plate	glass	PBS	0.38	(Bonnevie et al., 2016)
acellular meniscus scaffold (silk)	synthetic	pin-on-plate	AC	BSF	0.056	(Warnecke et al., 2017)
acellular meniscus scaffold (silk)	synthetic	pin-on-plate	glass	BSF	0.446	(Warnecke et al., 2017)
in vivo meniscus scaffold (polyurethane)	synthetic	pin-on-plate	glass	PBS	0.35-0.45	(Galley et al., 2011)
in vivo meniscus scaffold (polyurethane)	synthetic	pin-on-plate	glass	ESF	0.12-0.18	(Galley et al., 2011)

Abbreviations. AC: articular cartilage; Alg/PAAm IPN: alginate polyacrylamide interpenetrating network; BSF: bovine synovial fluid; ESF: equine synovial fluid; PBS: phosphate buffered saline; PCL: polycaprolactone; PVA: polyvinyl alcohol; PVP: polyvinylpyrrolidone;

*Boundary lubrication, average, equilibrium, kinetic coefficient of friction (μ)
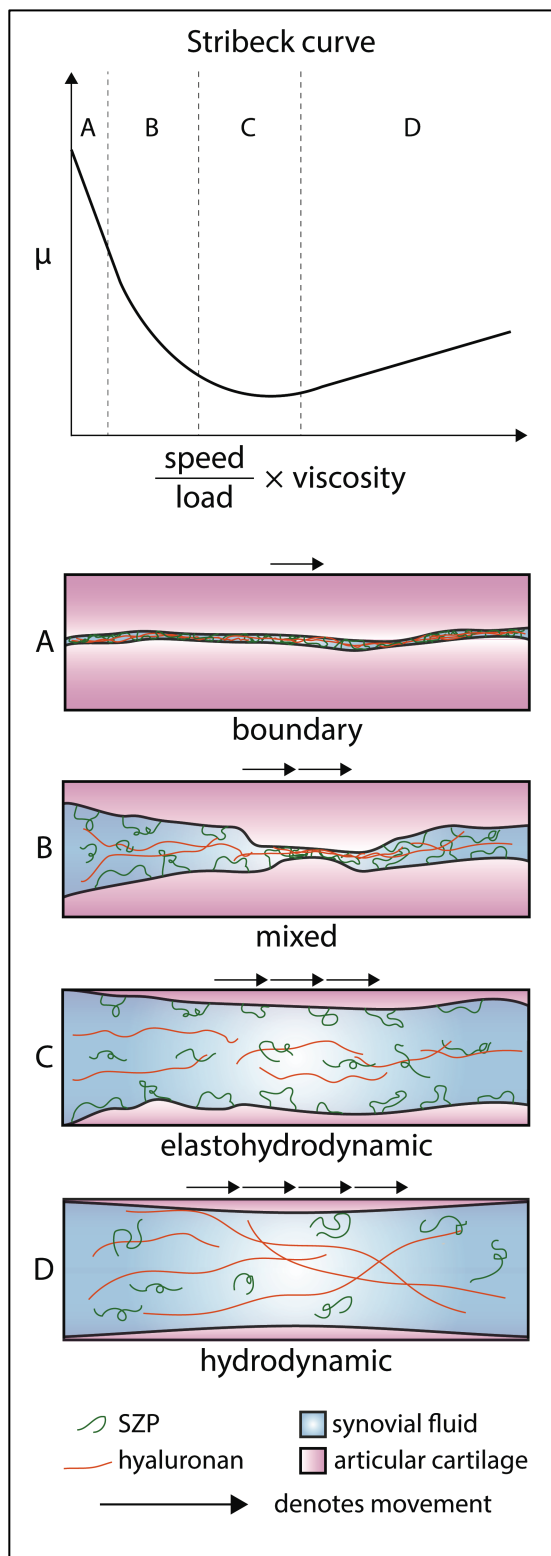
FIGURES

FIGURE 1

Figure 1- Lubrication regimes (A-D) within a synovial joint. The speed of articulation, magnitude of load, and fluid viscosity determine the mode of lubrication and affect the coefficient of friction (μ), as demonstrated in the Stribeck curve. Boundary lubrication **(A)** involves interaction of both articular surfaces resulting in a lack of fluid film. Mixed lubrication **(B)** combines aspects of boundary lubrication and fluid film lubrication. Elastohydrodynamic lubrication **(C)** is characterized by both a fluid film and deformation of articular cartilage. Hydrodynamic lubrication **(D)** involves a fluid film alone.

FIGURE 2
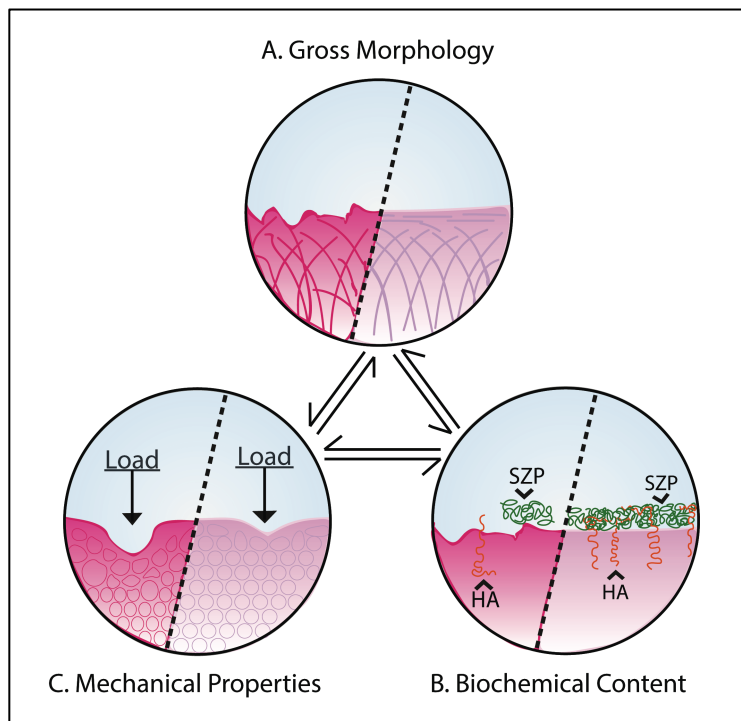
Figure 2 - A summary of how the gross morphology, biochemical content, and mechanical properties of cartilage feed into the maintenance of tribological function in the diarthrodial joint. In all panels, diseased cartilage is shown on the left and healthy cartilage is shown on the right. The gross morphology **(A)**, biochemical content **(B)**, and mechanical properties **(C)** of diseased cartilage (left) are compromised in comparison to healthy cartilage (right).
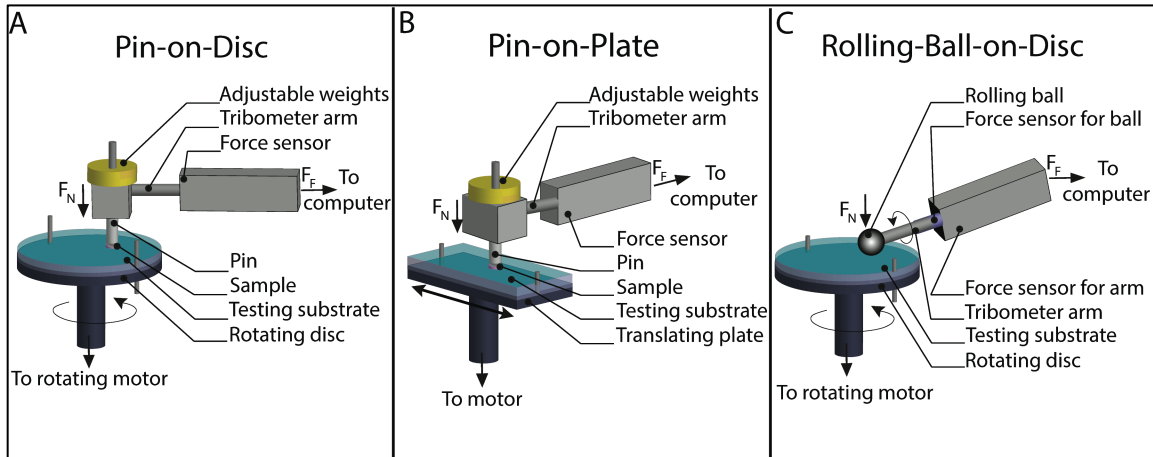
FIGURE 3

Figure 3- Tribometer configurations. Schematic of a pin-on-disc tribometer **(A)** where a sample is glued to the pin and tested on a substrate attached to the rotating disc. Schematic of pin-on-plate tribometer **(B),** which uses a translating plate instead of a disc. Schematic of rolling-ball-on-disc tribometer **(C),** primarily used to test orthopedic implants, where both the tribometer arm and the disc can be rotated independently. In each setup, the coefficient of friction is calculated by dividing the friction force (F_F), obtained from the force sensor, by the known F_N created by the adjustable weights or the movement of the tribometer arm.

REFERENCES

Ambrosio, L., Borzacchiello, A., Netti, P.A., Nicolais, L., 1999. Rheological study on hyaluronic acid and its derivative solutions. Journal of Macromolecular Science, Part A 36, 991-1000.

Antonacci, J.M., Schmidt, T.A., Serventi, L.A., Cai, M.Z., Shu, Y.L., Schumacher, B.L., McIlwraith, C.W., Sah, R.L., 2012. Effects of Equine Joint Injury on Boundary Lubrication of Articular Cartilage by Synovial Fluid: Role of Hyaluronan. Arthritis and Rheumatism 64, 2917-2926.

Athanasiou, K.A., Darling, E.M., Hu, J.C., DuRaine, G.D., Reddi, A.H., 2017. Articular Cartilage. CRC Press, Boca Raton.

Bell, C.J., Ingham, E., Fisher, J., 2006. Influence of hyaluronic acid on the time-dependent friction response of articular cartilage under different conditions. Proceedings of the Institution of Mechanical Engineers. Part H, Journal of engineering in medicine 220, 23-31.

Bergmann, G., Graichen, F., Rohlmann, A., 1993. Hip joint loading during walking and running, measured in two patients. Journal of biomechanics 26, 969-990.

Blum, M.M., Ovaert, T.C., 2013. Low friction hydrogel for articular cartilage repair: evaluation of mechanical and tribological properties in comparison with natural cartilage tissue. Materials science & engineering. C, Materials for biological applications 33, 4377-4383.

Bonnevie, E.D., McCorry, M.C., Bonassar, L.J., 2016. Mesenchymal Stem Cells Enhance Lubrication of Engineered Meniscus Through Lubricin Localization in Collagen Gels. Biotribology 8, 26-32.

Bonnevie, E.D., Puetzer, J.L., Bonassar, L.J., 2014. Enhanced boundary lubrication properties of engineered menisci by lubricin localization with insulin-like growth factor I treatment. Journal of biomechanics 47, 2183-2188.

Chan, S.M.T., Neu, C.P., DuRaine, G., Komvopoulos, K., Reddi, A.H., 2010. Atomic force microscope investigation of the boundary-lubricant layer in articular cartilage. Osteoarthritis and cartilage 18, 956-963.

Chan, S.M.T., Neu, C.P., DuRaine, G., Komvopoulos, K., Reddi, A.H., 2012. Tribological altruism: A sacrificial layer mechanism of synovial joint lubrication in articular cartilage. Journal of biomechanics 45, 2426-2431.

Chang, D.P., Guilak, F., Jay, G.D., Zauscher, S., 2014. Interaction of lubricin with type II collagen surfaces: adsorption, friction, and normal forces. Journal of biomechanics 47, 659-666.

Coles, J.M., Zhang, L., Blum, J.J., Warman, M.L., Jay, G.D., Guilak, F., Zauscher, S., 2010. Loss of cartilage structure, stiffness, and frictional properties in mice lacking PRG4. Arthritis and Rheumatism 62, 1666-1674.

Comper, W.D., Laurent, T.C., 1978. Physiological function of connective tissue polysaccharides. Physiol Rev 58, 255-315.

Cooper, B.G., Lawson, T.B., Snyder, B.D., Grinstaff, M.W., 2017. Reinforcement of articular cartilage with a tissue-interpenetrating polymer network reduces friction and modulates interstitial fluid load support. Osteoarthritis and cartilage 25, 1143-1149.

Cowman, M.K., Lee, H.-G., Schwertfeger, K.L., McCarthy, J.B., Turley, E.A., 2015. The Content and Size of Hyaluronan in Biological Fluids and Tissues. Frontiers in immunology 6, 261-261.

Flannery, C.R., Zollner, R., Corcoran, C., Jones, A.R., Root, A., Rivera-Bermúdez, M.A., Blanchet, T., Gleghorn, J.P., Bonassar, L.J., Bendele, A.M., Morris, E.A., Glasson, S.S., 2009. Prevention of cartilage degeneration in a rat model of osteoarthritis by intraarticular treatment with recombinant lubricin. Arthritis & Rheumatism 60, 840-847.

Flowers, S.A., Zieba, A., Örnros, J., Jin, C., Rolfson, O., Björkman, L.I., Eisler, T., Kalamajski, S., Kamali-Moghaddam, M., Karlsson, N.G., 2017. Lubricin binds cartilage proteins, cartilage oligomeric matrix protein, fibronectin and collagen II at the cartilage surface. Scientific reports 7, 13149-13149.

Galley, N.K., Gleghorn, J.P., Rodeo, S., Warren, R.F., Maher, S.A., Bonassar, L.J., 2011. Frictional properties of the meniscus improve after scaffold-augmented repair of partial meniscectomy: a pilot study. Clinical orthopaedics and related research 469, 2817-2823.

Ghosh, S., Abanteriba, S., 2016. Status of surface modification techniques for artificial hip implants. Science and technology of advanced materials 17, 715-735.

Ghosh, S., Bowen, J., Jiang, K., Espino, D.M., Shepherd, D.E., 2013. Investigation of techniques for the measurement of articular cartilage surface roughness. Micron 44, 179-184.

Gleghorn, J.P., Bonassar, L.J., 2008. Lubrication mode analysis of articular cartilage using Stribeck surfaces. Journal of biomechanics 41, 1910-1918.

Gleghorn, J.P., Jones, A.R.C., Flannery, C.R., Bonassar, L.J., 2009. Alteration of articular cartilage frictional properties by transforming growth factor β, interleukin-1β, and oncostatin M. Arthritis & Rheumatism 60, 440-449.

Grad, S., Loparic, M., Peter, R., Stolz, M., Aebi, U., Alini, M., 2012. Sliding motion modulates stiffness and friction coefficient at the surface of tissue engineered cartilage. Osteoarthritis and cartilage 20, 288-295.

Greene, G.W., Banquy, X., Lee, D.W., Lowrey, D.D., Yu, J., Israelachvili, J.N., 2011. Adaptive mechanically controlled lubrication mechanism found in articular joints. Proceedings of the National Academy of Sciences 108, 5255.

Grenier, S., Bhargava, M.M., Torzilli, P.A., 2014. An in vitro model for the pathological degradation of articular cartilage in osteoarthritis. Journal of biomechanics 47, 645-652.

Henrotin, Y., Chevalier, X., Raman, R., Richette, P., Montfort, J., Jerosch, J., Baron, D., Bard, H., Carrillon, Y., Migliore, A., Conrozier, T., 2018. EUROVISCO Guidelines for the Design and Conduct of Clinical Trials Assessing the Disease-Modifying Effect of Knee Viscosupplementation. Cartilage, 1947603518783521.

Higaki, H., Murakami, T., Nakanishi, Y., Miura, H., Mawatari, T., Iwamoto, Y., 1998. The lubricating ability of biomembrane models with dipalmitoyl phosphatidylcholine and gamma-globulin. Proceedings of the Institution of Mechanical Engineers. Part H, Journal of engineering in medicine 212, 337-346.

Hyun, K., Kim, S.H., Ahn, K.H., Lee, S.J., 2002. Large amplitude oscillatory shear as a way to classify the complex fluids. Journal of Non-Newtonian Fluid Mechanics 107, 51-65.

Iwakura, T., Sakata, R., Reddi, A.H., 2013. Induction of chondrogenesis and expression of superficial zone protein in synovial explants with TGF-beta1 and BMP-7. Tissue engineering. Part A 19, 2638-2644.

Iwasa, K., Reddi, A.H., 2017. Optimization of Methods for Articular Cartilage Surface Tissue Engineering: Cell Density and Transforming Growth Factor Beta Are Critical for Self-Assembly and Lubricin Secretion. Tissue engineering. Part C, Methods 23, 389-395.

Jahn, S., Seror, J., Klein, J., 2016. Lubrication of Articular Cartilage. Annual review of biomedical engineering 18, 235-258.

Jay, G.D., Torres, J.R., Rhee, D.K., Helminen, H.J., Hytinnen, M.M., Cha, C.J., Elsaid, K., Kim, K.S., Cui, Y., Warman, M.L., 2007. Association between friction and wear in diarthrodial joints lacking lubricin. Arthritis and Rheumatism 56, 3662-3669.

Jay, G.D., Waller, K.A., 2014. The biology of Lubricin: Near frictionless joint motion. Matrix Biology 39, 17-24.

Jia, H., Ma, X., Tong, W., Doyran, B., Sun, Z., Wang, L., Zhang, X., Zhou, Y., Badar, F., Chandra, A., Lu, X.L., Xia, Y., Han, L., Enomoto-Iwamoto, M., Qin, L., 2016. EGFR signaling is critical for maintaining the superficial layer of articular cartilage and preventing osteoarthritis initiation. Proceedings of the National Academy of Sciences of the United States of America 113, 14360-14365.

Kanca, Y., Milner, P., Dini, D., Amis, A.A., 2018a. Tribological evaluation of biomedical polycarbonate urethanes against articular cartilage. Journal of the mechanical behavior of biomedical materials 82, 394-402.

Kanca, Y., Milner, P., Dini, D., Amis, A.A., 2018b. Tribological properties of PVA/PVP blend hydrogels against articular cartilage. Journal of the mechanical behavior of biomedical materials 78, 36-45.

Lewis, P.R., McCutchen, C.W., 1959. Experimental evidence for weeping lubrication in mammalian joints. Nature 184, 1285.

Liao, I.C., Moutos, F.T., Estes, B.T., Zhao, X., Guilak, F., 2013. Composite three-dimensional woven scaffolds with interpenetrating network hydrogels to create functional synthetic articular cartilage. Advanced functional materials 23, 5833-5839.

Maiese, K., 2016. Picking a bone with WISP1 (CCN4): new strategies against degenerative joint disease. Journal of translational science 1, 83-85.

Majd, S.E., Kuijer, R., Kowitsch, A., Groth, T., Schmidt, T.A., Sharma, P.K., 2014. Both hyaluronan and collagen type II keep proteoglycan 4 (lubricin) at the cartilage surface in a condition that provides low friction during boundary lubrication. Langmuir 30, 14566-14572.

Marcelino, J., Carpten, J.D., Suwairi, W.M., Gutierrez, O.M., Schwartz, S., Robbins, C., Sood, R., Makalowska, I., Baxevanis, A., Johnstone, B., Laxer, R.M., Zemel, L., Kim, C.A., Herd, J.K., Ihle, J., Williams, C., Johnson, M., Raman, V., Alonso, L.G., Brunoni, D., Gerstein, A., Papadopoulos, N., Bahabri, S.A., Trent, J.M., Warman, M.L., 1999. CACP, encoding a secreted proteoglycan, is mutated in camptodactyly-arthropathy-coxa vara-pericarditis syndrome. Nat Genet 23, 319-322.

McCutchen, C.W., 1959. Mechanism of Animal Joints: Sponge-hydrostatic and Weeping Bearings. Nature 184, 1284.

McCutchen, C.W., 1962. The frictional properties of animal joints. Wear 5, 1-17.

McNary, S.M., Athanasiou, K.A., Reddi, A.H., 2012. Engineering Lubrication in Articular Cartilage. Tissue Engineering. Part B, Reviews 18, 88-100.

Middendorf, J.M., Griffin, D.J., Shortkroff, S., Dugopolski, C., Kennedy, S., Siemiatkoski, J., Cohen, I., Bonassar, L.J., 2017. Mechanical properties and structure-function relationships of human chondrocyte-seeded cartilage constructs after in vitro culture. Journal of orthopaedic research : official publication of the Orthopaedic Research Society 35, 2298-2306.

Moa-Anderson BJ, C.K., Hung CT, Ateshian GA, 2003. Bovine articular cartilage surface topography and roughness in fresh versus frozen tissue samples using atomic force microscopy, Proceedings of 2003 Summer Bioengineering Conference.

Moore, A.C., Burris, D.L., 2015. Tribological and material properties for cartilage of and throughout the bovine stifle: support for the altered joint kinematics hypothesis of osteoarthritis. Osteoarthritis and cartilage 23, 161-169.

Morgese, G., Cavalli, E., Muller, M., Zenobi-Wong, M., Benetti, E.M., 2017. Nanoassemblies of Tissue-Reactive, Polyoxazoline Graft-Copolymers Restore the Lubrication Properties of Degraded Cartilage. ACS nano 11, 2794-2804.

Morgese, G., Cavalli, E., Rosenboom, J.G., Zenobi-Wong, M., Benetti, E.M., 2018. Cyclic Polymer Grafts That Lubricate and Protect Damaged Cartilage. Angewandte Chemie (International ed. in English) 57, 1621-1626.

Morrell, K.C., Hodge, W.A., Krebs, D.E., Mann, R.W., 2005. Corroboration of in vivo cartilage pressures with implications for synovial joint tribology and osteoarthritis causation. Proceedings of the National Academy of Sciences of the United States of America 102, 14819-14824.

Murakami, T., Higaki, H., Sawae, Y., Ohtsuki, N., Moriyama, S., Nakanishi, Y., 1998. Adaptive multimode lubrication in natural synovial joints and artificial joints. Proceedings of the Institution of Mechanical Engineers. Part H, Journal of engineering in medicine 212, 23-35.

Murphy, M.K., DuRaine, G.D., Reddi, A., Hu, J.C., Athanasiou, K.A., 2013. Inducing articular cartilage phenotype in costochondral cells. Arthritis Res Ther 15, R214.

Nečas, D., Vrbka, M., Křupka, I., Hartl, M., 2018. The Effect of Kinematic Conditions and Synovial Fluid Composition on the Frictional Behaviour of Materials for Artificial Joints. Materials (Basel, Switzerland) 11, 767.

Neu, C.P., Komvopoulos, K., Reddi, A.H., 2008. The interface of functional biotribology and regenerative medicine in synovial joints. Tissue engineering. Part B, Reviews 14, 235-247.

Noyori, K., Takagi, T., Jasin, H.E., 1998. Characterization of the macromolecular components of the articular cartilage surface. Rheumatol Int 18, 71-77.

Oungoulian, S.R., Durney, K.M., Jones, B.K., Ahmad, C.S., Hung, C.T., Ateshian, G.A., 2015. Wear and Damage of Articular Cartilage with Friction Against Orthopaedic Implant Materials. Journal of biomechanics 48, 1957-1964.

Park, I.S., Choi, W.H., Park, D.Y., Park, S.R., Park, S.H., Min, B.H., 2018. Effect of joint mimicking loading system on zonal organization into tissue-engineered cartilage. PLoS One 13, e0202834.

Park, J.Y., Duong, C.T., Sharma, A.R., Son, K.M., Thompson, M.S., Park, S., Chang, J.D., Nam, J.S., Park, S., Lee, S.S., 2014. Effects of hyaluronic acid and gamma-globulin concentrations on the frictional response of human osteoarthritic articular cartilage. PLoS One 9, e112684.

Park, S., Costa, K.D., Ateshian, G.A., 2004. Microscale frictional response of bovine articular cartilage from atomic force microscopy. Journal of biomechanics 37, 1679-1687.

Peng, G., McNary, S.M., Athanasiou, K.A., Reddi, A.H., 2014. Surface zone articular chondrocytes modulate the bulk and surface mechanical properties of the tissue-engineered cartilage. Tissue engineering. Part A 20, 3332-3341.

Peng, G., McNary, S.M., Athanasiou, K.A., Reddi, A.H., 2015. The distribution of superficial zone protein (SZP)/lubricin/PRG4 and boundary mode frictional properties of the bovine diarthrodial joint. Journal of biomechanics 48, 3406-3412.

Peng, G., McNary, S.M., Athanasiou, K.A., Reddi, A.H., 2016. Superficial Zone Extracellular Matrix Extracts Enhance Boundary Lubrication of Self-Assembled Articular Cartilage. Cartilage 7, 256-264.

Rongen, J.J., van Tienen, T.G., van Bochove, B., Grijpma, D.W., Buma, P., 2014. Biomaterials in search of a meniscus substitute. Biomaterials 35, 3527-3540.

Sanchez-Guerrero, E., Chen, E., Kockx, M., An, S.W., Chong, B.H., Khachigian, L.M., 2012. IL-1beta signals through the EGF receptor and activates Egr-1 through MMP-ADAM. PLoS One 7, e39811.

Schmidt, T.A., Gastelum, N.S., Nguyen, Q.T., Schumacher, B.L., Sah, R.L., 2007. Boundary lubrication of articular cartilage: role of synovial fluid constituents. Arthritis and Rheumatism 56, 882-891.

Sedin, D.L., Rowlen, K.L., 2001. Influence of tip size on AFM roughness measurements. Applied Surface Science 182, 40-48.

Shi, L., Sikavitsas, V.I., Striolo, A., 2011. Experimental friction coefficients for bovine cartilage measured with a pin-on-disk tribometer: testing configuration and lubricant effects. Annals of biomedical engineering 39, 132-146.

Šimkovic, I., Hricovíni, M., Šoltés, L., Mendichi, R., Cosentino, C., 2000. Preparation of water-soluble/insoluble derivatives of hyaluronic acid by cross-linking with epichlorohydrin in aqueous NaOH/NH4OH solution. Carbohydrate Polymers 41, 9-14.

Singh, A., Corvelli, M., Unterman, S.A., Wepasnick, K.A., McDonnell, P., Elisseeff, J.H., 2014. Enhanced lubrication on tissue and biomaterial surfaces through peptide-mediated binding of hyaluronic acid. Nature Materials 13, 988.

Sun, S.-F., Hsu, C.-W., Lin, H.-S., Liou, I.-H., Chen, Y.-H., Hung, C.-L., 2017. Comparison of Single Intra-Articular Injection of Novel Hyaluronan (HYA-JOINT Plus) with Synvisc-One for Knee Osteoarthritis: A Randomized, Controlled, Double-Blind Trial of Efficacy and Safety. 99, 462-471.

Tamer, T.M., 2013. Hyaluronan and synovial joint: function, distribution and healing. Interdisciplinary Toxicology 6, 111-125.

Walker, P.S., Dowson, D., Longfield, M.D., Wright, V., 1968. "Boosted lubrication" in synovial joints by fluid entrapment and enrichment. Annals of the rheumatic diseases 27, 512-520.

Waller, K.A., Zhang, L.X., Elsaid, K.A., Fleming, B.C., Warman, M.L., Jay, G.D., 2013. Role of lubricin and boundary lubrication in the prevention of chondrocyte apoptosis. Proceedings of the National Academy of Sciences 110, 5852-5857.

Warnecke, D., Schild, N.B., Klose, S., Joos, H., Brenner, R.E., Kessler, O., Skaer, N., Walker, R., Freutel, M., Ignatius, A., Durselen, L., 2017. Friction properties of a new silk fibroin scaffold for meniscal replacement. Tribology international 109, 586-592.

Whitney, G.A., Jayaraman, K., Dennis, J.E., Mansour, J.M., 2017. Scaffold-free cartilage subjected to frictional shear stress demonstrates damage by cracking and surface peeling. Journal of tissue engineering and regenerative medicine 11, 412-424.

Whitney, G.A., Mansour, J.M., Dennis, J.E., 2015. Coefficient of Friction Patterns Can Identify Damage in Native and Engineered Cartilage Subjected to Frictional-Shear Stress. Annals of biomedical engineering 43, 2056-2068.

Woydt, M., Wäsche, R., 2010. The history of the Stribeck curve and ball bearing steels: The role of Adolf Martens. Wear 268, 1542-1546.

Wu, Y., Stoddart, M.J., Wuertz-Kozak, K., Grad, S., Alini, M., Ferguson, S.J., 2017. Hyaluronan supplementation as a mechanical regulator of cartilage tissue development under joint-kinematic-mimicking loading. Journal of the Royal Society Interface 14.

Zappone, B., Greene, G.W., Oroudjev, E., Jay, G.D., Israelachvili, J.N., 2008. Molecular Aspects of Boundary Lubrication by Human Lubricin: Effect of Disulfide Bonds and Enzymatic Digestion. Langmuir 24, 1495-1508.

APPENDIX B- CHARACTERIZATION OF ADULT AND NEONATAL ARTICULAR CARTILAGE FROM THE EQUINE STIFLE

ABSTRACT

Background: A significant portion of equine lameness is localized to the stifle joint. Effective cartilage repair strategies are largely lacking, however, recent advances in surgical techniques, biomaterials, and cellular therapeutics have broadened the clinical strategies of cartilage repair. To date, no studies have been performed directly comparing neonatal and adult articular cartilage from the stifle in a topographical manner. An understanding of the differences in properties between the therapeutic target cartilage (i.e., adult cartilage) as well as potential donor cartilage (i.e. neonatal cartilage) could aid in selection of optimal harvest sites within a donor joint as well as evaluation of the success of the grafted cells or tissues within the host.

Objective: Given the dearth of topographical characterization of the equine stifle joint, and in particular neonatal stifle cartilage, the goal of this study was to measure properties of both potential source tissue and host tissue.

Methods: Articular cartilage of the distal femur and patella was assessed in regards to two specific factors, age of the animal and specific site within the joint. Two age groups were considered: neonatal (<1 week) and adult (4-14 years). Cartilage samples were harvested topographically from 17 sites across the distal femur and patella. It was hypothesized that properties would vary significantly between neonatal and adult horses as well as within age groups on a topographic basis.

Results: Adult thickness varied topographically. With the exception of water content, there were no significant biochemical differences among sites within regions of the distal femur (condyles, trochlea) and the patella in either the adult or neonate. Neonatal cartilage had a significantly higher water content than adult. Surprisingly, biochemical measurements of cellularity did not differ significantly between neonatal and adult, however adult cartilage had a

significantly greater variability in cellularity compared to neonatal. Biochemical assays revealed that the medial condyle had the lowest glycosaminoglycan (GAG) content in both adult and neonatal cartilage. Overall, there were no significant differences between neonatal and adult GAG content. Collagen per wet weight was found to be significantly higher in adult cartilage compared to neonatal when averaged across all levels. Aggregate modulus varied significantly across the condyles of adult cartilage but not the neonate. Neonatal cartilage was significantly less permeable and the Young's modulus of neonatal cartilage was significantly higher compared to the adult. The tensile strength did not vary in a statistically significant manner between age groups.

Conclusions: An understanding of morphological, histological, biochemical, and biomechanical properties enhances the understanding of cartilage tissue physiology and structure-function relationships. This study revealed important differences in biomechanical and biochemical properties among the 17 topographical sites and among the six joint regions, as well as age-related differences between neonatal and adult cartilage. These topographical and age-related variations are informative toward determining the donor tissue harvest site.

Authors: White JL, Salinas EY, Link JM, Hu JC, Athanasiou KA

Manuscript Prepared for Submission

INTRODUCTION

The stifle joint is notable as the largest and most complex joint in the body. The stifle joint is comprised of the femoropatellar and femorotibial joints, and, in the equine, the femorotibial joint is further divided by synovial tissue into a non-communicating medial and lateral joint space, each containing a fibrocartilaginous meniscus [1]. The menisci serve to increase congruity between the condyles of the distal femur and proximal tibia [2]. In addition to the menisci,12 ligaments collectively serve to stabilize the stifle and facilitate the interdependent motion of the femoropatellar and femorotibial joints. The articular cartilage lining the ends of the long bones and articulating surface of the patella, plays a critical role in proper joint function. Damage or developmental abnormalities affecting any component of this complex synovial joint can result in decreased mobility and lameness.

Lameness associated with the stifle joint has been reported to be 40% of hindlimb lameness cases [3]. Osteochondrosis is among the most commonly diagnosed developmental disorders in the equine stifle. Osteochondrosis in its most severe form is known as osteochondritis dissecans (OCD) and presents as fissures or fragments of the articular cartilage and, in certain cases, subchondral bone cysts may also be present [4]. Subchondral bone cysts can also occur in the absence of OCD and are considered part of the family of orthopedic developmental disorders. These cysts are commonly localized to the equine stifle joint, with the highest incidence in the medial femoral condyle [5]. Non-cystic OCD lesions of the stifle are most commonly localized to the lateral trochlear ridge of the femur. The etiology of this disorder is not fully understood, and as with osteochondrosis, there appears to be a genetic component, as certain breeds are more commonly affected [6]. Left untreated, developmental disorders such as osteochondrosis and subchondral bone cysts can result in the condition of osteoarthritis.

In addition to developmental disorders, traumatic injury to the articular cartilage of the stifle joint, underlying subchondral bone, or soft tissue structures within and surrounding the joint, such as ligaments, menisci, or joint capsule, can also result in osteoarthritis [7]. Reports of the incidence of osteoarthritis ranges from 3 to 32% of all stifle lameness that may be attributed to the disease process, with the medial femorotibial joint compartment being the most commonly affected in horses [8]. Osteoarthritis in performance horses may be associated with high impact loading as a result of activities such as jumping, racing, etc., that has been shown to decrease proteoglycan content and increase catabolic enzymes and chondrocyte apoptosis [9-12]. Due to its progressive nature, osteoarthritis carries a relatively poor long-term prognosis, which is why treatment of joint lesions to preclude the onset of osteoarthritis is imperative for long-term health of the animal.

Effective cartilage repair strategies are largely lacking in both human and veterinary medicine, however, recent advances in surgical techniques, biomaterials, and cellular therapeutics have greatly broadened the clinical strategies of cartilage repair. In the equine, although a number of treatments have been shown to out-perform debridement, this procedure persists as a mainstay of treatment for equine cartilage pathology due its relative low cost and simplicity. Debridement is often performed in conjunction with microfracture, as it is thought that microfracture functions to promote formation of endogenous repair tissue. While repair tissue does form as a result of microfracture, it is largely fibrocartilaginous in adult individuals of most species, including horses, and does not withstand physiologic forces as well as hyaline cartilage [13,14]. Therefore, research efforts to develop new cartilage repair strategies aim to promote hyaline tissue formation over fibrocartilage formation. These strategies include grafting procedures such as osteochondral allograft transplantation system (OATS) and mosaicplasty, cellular based strategies such as autologous chondrocyte implantation (ACI) and matrix-assisted ACI (MACI), as well as particulated cartilage based procedures such as cartilage

autograft implantation system (CAIS) [15]. Some of these strategies utilize tissue from neonatal and juvenile tissue donor sources, including RevaFlex^{TM} DeNovo$^®$ Arthrex Biocartilage$^®$, capitalizing on the higher regenerative capacity of chondrocytes from younger donor sources [16].

While a number of these strategies are utilized routinely in human medicine, they are largely confined to the realm of research in the context of equine medicine. Technical considerations, including tissue harvest and banking, cellular expansion, and surgical implantation protocols, and their associated costs have prevented widespread adoption of these therapies. Stem cells, in particular mesenchymal stem cells (MSCs), show promise as a potential tool for cartilage repair, however, much work has yet to be done to identify the optimal parameters to direct these cells to function in a restorative capacity [17-21]. Much effort has also been put toward development of biocompatible scaffolds, both natural and synthetic, as well as chondroinductive factors that can be combined with these scaffolds to provide a multifactorial approach to cartilage regeneration [22-24]. An ideal articular cartilage repair product would result in production of novel hyaline cartilage tissue that recapitulated the zonal architecture and hyaline composition of native articular cartilage and achieve lateral integration into surrounding healthy cartilage and underlying subchondral bone. It is therefore important to understand the properties of native cartilage in order to establish design criteria for potential therapeutics.

Equine articular cartilage, as in other species, is an avascular tissue containing sparse chondrocytes and a high content of collagen type 2 and GAG; the exact composition of articular cartilage varies, however, with age and location within the body [25]. Properties of equine articular cartilage in health have been most extensively characterized in the metacarpophalangeal joint [26-35], however, limited studies have been conducted in other joints such as the carpus [36-41], cervical facet [42], and stifle [43]. To date, no studies have been performed directly comparing neonatal and adult articular cartilage from the stifle in a

topographical manner. An understanding of the differences between neonatal and adult cartilage can inform theories of the post-natal maturation process, especially when interpreted in conjunction with kinematic/loading force studies. Equine neonatal cartilage may also serve as donor tissue, both as a cell source for tissue engineering efforts as well as matrix source for allograft procedures [44,45]. An understanding of the differences in properties between the therapeutic target cartilage (i.e., adult cartilage) as well as potential donor cartilage (i.e., neonatal cartilage) could aid in selection of optimal harvest sites within a donor joint as well as evaluation of the success of the grafted cells or tissues within the host.

Given the dearth of topographical characterization of the equine stifle joint, and in particular neonatal stifle cartilage, the goal of this study was to measure properties of both potential source tissue and host tissue. Articular cartilage of the distal femur and patella was assessed in regards to two specific factors, age of the animal and site within the joint. Two age groups were considered specifically, neonatal (<1 week) and adult (4-14 years). Cartilage samples were harvested topographically from 17 sites across the distal femur and patella. It was hypothesized that properties would vary significantly between neonatal and adult horses as well as within age groups on a topographic basis.

MATERIALS AND METHODS

Native tissue sample preparation

Equine stifle joints were isolated from six skeletally mature horses (4-14 yrs old, mean = 6.7 yrs old) and six neonatal foals (<1 wk old). All animals died or were euthanized for reasons unrelated to stifle joint pathology. Upon opening the stifle joint, a macroscopic inspection of the cartilage was performed to check for signs of osteoarthritis (OA). Horses whose cartilage showed gross signs of OA were excluded from this study. Articular cartilage samples were isolated from the patella (P) and five different regions of the distal femur – the medial condyle (MC), the lateral condyle (LC) the medial ridge of the trochlea (MR), the lateral ridge of the trochlea (LR), and the trochlear groove (TG). Within each of these regions, multiple topographical sites were tested, three sites on MC, three sites on LC, three sites on MR, three sites on LR, three sites on TG, and two sites on P (Figure 1). Specific sites were isolated using an 8 mm biopsy punch. For adult samples, the cartilage was trimmed off the underlying subchondral bone with a #10 scalpel blade. Neonatal samples were trimmed to ~2mm thickness (approximate junction between articular cartilage and underlying epiphyseal growth plate cartilage) using a custom jig and microtome blade. Each 8 mm punch was portioned for histological, biochemical, and biomechanical evaluations.

Biomechanical evaluation

Creep indentation testing was performed on 3 mm cylindrical punches taken from the larger 8 mm specimens collected from each topographical region. This 3 mm punch was then photographed, and digital measuring tools (Image J) were used to determine the thickness of the sample. The sample was subsequently glued to the base of a cylindrical sample holder and submerged in PBS (Sigma). A 0.9 mm diameter, flat, porous indenter tip was applied to the samples under a 2 – 12 g load to achieve ~10% strain. The tissue was allowed to reach creep equilibrium while the deformation was recorded over time. Creep deformation data were then

used to determine the aggregate modulus, shear modulus, and permeability of each sample using a linear biphasic model [46].

For uniaxial tensile testing, specimens were trimmed into a dog-bone shape with a gauge length of 1.3 mm, in adherence with ASTM standards (ASTM D3039). Orientation of collagen fibers was determined by pricking the cartilage sample surface with a needle dipped in India Ink, which allowed for visualization of a split line running parallel to collagen fiber orientation. Specimens were trimmed such that the long-axis of the dog-bone was oriented parallel to collagen fiber alignment based on the India Ink staining. Samples were photographed to obtain the cross-sectional area of each sample using ImageJ. Paper tabs were glued to the samples outside the gauge length. These tabs were loaded into the grips of a TestResources mechanical tester (TestResources Inc.) and pulled at 1% of the gauge length per second until sample failure. Load measurements were recorded over the duration of the test and used to generate stress-stain curves. Young's modulus was obtained by a least-squares fit of the linear region of the curve and ultimate tensile strength (UTS) was determined from the maximum stress at failure.

Biochemical evaluation

Full-thickness samples were portioned from each 8 mm biopsy punch for biochemical analysis. Samples were weighed before and after lyophilization to obtain wet weights and dry weights respectively. Water content of the tissues was determined using the difference between wet and dry weight for each sample. Lyophilized samples were digested in 125 µg/mL papain (Sigma) in 50 mM phosphate buffer (pH = 6.5) containing 2 mM N-acetyl cysteine (Sigma) and 2 mM EDTA (Sigma) at 60°C for 18 hours. Sulfated GAG content was measured using the Blyscan dimethyl methylene blue assay kit (Accurate Chemical). Collagen content was quantified by a perchloric acid-free, chloramine-T modified hydroxyproline assay [47] following hydrolysis with 2 N NaOH for 20 mins at 110ºC and using Sircol collagen (Accurate Chemical) as a standard. The

Quant-iT Picrogreen dsDNA assay kit (Invitrogen) was used to measure the DNA content. Pyridinoline crosslinks were quantified using high-performance liquid chromatography (HPLC). For the HPLC assay, lyophilized samples were digested in 6N HCl at 100°C for 24 h and then dried in a vacuum concentrator. Digested samples were resuspended in 500 µL of a solution containing 1.67 nmol pyroxidine/mL, 8.3% acetonitrile, and 0.41% heptafluorobutyric acid (HFBA) in water and then injected into a 25 mm C18 column (Shimadzu). Two solvents, (1) 24% methanol and 0.13% HFBA in water and (2) 75% acetonitrile and 0.1% HFBA in water, were sequentially flowed through the column for sample elution and column washing, respectively [48].

Histological and immunohistochemical evaluation

Samples partitioned for histological processing were fixed in 10% neutral buffered formalin, embedded in paraffin, and sectioned into 4 µm sections to expose the full thickness of the tissue. Sections were stained with Hematoxylin and Eosin, Safranin O/Fast Green for sulfated GAGs, and Picrosirius red for collagen. Immunohistochemistry (IHC) was performed to visualize collagen type I and collagen type 2. Following antigen retrieval with citric acid (pH 6) at 95°C for 20 min and at room temperature for an additional 20 min, anti-collagen I antibody (ab34710, Abcam) was applied at a 1:300 dilution. Antigen retrieval using 4 mg/mL hyaluronidase (Sigma) in PBS for 30 minutes followed by 3 mg/mL pepsin (Sigma) in 0.5% acetic acid for 30 min was used prior to application of anti-collagen II antibody (ab34712, Abcam) at a 1:600 dilution.

Statistical Analysis

An O'Brien test for unequal variances was performed for all quantitative measures. If variances were unequal, a Welch's test was performed. In the case of equal variances, analysis was performed by linear mixed model ANOVA treating animal as a random effect followed by Tukey's *post hoc* test. The statistical model included joint region (lateral condyle, medial condyle, lateral trochlear ridge, medial trochlear ridge, trochlear groove, and patella), age (adult

vs. neonatal), and the interaction of joint region and age as fixed effects. Data are presented as mean ± standard deviation, and different letters denote significantly different groups at p<0.05.

RESULTS

<u>Gross morphology</u>

All animals used in this study had articular cartilage of the femoropatellar joint that appeared healthy, with a smooth, glossy, white appearance. For the purposes of mechanical testing, cartilage thickness was measured for all sites in both neonatal and adult cartilage (Table 1). Because the thickness of neonatal cartilage generally extended beyond the depth of the biopsy punch, the full thickness of articular cartilage could not be determined in the neonate. All sites in the neonate had a thickness greater than 2 mm with the exception of TG1 and TG3. The average thickness across the TG in the neonate was 1.94 ± 0.43mm.

The thicknesses of adult cartilage varied significantly among sites within a region (Figure 2A) and among different regions (Figure 2B). The thickness of the MC1, MC2, and MC3 sites were 1.51 ± 0.35 mm, 1.80 ± 0.40 mm, and 2.14 ± 0.34 mm, respectively. MC3 was significantly thicker than MC1 and MC2. The thicknesses of the LC1, LC2, and LC3 sites were 1.50 ± 0.51 mm, 0.98 ± 0.21 mm, and 0.75 ± 0.08 mm, respectively. LC1 was significantly thicker than LC3, but not LC2. Interestingly, the thickness increased when moving from axial to abaxial on the medial condyle but decreased when moving from axial to abaxial on the lateral condyle. The thicknesses of the TG1, TG2, and TG3 sites were 1.70 ± 0.23 mm, 1.56 ± 0.30 mm, and 1.60 ± 0.36 mm, respectively. The thicknesses of the MR1, MR2, and MR3 sites were 1.35 ± 0.32 mm, 1.15 ± 0.20 mm, and 1.41 ± 0.38 mm, respectively. The thicknesses of the LR1, LR2, and LR3 sites were 1.95 ± 0.34 mm, 1.78 ± 0.17 mm, and 2.09 ± 0.30 mm, respectively. No significant differences were observed among the three sites for each trochlear region, however, for all trochlear regions the middle site (TG2, MR2, and LR2) was the thinnest site. Lastly, the thicknesses of the P1 and P2 sites were 1.95 ± 0.28 mm and 1.66 ± 0.35 mm, respectively, and

did not differ significantly. In the adult, the overall thicknesses of each region were also compared and it was determined that the thickness of MC, G, LR, and P were significantly higher than those of MR and LC. The average thicknesses of MC, LC, TG, MR, LR and P were 1.82 ± 0.44 mm, 1.08 ± 0.44 mm, 1.62 ± 0.29 mm, 1.30 ± 0.31 mm, 1.94 ± 0.29 mm, and 1.80 ± 0.34 mm.

Histology

Histological staining was used to visualize tissue morphology and distribution of sulfated GAG and collagen (Figure 3). H&E staining of adult articular cartilage revealed that the condyles stained more basophilic throughout all zones, whereas trochlear cartilage possessed more eosinophilic staining at the surface, and patellar cartilage had an intermediate phenotype that was more basophilic than trochlear but less than condylar. In neonatal articular cartilage, this phenotype was reversed, with the condyles showing less basophilic staining than the trochlea and patella. Overall, neonatal cartilage appeared more homogeneous and more cellular, however cell lacunae were more pronounced in adult cartilage. Safranin-O (with a Fast green counterstain) was utilized to visualize sulfated GAG distribution. In both neonatal and adult cartilage, stain intensity was generally highest in the deep zone. In many regions of adult cartilage, staining was faint or absent in the most superficial region. This is likely an artifact of tissue processing, however, it suggests that this region may contain less GAG in adult cartilage compared to neonatal cartilage. A picrosirius red stain was used to visualize collagen distribution. Adult cartilage generally had higher staining intensity compared to neonatal cartilage, and in many cases, staining was more intense in the superficial zone. Immunohistochemistry for type I and II collaged showed consistently strong collagen II staining and faint collagen I staining for both adult and neonatal cartilages across all sites (Figure 4).

Biochemical properties

The biochemical content of articular cartilage in the different topographical sites for each age group is shown in Tables 1 and 2. With the exception of water content, there were no significant biochemical differences among sites 1, 2, and 3 for each region (MC, LC, TG, MR, LR, and P) in either the adult or neonate. In the adult, the water content of M1 was significantly greater than that of M2, whereas in the neonate, the water content of M3 was significantly less than M2 and M1, and L1 was significantly less than L3. Averaging across all sites, the water content of neonatal and adult cartilage differed significantly with a mean water content of 80.98 ± 1.33% and 78.36 ± 1.06%, respectively. The variability in water content in neonatal cartilage was also significantly greater than adult cartilage. Comparing different regions within the neonatal cartilage revealed that MR, LR, and P had significantly higher water content than both condyles, whereas in adult, the lateral and medial condyles had the highest water content (Figure 5A).

Collagen crosslinking was measured on a per collagen weight basis. There were no significant differences in collagen crosslinking between age groups or among sites and regions. Crosslinking, however, trended higher in adult cartilage and was significantly more variable among regions compared to neonatal cartilage (Figure 5B).

There were no significant differences between neonatal and adult GA/WW or GAG/DW, nor were there any significant differences among regions in neonatal cartilage. Adult cartilage, however, did differ significantly among regions with LC having significantly greater GAG/WW and GAG/DW than G and MC. Interestingly, MC had the lowest GAG content in both adult and neonatal cartilage. GAG/WW averaged 2.86 ± 0.32% and 3.44 ± 0.60% in the neonate and adult, respectively. GAG/DW averaged 15.16 ± 2.20% 16.05 ± 2.70% in neonatal and adult, respectively (Figures 5C and 5D).

In regards to collagen content, Col/WW varied significantly between neonatal and adult cartilage when averaged across all levels at 10.61 ± 2.23% and 13.80 ± 1.54%, respectively.

Col/DW, however, did not, with neonatal cartilage possessing 57.50 ± 14.24% and adult possessing 64.69 ± 9.27%. In the neonate, the regions of the trochlea had the highest collagen content, whereas in the adult, the condyles had the highest collagen content (Figures 5E and 5F). Cellularity did not differ significantly between neonatal and adult, however adult cartilage had a significantly greater variability in cellularity compared to neonatal. Making the assumption of 7.7 pg of DNA per cell, the cells/WW and cells/DW were calculated and averaged 18,631 ± 1720 cells/mg and 99,830 ± 12,674 cells/mg, respectively, in the neonate and 24,209 ± 8,466 cells/mg and 112,706 ± 43,074 cells/mg, respectively, in the adult. Also in the adult, the lateral condyle had significantly greater cellularity than all other regions (Figures 5G and 5H).

Biomechanical properties

The biomechanical properties at the different topographical sites for each age group are shown in Tables 3 and 4. In regards to compressive properties, aggregate modulus varied significantly among sites 1, 2, and 3 in MC and LC of adult cartilage but not neonatal. In the adult, LC1 had a significantly higher aggregate modulus than LC3, and both MC1 and MC2 were significantly higher than MC3. Comparing adult and neonatal compressive properties revealed that adult aggregate modulus had a significantly greater amount of variability compared to neonatal, and neonatal cartilage possessed on average a significantly higher aggregate modulus with an average of 354 ± 43 kPa compared to the adult with an average of 282 ± 47 kPa. There were no significant differences among regions in the neonate, but in the adult, P was significantly higher than MC (Figure 6A).

Shear moduli also varied significantly among sites 1, 2, and 3 in the adult only, with site 1 significantly higher than site 3 for both MC and LC. There was no significant difference between the overall shear modulus of neonatal and adult cartilage, which were 216 ± 28 kPa and 155 ± 24 kPa, respectively, nor were there significant differences among regions in either age group (Figure 6B).

Permeability of adult cartilage was significantly more variable than neonatal cartilage and also significantly higher on average. Neonatal cartilage had an average permeability of 3.26 ± 0.41 $m^4 \times 10^{-15}$/N.s, while adult cartilage had an average permeability of 5.09 ± 0.66 $m^4 \times 10^{-15}$/N.s. In the adult, permeability varied significantly among sites on the MC, with MC1 being significantly more permeable than both MC2 and MC3 (Figure 6C).

In regards to tensile properties, there were no significant difference among sites 1, 2, and 3 in either the neonatal or adult. The Young's modulus of neonatal cartilage was significantly more variable than the adult and also significantly higher on average. Neonatal cartilage had a Young's modulus of 16.2 ± 3.9 MPa and adult cartilage had a Young's modulus of 9.6 ± 2.1 MPa, on average. In the neonate, the Young's modulus of MR was significantly lower than the condyles and TG (Figure 7A). The UTS did not vary significantly between age groups. In the neonate, however, TG had a significantly higher UTS than MR and LR (Figure 7B).

DISCUSSION

Despite its role as the largest and most complex joint in the horse, the stifle joint is largely understudied in terms of its articular cartilage properties. Injury to the stifle joint is common in the equine athlete and repair strategies are lacking. Neonatal cartilage offers a potential source for both allogeneic tissue grafts or chondrocytes that may be used to generate repair tissue *in vitro* or *in vivo*. The purpose of this study, therefore, was to characterize the morphological, histological, biochemical, and biomechanical properties of the distal femur and patella in both neonatal and adult horses across the topography of the joint surface. It was hypothesized that these properties would vary between neonatal and adult horses as well as among topographical sites across the surface of the distal femur and patella. The hypothesis was confirmed as significant differences were found between adult and neonatal cartilage and among sites and

275

regions within each age group in regards to morphologic and histologic features, as well as biochemical and biomechanical properties.

In terms of morphology, thickness of adult cartilage was analyzed in this study for topographic variability. Variability in thickness was most pronounced in the condylar regions: MC3 was significantly thicker than MC1 and MC2, whereas LC1 was significantly thicker than LC3, but not LC2. This pattern of increasing thickness of the medial condyle and decreasing thickness of the lateral condyle while moving from cranial to caudal across each condylar surface is consistent with a previous study that topographically examined cartilage thickness of the equine distal femur [43]. The thinner areas of each condyle (the cranial aspect of the medial condyle and caudal aspect of the lateral condyle) correspond to areas that have been demonstrated to experience the greatest amount of contact with underlying meniscal tissue [49], supporting the theory that cartilage thickness may be influenced by mechanical forces [33,50].

Similar to thickness, compressive biomechanical properties, aggregate and shear moduli, varied significantly among sites 1, 2, and 3 of the MC and LC of adult cartilage. This variability was not observed in neonatal cartilage. While neonatal cartilage possessed on average a significantly higher aggregate modulus with an average of 354 ± 43 kPa compared to the adult with an average of 282 ± 47 kPa, adult aggregate modulus had a significantly greater amount of topographic variability compared to neonatal cartilage. This finding is consistent with a study comparing biomechanical properties of cartilage in fetal, juvenile and adult equine cartilage at multiple sites, which found that fetal and juvenile cartilage possessed higher compressive properties compared to adult cartilage, but did not vary significantly among topographical sites [33]. The results of this study are also consistent with a previous topographical study of the stifle, which found higher compressive properties at the cranial aspect of the condyles in adult horses [43]. Kinematic analysis of the equine study demonstrated that cranial and central area of the condyles corresponded with higher articular

276

contact intensity compared to the more caudal aspect of the condyles [51]. These regions of increased contact intensity correspond with regions of higher compressive properties in the adult but not the neonate, further supporting the concept of a functional adaptation process in response to physiologic loading.

Interestingly, in the adult, the MC region had both the lowest compressive and tensile properties compared to all other regions. In a relatively small study of 47 horses, lesions in the medial femoral condyle and medial meniscus were more prevalent compared to the lateral condyle and meniscus [52]. The cranial pole of the medial meniscus undergoes less cranial-caudal translation and higher axial compressive strain compared to the lateral meniscus during physiologic loading [53]. The forces required to generate this meniscal strain on the cranial pole of the medial meniscus are primarily transmitted through the cranial and central aspect of the medial femoral condyle during locomotion and correspond with areas of higher compressive properties within the medial condyle. Over time, the high strain experience by the medial condyle may result in accelerated wear to the cartilage in this joint compartment and may explain the lower biomechanical properties measured in this region.

Measurements of cellularity did not differ significantly between the neonate and adult, however adult cartilage had a significantly greater variability in cellularity compared to neonatal cartilage. Upon histological examination, neonatal cartilage appeared more homogeneous and more cellular compared to adult cartilage. Studies of the equine fetlock joint in the adult have demonstrated topographical variations in DNA content as great as 1.7-fold across this joint surface [29]. In this study, cellular content varied up to 1.9-fold in the adult equine stifle, with areas of higher cell content corresponding to areas with higher GAG content. This correlation between cellularity and GAG content was not found in neonatal cartilage, however. In general, cellularity of cartilage is thought to decrease with age, so the finding in this study of similar cellular content in both age groups was unexpected. Cellularity was determined by measuring

277

DNA content and calculating cell number based on the assumption that most mammalian cells contain approximately 7.7 pg of DNA per cell [54]. This study measuring DNA quantity was performed in adult rat cells, and it is uncertain whether neonatal cells also contain comparable levels of DNA. Another potential explanation for the relatively high cellularity of adult cartilage in this study is that there may have been some early degenerative changes in the samples tested that were not detected upon gross examination, as one of the early changes in osteoarthritis is an increase in cellularity as well as GAG content [55,56].

Histological staining also revealed that GAG distribution in both neonatal and adult cartilage was generally highest in the deep zone and the superficial-most region contained less GAG in adult cartilage compared to neonatal cartilage. This variation in GAG content corresponding with cartilage depth has also been observed in the equine fetlock [57]. Moreover, similar to fetlock cartilage, the degree of GAG variability across cartilage depth is higher in adult cartilage compared to neonatal cartilage [57]. Biochemical assays revealed that the MC region had the lowest GAG content in both adult and neonatal cartilage, although, overall, there were no significant differences between neonatal and adult GAG content. This lower GAG content in the MC in the adult may explain lower compressive properties observed in the adult in this region, as GAG content has been shown to correlate positively with compressive properties [58].

Adult cartilage generally had higher collagen staining compared to neonatal cartilage, and in many cases, staining was more intense in the superficial zone. Supporting this histological observation, Col/WW was found to be significantly higher in adult cartilage compared to neonatal when averaged across all levels (13.80 ± 1.54% and 10.61 ± 2.23%, respectively). This phenomenon of higher collagen content in the superficial zone of adult equine cartilage compared to neonatal equine cartilage has also been previously observed in the fetlock joint [57]. In the neonatal stifle joint, the regions of the trochlea had the highest

collagen content, whereas in the adult, the condyles had the highest collagen content. Collagen crosslinking trended higher in adult cartilage and was also significantly more variable compared to neonatal cartilage. This increase in crosslinking as well as overall collagen content is similar to that observed previously in a study comparing neonatal cartilage and cartilage from yearling horses [35].

While collagen content and crosslinking generally correlate positively with tensile properties [58], surprisingly, the stiffness (Young's modulus) of neonatal cartilage was significantly higher on average in the neonate compared to the adult. Neonatal cartilage had a Young's modulus of 16.2 ± 3.9 MPa and adult cartilage had a Young's modulus of 9.6 ± 2.1 MPa, on average. In the neonate, the Young's modulus of MR was significantly lower than the condyles and TG. Cartilage tensile strength (UTS) did not vary significantly between age groups. In the neonate, however, the TG had significantly higher UTS than the MR and LR. The UTS values measured in the adult stifle in this study are slightly lower (average 5.4 MPa), but comparable to those of a study in which tensile strength was measured at sites on the medial femoral condyle and medial trochlear ridge and found to be 6.7 MPa and 10.7 MPa, respectively [59]. Higher tensile stiffness in neonatal compared to adult cartilage has been observed in a previous study of the equine metacarpophalangeal joint. This study [57] examined tensile properties as well as collagen fiber arrangement in neonatal and adult cartilage and found that tensile stiffness correlated with the amount of collagen fibers that were arranged perpendicular to the surface (and thus perpendicular to the axis of tension). In adult cartilage, collagen fibers are primarily aligned parallel to the cartilage surface in the superficial zone and perpendicular to the surface in the deep zone. In neonatal cartilage, this collagen fiber alignment has not fully developed and, as a result, a greater proportion of collagen may have been aligned along the axis of tension, perhaps resulting in a higher measured stiffness [57].

While much of this discussion highlights the differences between neonatal and adult cartilage, there are a number of similarities between cartilages of neonatal and adult horses as well. Neonatal cartilage possesses mechanical and biochemical properties comparable to adult cartilage, suggesting that neonatal cartilage could withstand the loading forces incurred in the adult. This has implications for allograft techniques that may utilize a younger donor source for tissue. Good long-term outcome of a graft is undoubtedly a function of whether the graft tissue adequately recapitulates the properties of surrounding native tissue, such that it is able to withstand physiologic loading [60,61]. Furthermore, mismatch between repair tissue and surrounding native tissue results in stress concentrations at the interface between native and repair tissue, which can result in an acceleration of tissue degradation and failure of repair [62]. Using neonatal donor tissue offers the benefit of increased regenerative capacity of tissue from a younger donor source [16,44], which may facilitate lateral integration, while still closely matching properties of host cartilage at time of implantation. Similarities between adult and neonatal tissue properties may also be a consideration in regard to use of neonatal chondrocytes harvested from stifle joint tissue for tissue engineering purposes. It has been demonstrated that neocartilage generated from various topographical locations within a joint possess mechanical properties that corresponded to their tissue of origin, *i.e.* chondrocytes harvested from joint regions with higher mechanical properties produced neocartilage with higher mechanical properties compared to other joint regions [63]. Given that neonatal cartilage possesses properties comparable that of adult cartilage, neonatal chondrocytes may produce tissue engineered neocartilage with comparable properties to adult tissue as well.

Overall, this study characterized a wide topographical range of the distal femur and patella. As with any topographical study, the resolution of the topographical mapping of the measured properties was limited by the number of sampling sites tested; increasing the number of sample sites would have allowed for a higher level of understanding of the structure-function

280

relationship between tissue properties and tissue location within the joint. Loading forces experienced by the joint vary in a topographical manner as well. Therefore, in order to fully understand the relationship between tissue properties and tissue function, concomitant studies to determine forces experienced by articular cartilage during normal loading cycles will also need to be carried out. Additional age groups would further aid in the understanding of how loading influences maturation of articular cartilage, and how this maturation process manifests in regards to biochemical and biomechanical properties of the tissue. Another major limitation of this study was the heterogeneity of the patient population used in this study, which undoubtedly contributed to the large amount of variability in biochemical and biomechanical results. This study specifically compared neonatal and adult cartilage as neonatal cartilage and chondrocytes may serve as an ideal donor source for allografts or chondrocytes for tissue engineering strategies aimed at repair of damaged articular cartilage in the adult equine athlete. The results of this study, therefore, can be utilized in the establishment of design criteria for future engineered equine articular cartilage products as well as aid in assessment of the performance of engineered tissues in both *in vitro* and *in vivo* contexts.

CONCLUSION

This study provides qualitative and quantitative properties of native articular cartilage from the stifle of both neonatal and skeletally mature adult horses. This study represents the first time neonatal articular cartilage was comprehensively and quantitatively examined from the stifle and compared to adult cartilage in a head-to-head manner. The examination revealed important differences as well as similarities in morphological, histological, biochemical, and biomechanical properties among topographical sites within joint regions as well as age-related differences between neonatal and adult cartilage. An understanding of these topographical and age-related differences in properties between the therapeutic target cartilage (i.e., adult cartilage) as well as potential donor cartilage (i.e., neonatal cartilage) could aid in selection of optimal harvest sites

within a donor joint as well as evaluation of the success of the grafted cells or tissues within the host. Additionally, this work furthers the knowledge of cartilage tissue physiology and structure-function relationships.
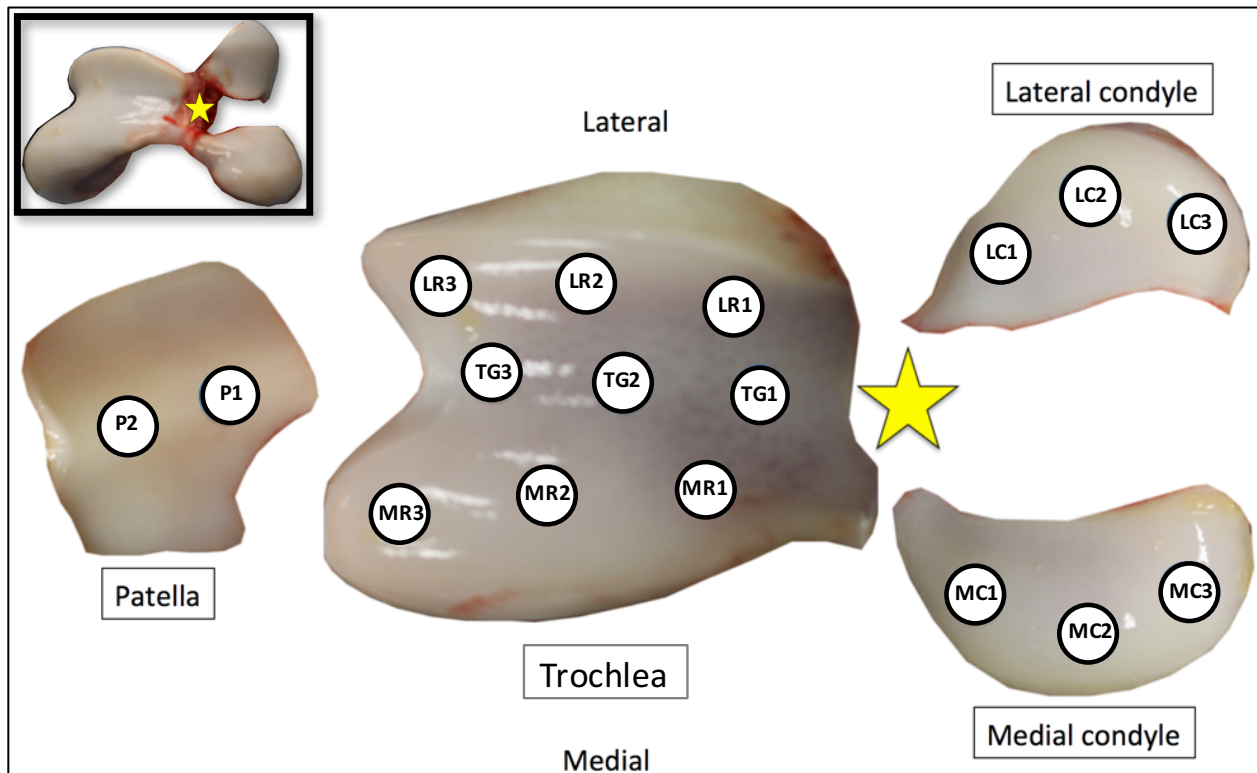
Figure 1- Articular cartilage from 17 sites across six regions of the distal femur and patella were characterized morphologically, histologically, biochemically, and biomechanically. The inset image at top left shows the distal femur with the star denoting the most axial portion of the joint surface. MC = medial condyle, LC = lateral condyle, LR = lateral ridge of the trochlea, MR = medial ridge of the trochlea, TG = trochlear groove, P = patella.

FIGURE 2
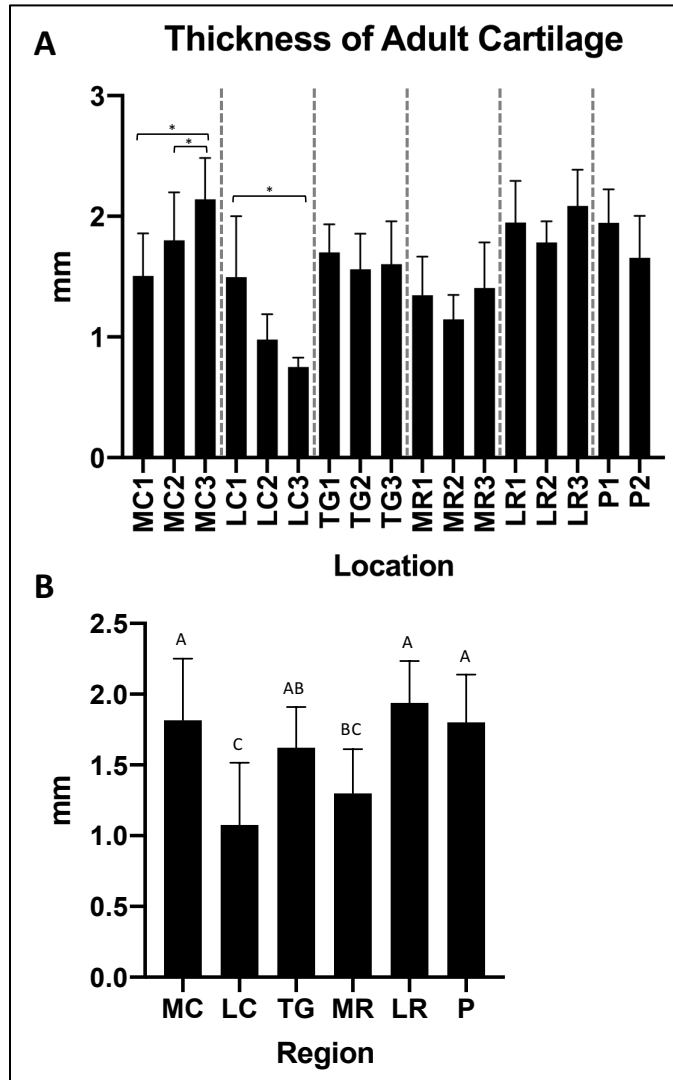
Figure 2 - Thickness of adult articular cartilage. All values are presented as mean ± s.d. Thickness of neonatal cartilage was not assessed as subchondral bone is not completely mineralized in neonates. A) Average thickness at all sampled sites across the joint. Each region is denoted by dashed gray vertical bars. Sites were compared within each region and starred bars (*) represent significant differences among sites within an individual region. MC3 is thicker than MC1 and MC2, whereas LC1 is significantly thicker than LC3. B) Average thickness across sites within each region. Regions that share the same letter above the error bars do not differ significantly. MC, TG, LR, and P are thicker than LC and MR.
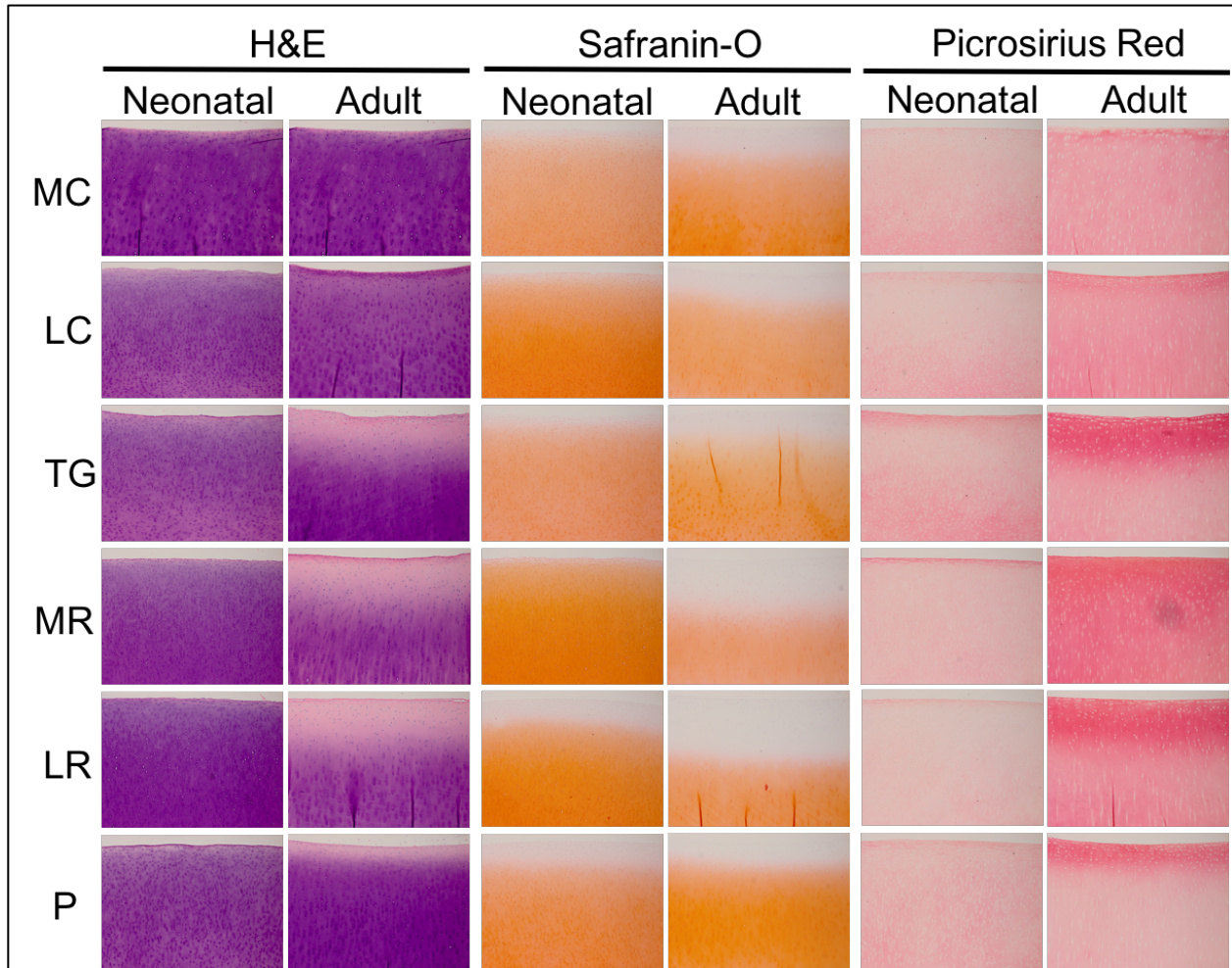
FIGURE 3

Figure 3- Histological evaluation of neonatal and adult articular cartilage cross sections. Neonatal cartilage stained more homogeneously basophilic with H&E stain as compared to adult cartilage. Adult cartilage stained eosinophilic in the superficial zone of the trochlear and patellar samples with H&E. Safranin-O stain for GAG was distributed through a greater proportion of neonatal cartilage compared to adult cartilage. Picrosirius red stain for collagen was more intense in adult cartilage compared to neonatal, particularly in the superficial zone.
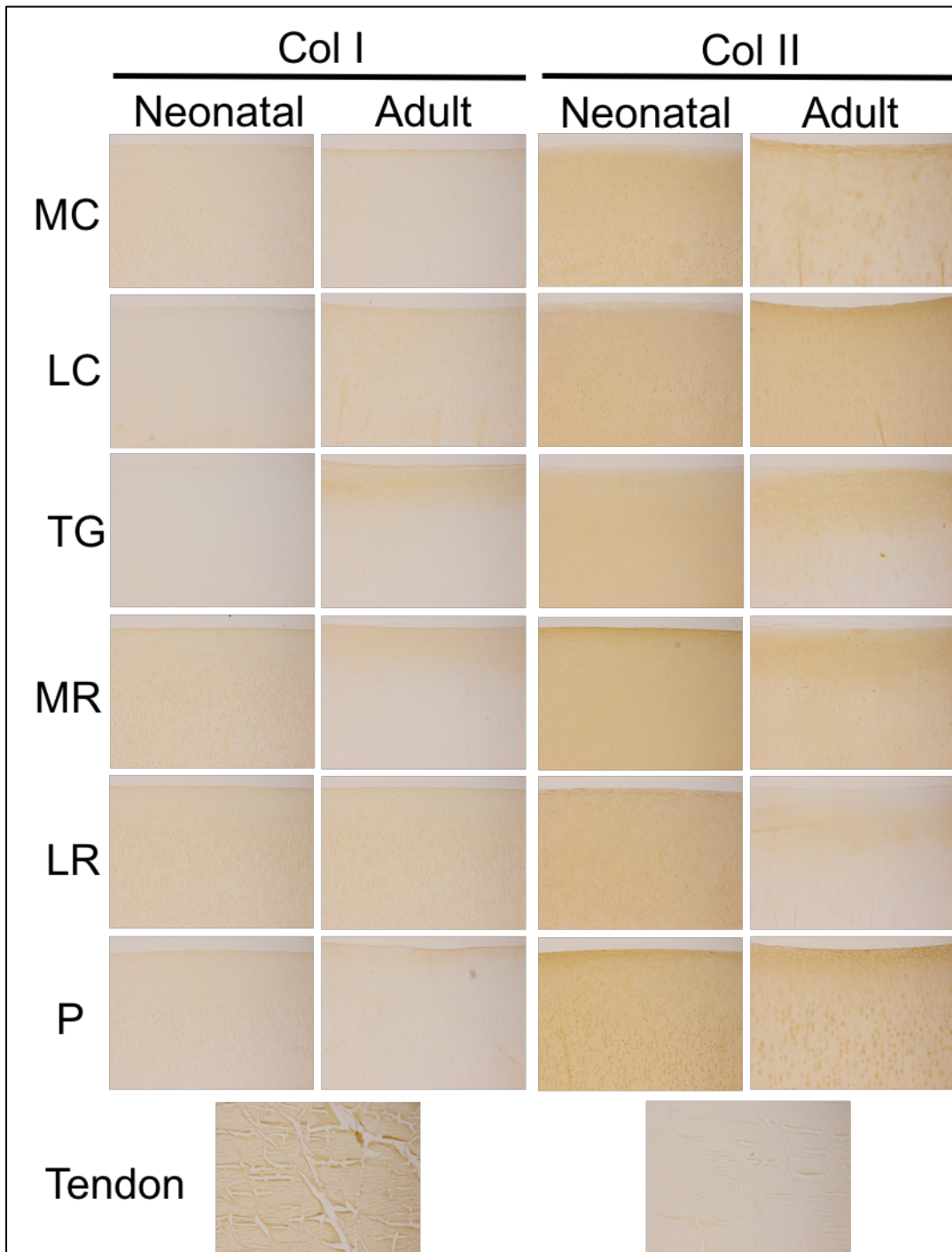
FIGURE 4

Figure 4- Immunohistochemical evaluation of neonatal and adult articular cartilage. Tendon, which is primarily comprised of collagen I, served as control. Both adult and neonatal cartilage stained more intensely for collagen II as compared to collagen I, whereas tendon stained more intensely for collagen I compared to collagen II. Overall, there were no dramatic differences between neonatal and adult cartilage in terms of specific collagen content staining using immunohistochemistry.
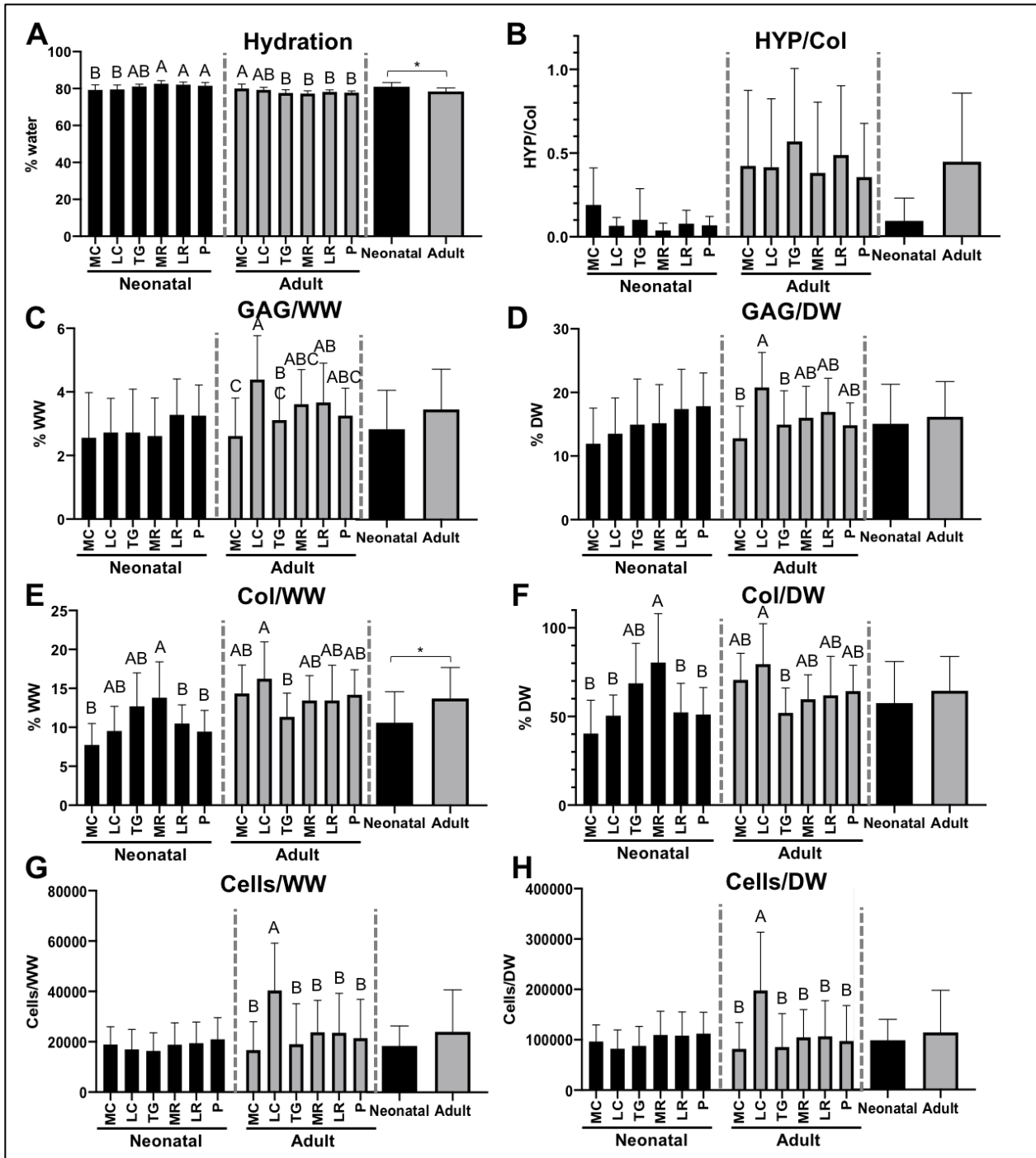
FIGURE 5

Figure 5- Biochemical characterization of regions and overall average for each age group: neonatal and adult. All values are presented as mean ± s.d. Starred bars (*) represent significant differences between age groups while regions that do not share the same letter within each age group differ significantly. (A) Hydration varied among regions in both the neonate and adult, and there was a significant difference of overall hydration between age groups. (B) Collagen cross linking (HYP) on a per collagen weight basis did not vary significantly among regions or between age groups, however, there was a trend for greater crosslinking in the adult. GAG varied among regions in the adult on a per wet weight (WW) (C) and per dry weight (DW) (D) basis. Collagen varied among regions in both the neonate and the adult on a per WW (E) and per DW (F) basis. Additionally, collagen/WW differed overall between the neonate and adult (E). Cellularity varied among regions in the adult on a per WW (G) and per DW (H) basis, but did not vary overall between the neonate and the adult. Topographical biochemical data are available in Tables 1 and 2.
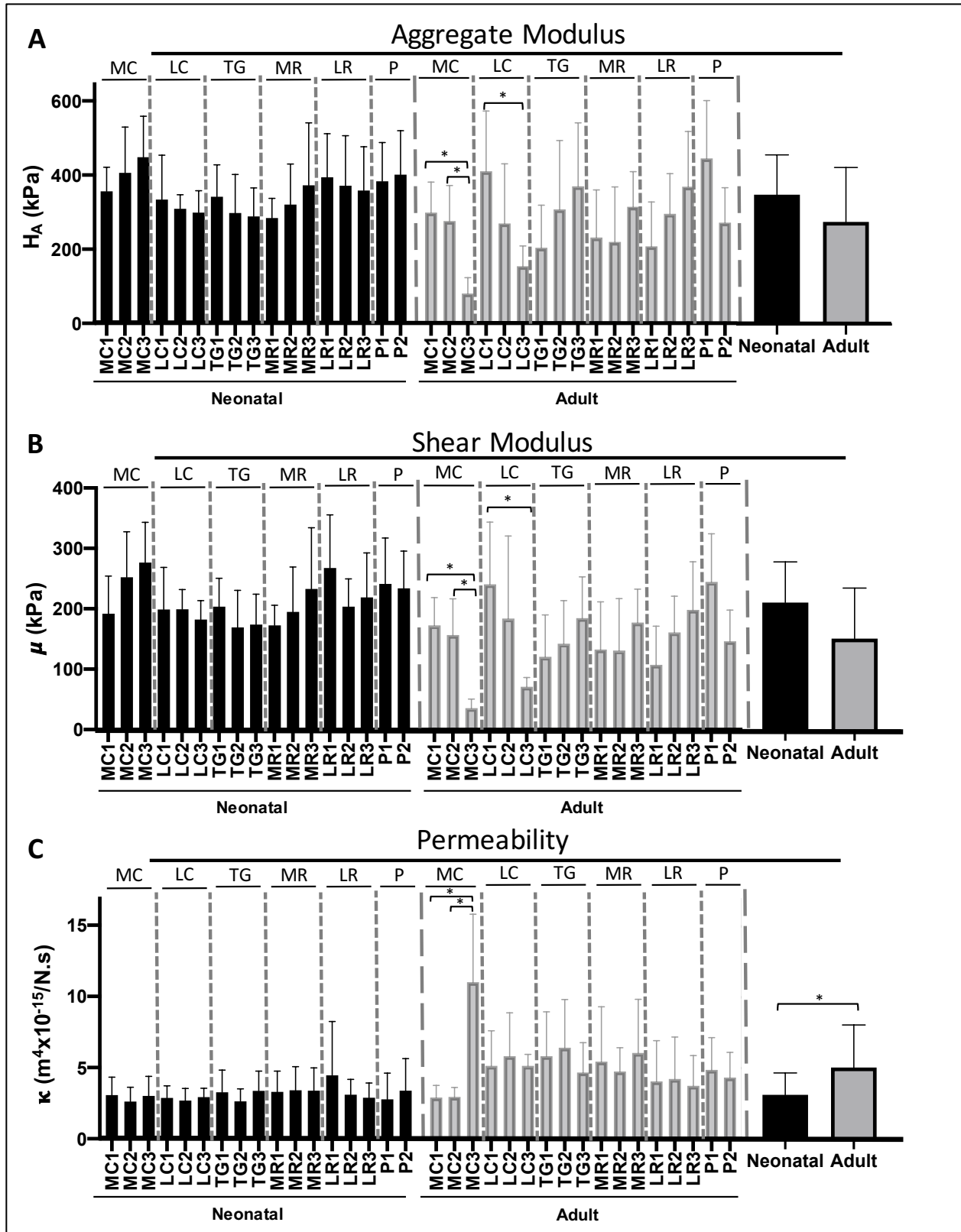
FIGURE 6

A Aggregate Modulus

B Shear Modulus

C Permeability

Figure 6- Characterization of compressive properties at each site within each region and overall average for each age group: neonatal and adult. All values are presented as mean ± s.d. Starred bars (*) represent significant differences among sites within each region as well as between overall averages of each age group. For both aggregate modulus (A) and shear modulus (B), MC1 and MC2 were significantly greater than MC3 and LC1 was significantly greater than LC3 in the adult. (C) Permeability was significantly greater in MC3 compared to MC1 and MC2 in the adult and varied significantly between the neonate and the adult overall. Topographical compressive property data are available in Table 3.
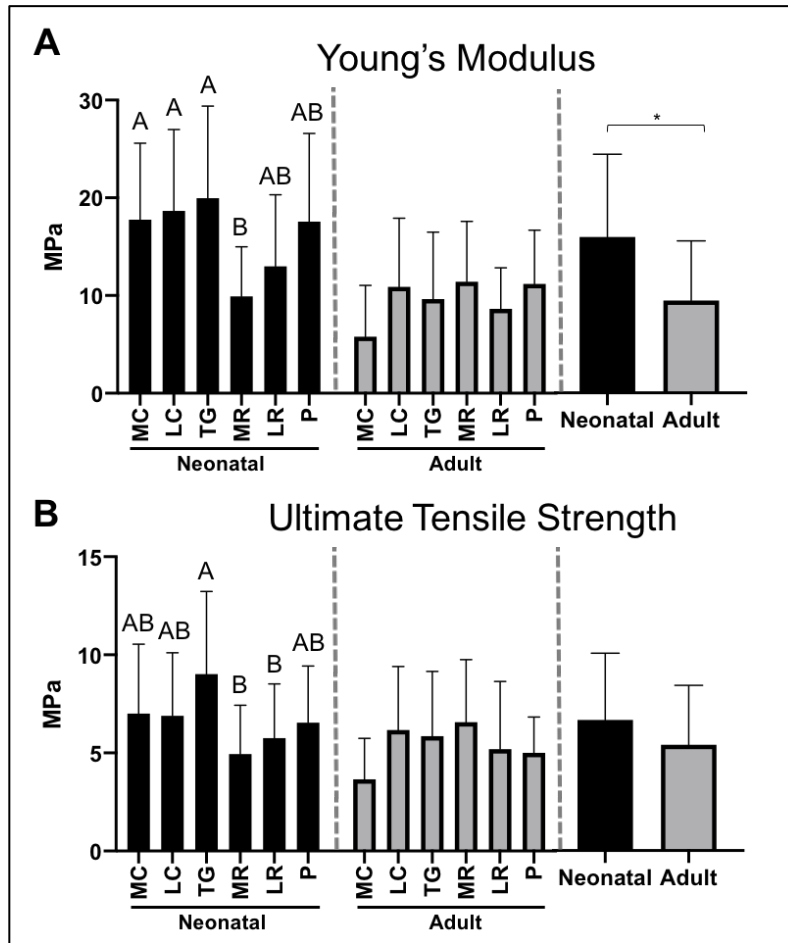
FIGURE 7

Figure 7- Characterization of tensile properties within each region and overall average for each age group: neonatal and adult. All values are presented as mean ± s.d. Starred bars (*) represent significant differences between age groups. Regions that do not share the same letter within each age group differ significantly. For both Young's modulus (A) and ultimate tensile strength (UTS) (B) there were significant differences among regions in the neonate but not adult cartilage. Neonatal cartilage had a significantly higher Young's modulus overall as compared to adult cartilage (A) as well.

TABLES

TABLE 1

Location		Neonatal	Adult	Neonatal	Adult	Neonatal	Adult
		Thickness (mm)		Hydration (%)		HPLC/Col (ug/ug)	
Medial Condyle (MC)	1	2.15 ± 0.60	1.51 ± 0.35	80.33 ± 1.75	78.00 ± 2.10	0.33 ± 0.33	0.19 ± 0.22
	2	2.31 ± 0.53	1.80 ± 0.40	80.20 ± 3.35	81.33 ± 1.51	0.10 ± 0.10	0.60 ± 0.45
	3	2.40 ± 0.22	2.14 ± 0.34	77.57 ± 2.07	80.67 ± 2.58	0.14 ± 0.12	0.48 ± 0.59
Lateral Condyle (LC)	1	2.05 ± 0.42	1.50 ± 0.51	77.33 ± 0.75	78.33 ± 0.82	0.06 ± 0.03	0.40 ± 0.38
	2	2.31 ± 0.30	0.98 ± 0.21	80.00 ± 1.67	79.17 ± 1.47	0.09 ± 0.08	0.40 ± 0.42
	3	2.28 ± 0.38	0.75 ± 0.08	81.00 ± 0.75	80.33 ± 1.21	0.05 ± 0.02	0.45 ± 0.51
Trochlear Groove (TG)	1	1.82 ± 0.32	1.70 ± 0.23	79.83 ± 2.50	78.00 ± 1.22	0.07 ± 0.08	0.65 ± 0.40
	2	2.06 ± 0.50	1.56 ± 0.30	81.50 ± 1.67	78.00 ± 2.61	0.05 ± 0.02	0.52 ± 0.53
	3	1.95 ± 0.50	1.60± 0.36	81.83 ± 1.55	76.83 ± 0.98	0.19 ± 0.32	0.54 ± 0.46
Medial Ridge (MR)	1	2.28 ± 0.48	1.35 ± 0.32	83.33 ± 2.42	76.50 ± 1.05	0.04 ± 0.06	0.55 ± 0.48
	2	2.34 ± 0.26	1.15 ± 0.20	82.50 ± 3.35	78.17 ± 1.60	0.02 ± 0.01	0.20 ± 0.30
	3	2.41 ± 0.19	1.41 ± 0.38	81.83 ± 2.07	77.17 ± 1.47	0.06 ± 0.05	0.40 ± 0.48
Lateral Ridge (LR)	1	2.24 ± 0.26	1.95 ± 0.34	81.67 ± 1.52	77.83 ± 0.75	0.06 ± 0.07	0.56 ± 0.49
	2	2.31 ± 0.35	1.78 ± 0.17	82.67 ± 1.75	78.33 ± 0.82	0.07 ± 0.07	0.57 ± 0.42
	3	2.34 ± 0.33	2.09 ± 0.30	81.83 ± 1.63	78.50 ± 1.52	0.11 ± 0.11	0.34 ± 0.38
Patella (P)	1	2.48 ± 0.28	1.95 ± 0.28	80.50 ± 1.37	77.33 ± 1.21	0.07 ± 0.03	0.32 ± 0.34
	2	2.24 ± 0.20	1.66 ± 0.35	82.33 ± 1.17	78.17 ± 0.41	0.06 ± 0.07	0.39 ± 0.33

Table 1- Thickness, hydration, and crosslinks per collagen of neonatal and adult articular cartilage from specific regions and sites within each region. Data are presented as mean ± s.d. Thickness of neonatal cartilage does not represent full thickness of cartilage layer, but rather the thickness of the trimmed explant used for biomechanical and biochemical testing.

TABLE 2

Location		Neonatal		Adult		Neonatal		Adult		Neonatal		Adult	
		GAG/WW (%)	GAG/DW (%)	GAG/WW (%)	GAG/DW (%)	Col/WW (%)	Col/DW (%)	Col/WW (%)	Col/DW (%)	Cell #/WW	Cell #/DW	Cell #/WW	Cell #/DW
Medial Condyle (MC)	1	2.33 ± 0.63	12.12 ± 6,55	3.17 ± 1.17	13.50 ± 3.62	6.67 ± 4.18	34.67 ± 19.03	16.17 ± 4.96	74.00 ± 21.20	19438 ± 7899	99897 ± 31054	22999 ± 13676	104887 ± 62547
	2	2.80 ± 1.47	13.00 ± 8.49	2.50 ± 1.38	13.83 ± 6.11	9.00 ± 1.22	57.00 ± 21.70	13.17 ± 2.79	68.00 12.38	20518 ± 6417	115661 ± 47423	12119 ± 6846	62445 ± 34672
	3	2.57 ± 1.26	11.14 ± 3.18	2.17 ± 0.98	11.00 ± 5.59	7.71 ± 1.80	33.43 ± 7.91	13.67 ± 2.66	69.83 ± 11.97	17330 ± 7519	79692 ± 45869	15005 ± 6967	78300 ± 55154
Lateral Condyle (LC)	1	2.33 ± 1.17	10.83 ± 5.53	4.50 ± 1.05	19.83 ± 4.36	11.67 ± 1.62	54.00 ± 10.53	16.33 ± 1.75	75.00 ± 8.85	17186 ± 9244	81223 ± 44140	37912 ± 7211	175210 ± 103385
	2	3.00 ± 1.51	15.83 ± 7.41	4.83 ± 1.94	22.33 ± 7.47	11.20 ± 1.92	55.40 ± 9.10	18.67 ± 6.86	87.83 ± 30.93	17884 ± 7535	87071 ± 30094	51355 ± 20022	201229 ± 124836
	3	2.83 ± 1.51	13.83 ± 2.79	3.83 ± 0.98	20.17 ± 4.88	8.67 ± 2.58	42.83 ± 12.06	13.20 ± 2.59	75.83 ± 24.59	15744 ± 8448	78426 ± 43025	32283 ± 8507	217376 ± 133904
Trochlear Groove (TG)	1	3.17 ± 1.37	16.00 ± 5.06	3.33 ± .82	16.50 ± 5.24	15.17 ± 4.67	77.67 ±24.97	11.33 ± 3.83	54.33 ± 20.75	15221 ± 7668	78098 ± 37127	11896 ± 7211	57553 ± 32795
	2	2.67 ± 1.10	15.33 ± 8.55	2.83 ± .75	14.33 ± 4.08	9.83 ± 3.54	55.33 ± 21.15	10.83 ± 3.54	49.67 ± 11.06	15975 ± 7124	86629 ± 37499	13830 ± 8104	64791 ± 3441
	3	2.33 ± 0.75	13.50 ± 8.46	3.17 ± 1.47	14.00 ± 6.90	13.00 ± 3.41	73.00 ± 18.37	11.83 ± 1.94	52.17 ± 9.89	17664 ± 8043	97495 ± 45014	30442 ± 21973	131066 ± 90432
Medial Ridge (MR)	1	3.00 ± 1.75	17.50 ± 5.68	3.50 ± 0.55	15.00 ± 3.52	12.17 ± 3.43	75.33 ± 23.01	13.50 ± 2.43	57.33 ± 10.11	16919 ± 7899	104931 ± 50480	28512 ± 11231	121703 ± 46462
	2	2.83 ±1.92	16.00 ± 5.66	4.00 ± 1.26	17.17 ± 5.71	12.00 ± 4.77	68.67 ± 28.32	12.50 ± 3.83	59.17 ± 16.62	17211 ± 9277	97576 ± 47413	25280 ± 16556	116364 ± 72597
	3	2.00 ± 0.79	12.00 ± 6.45	3.33 ± 1.37	15.83 ± 5.98	17.17 ± 4.12	97.33 ± 26.86	14.33 ± 3.44	62.67 ± 15.63	23163 ± 8873	129168 ± 45869	17374 ± 6967	74565 ± 28750
Lateral Ridge (LR)	1	3.50 ± 0.98	17.50 ± 3.39	3.50 ± 1.22	15.83 ± 4.31	9.67 ± 3.67	50.83 ± 17.17	11.33 ± 3.20	49.67 ± 14.56	15580 ± 7191	83247 ± 35566	20050 ± 17212	88966 ± 76922
	2	3.33 ± 0.82	19.83 ± 6.49	4.00 ± 1.79	19.00 ± 8.02	10.33 ± 3.50	59.33 ± 17.19	13.67 ± 6.50	64.33 ± 31.11	19387 ± 8238	113977 ± 49940	23565 ± 17936	107395 ± 78804
	3	3.00 ± 0.55	14.83 ± 7.99	3.50 ± 0.55	16.00 ± 2.19	8.50 ± 2.51	46.83 ± 14.81	15.33 ± 2.73	71.67 ± 13.03	23282 ± 9342	127229 ± 50080	27729 ± 13210	128023 ± 61199
Patella (P)	1	2.83 ± 1.21	15.17 ± 4.67	3.17 ± 1.17	14.33 ± 4.80	9.50 ± 3.21	48.83 ± 13.41	15.33 ± 3.93	69.50 ± 17.69	19214 ± 8540	97807 ± 39406	17374 ± 12545	77906 ± 55193
	2	3.67 ± 1.55	20.50 ± 4.59	3.33 ± 0.52	15.33 ± 1.97	9.33 ± 2.50	53.33 ± 17.80	13.00 ± 2.00	59.17 ± 9.50	22687 ± 9066	126603 ± 43078	26320 ± 18516	121318 ± 84902

Table 2: GAG, collagen, and cell number on a per wet weight (WW) and per dry weight (DW) basis of neonatal and adult articular cartilage from specific regions and sites within each region. Data are presented as mean ± s.d.

TABLE 3

Table 3: Compressive properties of neonatal and adult articular cartilage from specific regions and sites within each region. Data are presented as mean ± s.d.

Location		Neonatal			Adult		
		Aggregate Modulus (kPa)	Shear Modulus (kPa)	Permeability (m^4x10^{-15}/N.s)	Aggregate Modulus (kPa)	Shear Modulus (kPa)	Permeability (m^4x10^{-15}/N.s)
Medial Condyle (MC)	1	356 ± 53	192 ± 62	3.07 ± 1.26	307 ± 82	173 ± 79	2.9 ± 0.84
	2	406 ± 110	252 ± 75	2.61 ± 1.02	370 ± 96	157 ± 86	2.95 ± .65
	3	448 ± 169	277 ± 67	3.01 ± 1.34	81 ± 42	35 ± 56	11.00 ± 4.78
Lateral Condyle (LC)	1	334 ± 120	199 ± 70	2.87 ± 0.84	410 ± 162	241 ± 69	5.12 ± 2.46
	2	309 ± 38	199 ± 33	2.69 ± 0.84	270 ± 161	184 ± 72	5.80 ± 3.05
	3	299 ± 59	182 ± 31	2.92 ± 0.62	204 ± 54	71 ± 68	5.13 ± 0.80
Trochlear Groove (TG)	1	342 ± 86	204 ± 47	3.26 ± 1.57	204 ± 115	120 ± 103	5.80 ± 3.12
	2	297 ± 105	169 ± 61	2.63 ± 0.88	307 ± 186	142 ± 137	6.40 ± 3.39
	3	289 ± 76	174 ± 50	3.36 ± 1.40	370 ± 171	185 ± 15	4.66 ± 2.10
Medial Ridge (MR)	1	284 ± 53	172 ± 33	3.30 ± 1.45	231 ± 128	132 ± 46	5.42 ± 3.86
	2	320 ± 110	195 ± 74	3.40 ± 1.66	220 ± 148	131 ± 60	4.73 ± 1.68
	3	372 ± 169	233 ± 101	3.38 ± 1.60	315 ± 95	177 ± 15	6.03 ± 3.78
Lateral Ridge (LR)	1	394 ± 118	267 ± 88	4.45 ± 3.79	208 ± 120	107 ± 80	4.03 ± 2.87
	2	372 ± 134	204 ± 46	3.09 ± 1.08	295 ± 108	161 ± 52	4.20 ± 2.94
	3	358 ± 118	219 ± 74	2.88 ± 1.04	369 ± 149	198 ± 64	3.72 ± 2.12
Patella (P)	1	394 ± 118	267 ± 88	4.45 ± 3.79	445 ± 156	244 ± 60	4.84 ± 2.27
	2	401 ± 119	234 ± 62	3.38 ± 2.25	272 ± 95	146 ± 80	4.30 ± 1.77

TABLE 4

Location		Neonatal		Adult	
		Young's Modulus (MPa)	UTS (MPa)	Young's Modulus (MPa)	UTS (MPa)
Medial Condyle (MC)	1	14.0 ± 4.1	6.6 ± 3.7	10.9 ± 6.2	4.9 ± 2.3
	2	17 ± 5.9	7.5 ± 3.6	4.1 ± 2.4	2.0 ± 1.7
	3	22.4 ± 10.7	7.0 ± 3.9	2.4 ± 1.1	3.7 ± 4.7
Lateral Condyle (LC)	1	21.2 ± 8.9	6.2 ± 2.5	12.5 ± 11.2	5.8 ± 3.5
	2	16.4 ± 8.9	6.2 ± 3.7	9.1 ± 3.1	5.3 ± 1.8
	3	18.4 ± 10.9	8.2 ± 3.5	11.1 ± 5.1	7.4 ± 4.1
Trochlear Groove (TG)	1	25.3 ± 10.7	12.1 ± 4.9	7.0 ± 7.0	4.1 ± 2.2
	2	22.0 ± 9.6	8.6 ± 2.4	9.4 ± 6.3	6.0 ± 2.8
	3	13.5 ± 4.1	6.4 ± 3.2	12.5 ± 7.1	7.5 ± 4.1
Medial Ridge (MR)	1	10.2 ± 7.3	5.1 ± 2.2	10.3 ± 6.4	7.2 ± 2.8
	2	11.0 ± 4.3	5.4 ± 2.0	9.5 ± 3.5	5.4 ± 1.7
	3	8.6 ± 3.6	4.4 ± 3.4	14.4 ± 7.7	7.1 ± 4.7
Lateral Ridge (LR)	1	15.2 ± 11.0	5.9 ± 2.5	8.8 ± 4.1	6.4 ± 4.3
	2	13.7 ± 6.8	6.4 ± 3.2	9.7 ± 5.3	5.1 ± 3.4
	3	10.1 ± 4.4	4.9 ± 2.9	7.4 ± 3.5	4.0 ± 2.6
Patella (P)	1	20.0 ± 11.3	7.5 ± 2.9	11.4 ± 4.7	5.4 ± 1.7
	2	15.1 ± 4.3	5.6 ± 2.8	11.0 ± 6.6	4.6 ± 2.0

Table 4- Tensile properties of neonatal and adult articular cartilage from specific regions and sites within each region. Data are presented as mean ± s.d.

REFERENCES

1. Vacek, J.R., Ford, T.S. and Honnas, C.M. (1992) Communication between the femoropatellar and medial and lateral femorotibial joints in horses. *Am J Vet Res* **53**, 1431–1434.

2. Bryceland, J.K., Powell, A.J. and Nunn, T. (2016) Knee Menisci. *Cartilage* **8**, 99–104.

3. Singer, E.R., Barnes, J., Saxby, F. and Murray, J.K. (2008) Injuries in the event horse: Training versus competition. *The Veterinary Journal* **175**, 76–81.

4. Olstad, K., Ekman, S. and Carlson, C.S. (2015) An Update on the Pathogenesis of Osteochondrosis. *Vet. Pathol.* **52**, 785–802.

5. Auer, J.A. (1992) *Equine Surgery*, W B Saunders Company.

6. Desjardin, C., Riviere, J., Vaiman, A., Morgenthaler, C., Diribarne, M., Zivy, M., Robert, C., Le Moyec, L., Wimel, L., Lepage, O., Jacques, C., Cribiu, E. and Schibler, L. (2014) Omics technologies provide new insights into the molecular physiopathology of equine osteochondrosis. *BMC Genomics* **15**, 947–12.

7.   Jiménez, G., Cobo-Molinos, J., Antich, C. and López-Ruiz, E. (2018) Osteoarthritis: Trauma vs Disease. In: *Osteochondral Tissue Engineering*, Springer International Publishing, Cham. pp 63–83.

8.   De Lasalle, J., Alexander, K., Olive, J. and Laverty, S. (2016) Comparisons among radiography, ultrasonography and computed tomography for ex vivo characterization of stifle osteoarthritis in the horse. *Veterinary Radiology & Ultrasound* **57**, 489–501.

9.   Schlueter, A.E., Orth, M.(null) Equine osteoarthritis: a brief review of the disease and its causes. Equine Comp. *Equine and Comparative Exercise Physiology* **1**, 221–231.

10.   Jeffcott, L.B. and Kold, S.E. (1982) Stifle lameness in the horse: A survey of 86 referred cases. *Equine Veterinary Journal* **14**, 31–39.

11.   Fowlie, J.G., Arnoczky, S.P., Lavagnino, M. and Stick, J.A. (2011) Stifle extension results in differential tensile forces developing between abaxial and axial components of the cranial meniscotibial ligament of the equine medial meniscus: A mechanistic explanation for meniscal tear patterns. *Equine Veterinary Journal* **44**, 554–558.

12.   Dubuc, J., Girard, C., Richard, H., De Lasalle, J. and Laverty, S. (2017) Equine meniscal degeneration is associated with medial femorotibial osteoarthritis. *Equine Veterinary Journal* **50**, 133–140.

13.   Morisset, S., Frisbie, D.D., Robbins, P.D., Nixon, A.J. and McIlwraith, C.W. (2007) IL-1ra/IGF-1 Gene Therapy Modulates Repair of Microfractured Chondral Defects. *Clinical Orthopaedics and Related Research* **462**, 221–228.

14.   Johnson, S.A. and Frisbie, D.D. (2016) Cartilage Therapy and Repair in Equine Athletes. *Operative Techniques in Orthopaedics* **26**, 155–165.

15.   McIlwraith, C.W., Fortier, L.A., Frisbie, D.D. and Nixon, A.J. (2011) Equine Models of Articular Cartilage Repair. *Cartilage* **2**, 317–326.

16.   Smeriglio, P., Lai, J.H., Dhulipala, L., Behn, A.W., Goodman, S.B., Smith, R.L., Maloney, W.J., Yang, F. and Bhutani, N. (2015) Comparative Potential of Juvenile and Adult Human Articular Chondrocytes for Cartilage Tissue Formation in Three-Dimensional Biomimetic Hydrogels. *Tissue Engineering Part A* **21**, 147–155.

17.   Jiang, Y. and Tuan, R.S. (2014) Origin and function of cartilage stem/progenitor cells in osteoarthritis. *Nat Rev Rheumatol* **11**, 206–212.

18.   Wang, A.-T., Feng, Y., Jia, H.-H., Zhao, M. and Yu, H. (2019) Application of mesenchymal stem cell therapy for the treatment of osteoarthritis of the knee: A concise review. *WJSC* **11**, 222–235.

19.   Ortved, K.F. and Nixon, A.J. (2016) Cell-based cartilage repair strategies in the horse. *The Veterinary Journal* **208**, 1–12.

20.   Monaco, Lo, M., Merckx, G., Ratajczak, J., Gervois, P., Hilkens, P., Clegg, P., Bronckaers, A., Vandeweerd, J.-M. and Lambrichts, I. (2018) Review Article Stem Cells for Cartilage Repair: Preclinical Studies and Insights in Translational Animal Models and Outcome Measures. *Stem Cells International* 1–22.

21.   Wilke, M.M., Nydam, D.V. and Nixon, A.J. (2007) Enhanced early chondrogenesis in

articular defects following arthroscopic mesenchymal stem cell implantation in an equine model. *J. Orthop. Res.* **25**, 913–925.

22. Makris, E.A., Gomoll, A.H., Malizos, K.N., Hu, J.C. and Athanasiou, K.A. (2014) Repair and tissue engineering techniquesfor articular cartilage. *Nature Publishing Group* 1–14.

23. Huang, B.J., Hu, J.C. and Athanasiou, K.A. (2016) Cell-based tissue engineering strategies used in the clinical repair of articular cartilage. **98**, 1–22. http://linkinghub.elsevier.com/retrieve/pii/S0142961216301296.

24. Kwon, H., Paschos, N.K., Hu, J.C. and Athanasiou, K. (2016) Articular cartilage tissue engineering: the role of signaling molecules. *Cell. Mol. Life Sci.* **73**, 1173–1194.

25. McIlwraith, C.W. (2015) *Joint Disease in the Horse*, Elsevier Health Sciences.

26. Brama, P.A.J., Holopainen, J., van Weeren, P.R., FIRTH, E.C., Helminen, H.J. and Hyttinen, M.M. (2009) Influence of exercise and joint topography on depth-related spatial distribution of proteoglycan and collagen content in immature equine articular cartilage. *Equine Veterinary Journal* **41**, 557–563.

27. Brama, P.A.P., Tekoppele, J.M.J., Bank, R.A.R., van Weeren, P.R.P. and Barneveld, A.A. (1999) Influence of different exercise levels and age on the biochemical characteristics of immature equine articular cartilage. *Audio, Transactions of the IRE Professional Group on* 55–61.

28. Brama, P.A.J., Holopainen, J., van Weeren, P.R., Firth, E.C., Helminen, H.J. and Hyttinen, M.M. (2009) Effect of loading on the organization of the collagen fibril network in juvenile equine articular cartilage. *J. Orthop. Res.* **27**, 1226–1234.

29. Brama, P.A.J., Tekoppele, J.M., Bank, R.A., Karssenberg, D., Barneveld, A. and van Weeren, P.R. (2006) Topographical mapping of biochemical properties of articular cartilage in the equine fetlock joint. 1–8.

30. Hyttinen, M.M., Holopainen, J., René van Weeren, P., Firth, E.C., Helminen, H.J. and Brama, P.A.J. (2009) Changes in collagen fibril network organization and proteoglycan distribution in equine articular cartilage during maturation and growth. *Journal of Anatomy* **215**, 584–591.

31. Holopainen, J.T., Brama, P.A.J., Halmesmäki, E., Harjula, T., Tuukkanen, J., van Weeren, P.R., Helminen, H.J. and Hyttinen, M.M. (2008) Changes in subchondral bone mineral density and collagen matrix organization in growing horses. *Bone* **43**, 1108–1114.

32. van der Harst, M.R., van de Lest, C.H.A., DeGroot, J., Kiers, G.H., Brama, P.A.J. and van Weeren, P.R. (2005) Study of cartilage and bone layers of the bearing surface of the equine metacarpophalangeal joint relative to different timescales of maturation. 1–7.

33. Brommer, H., Brama, P.A.J., Laasanen, M.S., Helminen, H.J., van Weeren, P.R. and Jurvelin, J.S. (2005) Functional adaptation of articular cartilage from birth to maturity under the influence of loading: a biomechanical analysis. *Equine Veterinary Journal* **37**, 148–154.

34. Weeren, P.R., Firth, E.C., Brommer, H., Hyttinen, M.M., Helminen, H.J., Rogers, C.W.,

DeGroot, J. and Brama, P.A.J. (2010) Early exercise advances the maturation of glycosaminoglycans and collagen in the extracellular matrix of articular cartilage in the horse. *Equine Veterinary Journal* **40**, 128–135.

35. Brama, P., Tekoppele, J.M., Bank, R.A., Barneveld, A. and van Weeren, P.R. (2000) Functional adaptation of equine articular cartilage: the formation of regional biochemical characteristics up to age one year. *Equine Veterinary Journal* **32**, 217–221.

36. Vachon, A.M., Keeley, F.W., McIlwraith, C.W. and Chapman, P. (1990) Biochemical analysis of normal articular cartilage in horses. *Am J Vet Res* **51**, 1905–1911.

37. Palmer, J.L., Bertone, A.L., Malemud, C.J., Carter, B.G., Papay, R.S. and Mansour, J. (1995) Site-specific proteoglycan characteristics of third carpal articular cartilage in exercised and nonexercised horses. *Am J Vet Res* **56**, 1570–1576.

38. Palmer, J.L., Bertone, A.L., Malemud, C.J. and Mansour, J. (1996) Biochemical and biomechanical alterations in equine articular cartilage following an experimentally-induced synovitis. *Osteoarthritis and Cartilage* **4**, 127–137.

39. Murray, R.C., DeBowes, R.M., Gaughan, E.M., Zhu, C.F. and Athanasiou, K.A. (1998) The effects of intra-articular methylprednisolone and exercise on the mechanical properties of articular cartilage in the horse. *Osteoarthritis and Cartilage* **6**, 106–114.

40. Murray, R.C., DeBowes, R.M., Gaughan, E.M., Mosier, D.E. and Athanasiou, K.A. (1995) Variations in the Biomechanical Properties of Articular Cartilage of the Midcarpal Joint of Normal Horses. *Veterinary and Comparative Orthopaedics and Traumatology* **8**, 11–18.

41. Murray, R.C., Zhu, C.F., Goodship, A.E., Lakhani, K.H., Agrawal, C.M. and Athanasiou, K.A. (1999) Exercise affects the mechanical properties and histological appearance of equine articular cartilage. *J. Orthop. Res.* **17**, 725–731.

42. O'Leary, S.A., White, J.L., Hu, J.C. and Athanasiou, K.A. (2018) Biochemical and biomechanical characterisation of equine cervical facet joint cartilage. *Equine Veterinary Journal* **50**, 800–808.

43. Changoor, A., Hurtig, M.B., Runciman, R.J., Quesnel, A.J., Dickey, J.P. and Lowerison, M. (2006) Mapping of donor and recipient site properties for osteochondral graft reconstruction of subchondral cystic lesions in the equine stifle joint. *Equine Veterinary Journal* 1–7.

44. Yanke, A.B., Tilton, A.K., Wetters, N.G., Merkow, D.B. and Cole, B.J. (2015) DeNovo NT Particulated Juvenile Cartilage Implant. *Sports Med Arthrosc Rev* **23**, 125–129.

45. Taylor, S.E.B., Lee, J., Smeriglio, P., Razzaque, A., Smith, R.L., Dragoo, J.L., Maloney, W.J. and Bhutani, N. (2016) Identification of Human Juvenile Chondrocyte-Specific Factors that Stimulate Stem Cell Growth. *Tissue Engineering Part A* **22**, 645–653.

46. Athanasiou, K.A., Agarwal, A., Muffoletto, A., Dzida, F.J., Constantinides, G. and Clem, M. (1995) Biomechanical properties of hip cartilage in experimental animal models. *Clinical Orthopaedics and Related Research* 254–266.

47. Cissell, D.D., Link, J.M., Hu, J.C. and Athanasiou, K.A. (2017) A Modified Hydroxyproline Assay Based on Hydrochloric Acid in Ehrlich's Solution Accurately Measures Tissue

Collagen Content. *Tissue Engineering Part C: Methods* **23**, 243–250.

48. Bank, R.A., Beekman, B., Verzijl, N., de Roos, J.A., Sakkee, A.N. and Tekoppele, J.M. (1997) Sensitive fluorimetric quantitation of pyridinium and pentosidine crosslinks in biological samples in a single high-performance liquid chromatographic run. *J Chromatogr B Biomed Sci Appl* **703**, 37–44.

49. Ionescu, L.C., Lee, G.C., Garcia, G.H., Zachry, T.L., Shah, R.P., Sennett, B.J. and Mauck, R.L. (2011) Maturation state-dependent alterations in meniscus integration: implications for scaffold design and tissue engineering. *Tissue Engineering Part A* **17**, 193–204.

50. Wong, M. and Carter, D.R. (2003) Articular cartilage functional histomorphology and mechanobiology: a research perspective. *Bone* **33**, 1–13.

51. Halley, S.E., Bey, M.J., Haladik, J.A., Lavagnino, M. and Arnoczky, S.P. (2013) Three dimensional, radiosteriometric analysis (RSA) of equine stifle kinematics and articular surface contact: A cadaveric study. *Equine Veterinary Journal* **46**, 364–369.

52. Adrian, A.M., Barrett, M.F., Werpy, N.M., Kawcak, C.E., Chapman, P.L. and Goodrich, L.R. (2016) A comparison of arthroscopy to ultrasonography for identification of pathology of the equine stifle. *Equine Veterinary Journal* **49**, 314–321.

53. Fowlie, J.G., Arnoczky, S.P., Stick, J.A. and Pease, A.P. (2010) Meniscal translocation and deformation throughout the range of motion of the equine stifle joint: An in vitro cadaveric study. *Equine Veterinary Journal* **43**, 259–264.

54. Bibbiani, C., Tongiani, R. and Viola-Magni, M. (1969) I. Quantitative determination of the amount of DNA per nucleus by interference microscopy. *J Cell Biol* **42**, 444–451.

55. Poole, C.A., Matsuoka, A. and Schofield, J.R. (1991) Chondrons from articular cartilage. III. Morphologic changes in the cellular microenvironment of chondrons isolated from osteoarthritic cartilage. *Arthritis Rheum* **34**, 22–35.

56. D'Lima, D.D., Hashimoto, S., Chen, P.C., Colwell, C.W. and Lotz, M.K. (2001) Impact of mechanical trauma on matrix and cells. *Clinical Orthopaedics and Related Research* **391**, S90–9.

57. Oinas, J., Ronkainen, A.P., Rieppo, L., Finnilä, M.A.J., Iivarinen, J.T., van Weeren, P.R., Helminen, H.J., Brama, P.A.J., Korhonen, R.K. and Saarakkala, S. (2018) Composition, structure and tensile biomechanical properties of equine articular cartilage during growth and maturation. *Sci. Rep.* **8**, 1–12.

58. Athanasiou, K.A., Darling, E.M., Hu, J.C., DuRaine, G.D. and Reddi, A.H. (2017) *Articular Cartilage*, CRC Press.

59. Lewis, C.W., Williamson, A.K., Chen, A.C., Bae, W.C., Temple, M.M., Wong, W.V., Nugent, G.E., James, S.P., Wheeler, D.L., Sah, R.L. and Kawcak, C.E. (2005) Evaluation of subchondral bone mineral density associated with articular cartilage structure and integrity in healthy equine joints with different functional demands. *Am J Vet Res* **66**, 1823–1829.

60. Koh, Y.-G., Lee, J.-A., Kim, Y.S., Lee, H.Y., Kim, H.J. and Kang, K.-T. (2019) Optimal

mechanical properties of a scaffold for cartilage regeneration using finite element analysis. *Journal of Tissue Engineering* **10**, 2041731419832133.

61.   Bowland, P., Ingham, E., Jennings, L. and Fisher, J. (2015) Review of the biomechanics and biotribology of osteochondral grafts used for surgical interventions in the knee. *Proc Inst Mech Eng H* **229**, 879–888.

62.   Kock, N.B., Smolders, J.M.H., van Susante, J.L.C., Buma, P., van Kampen, A. and Verdonschot, N. (2008) A cadaveric analysis of contact stress restoration after osteochondral transplantation of a cylindrical cartilage defect. *Knee Surg Sports Traumatol Arthrosc* **16**, 461–468.

63.   Paschos, N.K., Makris, E.A., Hu, J.C. and Athanasiou, K.A. (2014) Topographic Variations in Biomechanical and Biochemical Properties in the Ankle Joint: An In Vitro Bovine Study Evaluating Native and Engineered Cartilage. *Arthroscopy: The Journal of Arthroscopic and Related Surgery* **30**, 1317–1326.

APPENDIX C - EFFECT OF CONTROLLING GROUP HETEROGENEITY ON STUDENT PERFORMANCE IN A GRAPHICAL PROGRAMMING COURSE

ABSTRACT

This study assesses whether students perform better in an introductory programming course if they are placed in groups with people of the same or varying programming aptitude. Although the push for teaching code in U.S K-12 classrooms is growing, students arrive to college with a variety of coding experience because only not all schools include coding in their curriculum. Understanding what makes a group productive and efficient is important as the use of active-learning pedagogies across college classrooms grows. The studies presented here aim to 1) predict how well a student will perform in an introductory programming course based on a pre-assessment administered at the beginning of the course and 2) determine whether students perform better in an introductory programming course if they participate in team based projects with people of the same or varying programming aptitude. During the first week of class, students were administered a pre-assessment. Their score determined individual student programming aptitude. Students were assigned to groups based on their performance, where control groups consisted of students who only scored as high programming aptitude or only scored low programming aptitude, and experimental teams consisted of a mix of both. Evidence was found to indicate that the group formation pre-assessment was a good indicator of programming aptitude. The positive findings and their effect on students' abilities to learn a programming language demonstrated that the technique of a short assessment and assigned groups may become an important tool to create more effective groups in large introductory programming courses. Although further testing is required, this technique may shape the future of group formation in large programming courses.

INTRODUCTION

In recent decades, science education policy has moved toward advocating for course curriculums involving teamwork (also known as group work) [1]. Primarily, group work has been shown to play a role in improving problem-solving, critical thinking, and communication skills [2]–[5]. The inclusion of group work assignments in engineering course curriculums is also motivated by survey studies in which both employees and employers participate. For example, when industry employers were asked which skillsets they found to be most valuable in their employees, the most common response was teamwork and communication [6], [7]. Furthermore, when engineering graduates were inquired about the skills they developed as undergraduate students, engineering graduates in both academia and industry rated teamwork, communication, and data analysis to be the most salient skillsets [8]. Thus, group work has been integrated in most course curriculums by utilizing several different strategies such as collaborative and cooperative learning [5], [9].

In large, undergraduate, introductory programming courses for engineers however, instructors are often met with obstacles when attempting to implement collaborative and cooperative learning activities. In particular, students enter their undergraduate careers with a variety of science, math, and coding backgrounds. Coding backgrounds and knowledge of programming languages have notably been found to be a major disparity among engineering undergraduate students. [10], [11]. Although industry leaders in Silicone Valley and biotechnology push for, and even fund, the development of coding skills in K-12 schools, only 1 in 4 high schools in the United States include coding and programming in their course curriculum [10]. The difference in academic backgrounds can affect group dynamics, and the outcomes of group work vary depending on levels of experience [1]. Understanding what makes a group beneficial to student learning is important as the need for coding ability becomes inevitable and the use of active-learning pedagogies across college classrooms grows.

Currently, there is a lack of consensus on what group formation should be based on [1]. Although allowing students to choose their own groups alleviates administrative duties for instructors, especially in large college classrooms, this may not necessarily be the most beneficial for student learning. For instance, in class activities, it may be more beneficial for students to be placed in groups with other students of homogeneous academic backgrounds or abilities so that the instructor can focus on groups of students who are behind in the course material [12], [13]. Conversely, for group work done outside the classroom, homogeneous groups may cause groups of students who lack in ability and academic background to fall further behind. Furthermore, if students are to be placed in heterogeneous groups, it is unclear whether heterogeneity should be based on intellectual aptitude, grade point average, motivation, or other latent factors [6],[14],[15].

In this study, how students perform in an introductory graphical programming course if they are placed in groups with people of the same or varying coding aptitude is assessed. First, a group formation pre-assessment was distributed to the study participants of a large lower-division programming course. The group formation pre-assessment consisted of three sections: an academic coding background survey, a motivation survey, and a diagrammatic reasoning pre-assessment. The students were divided into groups based on the section of the pre-assessment that indicated the most disparity amongst students. This study first assessed whether the group formation pre-assessment was a good indicator of how well the students would perform in the class. Next, by inspecting both individual and group outcomes, the hypothesis that students would perform better if placed in a heterogeneous group was tested. Finally, student enjoyment of group work and approval of group members was quantified through the administration of a survey at the end of the course. The following sections describe related research executed by other investigators, the specific methods and results of this particular study, as well as the implications and future directions of this work.

RELATED WORK

As stated previously, there is a lack of clear consensus from the literature on effective characteristics for group formation [1]. Group work in the classroom may involve active learning strategies implemented in the classroom, such as collaborative learning and peer grading [9], [9], [16]. For these group activities in the classroom, enabling students to choose their groups themselves alleviates administrative duties and an instructor is present to guide students towards achieving learning goals. However, there is evidence for heterogeneous groups being beneficial in group work completed outside of the classroom, where learning and progress responsibilities are placed on groups of students. For example, in [1], it was found that groups with at least one "high-scoring student" attained better grades on group work than groups with only "low-scoring students." This study aimed to investigate several aspects of group dynamics, and the classroom instructors did not assign groups. In spite of the lack of group formation design, it was indicated that heterogeneous groups are beneficial to both high and low performing students.

Diversity of team skill levels have also been heavily investigated in attempts to improve efficiency and moral in the workplace. It has been shown that diversity in workplace teams can generally reduce company costs in communication to customers, but may raise communication costs with team members. [17] Contrary to this belief though, heterogeneity of team skill levels has been shown to increase team productivity. [17] The same concept has been shown in different workplace settings such as in action-teams. In particular, 30 teams from the National Basketball Association were studied, and a positive correlation between job-skill level team heterogeneity and action-team performance was found. [18] These studies show that a diversity of team skill levels can be beneficial not only in the classroom, but also in a variety of different workplaces.

Writing in a programming language or coding in a graphical interface is typically seen as an individual task. Therefore, introductory programming courses typically require students to produce short, functional scripts individually [14]. However, it has been shown that students who perform "pair programming" write better code [9], [19], [20]. This further supports the rationale for investigating the factors of group formation design in an introductory programming course.

Despite improved performance being a critical outcome of group work in coding, student satisfaction with their group members is also a salient factor in the success of group work in and out of the classroom. Previous studies have indicated that, regardless of the active learning strategy utilized, most students enjoy group work such as peer-assessment assignments or team learning [3], [4], [21]. In particular, students have confirmed their preference of "pair programming" over completing individual programming tasks [9], [22]. The study presented below also assesses student satisfaction with their group mates.

METHODS

Objectives

To assess how students perform in an introductory graphical programming course if they are placed in groups with people of the same or varying coding aptitude as determined by a group formation pre-assessment, the following research questions were posed:

1. Can student performance in an introductory programming class be predicted using a pre-assessment?

2. How do students perform in an introductory programming course if they complete group projects with people of the same or different coding aptitude?

These research questions have significant implications for courses designed to implement active-learning strategies associated with group work by determining how group formation and group dynamics affect individual student learning outcomes. Groups that consist of students of the same coding aptitude are referred to as homogeneous groups (HOMO) and groups that

305

consist of students of different coding aptitudes are referred to as heterogeneous groups (HET). It was hypothesized that the group formation pre-assessment would be a good indicator of student coding aptitude and that students in heterogeneous groups would outperform students in homogeneous groups.

Recruitment and Participation

Students in a large introductory programming course at an R1 (highest research activity) university participated in three group projects and individual weekly quizzes. A total of 146 students (42% female and 30% URM) from Biomedical Engineering 60A: Engineering Analysis, Design, Data Acquisition, a course that overviews Labview and the first introduction to coding for undergraduate biomedical engineering students, were recruited to participate in this study. This course was co-instructed by two instructors and one teaching assistant, and provided three one-hour lectures and one one-hour discussion sections each week for ten weeks. All students of the course participated in this study and provided informed consent (University of California Irvine IRB Approval Number 2018 – 4211).

Table 1.   Participant demographics

Study Participants (146 total)	
Low Income	26 (17.8%)
First Generation	52 (35.6%)
Females	62 (42.4%)
Underrepresented Minorities	45 (30.8%)

A group formation pre-assessment was issued to all students during the first week of the course. All 146 students were motivated to participate because they were graded for completion of the pre-assessment. The student demographics for students who participated in this study are presented in Table 1.

Prior to the completion of the course, a survey was also issued where students were asked to voluntarily complete a brief online survey to ascertain whether the students enjoyed

the groups that they were assigned after taking the group formation pre-assessment. To maximize compliance, completion of the survey awarded the students with half an extra credit point towards their final grade. Out of 146 students that participated in the study, 127 students responded to the online survey.

Group Formation

The group formation pre-assessment was created by the first author and consisted of three sections with three to four questions each: three questions about prior coding experience, three questions about motivation in the classroom [23], and three diagrammatic reasoning questions [24]. The pre-assessment section that most evenly split the students into homogeneous and heterogeneous groups was chosen. The score the students received on that pre-assessment section determined individual student coding aptitude and students were assigned to the following categories:

  a. Only high coding aptitude students (HCA)

  b. Only low coding aptitude students (LCA)

  c. Both HCA and LCA students.

Thus, the studies participants were divided into four experimental groups:

  a. HCA grouped with LCA -   (HET + HCA)

  b. HCA grouped with HCA -   (HOMO + HCA)

  c. LCA grouped with HCA -   (HET + LCA)

  d. LCA grouped with LCA -   (HOMO + LCA)

The number of students in each group are presented in Table 3, as well as how many of each group were formed. Students worked in these groups for project 1 of the course, but were allowed to form their own groups for subsequent group projects, project 2 and project 3. All projects were completed outside of the classroom.

Table 2. Group formation assessment survey

Question	Answer Choices
Did you like your group members in Project 1?	Yes/No
Did you like your group members in Project 2?	Yes/No
Did you prefer group members in Project 1 or 2?	1/2/both

Group Formation Pre-Assessment Results

The outcomes collected to assess the ability of the group formation pre-assessment to predict coding aptitude were quantitative. This assessment included comparing the z-scores of HCA and LCA final course grades using a student's t-test. A second outcome was also collected for the group formation pre-assessment. In particular, a short survey, shown in Table 2, was administered and assessed whether or not the students liked their teammates. Because the responses to this survey were binary, either "yes" or "no," the responses were tallied and quantified. The results of this survey are presented as percentages of students who answered yes and percentage of students who answered no.

For project 2, students were allowed to choose their own group members. Counting how many students answered yes to the first question of the survey was a second quantitative outcome of the group formation pre-assessment.

Group and Student Performance Assessment

The outcome measures collected to assess the effect of group formation on group performance were the group project scores. The final grade distribution was skewed and not normally distributed, so the grades were normalized to the average by converting to z-scores. The average z-scores of the grades for the three group projects were calculated for the four experimental groups listed previously.

The outcome measures collected to assess the effect of group formation on individual student improvement were quiz grades. These quizzes were completed individually. Quiz 1 and

2 were based on course material for group project 1, and quiz 3, 4, and 5 were based on course material presented for group project 2 and 3. As was done with the final grades, the grades for quizzes and projects had to be converted to z-scores because of a skewed and not normal distribution. The average z-scores of the grades for all quizzes were calculated for the four experimental groups.

RESULTS

It was found that the diagrammatic reasoning section of the group formation pre-assessment best split the classroom compared to other pre-assessment sections. Additionally, according to final course grades, it was found that the diagrammatic reasoning section of the pre-assessment was also a good indicator for determining LCA students and HCA students. It was also found that students placed in heterogeneous groups for projects performed better on individual quizzes that pertained to the same course material covered by the group project. Finally, it was shown that students enjoyed the groups they were assigned to.
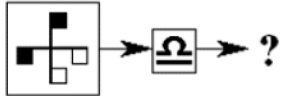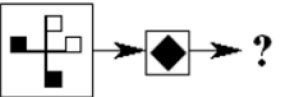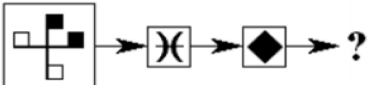
Group Formation Results

All students in the course participated in the group formation pre-assessment as it was part of their Project 1 assignment. It was found that the variability in student answers was highest for section 3 of the group formation pre-assessment, entitled "diagrammatic reasoning". Using the diagrammatic reasoning section of the group formation pre-assessment allowed the investigators to split the classroom as evenly as possible amongst groups, as shown in Table 3.

Table 3. Group formation results

Group	# of students/group	# of groups
HET + HCA	4-6	8
HOMO + HCA	4-6	6
HET + LCA	4-6	8
HOMO + LCA	4-6	15

In particular, as shown in Table 4, 31% of students answered all three questions correctly. This can be compared to the 25% of students that acknowledge previously taking a formal coding course before. Although overlap between these two sections was not calculated, the variability of student answers in these two sections was far greater than that of motivation. According to the group formation pre-assessment, student motivation to do well in the course was shared throughout the majority of the classroom.

Table 4. Group formation pre-assessment results

Section 1: Coding Background		
Question	Response (%)	
Did you transfer into BME from a different major or undecided?	Yes (19%)	No (81%)
Have you ever completed a formal class on coding or programming before?	Yes (25%)	No (75%)
Have you completed a college-level class on coding or programming before?	Yes (15%)	No (85%)
Have you attempted coding on your own or just for fun or out of curtiosity?	Yes (45%)	No (55%)
Section 2: Motivation for Doing Well		
In a class like this, ...	Response (%)	
I prefer course material that reallly challenges me so I can learn new things	0-3 (6%)	4-7 (94%)
I prefer course material that arouses my curiosity, even if it is difficult to learn	0-3 (3%)	4-7 (97%)
The most satisfying thing for me is trying to understand the content as thoroughly as possible.	0-3 (1%)	4-7 (99%)
I choose course assignments that I can learn from even if they dont guarantee a good grade.	0-3 (28%)	4-7 (72%)
Section 3: Diagramattic Reasoning		
What is the output for the following processes?	Response (%)	
	Correct (35%)	Not Correct (65%)
	Correct (33%)	Not Correct (67%)
	Correct (31%)	Not Correct (69%)

GROUP FORMATION PRE-ASSESSMENT CAPABILITIES

The final course grades of all students were determined based on their performance of all group projects and quiz grades. According to the trends of z-scores for final course grades, it was found the diagrammatic reasoning section of the group formation pre-assessment was an adequate indicator of coding aptitude. As shown in Figure 1, students who were classified as HCA trended above the final course grade average, and students who were classified as LCA trended below the final course grade average. In Figure 1 A, it is shown that the average final course grade of an LCA student was 0.3 standard deviations below the class average. Furthermore, 75.75% of

HCA students, individually received final course grades above the class average, compared to only 25.24% of LCA students (Figure 1B). These results provide evidence that student performance on a diagrammatic reasoning pre-assessment may indicate how they will perform in an introductory graphical programming course.
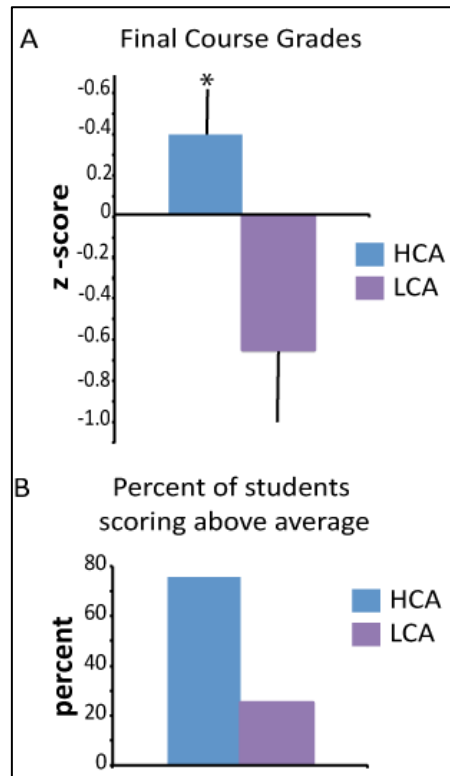
FIGURE 1

Fig. 1. (A) The average z-scores of the final grades for high coding aptitude (HCA) students and low coding aptitude (LCA) students. HCA students typically score above the average, and LCA students typically score below the average (p<0.05) (B) The percent of HCA students scoring above average on the final course grade is 75.75%. The percent of LCA students scoring above average on the final course grade is 25.24%.

A survey was administered to determine whether or not students were satisfied with their assigned group members for Project 1. Although the questions presented in the survey were qualitative, we were able to make the outcome quantitative by counting the number of students who answered yes or no to each question. The student responses are shown in Table 5 as

percent of students per experimental group. The survey responses show that, in all experimental groups, a majority of the students were satisfied with their group members for Project 1. Interestingly, students who were paired with students of the same coding aptitude (experimental groups HOMO + HCA and HOMO + LCA) were more inclined to answer that they enjoyed working with their group members. In contrast, only 68.75% of students in the HET + LCA group enjoyed working with their team members for Project 1.

Table 5. Group satisfaction

Did you like your group members in Project 1?		
Group	Yes (%)	No (%)
HET + HCA	83.33%	16.66%
HOMO + HCA	86.48%	13.51%
HET + LCA	68.75%	31.25%
HOMO + LCA	88.15%	11.84%

STUDENT PERFORMANCE

By comparing scores on all group projects, group work performance was assessed. Similarly, z-scores were utilized to indicate how experimental groups performed compared to the rest of the class. In Figure 2, it can be seen that groups who contained group members of the same coding aptitude performed above the class average in project 1. However, for project 2, where the groups were formed by the students' choice, students who were previously placed in groups with students of different coding aptitudes performed above the class average. This is a counterintuitive result because for project 1, it was hypothesized that groups with at least one HCA student in a group would perform better in group tasks, yet both homogenous groups scored above the average. Groups who contained all LCA students performed only slightly about the average, and not so surprisingly, students who were in groups with all HCA students attained the highest scores in their group projects.

313

Individual student performance outcomes consisted of individual quiz grades related to the course material of each project. The average z-scores pertaining to experimental groups is shown in Figure 3. Quizzes 1 and 2 were based on material covered in Project 1, and quizzes 3, 4, and 5 were based on material covered in Projects 2 and 3. Interestingly, for quizzes 1 and 2, which pertained to the course material of project 1, students who were placed in heterogeneous groups outperformed students who were placed in homogeneous groups. This trend was consistent for both LCA and HCA students in both quiz 1 and quiz 2. HCA students placed in heterogeneous groups, outperformed HCA students placed in homogeneous groups for both quiz 1 and quiz 2. Similarly, LCA students placed in heterogeneous groups outperformed

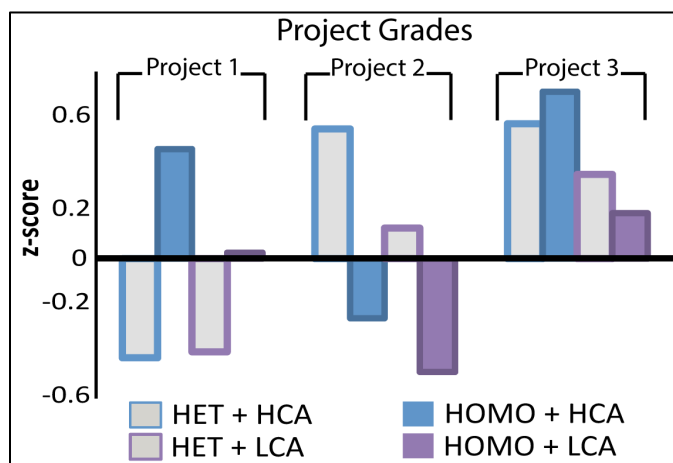LCA students placed in homogeneous groups.

FIGURE 2

Fig. 2. The average z-score of all groups for project 1, project 2, and project 3. All projects were completed in groups, but only the first groups were formed using the diagrammatic reasoning section of the group formation pre-assessment. For project 2 and project 3, students were allowed to choose their own group. Groups are labeled as was stated in methods section.

Alternatively, for quizzes 3 through 5, where groups were no longer assigned for projects pertaining to the course material, students who were categorized as LCA dropped below the class average regardless of their original group placement in project 1.
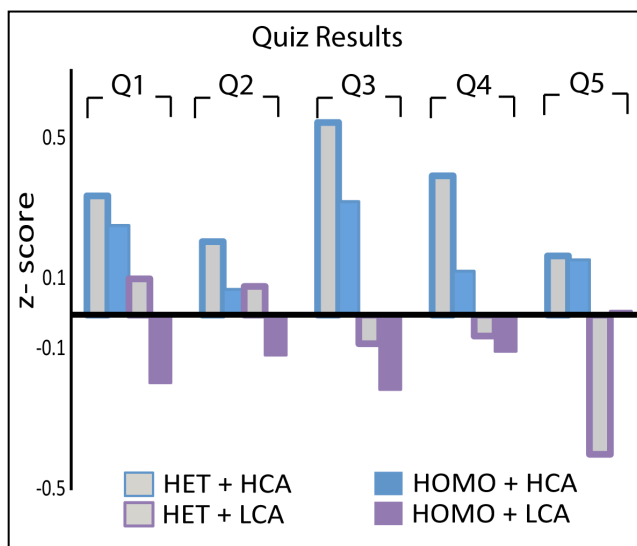
FIGURE 3

Fig. 3. The average z-score for all groups of all quizzes are shown. Quizzes 1 and 2 covered course material that pertained to project 1, and quizzes 3,4, and 5, covered course material that pertained to project 2 and project 3. Q1, Q2, Q3, Q4, and Q5, pertain to quiz numbers. Groups are labeled as was stated in methods section.

Furthermore, HCA students who were placed in groups with LCA students also outperformed HCA students who were placed with HCA students for quizzes 1 and 2. For quizzes 3, 4, and 5, all LCA students, regardless of their experimental group, scored below the class average. These results indicate that when students are grouped with students of different coding aptitudes, both types of students benefit in terms of understanding the course material.

DISCUSSION

The results of this study indicate that it is feasible to create student groups based on coding aptitude in a large introductory programming course. Furthermore, as is mentioned in prior studies [11], [15], it was shown that students enter their undergraduate education with a variety of coding backgrounds and coding aptitudes. This study aimed to determine if the consequences of these student differences could be mitigated. It was hypothesized that the group formation pre-assessment would be a good indicator of student coding aptitude and that students in heterogeneous groups would outperform students in homogeneous groups.

One important finding of this study was that there were less students who had previously taken a coding course than students who had a high coding aptitude according to the diagrammatic reasoning section of the group formation pre-assessment. This indicates that there may be other factors, such as high-level math and science courses or problem solving and spatial reasoning skills, that effect coding ability as well [25], [26]. Further research, such as exploring students' previous course histories, may explain disparities in performance levels in introductory programming courses.

The diagrammatic reasoning section of the group formation pre-assessment was found to be adequate at determining which students would fall above and below average final course grades. Although neither of the z-scores for HCA or LCA students fell above or below two standard deviations from the average final course grade, 75.75% of HCA students scored above the average final course grade. Conversely, only 25.24% of LCA students scored above the average final course grade. This indicates that a diagrammatic reasoning test may predict how well a student will perform in an introductory programming course. Future studies that aim to confirm the abilities of a diagrammatic reasoning pre-assessment as a predicting measure should be based solely on individual performance in an introductory graphical programming course. Although most of the students in this study said they liked their group members, future

studies should also verify whether or not they found their group members to be effective or good to work with. This will likely improve the understanding of the qualitative outcomes of group heterogeneity.

When students were placed into either heterogeneous groups or homogeneous groups for project 1, it was found that the homogeneous groups attained higher scores than heterogeneous groups. However, once the students were allowed to choose their own teammates for project 2, it was found that the students who were originally in heterogeneous groups attained higher scores than those in homogeneous groups for project 1. This may be due to a temporal development of team skills. [27] Students who were placed in heterogeneous groups originally had to learn how to work with people of different skillsets during project 1, so when they worked with their own self-chosen teams in project 2, they had already developed better management and team work skills than those placed in homogeneous groups. This pattern has been noted in other teamwork related studies, suggesting that it takes time to foster and build team skills. [27] Furthermore, those students who were placed in homogeneous groups for project 1 were unprepared for working with team members of different skill levels in project 2.

Students who were identified as LCA and were placed in heterogeneous groups were found to outperform LCA students who were placed in homogeneous groups in certain tasks. In particular, HET + LCA students performed above the class average in quizzes pertaining to project 1 course material. Interestingly, HET + HCA students attained better scores than HOMO + HCA students in the quizzes pertaining to project 1 course material as well. When taking quizzes pertaining to course material in projects 2 and 3 however, students who were originally in HET + LCA groups for project 1 scored below the class average. These data suggest that students who are placed in heterogeneous groups, regardless of their coding aptitude status, benefit from being in groups with students of different coding aptitudes.

CONCLUSION

The findings of this study indicate that group formation appears to play a role in student learning of a graphical programming language. If group formation strategies are further studied, the obstacles that arise in an introductory programming course from disparities in student coding backgrounds may be overcome. For example, student groups for group projects may be assigned based on different sections of the above mentioned group formation pre-assessment to determine which is the most effective at minimizing the range of individual performance scores. Furthermore, in depth data analysis to determine the factors of student academic backgrounds that play salient roles in student learning of a programming language could have major implications in the ways active and group learning are addressed in large, introductory, undergraduate classrooms.

REFERENCES

[1] Y. Chang and P. Brickman, "When Group Work Doesn ' t Work : Insights from Students," pp. 1–17, 2018.

[2] R. E. Slavin, "Synthesis of research of cooperative learning.," *Educ. Leadersh.*, vol. 48, no. 5, pp. 71–82, 1991.

[3]   S. Freeman *et al.*, "Active learning increases student perfor- mance in science, engineering, and mathematics.," *Proc. Natl. Acad. Sci.*, vol. 111, no. 23, pp. 8410–8415, 2014.

[4]   Z. Batz, B. J. Olsen, J. Dumont, F. Dastoor, and M. K. Smith, "Helping struggling students in introductory biology: A peer-tutoring approach that improves performance, perception, and retention.," *CBE—Life Sci. Educ.*, vol. 14, no. 2, 2015.

[5]   M. Armstrong, N., Chang, S.-M., & Brickman, "Cooperative learning in industrial-sized biology classes.," *CBE—Life Sci. Educ.*, vol. 2, no. 6, pp. 163–171, 2007.

[6]   M. Richardson, R. Bond, and C. Abraham, "Psychological Correlates of University Students ' Academic Performance : A Systematic Review and Meta-Analysis," *Psycological Bull.*, vol. 138, no. 2, pp. 353–387, 2012.

[7]   S. Bhavnani and D. Aldridge, "Teamwork across Disciplinary Borders : A Bridge between College and the Work Place," *J. Eng. Educ.*, pp. 13–17, 2000.

[8]   H. Passow, "Which ABET Competencies Do Engineering Graduates Find Most Important in their Work ?," *J. Eng. Educ.*, vol. 101, no. 1, pp. 95–118, 2012.

[9]   L. Williams, E. Wiebe, K. Yang, M. Ferzli, and C. Miller, "In Support of Pair Programming in the Introductory Computer Science Course," *Comput. Sci. Educ.*, vol. 12, no. 3, pp. 197–212, Sep. 2002.

[10]   N. Singer, "How Silicone Valley Pushed Coding into American Classrooms," *New York Times*, 2017.

[11]   The Computer Science Teachers Association, "State of Computer Science Education : Policy and Education," 2018.

[12]   S. L. Rebecca Wing-yi Cheng and J. C. Chan, "When high achievers and low achievers work in the same group: The roles of group heterogeneity and processes in project-based learning," *Br. J. Educ. Psychol.*, vol. 78, no. 205–221, 2008.

[13]   H. M. Levy, "Meeting the Needs of All Students through Differentiated Instruction: Helping Every Child Reach and Exceed Standards," *Clear. House A J. Educ. Strateg. Issues Ideas*, vol. 81, no. 4, pp. 161–164, Mar. 2008.

[14]   I. Stamouli, E. Doyle, and M. Huggard, "Establishing structured support for programming students," in *34th Annual Frontiers in Education, 2004. FIE 2004.*, 2004, p. F2G–5.

[15]   R. M. Felder and R. Brent, "Understanding Student Differences," *J. Eng. Educ.*, vol. 94, no. 1, pp. 57–72, Jan. 2005.

[16]   M. Prince, "Does Active Learning Work? A Review of the Research," *J. Eng. Educ.*, vol. 93, no. 3, pp. 223–231, Jul. 2004.

[17]   B. Hamilton, J. Nickerson, H. Owan, "Diversity and productivity in Production Teams," *Advances in the Economic Analysis of Participatory and Labor-Managed Firms.* Emerald Group Publishing Limited, pp.99-138.

[18]   J. De La Torre-Ruiz, J. Aragon-Correa, V. Ferron-Vilchez, "Job-related skill heterogeneity and action team performance," Management Decision. Vol. 49 Issue:7, pp.1061-1079

[19]   L. M. M. Giraffa, M. C. Moraes, and L. Uden, "Teaching Object-Oriented Programming in First-Year Undergraduate Courses Supported By Virtual Classrooms BT - The 2nd International Workshop on Learning Technology for Education in Cloud," 2014, pp. 15–26.

[20]   C. McDowell, L. Werner, H. Bullock, and J. Fernald, "The Effects of Pair-programming on Performance in an Introductory Programming Course," in *Proceedings of the 33rd SIGCSE Technical Symposium on Computer Science Education*, 2002, pp. 38–42.

[21]   C. E. King, "Feasibility and Acceptability of Peer Assessment for Coding Assignments in Large Lecture Based Programming Engineering Courses," *Proc. IEEE Front. Educ. Natl. Meet.*, 2018.

[22]   L. Williams, R. R. Kessler, W. Cunningham, and R. Jeffries, "Strengthening the case for pair programming," *IEEE Softw.*, vol. 17, no. 4, pp. 19–25, 2000.

[23]   P. R. Pintrich, T. G. D. A. F. Smith, and W. J. McKeachie., "Motivated Strategies for Learning Questionnaire Manual.," *Ann Arbor, MI Natl. Cent. Res. to Improv. Postsecond. Teach. Learn.*, 1991.

[24]   "Diagrammatic Reasoning," *Wikijob*, 2018. .

[25]   J. Shah, J. Woodward, S.M. Smith, "Applied tests of design skills—part II: visual thinking," *Journal of Mechanical Design*, vol. 135, no. 7, pp.071004, 2013.

[26]   S. Grigg, and L. Benson, "Promoting problem-solving proficiency in first-year engineering:PROCESS assessment." In American Society for Engineering Education: Proceedings of the2015 American Society for Engineering Education Annual Conference Exposition, Seattle, WA,June 14-17, 2015, pp. 13759.

[27]   T. Rapp, J. Matthew, "Evaluating and Individually Self-Administered Generic Teamwork Skills Training Program Across Time and Levels" *Small Group Research*, vol. 38. No. 4, pp532-5